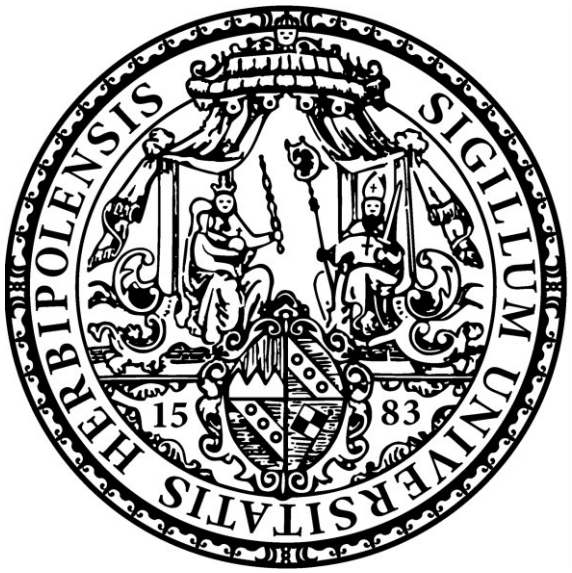

Determinants of macrophage and neutrophil heterogeneity in cardiac repair after myocardial infarction

Determinante der Makrophagen- und Neutrophilien-Heterogenität bei der Herzreparatur nach Myokardinfarkt

Doctoral thesis for a doctoral degree

at the Graduate School of Life Sciences,

Julius-Maximilians-Universität Würzburg,

Section: Biomedicine

submitted by

Rizzo Giuseppe

from

Rome (Italy)

Würzburg, 2022

Submitted on:

Members of the Thesis Committee

Chairperson: Prof. Dr. Georg Gasteiger

Primary Supervisor: Clément Cochain, PhD

Supervisor (Second): Prof. Dr. Alma Zernecke

Supervisor (Third): Prof. Dr. Med. Ulrich Hofmann

Supervisor (Fourth): PD Dr. rer. nat Heike Hermanns

1 Table of contents

2 Chapter 1: Introduction

2.1 Myocardial infarction

Cardiovascular diseases are the leading cause of death worldwide, with an estimated incidence of death of 17.9 million people per year. [1] Cardiovascular diseases are disorders of the heart and blood vessels, including coronary artery diseases, cerebrovascular diseases, peripheral arterial diseases, rheumatic heart diseases, congenital heart diseases, thrombosis and embolisms. [1,2] Myocardial infarction (MI) is a cardiac disease caused by coronary artery occlusion, leading to ischemic damage of the myocardium and characterized by left ventricle remodeling, reduced cardiac function and development of heart failure. [3,4]

Myocardial infarction is mainly initiated by rupture or erosion of an unstable atherosclerotic plaque, leading to thrombosis, interruption of blood flow to the heart and ischemia-induced death of cardiomyocytes. Disruption of endothelial cells integrity facilitates the infiltration of leukocytes in the tissue.[3] Danger-associated molecular patterns (DAMPs) are released by necrotic cells and recognized by infiltrating leukocytes-expressing pattern recognition receptors (PRRs), initiating an inflammatory response crucial for the clearance of damaged and dead cells and extracellular matrix debris. [3] Inflammation is then followed by a reparative phase with resolution of inflammation, myofibroblasts proliferation, collagen deposition and scar formation (**Figure 1**).[3]

Several pathophysiological complications are associated with MI. Rupture of the infarcted tissue is the most dramatic consequence in patients with MI and, although the incidence in MI patients is below 1%, mortality is extremely high.[5] It is suggested that rupture is caused by prolonged inflammation or impairment of the reparative processes.[6] Other complications include cardiogenic shock, reduced cardiac output that leads to ischemic dysfunction of vital organs like kidney and brain, and defects in the heart electric conduction, causing arrhythmias during early and late phase after myocardial infarction.[6] Among the patients surviving the initial cardiac events after myocardial infarction, a large proportion develop Heart Failure (HF) with reduced ejection fraction (HFrEF). [4] HFrEF is

associated with drastic morphological changes, such as progressive chamber dilation, increased ventricle stiffness and scarring. [4]

To overcome the complications caused by ischemic damage to the myocardium, many therapeutic strategies have been developed. Restoration of the blood flow via re-opening of affected coronary arteries through percutaneous coronary intervention, especially performed shortly after the ischemic damage, improved cardiomyocytes survival and reduced scar size.[3] Beta-blockers administration have been shown to decrease heart rate, blood pressure, and infarct size after MI, but some studies in experimental MI revealed that Beta-blockers administration did not alter infarct size,[7] despite reduced incidence of cell death.[8–11] Patients treated with angiotensin-converting enzyme (ACE) inhibitors displayed decreased in mortality and heart failure development.[12] ACE inhibitors treatment showed reduced angiotensin II levels, correlated with reduced cell apoptosis and inflammation, reduced cardiac hypertrophy and interstitial fibrosis.[13,14,15,16] Also, in patients with myocardial infarction statins treatment reduced mortality and fibrosis in experimental myocardial infarction through suppression of matrix metalloproteinases (MMP) expression.[17–20]

Tissue healing after MI is a finely orchestrated process of events in which different cell types and molecular components are involved. Inflammation is known to play a critical role in cardiac remodeling, supporting both tissue damage and repair.[3] Because of its dualism, modulating inflammation has been proposed as a potential therapeutic strategy to improve cardiac repair and functional recovery after myocardial infarction.[3]

However, trials employing non-targeted inhibition of the inflammatory response after MI, using non-steroidal anti-inflammatory drugs acting via cyclooxygenase inhibition, were unexpectedly harmful, leading to increased rupture and adverse remodeling, highlighting the crucial role of the inflammatory response in the reparative processes.[21] In more recent clinical trials, patients with MI treated with Colchicine, an anti-inflammatory medication, had lower risk of ischemic cardiovascular events compared to the placebo group. [22] On the same line, treatment with Canakinumab, a monoclonal antibody against Interleukin-1β (IL1β), in MI patients led to reduced cardiovascular events compared to the placebo group. [23] However, it remains unknown how these treatments are affecting cardiac

healing and function after myocardial infarction, although initial data indicate that IL1β blockade might have beneficial effects and reduce the development of heart failure in MI patients. Recently, treatment with anakinra, an IL1-receptor antagonist, in patients with MI led to reduced incidence of new-onset of heart failure and hospitalization at 1 year follow-up. [24]

Because of the dual role of inflammation in cardiac remodeling after myocardial infarction, it is crucial to develop therapeutic strategies able to inhibit inflammation deleterious functions and not affect or increase its beneficial role. For this reason, a selective targeting of specific subsets of immune cells or specific signaling pathways is needed. Nevertheless, there are several complications on targeting the immune response mediators. First of all, the inflammatory mediators are pleiotropic, and can for example exert different functions in different cell types. [25–28] Second, the inflammatory response is a highly dynamic process and finding the precise time window to target a specific cell type or pathway is quite challenging. Finally, post-MI remodeling in patients is greatly affected by different aspects, such as genetic background, comorbidities (like hypertension and diabetes), age and sex, and the influence of these factors on the post-MI inflammatory response are poorly known. Taken together, these considerations limit the therapeutic approaches.

In this thesis, I am focusing on the inflammatory response after experimental myocardial infarction, especially in defining the main drivers of neutrophil and macrophage functional heterogeneity in the ischemic heart and how they are involved in cardiac remodeling after MI.

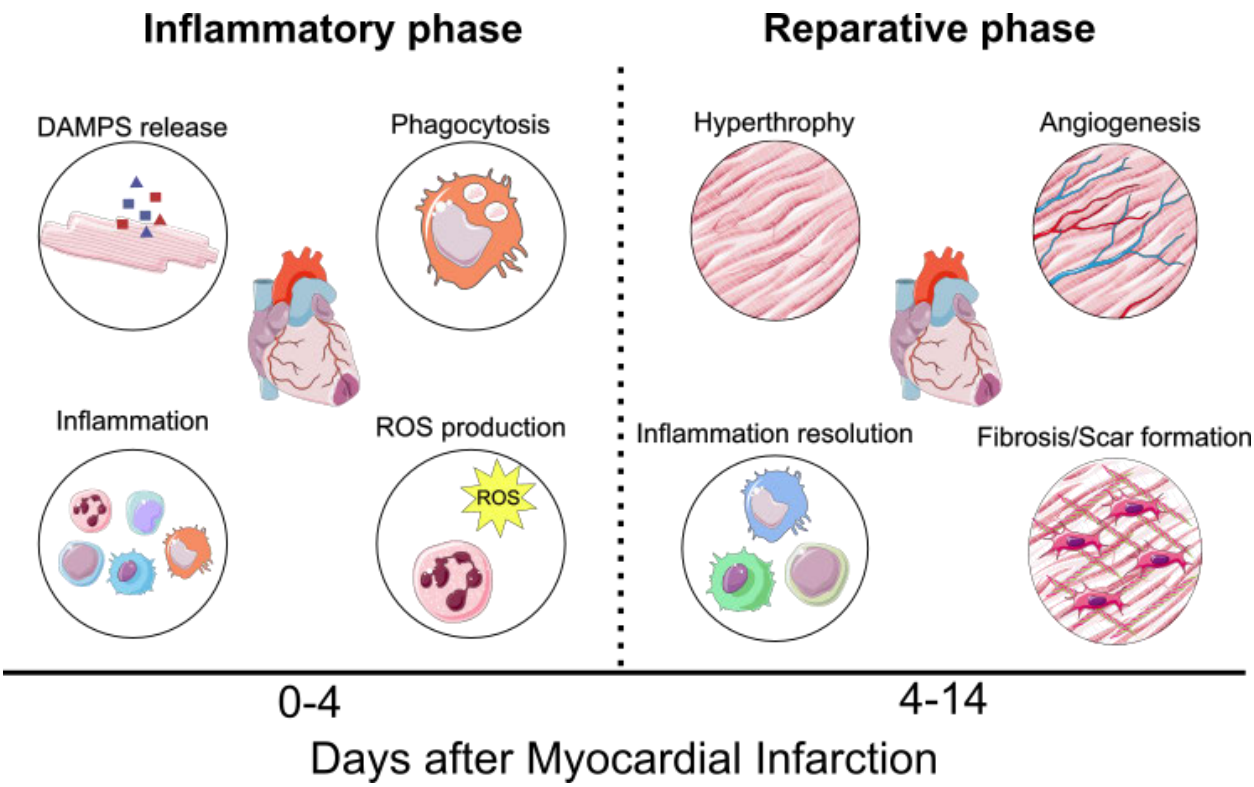

Figure 1: Phases of cardiac healing after myocardial infarction. Ischemic damage triggers tissue injury and cardiomyocyte death initiating the inflammatory phase, characterized by acute inflammation with recruitment of immune cells including neutrophils, monocytes/macrophages, dendritic cells, and lymphocytes. After 4 days in mice, the inflammatory phase is followed by a reparative phase, characterized by inflammation resolution, angiogenesis, myofibroblast proliferation, collagen deposition, and scar formation. These are necessary processes for a proper wound healing. Images are taken from Servier Medical Art (smart.servier.com*)* and arranged with Inkscape.

2.2 Inflammation in the ischemic heart

2.2.1 Molecular drivers of the inflammatory response

2.2.1.1 Danger-associated Molecular Patterns (DAMPs) involved in immune cell activation

DAMPs released by necrotic cells and their recognition by PRRs of the innate immune system is the starting point of an inflammatory response. Upon PRRs activation, a cascade of inflammatory mediators is activated, including inflammatory cytokines, chemokines, and cell adhesion molecules.[29–34] In the ischemic heart, some DAMPs are released by stressed cardiomyocytes, fibroblast and activated leukocytes. [29,31,32]

High mobility group box-1 (HMGB1) is released by necrotic cells, monocytes, macrophages, and stressed cardiomyocytes.[35] HMGB1 binds and activates different Toll-like receptors (TLRs), including TLR2, TLR3 and TLR4, and receptor for advanced glycation end-products (RAGE) initiating NF-kB translocation in the nucleus and activating the proinflammatory signaling cascade.[34,36–38]

S100A8 (calgranulin A) and S100A9 (calgranulin B) are DAMPs secreted by neutrophils, monocytes and macrophages during inflammation and activate RAGE and TLR4 receptors, initiating their signaling pathways. In a mouse model of ischemia/reperfusion injury, S100A8/A9 heterodimer is released immediately after hypoxic damage, inducing pro-inflammatory cytokines expression in cardiac fibroblasts and macrophages.[39] High level of S100A8/A9 are present in patients with acute MI correlating with circulating neutrophils count, recurrent cardiovascular events and increased risk of cardiovascular death or MI.[40,41]

S100A1 is a DAMPs secreted specifically by cardiomyocytes during MI. High levels of S100A1 were found in both experimental MI and patient with acute MI. Cardiac fibroblast engulf S100A1 via endocytosis, initiating TLR4 dependent-activation via MAP kinases and NF-kb, exerting a immunomodulatory and anti-fibrotic effect.[42]

Fibronectin is an extracellular matrix protein released by fibroblasts in the cardiac tissue during myocardial hypertrophy and failure.[43] Secretion of inflammatory cytokines (e.g. TNFα, IL6, and IL1β) were induced in bone marrow-derived mast cell in a TLR4-dependent manner after fibronectin treatment.[44] In fibronectin knock-out mice, left ventricular dilation was decreased and systolic performance was increased after MI. Moreover, inflammation, and metalloproteinase 2 and 9 activity were also decreased.[45]

2.2.1.2 Pattern recognition receptor (PRRs) in myocardial infarction

PRRs are proteins expressed on the cellular and endosomal membranes but they can also be found in the bloodstream and interstitial fluids. The main PRRs associated with inflammation after MI are the Toll - like receptors (TLRs) and the nucleotide-binding oligomerization domain - like receptors (NLRs).[46]

TLRs are mostly expressed on leukocytes, but they can also be found in parenchymal cells, like cardiomyocytes, fibroblasts, and endothelial cells [47,48]. The signaling pathway activated by TLRs relies on a cytoplasmatic Toll/interleukin (IL) 1 receptor (TIR) domain that serve as docking site for an adaptor protein called MyD88, that can engage the domain directly, for TLR-1-5-6-7-9, or in combination with another adaptor like TIRAP/MAL, for TLR2-4. Activated MyD88 recruits IL1 receptor associated kinases 4, 1 and 2 (IRAK4, IRAK1, and IRAK2) to the complex. In particular, phosphorylation of IRAK1 recruits tumor necrosis receptor associated factor 6 (TRAF6) that associates with the ubiquitin-conjugating enzyme 13 (UBC13) and ubiquitin-conjugating enzyme E2 variant 1 (UEV1A). This leads to TRAF6 ubiquitination, activating TAK1 that subsequently phosphorylates IKKα, IKKβ, and IKKγ leading to IkB degradation and allowing the translocation of NF-kb to the nucleus inducing the expression of its target genes. [29,30]
The TLRs most expressed in the heart are TLR4, TLR2, TLR3, and TLR5, among which TLR4 and TLR2 are the most studied in the context of myocardial injury. [3] In circulating leukocytes from humans with acute MI increased activation of TLR2 and TLR4 and their signaling cascade mediators has been observed, correlating with the development of HF.[49–52] In a mouse model of ischemia/reperfusion injury, disruption or deficiency of TLR4, TLR2, MyD88, or TLR3 reduced infarct size and, on a complementary approach, treatment with an a TLR4 antagonist in mice and with an anti-TLR2 antibody in mice and pigs also reduced infarct size. [53–59] According to these findings, sustained TLRs activation exacerbates cell death, inflammation, oxidative stress, interstitial fibrosis, and leukocyte infiltration. In contrast, a study showed a beneficial effect of TLR5 in a model of ischemia/reperfusion injury, in which TLR5 deficiency increased infarct size, oxidative

stress, inflammation and left ventricular dysfunction.[60] It was also shown that TLR2, TLR4 and TLR9 activation before ischemia/reperfusion injury induced cardioprotection, reducing infarct size and cardiomyocytes survival, via activation of TIR domain and PI3K/Akt.[61–65] Similar protective effects were shown after short-term activation of some immune signaling.[26,66–68] These findings suggest that short-term activation of immune cell pathways has beneficial effect impacting primarily on cardiomyocyte survival, whereas a prolonged activation exacerbates the inflammatory response recruiting high number of leukocytes in the heart inducing tissue injury.[26,30,66,69]

NLRs are sensors that recognize intracellular DAMPs and pathogen-associated molecular patterns (PAMPs). They are divided in 4 subfamilies based of their N-terminal domain: NLRA, NLRB/NAIP, NLRC, and NLRP. NLRs consist of three different domains: a leucine rich repeat (LRR) domain at the C terminus involved in the recognition of ligands; a CARD (caspase recruitment domain) and PYD (pyrin domain) domain at the N-terminal which link the NLRs to the different adaptor proteins and effector molecules; and a NACHT (neuronal apoptosis inhibitory protein CIITA HET-E TP1) domain which is important for NLRs activation.[70] NLRs are involved in a wide range of molecular functions, including NFkB signaling pathway, retinoic acid-inducible gene-I-like receptor signaling, autophagy, major histocompatibility complex (MHC) gene regulation, reproduction and development.[71] In particular, the NLRs most studied in the context of myocardial infarction are NLRP3 and NOD1.

NLRP3 is associated with the inflammasome, a macroprotein complex that activates a series of pro-inflammatory cytokines, such as IL1β and IL18.[72–74] NLRP3 inflammasome is widely studied in different cardiovascular diseases, such as hypertension, heart failure, atrial fibrillation and acute MI, promoting adverse inflammatory response in such diseases. [75,76,76,77] In the mouse heart after ischemia/reperfusion injury, NLRP3 and the downstream components of inflammasome activation caspase-1, IL1β and IL18 are upregulated. [78,79] Moreover, in a NLRP3 knock-out mouse model reduced infarct size, fibrosis, left ventricular dysfunction and decreased macrophage and neutrophils infiltration were observed.[80] Other findings described a link between reactive oxygen species (ROS) production and NLRP3 inflammasome activation, in which mice after

ischemia/reperfusion injury treated with antioxidant displayed reduced infarct size correlated to a diminished level of NLRP3, active caspase-1 and IL1β levels.[81,82]

NOD1 is an intracellular scaffold protein that consists of CARD, NOD, and leucine-rich repeat domain. Inactive NOD1 exists in monomer form in the cytosol, while upon activation, it self-oligomerizes recruiting several accessory/scaffold proteins ending up with NF-kB activation and its translocation in the nucleus.[83] In a model of ischemia/reperfusion injury, a deleterious effect of NOD1 in cardiac healing was shown. In fact, activation of NOD1 with its activator DAP (D-glutamyl-meso-diaminopimelic acid) aggravated ischemic injury promoting cardiomyocytes apoptosis and inflammation. [84] In particular, activation of NOD1 in cardiomyocytes displayed decreased in L-type Ca^{2+} current, intracellular Ca^{2+} transients and slow intracellular Ca^{2+} decay, features that are common in different cardiovascular diseases. [85] NOD1 deletion or pharmacological inhibition prevented Ca^{2+} mishandling in ventricular cells in a murine model of heart failure.[86] These findings highlight the role of NOD1 as regulator of Ca^{2+} dynamic in cardiac excitation-contraction.

2.2.1.3 Cytokines

Cytokines are biologically active proteins with low molecular weight that act in an autocrine or a paracrine manner to modulate cell function. After myocardial infarction, cytokines and chemokines produced by stromal cells or resident immune cells induce immune cell recruitment in the heart in which they exert their role by also producing a variety of cytokines and chemokines. [87]

Proinflammatory cytokines like TNFα, IL1 and IL6 are among the most important and widely studied in the context of heart diseases, including myocardial infarction. [6]

TNFα is produced in high level in the heart after acute injury or cardiac stress (such as myocyte stretch, ischemia, pressure, or volume overload), while in physiological condition it is not present. [88] TNFα has a controversial role, contributing to the development of cardiac dysfunction, but also known to have cardioprotective effects. [88] On one hand,

increase in TNFα levels upregulate the expression of antioxidant enzyme manganese superoxide dismutase and mitochondrial protein A20, supporting a protective role [89]. On the other hand, TNFα exerts direct toxicity on cardiomyocytes and promotes reactive oxygen intermediates generation, supporting a role in tissue damage. [90] There are two types of TNFα cell membrane receptors: TNFR-1 and TNFR-2. TNFR-1 is known to exert deleterious effects, while TNFR-2 exerts a protective effect in the heart. [91] Clinical studies on anti-TNFα antagonists showed contradictory results. In a first study, high risk of death and hospitalization was increased in patients with heart failure treated with TNFα antagonist compared to the control group. [92] In a second study, TNFα antagonist treatment in patients with chronic heart failure showed lower death rate and hospitalization. [93] In a third study, patients with myocardial ischemia treated with a TNFα antagonist displayed less blood neutrophils and plasma IL6 but increased platelet-monocyte aggregation. [94] These studies suggest that blockage of TNFα eliminates both its beneficial and detrimental function.

IL1 is a group of 11 cytokines that are known to initiate proinflammatory processes. The most studied are IL1α and IL1β which both bind to the IL1 receptor (IL1R) and exert similar pro-inflammatory effects. IL1R knock-out mice displayed reduced left ventricular dysfunction and dilation in a model of ischemia/reperfusion injury.[95] Moreover, in experimental MI, treatment with an IL1R antagonist inhibited myocyte apoptosis, supporting the notion that the IL1 signaling pathway promotes tissue damage after ischemic injury.[96] IL1β is expressed as inactive precursor and is activated by the inflammasome after cleavage at specific sites. [97] As previously mentioned, myocardial infarction patients treated with an IL1β blocking antibody showed reduced cardiovascular events. [23] Although cardiac function readouts were not evaluated in this trial, it supports the notion that IL1β promotes cardiovascular disease progression.

IL6 is a cytokine with proinflammatory properties and secreted by different cell types. IL6 binding to IL6 receptor (IL6R) and gp130, a transmembrane protein required for IL6/IL6R recognition, activates various signaling pathways involving different transcription factors, including STAT1 and STAT3. [98] Cardiomyocytes-specific over-expression of gp130 in experimental myocardial infarction led to increased inflammation, adverse remodeling, mortality rate and heart failure in a STAT3-dependent way. Indeed, genetic STAT3

reduction in gp130-enhancing condition improved the healing outcomes, lowered inflammation, left ventricular rupture and heart failure after myocardial infarction. [99]

Anti-inflammatory cytokines are necessary for inflammation resolution, an important process that reduces the inflammation and initiates the proliferative phase in myocardial infarction. The most studied anti-inflammatory cytokine is IL10, a homodimer protein homodimer produced by many types of cells, such as monocytes, T-helper lymphocytes, mast cells, T regs, macrophages and some subsets of B cells. IL10 is responsible to reduce TNFα, IL1 and IL6 production.[100] Infarcted mice treated with IL10 showed decreased left ventricular dilation and improved cardiac function, despite unchanged infarct size and mortality rate. Moreover, IL10 significantly upregulate a pro-reparative phenotype in heart macrophages isolated after MI. [101] IL10 is required for the induction of an osteopontin-producing reparative macrophage phenotype in the heart after myocardial infarction, contributing to fibrosis and clearance of apoptotic cells. [102]

2.2.1.4 Transforming growth factor β (TGFβ)

Transforming growth factor β (TGFβ) comprises a large group of proteins, including the TGFβ1, TGFβ2 and TGFβ3, the bone morphogenetic proteins (BMPs), the growth differentiation factors (GDFs), the activins, the inhibins, the nodal, and the anti-Mullerian hormone proteins. [103] In homeostasis, TGFβ is constitutively expressed in the embryonic and adult heart, localizing specifically in cardiomyocytes, or bound to the extracellular matrix. [104] TGFβ is crucial during cardiac development. Indeed, mice deficient for several TGFβ isoforms, mainly TGFβ1 and TGFβ2, showed impaired heart development and impaired cardiac valve formation. [105,106] In adult mice, cardiomyocyte-specific deletion of Smad4, an intracellular mediator of the TGFβ signaling pathway, is associated with defective cardiac function, fibrosis, increased cardiomyocytes cross-sectional area and decreased ion channel gene expression. [107]

Myocardial infarction is associated with TGFβ and the Smad signaling cascade activation. [108,109] The TGFβ isoforms seem to follow a time-dependent expression. [104,108,110–113] In a

model of ischemia/reperfusion injury, TGFβ1 and TGFβ2 peak between 6-72 hours, while TGFβ3 is upregulated after 7 days. [113] TGFβ isoforms are secreted in a latent form that includes the TGFβ dimer, the latency-associated peptide (LAP), and the latent TGFβ-binding protein (LTBP). [114–116] The activation of TGFβ signaling pathway involves the release of the LAP and the LTBP complexes. [114–116] However, which are the signals triggering TGFβ activation after myocardial infarction are still unknown, but several hypotheses have been suggested. *In vitro* studies suggested that αvβ5 and αvβ3 integrins are involved in TGFβ activation and myofibroblast conversion, but the relevance of these studies *in vivo* remain to be clarified. [117] Proteases, such as serine proteases, cathepsins, matrix metalloproteinases, and cysteine proteases, are implicated in TGFβ activation following injury, and, since they are highly activated following cardiac injury, they have been suggested as potential TGFβ activators in the infarcted heart. [118–120] Thrombospondin-1 (TSP-1) interacts with the LAP complex promoting TGFβ dimer release and activation. [121] In a murine and canine model of myocardial infarction, TSP-1 is upregulated in the border zone and is associated with an increased level of TGFβ. [122]

Several cell types can produce and release TGFβ after myocardial infarction. In particular, macrophages seem to be the main producers of TGFβ in mice. [123] In CCL2/MCP-1-deficient mice, a mouse model in which monocyte and macrophage recruitment is impaired, expression of TGFβ2 and TGFβ3 was reduced, supporting the hypothesis that monocytes/macrophage compartments contribute to TGFβ production. [124] In contrast, cardiomyocytes were the major source of TGFβ in a porcine model of myocardial infarction, suggesting that cell type-specific TGFβ production might variate across species. [112] Fibroblast, endothelial cells, mast cells, and lymphocytes are populating the infarcted heart and can produce TGFβ, but whether they contribute significantly to TGFβ availability in the heart remain still unknown. [125–128]

TGFβ act on different cell types. TGFβ1 administration in a feline model of ischemia/reperfusion reduced cardiomyocyte death. [129] *Ex vivo* TGFβ1 infusion in the infarcted heart decreased cardiomyocytes apoptosis via activation of the p42/p44 signaling pathway. [129] In contrast to these findings, TGFβ enhanced apoptosis via Smad signaling pathway in isolated rat cardiomyocytes treated with angiotensin II. [130] Moreover, in experimental myocardial infarction, cardiomyocyte-specific knock-out of TGFβ1 and

TGFβ2 increased mice survival due to cardiac rupture. [131] The controversial effect of TGFβ on cardiomyocytes might be explained by a dose- and time-dependent action, and by the different experimental conditions. TGFβ plays a crucial role in fibroblast activation in the healing heart. Indeed, TGFβ induces cardiac fibroblast activation, their conversion in myofibroblast, and promotes the synthesis and secretion of collagen I, collagen III, and fibronectin. [130,132–134] In experimental myocardial infarction, systemic TGFβ inhibition reduced collagen synthesis and increase MMP expression in the infarcted heart, supporting the hypothesis that TGFβ might be involved in regulating cardiac fibroblast phenotype and function. [135] TGFβ is also a modulator of the response of the immune cells. It can act as a neutrophil and monocyte chemoattractant and stimulates pro-inflammatory cytokines and chemokines in monocytes *in vitro*. [109,136–138] In contrast, systemic TGFβ inhibition increased neutrophil recruitment and production of pro-inflammatory cytokines in experimental myocardial infarction. [139] TGFβ can also modulate macrophage function. Indeed, *in vitro* macrophage stimulation with TGFβ induced M2 macrophage polarization with suppression of pro-inflammatory cytokines, augmented macrophage proliferation, reduced nitrogen oxide production, and suppressed cytotoxic activity against Leishmania parasite infection. [140–144]

2.2.1.5 Chemokines

Chemokines are a family of small secreted proteins that are known for their ability to stimulate leukocyte migration. They are divided into CC, CXC, and CX3C subtypes. [28] Chemokines receptors are expressed in a cell-type specific manner. CCR2 is expressed in Ly6C^{hi} monocytes and is required for their release from the bone marrow. [145] CXCR2 and CXCR4 are expressed in neutrophils and control neutrophil egress and return in the bone marrow. [146,147] The just mentioned chemokines receptors are called “conventional chemokine receptors”, but also “atypical chemokine receptors” exist. [148] The latter are involved in leukocyte recruitment acting mainly as decoy receptors, controlling the chemokine-chemokine receptor interaction. [149] For example, ACKR1 carries chemokines

across the endothelial cells for presentation to blood leukocytes. [150,151] Moreover, although the mechanisms remain unclear, ACKR1 controls neutrophil phenotype and numbers in the blood. [152] ACKR2 act as a scavenger receptor, switching from the cell surface and the cytoplasm and internalizing the chemokines that it encounters while exposed to the extracellular space. [153,154] Chemokines internalized in this way are released by ACKR2 and degraded. [153,154] ACKR2 deficiency in mice leads to increased neutrophils and Ly6C^{hi} monocytes infiltration, decreased in survival and cardiac function, and increase left ventricular dilation after MI. [155]

2.2.2 Cardiac cellular composition and specific cellular roles in the post-MI inflammatory response

Different immune and non-immune cell types contribute to the initiation and maintenance of the inflammatory response after myocardial infarction. A study analyzing the cardiac cellular components in the normal heart showed that more than 60% of non-myocyte heart cells are endothelial cells, while leukocytes comprise 5% to 10%, and fibroblasts constitute less than 20%. [156] It has been widely studied how specific cell populations affect cardiac remodeling after injury and how the different cellular components interact with each other. Nevertheless, their relative role in activation of specific inflammatory cascades remain unclear. For this reason, I am going to describe in this section the different immune and non-immune cells present in the infarcted heart and how they participate in the inflammatory processes.

2.2.2.1 Non-immune cell component

2.2.2.1.1 Cardiomyocytes

Cardiomyocytes are the cellular unit of the myocardium responsible for the heart contraction. Upon ischemic damage, cardiomyocyte die because of necrosis, releasing DAMPs and providing the main stimulus for the initiation of the inflammatory response. Live cardiomyocytes in the border zone are supporting inflammation following activation with IL1, TLR ligands or ROS. Moreover, different studies have also shown that cardiomyocytes in the border zone express intercellular adhesion molecule-1 (ICAM1) and might be involved in supporting inflammation by producing cytokines and chemokines. [157–159] H9c2 cardiomyocytes cell line treated with LPS showed secretion of inflammatory cytokines (e.g. TNFα, IL1β and IL6), suggesting a potential role of cardiomyocytes in supporting the inflammatory response. [160] TGFβ deletion in cardiomyocytes reduced neutrophils infiltration, increased MMP9 activation and survival in mice over 40 days after myocardial infarction. [131] Although these findings highlight a potential role of cardiomyocytes in supporting inflammation, their real contribution to inflammatory processes is still poorly understood and remains to be more precisely evaluated.

2.2.2.1.2 Endothelial cells

Endothelial cells are the cellular component of the endothelium, the interior surface of blood vessels. Endothelial cells are required for lymphocytes extravasation from the circulation into the tissue, in this case the infarcted heart. Upon endothelial cells activation a series of adhesion molecules are upregulated, such as P-selectin and E-selectin. [161] Selectins bind activated leukocytes, mediating their extravasation through the endothelium and tissue infiltration. [162] Moreover, activated endothelial cells in the infarcted area are also an important source of cytokines and chemokines.[163,164]

Lymphatic endothelial cells are also involved in cardiac inflammation. Augmented lymphangiogenesis in the heart after MI improved clearance of immune cells from the heart to the lymph node in a LYVE-1-dependent manner. [165] Moreover, *Lyve-1* deletion exacerbated inflammation and reduced cardiac function. [165] On the contrary, lymphangiogenesis inhibition using VEGFR3 deletion in endothelial cells or loss of VEGF-C and VEGF-D did not affect leukocytes infiltration and cardiac function, highlighting that the role of lymphangiogenesis in MI needs further evaluation. [166]

2.2.2.1.3 Fibroblast

Fibroblasts are the most common cells in connective tissue and are responsible for producing collagen and extracellular matrix, the structural and biochemical support for every cell type. In the normal myocardium, fibroblasts are quiescent and provide maintenance of the extracellular matrix network. In contrast, when fibroblasts are stimulated with DAMPs, they secrete inflammatory cytokines and chemokines. [167] IL1 signaling pathway seems to have an important role in fibroblast activation during myocardial infarction. Indeed, activation of IL1 signaling in fibroblasts was described to promote a proinflammatory phenotype, to inhibit α-smooth muscle actin (α-SMA) and to promote a matrix-degrading phenotype. [168] scRNA-seq analysis of cardiac fibroblasts described upregulation of NF-kb-related genes and *Ccl2* chemokine, essential for Ly6C^{hi} monocyte recruitment, in a model of pressure overload. [169] In the same study, blockage of NF-kb signaling pathway in cardiac fibroblasts attenuated Ly6C^{hi} monocytes recruitment and preserved cardiac function.[169] Another study highlighted the ability of cardiac fibroblast to engulf dead cells via secretion of milk fat globule-epidermal growth factor 8 (MFG-E8). [170] MFG-E8 deficiency led to accumulation of dead cells, exacerbation of the inflammatory response and decreased survival in experimental MI. [170] Overall, these data show that fibroblasts can modulate inflammation after myocardial infarction.

2.2.2.2 Immune cell component

Inflammatory cells infiltrate the infarcted heart dynamically during the different phases of the healing process, acquiring specialized function (**Figure 2**). [87] In this section I am going to describe the different immune cells invading the heart and how they affect cardiac healing.

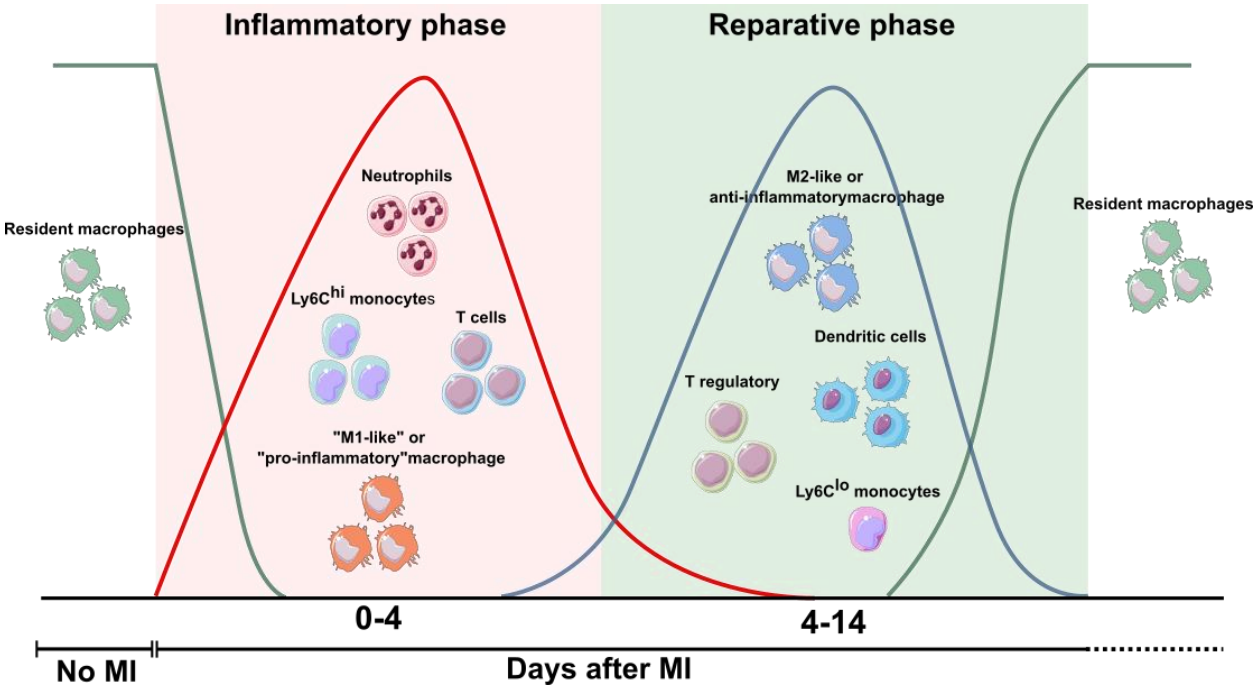

Figure 2: Immune cell kinetic after myocardial infarction. Inflammatory cells dynamically infiltrate the infarcted heart. Shortly after MI, resident macrophages die and pro-inflammatory immune cells, such as neutrophils, Ly6C^{hi} monocytes, T cells, and pro-inflammatory macrophages, infiltrate the heart during the inflammatory phase. The reparative phase is characterized by immune cell population with an anti-inflammatory response, including anti-inflammatory macrophages, dendritic cells, T regulatory cells, and Ly6C^{lo} monocytes. During the reparative phase, the resident macrophage pool is replenished. Images are taken from Servier Medical Art (smart.servier.com) and arranged with Inkscape.

2.2.2.2.1 Dendritic cells

Dendritic cells are a heterogeneous population of immune cells known also as “antigen-presenting cells”. Their function consist in antigen presentation to T cell and secretion of cytokines and growth factors, regulating the immune response and inflammation.[171] Dendritic cells are classified in two main subpopulation: plasmacytoid dendritic cells (pDCs) and conventional dendritic cells (cDCs). [172] cDCs can be additionally classified in cDCs1, defined as $CD8a^{+}CD103^{+}XCR1^{+}$ in mice and $CD141^{+}CLEC9A^{+}XCR1^{+}$ in human, and cDCs2, defined as $CD172a^{+}CD11b^{+}$ in mice and $CD1c^{+}CD172a^{+}$in human. [173]

The steady state heart is populated by pDCs, cDCs, a pre-cDCs subset and a population of monocyte-derived DCs (moDCs). [174] In homeostatic condition DCs are essential to maintain peripheral tolerance to the heart. Indeed, IRF8-dependent cDC1 are able to present cardiac self-antigen in the heart draining lymph nodes stimulating myosin-specific Treg development. [175] After myocardial infarction in mice, cDCs and moDCs populations increase in number. [175] In a mouse model of genetic cDCs depletion , improved cardiac function, reduced fibrosis and immune cells infiltration, including macrophages, neutrophils and T cells were observed after MI. [174] cDCs2 are migrating to the lymph node promoting autoreactive priming of Th1/Th17 T cells response. [175] Injection of tolerogenic DCs in mice induced Tregs systemic activation (in heart, spleen, inguinal and mediastinal lymph node) and pro-reparative macrophage responses, increasing cardiac function, improving survival and promoting angiogenesis. [176] Although cDCs depletion in mice ameliorated adverse remodeling after MI, cDCs comprise heterogeneous subsets that exert different function. [174] For instance, cDCs1 are able to “cross-prime” both CD4+ helper and CD8+ cytotoxic T cells. [177] Indeed, cross-priming inhibition in *Clec9a*-knock out mice exacerbated adverse remodeling after MI reducing collagen deposition and cardiac function, pointing out that not all cDCs subset are deleterious for the healing myocardium. [178] In line with this finding, decreased dendritic cells infiltration is associated with impaired collagen deposition and development of cardiac rupture in human after MI. [179]

2.2.2.2.2 T and B lymphocytes

T cells and B cells are immune cells of the adaptive immune system. They carry unique antigen receptors (T-cell receptor (TCR) for T cells and B-cell receptor (BCR) for B cells) generated by random somatic recombination.

T cells activation takes place in the secondary lymphoid organs (such as lymph node and spleen) and is mediated by antigen-presenting cells (like dendritic cells, monocytes, macrophages, and B cells) that internalize the antigen and present it to the TCR via the major histocompatibility complex (MHC) class I and class II molecules.[180] Once activated, T cells secret IL2 inducing their expansion and differentiation and, eventually, migrate from the lymph node to the target organ where they exert specific functions.

Flow cytometry data showed infiltration in the heart of mature B cells, conventional and unconventional T cells peaking at day 7 after MI. They also showed activation and proliferation of CD4+ T and T regulatory (Treg) cells in the heart draining lymph nodes. Conventional CD4+ T cells in the infarcted heart are mainly Th1 polarized, while Th17 and Th2 T cells are hardly detectable.[181–184]

First studies on the role of the different T cells subsets in a mouse model of ischemia/reperfusion injury showed that CD4+ T cells, but not CD8+ T cells, contribute to myocardial ischemia injury after 60 minutes of reperfusion.[185] On the contrary, more recent works better defined the role of CD4+ T cells in cardiac remodeling, showing in CD4+ knock-out (KO) mice increased left ventricular dilation, impaired neovascularization and collagen deposition, and increased infiltration of proinflammatory monocytes, suggesting a protective role of CD4+ T cells probably via modulation of the innate immune response. [186] Several studies illustrate that especially Tregs play a beneficial role after MI. Tregs ablation experiments, using cell mediated depletion approach or specific knock out mouse model, revealed increase in neutrophils and pro-inflammatory Ly6C^{hi} monocytes infiltration in the heart enhancing the pro-inflammatory milieu leading to left

ventricular dilation. [125,126,181] Also Treg drive macrophage towards a pro-repair phenotype. [181]

Cytotoxic CD8+ T cells infiltrate in the heart after MI. Genetic CD8+ T cells deficiency increased neutrophils and macrophages recruitment, delayed necrotic tissue removal and poor scar formation. Nevertheless, these mice display increased survival and cardiac function. [187] Poor scar formation in CD8+ T cells deficient mice show increased cardiac rupture events compared to wild type mice, suggesting that CD8+ T cells contribute to both cardiac repair and damage after MI. [187] A more recent work using antibody mediated depletion of CD8+ T cells and CD8+ T cell transfer experiments in mice and pigs suggested a pathogenic role of CD8+ T cells after myocardial infarction, and revealed that the deleterious effect of CD8+ T cells is due to release of Granzyme B. This work also showed that high level of circulating Granzyme B was detected in patients with acute MI and positively correlate with increased risk of death at 1-year follow-up. [188]

B cells deletion in KO mice or via antibody-mediated depletion showed reduced infarct size and left ventricular dilation, suggesting a pathogenic role of B cells. [189] Moreover, in these mice models lower levels of the chemokine CCL7 were detected, which is associated with less pro inflammatory Ly6C^{hi} monocytes infiltration presumably because of increased retention in the bone marrow. [183] In contrast, intramyocardial injection of isolated bone marrow B cells reduced apoptosis and improved cardiac function after MI, suggesting a possible protective role of B cells. [189] In depth analysis of the B cell population in the infarcted heart using scRNA-seq highlighted the infiltration of a heart-specific B cell subset recruited via the CXCL13-CXCR5 axis and contributing to local TGFβ production. [190] Nevertheless, in CXCR5-deficient mice and in mice treated with a neutralizing antibody for CXCL13, the ligand of CXCR5, no improvement in cardiac function was observed despite reduced B cells infiltration and TGFβ levels in the infarcted heart. [190] Spleen marginal zone B cells were recently shown to promote adverse remodeling by increasing inflammatory monocyte mobilization via upregulation of the monocyte chemoattractant CCL7. [191] Furthermore, B-cell produced antibodies were shown to play a detrimental role in cardiac remodeling after MI. [192] Indeed, mice in which antibody production is impaired exhibited improved cardiac function that correlated with

a decrease in transcripts known to promote adverse remodeling, such as MMP9, collagenase type I and III, and IL6. [192]

2.2.2.2.3 γδT cells and Innate lymphoid cells

Unconventional γδT cells are lymphocytes that have a γδ TCR. They represent 0.5-10% of circulating lymphocytes in humans and mice, and they are residing in specific tissue sites, such as skin, intestine, liver, and lungs. [193–198]

γδT cells infiltrate in the myocardium at day 7 after MI.[199] γδT cells are the major IL17 producing-cells in the infarcted heart. In IL17A KO mice, survival and left ventricular dilation was improved over 28 days after MI. Moreover, decreased inflammation was described in these mice, reducing neutrophils and monocytes infiltration and their ability to produce inflammatory cytokines, suggesting a deleterious role of γδT cells via IL17A-mediated modulation of the innate immune response.[200]

Innate lymphoid cells (ILCs) arise from common lymphoid progenitors but, unlike T cells, they are activated by stress signals, microbial compounds, and cytokines from the microenvironment rather than antigens. [201] They are also divided in 3 groups based of the cytokine profile of the classical CD4+ T helper cells: ILC1s, ILC2s, and ILC3s. [201] In experimental MI, ILC2s depletion decreased mice survival, heart function, collagen deposition and increased infarct size. [202] Moreover, ILC2s isolated from pericardial adipose tissue after MI showed enrichment of the IL2 pathway. [202] Infarcted mice treated with IL2 showed improved cardiac function and reduced infarct size. [202]

2.2.2.2.4 Neutrophils

Neutrophils are the most abundant granulocytes, and they are part of the innate immune system. They originate from the common myeloid progenitors (CMPs) in the bone marrow that differentiate in granulocyte macrophage progenitor (GMP). [203–208] Granulocyte colony-stimulating factor (G-CSF) is the main growth factor initiating the differentiation processes from GMP to mature neutrophils (**Figure 3**). [209–212] Three different intermediate populations of unipotent neutrophil progenitors are described in humans and mice from the GMP to mature neutrophil stage: an early neutrophil progenitor stage, followed by a preneutrophil stage, and lastly with the immature neutrophil stage. [205,208,213] These neutrophil precursor stages rapidly differentiate into mature neutrophils, and these processes involve several transcription factors, such as PU.1, C/EBPα, or GFI1 (**Figure 3**). [214] Neutrophils are also produced in extramedullary organs. Indeed, neutrophils progenitors can be found in the spleen. [215]

Retention of neutrophils in the bone marrow is mediated by CXCL12-CXCR4 signaling, in which CXCL12 produced by bone marrow stromal cells provides a retention signal for neutrophils through activation of CXCR4 expressed on neutrophils. [216] During tissue injury or infection, neutrophils are produced through emergency or reactive granulopoiesis in the bone marrow or via extramedullary hematopoiesis in the spleen. [217] Their mobilization into the circulation is mediated by the CXCL1/2-CXCR2 signaling. [216]

In the steady state, mature neutrophils are present in the blood in two ways: circulating, or residing intravascularly in certain tissues (named marginated neutrophils). [218] Marginated neutrophils can be found in liver, spleen and bone marrow. [219] *In vivo* labeling revealed that the life span of neutrophils in circulation is around 5 days in human and 18 hours in mice. [220] However, neutrophils half-life can variate under different inflammatory condition, such as presence of cytokines, growth factor and LPS, hypoxia and viral infections. [221–225]

Different studies in mice described two subsets of blood neutrophils, named “young” and “aged”, which are controlled by circadian oscillations. [226] Aged neutrophils peak during the day and they are expressing low level of CD62L ($CD62L^{low}$), while young nonaged neutrophils express high level of CD62L ($CD62L^{high}$) and they peak in the circulation during the night. [226,227] The ageing process has been proposed to favor neutrophils clearance, while other studies reported that aged neutrophils are the most rapid to

infiltrate to the sites of inflammation. [226,228] Changes in CD62L expression in neutrophils according to the circadian cycle were detected also in human blood. [226,229] Aged neutrophils home back to the bone marrow, spleen or liver for clearance. [230,231]

Upon infection or tissue damage, neutrophils rapidly migrate to the target organs thank to release of inflammatory chemokines, such as CXCL1 and CXCL2. [232] Moreover, PAMPs and DAMPs can also directly interact with PRRs expressed in neutrophils to induce their recruitment. [233] Once activated, they switch on a wide range of effector mechanisms, such as phagocytosis, production of ROS, and neutrophil extracellular traps (NETs). [234] Regarding tissue injury, neutrophils have always been associated to cause tissue damage by amplifying the inflammatory response or releasing cytotoxic effectors. [235] However, neutrophils can also promote tissue repair by performing phagocytosis and releasing growth or pro-angiogenic factors.[235]

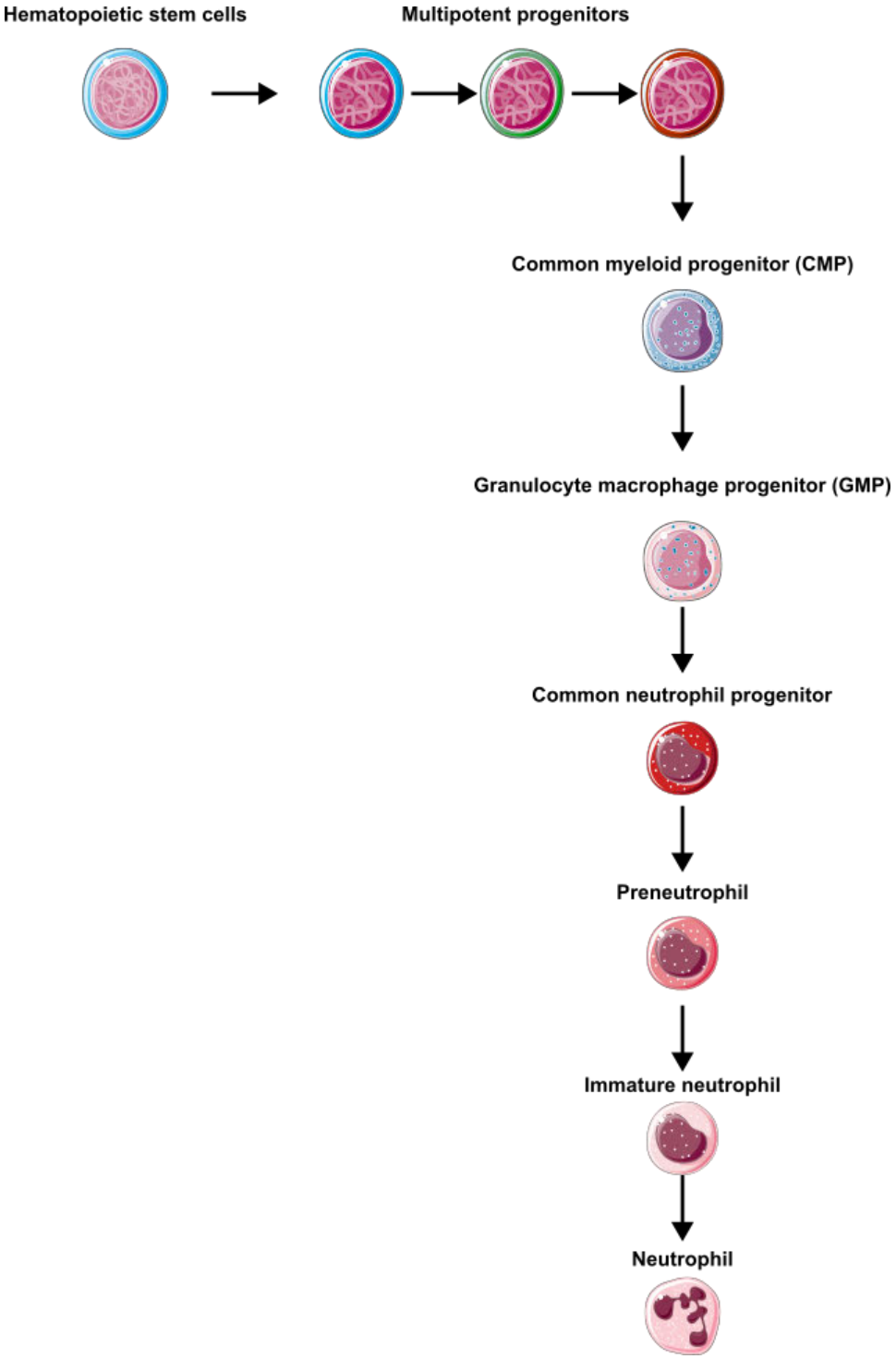

Figure 3: **Neutropoiesis.** Neutrophils originate in the bone marrow following a series of commitment states. The hematopoietic stem cell progenitor differentiates into several multipotent progenitor cells, giving rise to common myeloid progenitors (CMP) and then to granulocyte-macrophage progenitors (GMP). From the GMP state neutrophil commitment starts with the generation of the common neutrophils progenitor that goes under the maturation process, generating a pre-neutrophil state followed by the immature neutrophils state. Mature neutrophils are then produced. Images are taken from Servier Medical Art (smart.servier.com) and arranged with Inkscape.

2.2.2.2.4.1 Neutrophil heterogeneity

Neutrophils have long been considered as a homogeneous terminally differentiated cell population with a conserved function. However, neutrophil heterogeneity is starting to be appreciated and many nomenclature definitions have been proposed.

In healthy subjects, several blood neutrophils subsets were described: CD177+ neutrophils, olfactomedin-4+ neutrophils, a subset of neutrophils expressing variable TCR-like immune receptors (TCRαβ), and a $CD49d^{+}CXCR4^{+}VEGFR1^{+}$. [236–242] CD177 is a receptor required for surface presentation of proteinase 3, which mediates transendothelial migration of CD177+ neutrophils. [241,243] Olfactomedin-4 is expressed in 20-25% of human blood neutrophils, and in mice enhances bactericidal capacity against *Staphylococcus aureus*. [238,240] $CD49d^{+}CXCR4^{+}VEGFR1^{+}$ neutrophils are able to interact with VEGFR2 expressed on endothelial cells and their interaction is required for Vascular endothelial growth factor A (VEGF-A)-induced recruitment of circulating neutrophils during skeletal muscle hypoxia, supporting angiogenesis. [244] TCRαβ neutrophils are around 3-5% in human, but their functions remain still unknown. [245] As previously mentioned (see **1.2.2.2.4 Neutrophil**), neutrophils are also classified based on expression of specific aging markers. [231]

A more recent work employed scRNA-seq on human blood neutrophils to characterize their heterogeneity. [246] In steady sate condition, peripheral blood contained three distinct transcriptional neutrophils states named: PMNa, PMNb, and PMNc. [246] Although PMNc subset express high aging score comparing to PMNa and PMNb, the latter also express aging markers, albeit at lower level, suggesting that these three neutrophils subsets might undergo two distinct aging processes. [246]

Gradient density centrifugation of blood from patients with acute or chronic inflammatory diseases revealed neutrophils enriched in two phases named: “low-density” neutrophils (LDNs) and “normal-density” neutrophils (NDNs). [247] LDNs include immature and mature cells that are described to have an immunosuppressive role in cancer, pregnancy,

infections and systemic inflammation, while a pro-inflammatory role in autoimmune diseases. [248–251] NDNs represent the neutrophils obtained after red blood cell lysis without performing any density gradient centrifugation. [247,250,252]

During inflammation, neutrophils sense and respond to various PAMPs and DAMPs, integrating these signals which induce phenotypic and functional changes.[253] For instance, LPS administration to healthy volunteers showed increase of $CD16^{dim}$ neutrophils with impaired antimicrobial function and a mature CD16+ neutrophil subset with the ability to suppress T cell response and proliferation. [254,255]

Similar to macrophages, a N1/N2 neutrophil classification has been proposed. [256,257] A "N1" neutrophils population is characterized by hypersegmented nuclei, production of inflammatory cytokines, and a potent tumor killing capacity, while a N2 subset is defined with an immature phenotype, increased arginase activity and promote tumor growth. [257]

In a mouse model of lung cancer, neutrophils expressing high level of SiglecF with tumor-promoting functions, such as active production of ROS and upregulation of angiogenesis-related gene, were described. [258] We also found in the context of MI infiltration of $SiglecF^{hi}$ neutrophils in the ischemic heart (**Chapter 3**)

2.2.2.2.4.2 Neutrophil heterogeneity in the infarcted heart

In response to ischemic heart damage, neutrophils mobilize from the bone marrow and infiltrate the heart tissue. [3] Isolated neutrophils at Day1, 3, 5, and 7 after MI showed dynamic changes of their proteome profile. [259] Day1 neutrophils showed a pro-inflammatory profile and have increased degranulation and MMP activity. Day3, Day5, Day7 neutrophil showed increase in proteins involved in extracellular matrix organization (e.g. fibronectin, fibrinogen, galectin-3), suggesting a role in supporting scar formation by stimulating extracellular matrix reorganization. [259]

Yonggang et al. described two distinct neutrophil subsets in the heart after MI. One was named N1, defined as Ly6G+CD206-, while the other was named N2, defined as

Ly6G+CD206+. [260] N1 neutrophils represent more than 80% of the total neutrophils in the heart and are enriched in pro-inflammatory markers, such as *Ccl3*, *Il1b*, *Il12a*, and *Tnfα*, while N2 are increasing in number over 7 days and they are enriched in anti-inflammatory markers, like *Cd206* and *Il10*. [260,261] Correlation analysis revealed that N1 neutrophils are associated with infarct wall thinning. Moreover, N2 neutrophils were not found in the peripheral blood, suggesting that N2 phenotype is acquired in the ischemic heat (**Figure 4**). [261]

In this thesis, we used single-cell RNA sequencing (scRNA-seq) techniques to better define neutrophils heterogeneity in the heart after MI, see **Chapter 3**.

2.2.2.2.4.3 Neutrophils in cardiac injury and repair

Large amount of neutrophils infiltrates the ischemic heart within few hours after ischemic damage (**Figure 2**). [262,263] DAMPs and alarmins released by damaged cells are recognized by cardiac resident macrophages and by the endothelium, initiating neutrophil recruitment. [264] Infiltrating neutrophils phagocyte dead cell debris caused by the ischemic damage. However, they also release ROS, proteolytic enzymes, and inflammatory mediators contributing to cardiac injury. Additionally, they produce NET and release extracellular vesicles (EV) that contain a high amount of inflammatory mediators (**Figure 5**). [265,266] Several evidence also showed a beneficial role of neutrophils in cardiac repair, promoting anti-inflammatory response, angiogenesis, and pro-reparative effects. [262,264,267]

2.2.2.2.4.4 Neutrophils promote cardiac injury

Clinical and experimental studies associated neutrophils infiltration with worsening of cardiac healing. Indeed, high circulating neutrophils correlate with increased infarct size, sudden death, and heart failure development. [262,267] Neutrophils depletion or inhibition

experiments reduced cardiac injury and infarct size in experimental MI, supporting the evidence that neutrophils have deleterious effect. [268–271]

Active neutrophils in the ischemic heart produce a large amount of ROS through a process called respiratory burst, that is mediated by Nicotinamide adenine dinucleotide phosphate (NADPH). ROS are responsible to induce tissue injury and to promote release of pro-inflammatory cytokines.[272–274] Neutrophils also release a wide range of granular proteins, such as Myeloperoxidase (MPO), serine proteases, and MMP. These proteins promote cardiomyocyte death and extracellular matrix degradation (ECM) supporting tissue damage after MI. Moreover, neutrophils secrete cytokines (such as TNF-α, IL1β, and IL8) and chemokines (such as CXCL1, CXCL2, CXCL3, and CXCL8), exacerbating inflammation and adverse remodeling. [27,275,276]

Neutrophil extracellular traps (NETs) are detected in patients with acute MI and they positively correlate with cardiac events, increased infarct size and cardiac dysfunction. [277–280] A report showed that plasma thrombin is responsible for NET generation via platelet activation, contributing to fibrin deposition and formation of fibrin network, suggesting that NETs might be involved in MI occurrence. Supporting this hypothesis, PAD4 deficiency or pharmacological inhibition reduced NET formation, inflammation, cardiomyocyte apoptosis, and improved cardiac function in experimental MI. [281,282]

Neutrophils are produced by granulopoiesis in the bone marrow, and, upon MI, their production is enhanced. [281,282] DAMPs and inflammatory cytokines, and also neutrophils themselves, can induce granulopoiesis. [283–285]Neutrophils recruited in the infarcted heart release the alarmins S100A8/A9, stimulating IL1β secretion by neutrophils. IL1β enters in the circulation and binds with its receptor expressed on hematopoietic stem cells in the bone marrow, promoting granulopoiesis. Disruption of S100A8/A9 and inhibition of downstream signaling cascade inhibit granulopoiesis and improve cardiac function after MI. [283] In hypokalemia condition, neutrophils increased cardiac arrythmias in a lipocalin-2 (LCN2)-dependent manner in infarcted mice, while in human neutrophilia is associated with tachycardia in MI patients. [286]

2.2.2.2.4.5 Neutrophils promote cardiac healing

On the other hand, several evidence show that neutrophils are required for a proper healing after MI.

One of the main function of neutrophils is the phagocytosis of necrotic myocardium and cellular debris. [287] Phagocytosis by neutrophils is initiated by the interaction between neutrophil integrins and cellular debris, leading to an increase in intracellular calcium and calpain activation. Activated calpain induces its translocation to the cell membrane and contributes to the formation of the phagocytic cup. [287] Moreover, p81 cleavage by calpain creates a space between the F-actin protrusions and the F-actin membrane which increases neutrophil membrane size and allows neutrophils to engulf cellular debris. [287]

After fulfilling their role, neutrophils are removed from the tissue mainly by apoptosis. [288,289] Apoptotic neutrophils expose phosphatidylserine on the cell surface, which is recognized by macrophages initiating neutrophils clearance by efferocytosis. [288,289] Lipid mediators and proteins, like Lipoxin A4, resolving E1, and AnxA1, contribute to neutrophil apoptosis and promote their removal by efferocytosis. [290] Efferocytosis stimulates macrophages to produce anti-inflammatory and pro-resolving mediators, like TGF-β, IL10, VEGF, and specialized pro-resolving mediators, supporting inflammation resolution and cardiac repair. [291–294] Moreover, apoptotic neutrophils prevent the binding of inflammatory mediators from viable cells by acting as scavenger cells. [295–297] Delays in neutrophil apoptosis and persistent neutrophil response cause tissue damage and exacerbate inflammation, as it was shown in human acute coronary syndromes. [288,298]

Neutrophils also contribute to macrophage acquisition of a pro-reparative phenotype.

Indeed, in neutrophil-depleted mice macrophages displayed low expression of MerTK, a receptor involved in clearance of apoptotic cells, leading to reduced cardiac function, increased fibrosis and accumulation of apoptotic cells. [299] In the same work, LCN2 was suggested as a key inducer of pro-reparative macrophage phenotype. [299] Several reports showed that short-term blockade of S100A9 exert beneficial effect in myocardial repair and function. In details, S100A9 contributes to monocyte transition towards a reparative macrophage phenotype, promoting clearance of dead cells and debris. [300]

Angiogenesis is a critical process for a proper wound healing after MI. *In vitro* studies showed that adenosine induces macrophages to produce VEGF, an important growth factor necessary for angiogenesis. [301] It was shown that activated neutrophils produce and release adenosine. Moreover, they also release adenosine triphosphate (ATP) after stimulation, providing a substrate for extracellular generation of adenosine. [302] Neutrophils are the primary source of AnxA1 in the infarcted heart, a protein that drive macrophages towards a pro-angiogenic phenotype. [301] These findings suggest that they might have an indirect role in angiogenic processes in the heart after MI.

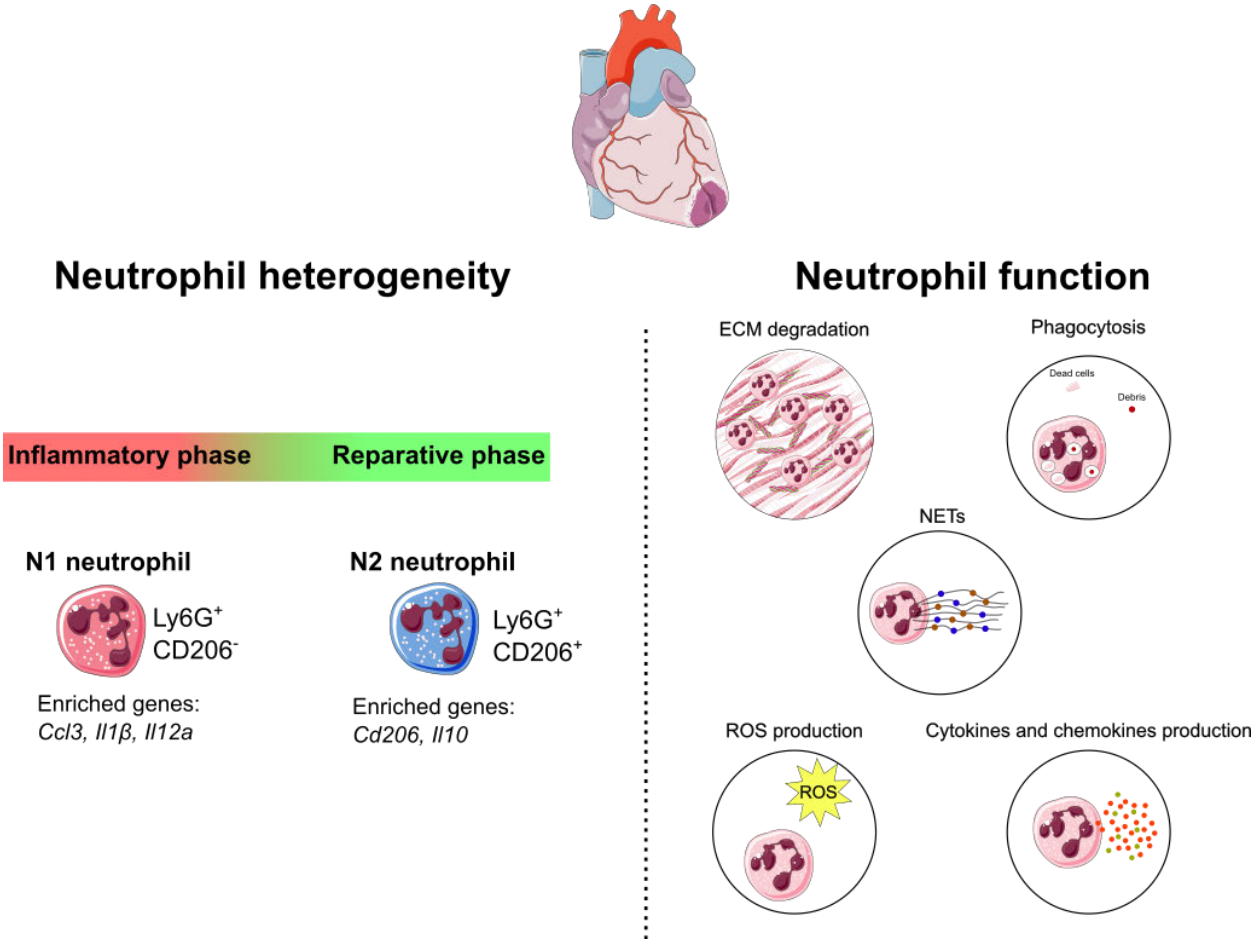

Figure 4: Neutrophils heterogeneity and function after myocardial infarction. Neutrophils infiltrate the infarcted heart within a few hours after ischemic damage. N1 neutrophils enriched in pro-inflammatory genes, such as *Ccl3*, *Il1β*, and *Il12a*, are infiltrating the heart during the inflammatory phase, while N2 neutrophils, enriched in anti-inflammatory genes, such as *Cd206* and *Il10*, are populating the heart during the reparative phase. Neutrophils performed a variety of functions in the infarcted heart, supporting both tissue damage and repair. For instance, neutrophils produce cytokines and chemokine, reactive oxygen species (ROS) and neutrophil extracellular traps (NETs), are involved in extracellular matrix (ECM)

degradation and removal of debris and dead cells. Images are taken from Servier Medical Art (smart.servier.com*)* and arranged with Inkscape.

2.2.2.2.5 Monocytes and macrophages

2.2.2.2.5.1 Monocytes

Monocytes and macrophages are myeloid cells part of the mononuclear phagocyte system.

Monocytes are short-lived cells that develop in the bone marrow during a process called "monopoiesis". Pluripotent hematopoietic stem cells (HSCs) develop into multipotent precursors (MMPs) giving rise then to common myeloid progenitors (CMPs). CMPs commit to become granulocyte and macrophage precursors (GMPs), the progenitor cells giving rise to granulocytes. The classical hierarchical model of hematopoiesis states that GMPs commit to become monocyte-macrophage/dendritic cell precursors (MDPs) before differentiating in common monocyte precursor (cMoP), the cells giving rise to monocytes and macrophages. [303] However, scRNA-seq analyses revealed that monocytes could also be produced by GMPs and MDPs during inflammation (**Figure 5**). [304]

Monocytes exist in two main subsets: classical and non-classical monocytes. [305,306]

Classical circulating monocytes comprise over 90% of monocytes in human and ~50% in mice and are defined as $CD14^{+}CD16^{-}$ and $Ly6C^{hi}$, respectively. Upon inflammation, they egress from the bone marrow and extramedullary sites, such as the spleen, and transit to the target organ in a CCR2-dependet manner. Upon entering the tissue, they contribute to inflammation via direct effect, producing TNF-α and nitric oxide, or indirectly, by differentiating into macrophages and dendritic cells. Classical monocytes also activate T cells via antigen presentation. [307–309]

On the other hand, non-classical monocytes comprise less than 10% of monocytes in human and ~50% in mice and they are defined as $CD14^{+}CD16^{+}$ and $Ly6C^{lo}$, respectively. [308] They persist in the circulation and their role during inflammation is still not clear.

Human and murine non-classical monocytes express high level of CX3CR1 and this receptor is essential for their survival. [308,310,311]. They circulate in the blood and play a role in immune surveillance. [312,313] Non-classical monocytes patrol healthy tissues by crawling the endothelium in a LFA-1-dependent way. [312] Upon infection, they rapidly invade tissues via CX3CR1, initiating the immune response and differentiating into macrophages. [312]

Human and mouse monocytes differ in some surface markers expression. For instance, human monocyte can be identified by their HLA-DR expression, while only a portion of mouse monocytes expresses MHCII. [314] On the other hand, mouse monocytes, but not human monocytes, are characterized by PPARγ and phagocytic genes expression. [315]

During homeostasis, classical monocytes remain in the circulation for almost a day before infiltrating tissues and replacing a proportion of tissue resident macrophages ,or differentiate in non-classical monocytes in the circulation. [307,316,325,317–324] Although monocytes contribute to the tissue resident macrophage pool during adulthood, little or no monocyte engraftment have been observed in epidermis, central nervous system, and the alveolar space. [325–331] Moreover, different works showed that the majority of classical monocytes are recruited in the peripheral tissues in which they differentiate into monocyte-derived macrophages, especially during diseases, or become part of a reservoir of undifferentiated monocytes. [316,332] ScRNA-seq of mouse monocytes showed rather homogenous populations of both classical Ly6C^{hi} and non-classical Ly6C^{lo} monocytes. [333] However, in the same work two populations of Ly6C^{int} monocytes population were described: one characterized by CD209a and MHCII expression, while the other is described as an intermediate state of Ly6C^{hi} to Ly6C^{lo} differentiation state. [333] A Ly6C^{hi} monocyte subset with a neutrophil-like gene expression signature is described in both homeostatic and inflammatory condition. [304,334] Non-classical monocytes circulate in the blood approximately for 2 days in mice and 7 days in human, but their lifespan can change based on the microenvironment (e.g. CSF1 availability). [316,325] The transition from Ly6C^{hi} to Ly6C^{lo} monocytes is dependent on C/EBPβ, NR4A1, and KLF2. Indeed, absence of one of these three transcription factors lead to absence or reduced Ly6C^{lo} monocyte number. [335–337] Human monocytes are enriched in C/EBPβ and NR4A1 motifs, suggesting that classical to non-classical monocyte transition follows similar mechanisms

to the ones described in mice. [338] The proportion between classical and non-classical monocytes depends on many factors. For instance, mice treated with a bacteria peptide show a shift from Ly6C^{hi} to Ly6C^{lo} monocytes. [339] On the other hand, low concentration of TLR ligands stimulate monocyte mobilization from the bone marrow increasing circulating Ly6C^{hi} monocytes. [340] Non-classical monocytes are also increasing with age and exercise. [341,342]

Inflammation triggers a process defined as “emergency monopoiesis”. During this process, monocytes are produced in high quantity also bypassing the canonical MDP-cMoP-monocytes development. In fact, neutrophil-like Ly6C^{hi} monocytes deriving from GMP have been described under inflammatory conditions. [304] Moreover, segregated nucleus-containing atypical Ly6C^{lo} monocytes (SatM) have been described during inflammation. [343] During emergency monopoiesis monocytes are also released by the spleen and recruited to the injured tissue, such as in the vessel wall during atherosclerosis and in the heart after myocardial infarction. [344–346] Monocytes recruited in the inflamed tissue exert different functions. They are known to actively promote inflammation via producing inflammatory cytokines in many disease contexts. [323,347] Moreover, monocyte can differentiate in monocyte-derived dendritic cells and acquire antigen-presentation ability. For instance, mouse monocytes treated with IL-4 and CSF2 were shown to efficiently cross-present cell-associated antigen to CD8^{+} T cells. [348] Monocytes are also involved in tissue remodeling. For instance, in a model of liver injury, monocytes contribute to hepatic regeneration and neutrophil clearance. [349,350] Moreover, in a model of retina injury, monocytes contribute to retinal progenitor cells survival and proliferation by producing IL10. [351]

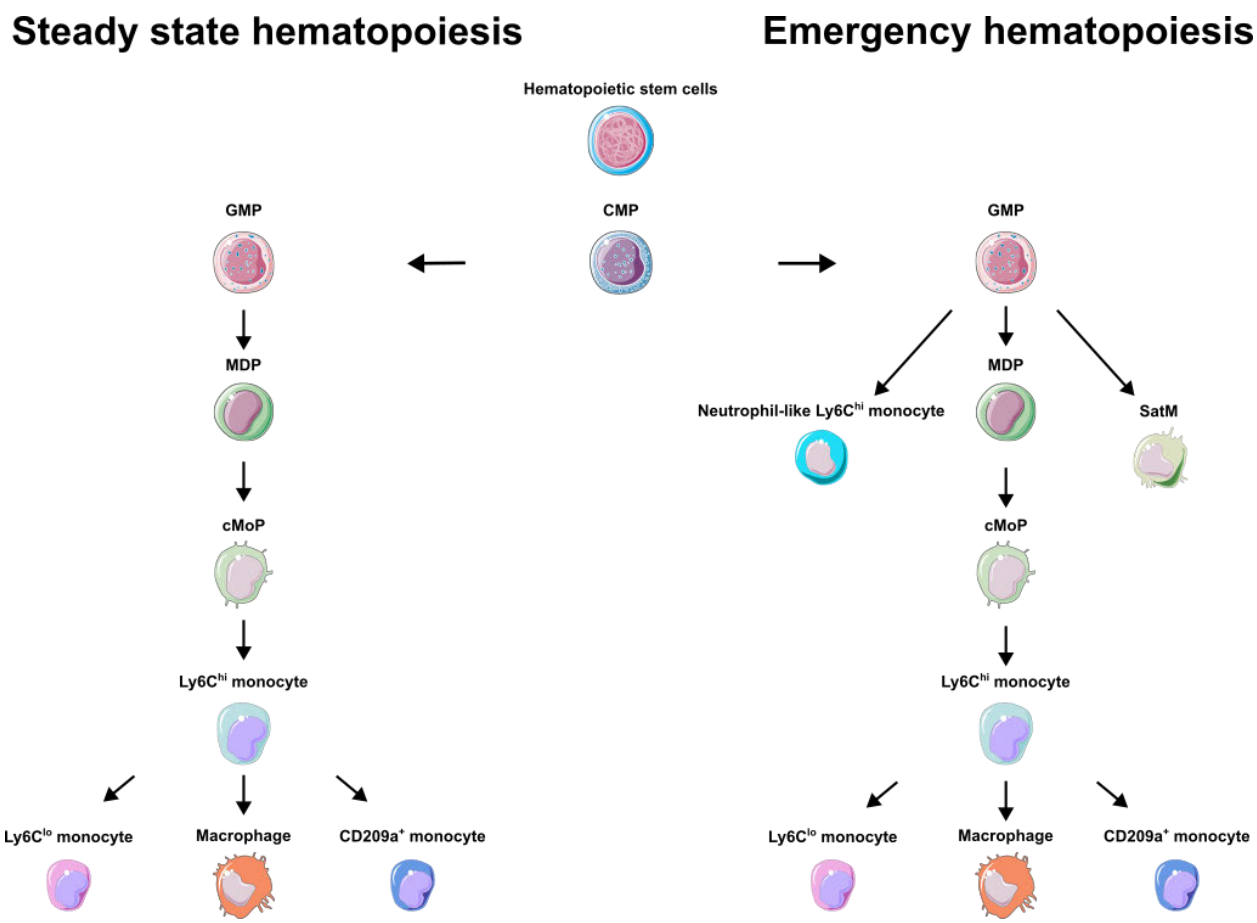

Figure 5: **Monopoiesis during steady state and emergency hematopoiesis.** Monocytes arise in the bone marrow from the hematopoietic stem cell progenitors. In the steady state (**left**), monocyte commitment starts from the GMP state that differentiates in monocyte-macrophage/dendritic cell precursor (MDP) and then in common monocyte progenitor (cMoP), giving rise ultimately to Ly6C^{hi} monocytes. Once mature Ly6C^{hi} monocytes enter the circulation, they differentiate in Ly6C^{lo} monocytes or CD209a+ monocyte, or, after infiltrating the tissue, they can differentiate in macrophages. During emergency hematopoiesis (**right**), monocytes are produced in high numbers and also bypassing the canonical MDP-cMoP-monocytes development. Neutrophils-like Ly6C^{hi} monocytes and segregated nucleus-containing atypical Ly6C^{lo} monocytes (SatM) are produced from the GMP precursor. Images are taken from Servier Medical Art (smart.servier.com*)* and arranged with Inkscape.

2.2.2.2.5.2 Macrophages

Macrophages are large phagocytes found in all tissues, where they exert a function of immunosurveillance and participate in normal tissue homeostasis.[352] Macrophages highly express CD68 in both mice and human, and F4/80 in mice. They are described as phagocytic cells, but further research highlights their role in many physiological and

pathological processes, such as cytokine production, phagocytosis, organ-specific homeostatic functions and the ability to coordinate the formation of granulation tissue. [353] Macrophages arise in two distinct ways: they develop from different progenitors during embryogenesis (giving rise to tissue-resident macrophages) or, mainly in inflammatory condition, via differentiation from monocytes (giving rise to monocyte-derived macrophages). Tissue-resident macrophages are mainly self-renewing in the tissue with restricted monocyte contribution to a few specific tissues and subsets.[354]

Macrophages develop during successive distinct waves during embryonic hematopoiesis and invade the developing organs before and shortly after birth (**Figure 6**). [355,356] In mice, at E7.0 a first primitive wave of hematopoiesis developing from the yolk sac occurs, giving rise to primitive erythroblasts, megakaryocytes, and macrophages. [357,358] A second wave of hematopoietic progenitors, named erythro-myeloid precursors (EMPs), with erythroid and myeloid potential, develop from the yolk sac between E8.0 and E8.5. [359] From E8.5 EMPs migrate to the fetal liver where they differentiate in different lineage of cells, including monocytes. [360,361] Moreover, at E8.5 a new wave of hematopoietic progenitor cells from the intraembryonic hemogenic endothelium give rise to fetal hematopoietic stem cells in the aorta, gonads, and mesonephros region. [362,363] At E10.5 these precursors cell migrate and invade the fetal liver where they establish definitive hematopoiesis. [362,363] Given that embryonic hematopoiesis is characterized by consecutives or parallel waves, macrophages can arise from different embryonic hematopoietic progenitors. For instance, microglia in the brain mainly originate from yolk sac macrophage progenitor, while in other tissue, such as Langerhans cells in the epidermis, alveolar macrophages in the lungs, and Kupfer cells in the liver, arise from both yolk sac macrophages as well as fetal liver monocytes. In tissues like the heart and the gut, monocyte infiltrate in the tissue and partially contribute to the resident-macrophage pool. [354]

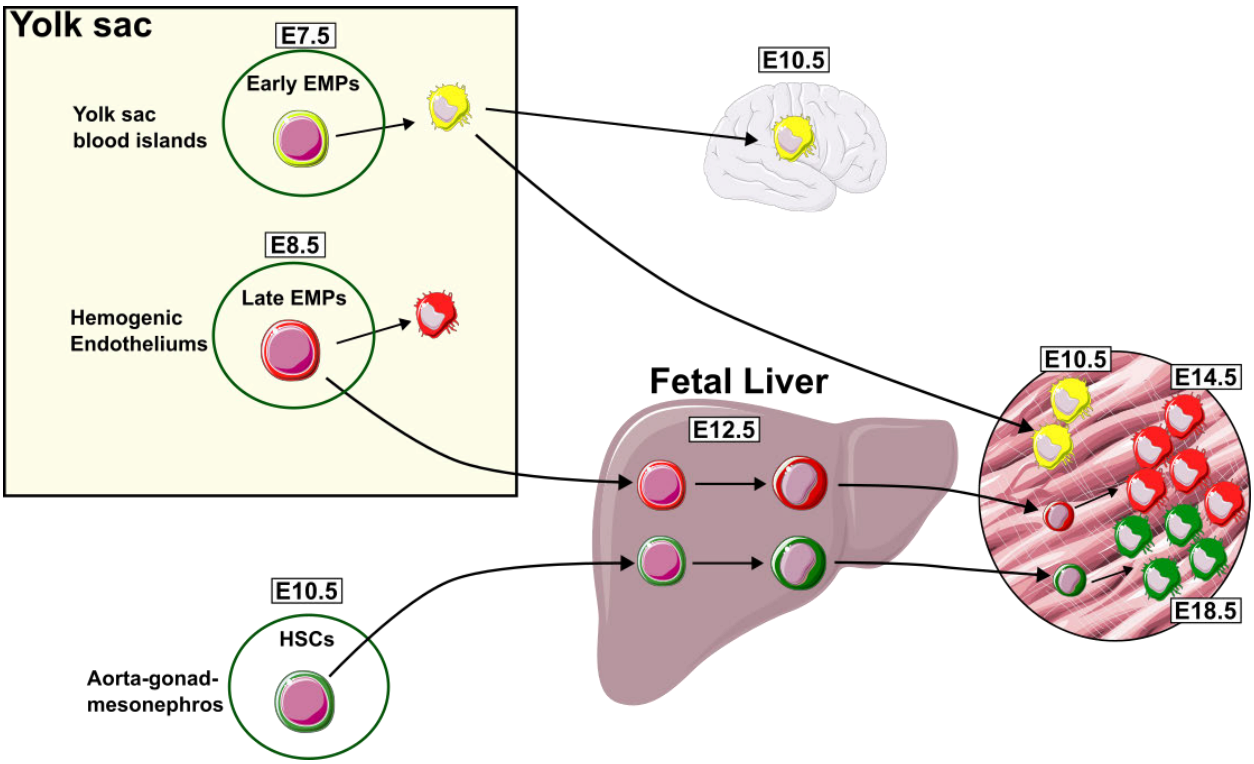

Figure 6: **Tissue-resident macrophage ontogeny.** Most of the tissue-resident macrophages originate during embryonic development and mainly self-renew in the tissue. Embryonic-derived macrophages develop in successive waves. A first wave starts at E7.5 in the Yolk sac, where early erythro-myeloid precursors (EMPs) generate macrophages that invade the developing tissue around E10.5, especially the brain. At E8.5 a second wave of late EMP invades the fetal liver where they differentiate in monocytes around E12.5. These monocytes are then invading the developing tissue and differentiate into macrophages around E14.5. At E10.5 a third wave comprises hematopoietic stem cells (HSCs) precursors that invade the fetal liver around E12.5, establishing definite hematopoiesis. Monocytes derived from HSCs in the fetal liver migrate to the developing tissue and differentiate in macrophages around E18.5. Images are taken from Servier Medical Art (smart.servier.com*)* and arranged with Inkscape. Figure re-adapted from Ginhoux F. et al, 2016. [354]

2.2.2.2.5.3 Macrophage Heterogeneity

Macrophages are plastic cells that can switch from one phenotype to another based on the stimuli they receive from the microenvironment, a phenomenon called “macrophage polarization”. [364,365]

Commonly, macrophages have been classified based on their *in vitro* response to cytokines stimulation. Based on this model, macrophages exist in two main subsets:

inflammatory M1 and anti-inflammatory M2 macrophages. [366–370] Stimulation of bone marrow-derived macrophages (BMDM) with IFNγ and TNFα, or with lipopolysaccharide (LPS) drive them towards M1 phenotype. These macrophages produce high levels of pro-inflammatory cytokines, such as TNFα, Il1α, IL1β, IL6, IL12, IL23 and cyclooxygnase-2 (COX-2). M1 macrophages have enhanced glycolytic pathway to sustain their rapid energy requirements and their increased demands for biosynthetic precursors used for the synthesis of pro-inflammatory cytokines.[371] On the contrary, BMDM polarize towards M2 phenotype by stimulation with IL4 and IL13, via STAT6 activation. [372,373] M2 macrophages have an anti-inflammatory cytokine profile, which is characterized by IL10 and TGFβ production. On the contrary to M1 phenotype, M2 macrophages mainly rely on oxidative phosphorylation.[371] M2 macrophages are also capable of "re-polarization", in which exposure with M1 stimuli leads to phenotypic switch towards M1 phenotype. The latter is also valid for M1 macrophages exposed to M2 stimuli.[353]

Macrophages are able to integrate multiple signals, such as microbes, damaged, dying and dead cells, cytokines, lipid mediators, etc… making the *in vitro* classification insufficient to describe their real heterogeneity.[353] Indeed, scRNA-seq together with fate mapping strategies revealed high heterogeneity in the macrophage pool in both health and disease. [334,374–376]. Macrophage ontogeny and normal tissue microenvironment are also influencing their function. Indeed, tissue-resident macrophage are involved in tissue homeostatic processes. [377] For instance, intestinal macrophages support immune tolerance against the microbiota and dietary products, while alveolar macrophages maintain gas exchange by carrying out the uptake and degradation of dead epithelial cells and debris preventing respiratory failure. [378,379] Another important consideration to make is that not all tissue-resident macrophages are embryonic-derived, but also adult monocytes contribute partially or totally to the resident macrophage pool. [354,377] For instance, microglia in the brain are known to have embryonic origin, self-renew in the tissue, and promote apoptotic neutrons removal and synaptic plasticity. [380,381] On the other hand, intestinal lamina propria macrophages are replenished by bone marrow-derived macrophages shortly after weaning, a process that continues during adulthood. [382] Kupffer cells are embryonic-derived macrophages residing in the liver that, upon liver injury, are partially replenished by adult monocytes. [377] Although some reports showed

similar behavior between embryonic-derived and monocyte-derived Kupffer cell, other studies described distinct functions raising the question that tissue-resident macrophage replaced by monocytes behave differently compared to the embryonic-derived counterpart. [383–386] A recent work employing scRNA-seq of isolated tissue-resident macrophages from different organs defined a conserved gene expression signature across tissues. They described three different subsets: TLF^{+} (expressing TIMD4 and/or LYVE1 and/or FOLR2) self-renewing macrophages; $MHCII^{hi}TLF^{-}$ macrophages renewed partially by monocytes; $CCR2^{+}TLF^{-}$ macrophages replaced entirely by monocytes. [376]

Macrophage function is also influenced in disease conditions and different types of macrophages can coexist at the same time. [353] For instance, scRNA-seq analysis of atherosclerotic plaque macrophages described diverse macrophage transcriptional states: a pro-inflammatory macrophage subset, resident-like macrophages, and foamy-$TREM2^{hi}$ macrophages. [374,387] In obese mouse adipose tissue three subset of macrophages have also been characterized: a resident-macrophage subset, and two $TREM2^{hi}$ macrophage subsets with a lipid-associated macrophage signature (LAM). [388] The $TREM2^{hi}$ LAM macrophage state was described in the last years in different disease contexts. [387,389–392] I will extensively discuss about this specific subset in another paragraph (see **Triggering receptor expressed on myeloid cells-2 (TREM2)**).

To summarize, macrophages are plastic cells that originate in a large part during embryonic development and seed the organs prior and immediately after birth, in which they contribute to tissue homeostasis. Monocytes produced during definitive hematopoiesis can to some extent and in an organ and macrophage subset-specific manner contribute to replenishment of tissue resident macrophage pools. During inflammation, monocyte-derived macrophages abundantly infiltrate tissues. Tissue microenvironment drives macrophages to specific phenotypes and, especially during diseases, different macrophage states with different function coexist at the same time. For these reasons, studying macrophage functional heterogeneity is challenging.

2.2.2.2.5.4 Origin of macrophages in the healthy and ischemic heart

Cardiac tissue resident macrophages (cRTMs) comprise 6-8% of non-cardiomyocytes cells in both human and mouse heart. [393,394] cRTMs consist of three different populations: $TIMD4^{+}Lyve1^{+}MHCII^{lo}CCR2^{-}$ macrophages, $TIMD4^{-}Lyve1^{-}MHCII^{hi}CCR2^{-}$ macrophages and $TIMD4^{-}Lyve1^{-}MHCII^{hi}CCR2^{+}$ macrophages. The $TIMD4^{+}Lyve1^{+}MHCII^{lo}CCR2^{-}$ subset mostly self-renew in tissue, while monocytes partially replenish the $TIMD4^{-}LYVE1^{-}MHCII^{hi}CCR2^{-}$ and fully replace the $TIMD4^{-}Lyve1^{-}MHCII^{hi}CCR2^{+}$ subset. [375] Fate mapping analysis using $Cx3Cr1^{CreERT2}$, $Csf1R^{CreERT2}$ and $Flt3^{Cre}$ mice described contribution of both yolk sac macrophages and fetal liver monocytes to the cRTMs pool. [325,331] In the neonatal heart, embryonic macrophages expand and differentiate in $MHCII^{hi}CCR2^{-}$ macrophages within weeks after birth. [319,395] $CCR2^{-}$ yolk sac macrophages have been described to promote coronary vessel formation and maturation in a IGF-1 dependent-manner. [396]

After MI, a large number of blood monocytes infiltrate the ischemic area within 30 minutes peaking between day 3 and 5 (**Figure 2**). [393] $Ly6C^{hi}$ monocytes are recruited in in the ischemic area from the bone marrow and spleen via MCP-1/CCR2 chemokine receptor interaction by a process named “emergency hematopoiesis”. [124,397–399] Emergency hematopoiesis is triggered during an inflammatory responses, in which pro-inflammatory factors, such as DAMPS and pro-inflammatory cytokines, reach and stimulate the hematopoietic stem cell niche in the bone marrow to proliferate and produce high amount of leukocytes, including monocytes. [400] Monocytes remain in the infarcted heart for about 20 hours and then they are cleared mostly by local cell death or differentiate into macrophages. [401] Nevertheless, their numbers in the infarcted heart are maintained extremely high due to infiltration of newly recruited monocytes. [401]

$Ly6C^{hi}$ monocytes are also mobilizing from the spleen. [399,401] Two different studies demonstrated that the majority of the heart infiltrating monocytes after MI are recruited from the splenic monocyte compartment. [399,401] Indeed, one of these studies showed activation of emergency hematopoiesis in the spleen, in which monocyte-dendritic cell progenitors (MDP) precursors cells significantly increase in number starting at Day3 and peaking at Day6 after MI. [401] Interestingly, considering that MI increases angiotensin II level in serum, it was shown that angiotensin II type-1 receptor promote monocyte

recruitment from the spleen, suggesting a connection between angiotensin II serum levels and splenic monocytes mobilization. [399] Another work highlighted that chronic heart failure in mice induces spleen remodeling by increased marginal zone and germinal center size, accompanied by increased number of cDCs, pDCs, $CD4^+$ and $CD8^+$ T cells, and decreased number of monocytes. [402] Moreover, splenectomy in heart failure mice improved pathological remodeling and improved cardiac function. [402] Although in this work the specific contribution of $Ly6C^{hi}$ monocytes in the healing processes after MI was not described, it definitely pointed out that splenic leukocytes are involved in adverse remodeling.

A study described the *in vivo* $Ly6C^{hi}$ and $Ly6C^{lo}$ monocytes function by injecting fluorescent probes to evaluate phagocytosis capacity, cellular matrix digestion, and cytokines and growth factors expression. [403] $Ly6C^{hi}$ monocytes displayed higher proteinase activity, suggesting higher extracellular matrix remodeling ability, and inflammatory cytokines production, such as TNFα. On the other side, $Ly6C^{lo}$ monocytes express high level of vascular endothelial growth factor (VEGF) and equal phagocytic capacity as $Ly6C^{hi}$ monocytes. [403] Although this work could evaluate monocytes function *in vivo*, their $Ly6C^{lo}$ monocytes gating strategy also included a macrophage population that can bias interpretation. [403] The transcription factor NR4A1 was shown to have an important role in dictating monocyte infiltration and macrophage phenotype. [404] Indeed, mice lacking NR4A1 display increased number of $Ly6C^{hi}$ monocytes and augmented inflammatory cytokines expression in macrophages in the heart after MI, and inability of $Ly6C^{hi}$ monocytes to differentiate into non-inflammatory macrophages. [404]

Mice lacking GM-CSF or its receptor showed decreased leukocytes infiltration, including monocytes, neutrophils and macrophages, accompanied by improved survival and enhanced cardiac function after MI. [405] In another work, atherosclerotic ApoE-deficient mice displayed enhanced pro-inflammatory gene expression, such as TNFα, and $Ly6C^{hi}$ monocytes recruitment in the infarcted heart after coronary artery ligation, associated with reduced cardiac function and increased ventricular dilation. [406] Lastly, increased infiltration of $Ly6C^{hi}$ monocytes together with increased cardiac rupture events and reduced cardiac function was described in ACKR2-deficient mice after MI. [155] Overall,

these data indicate that an increase of Ly6C^{hi} monocytes infiltration is generally associated with adverse myocardial remodeling after MI. [155,405,406]

Different regional zone can be delineated in the infarcted heart: the infarct zone, the peri-infarct zone (also called border zone), and the remote zone. [375] Within the infarct zone cRTMs are reduced due to cell death. In the peri-infarct zone cRTMs increase in number, while in the remote zone their numbers do not change but they transiently proliferate. [375,393] ScRNA-seq of immune cells isolated from normal and infarcted heart after 11 days showed replacement of the cRTM compartment by monocytes and four additional MI-associated macrophage clusters with distinct gene-expression profile and unknown function were described. [375] Moreover, single-cell transcriptome analysis of macrophages at day 4 after MI revealed the presence of an interferon inducible cell cluster, named "Interferon-inducible cells" (IFNICs). [407] These macrophages are enriched in expression of genes of the IRF3-IFN pathway, which detects cytosolic DNA and initiates an interferon response. A recent work described the presence of a macrophage subset in the pericardial cavity with a phenotype similar to serous cavity GATA6+ macrophages. [408] ScRNA-seq analysis of mouse heart at different time points after infarction described different macrophages transcriptional states populating the infarcted heart in a time-dependent manner. [334,409] My work is also focusing on defining macrophage functional heterogeneity using scRNA-seq, and I will discuss that extensively in **Chapter4**.

2.2.2.2.5.5 Functions of macrophages in the healthy and ischemic heart

cRTMs play a role in many physiological and pathological processes (**Figure 7**). In the steady state, cRTMs are able to phagocyte pathogens and apoptotic cells via TIMD4 or MerTK. [410–412] They are also involved in the electrical conduction of the heart, regulating cardiomyocytes membrane potential via connexin-43 gap junction connection. [394] Indeed, CD11b^{DTR} mice, a model of macrophage ablation, develop atrioventricular block. [394] cRTMs are also involved in maintaining cardiomyocytes homeostasis by taking up

material released in form of exophers derived from cardiomyocytes, which contain dysfunctional mitochondria and sarcomeric proteins. [413] Mice with cRTMs depletion or MerTk-deficiency showed accumulation of dysfunctional mitochondria in cardiomyocytes, impaired cardiac function, autophagy, and inflammasome activation. [413] In various inflammatory contexts (e.g., Lyme disease, viral myocarditis) macrophages can cause atrial fibrillation or arrhythmias. [414–416] In a mouse model of hypertension, upregulation of a reparative genes program in cRTMs was shown, in particular with elevated expression of insulin-like growth factor-1 (*Igf1*) that correlates with cardiomyocytes hypertrophy and with preservation of cardiac function. [417] Moreover, depletion of cRTMs in a mouse model of dilated cardiomyopathy induced increased mortality, impaired ventricular remodeling and angiogenesis, suggesting a role of cRTMs in cardiac healing. [418] In a similar way, increased fibrosis, hypertrophy, and decreased cardiac function and survival were described in a mouse model of cRTMs depletion after MI. [375]

After MI, cRTMs die and monocyte-derived macrophages are populating the infarcted heart. During the inflammatory phase, macrophages are involved in clearance of apoptotic cells, especially cardiomyocytes, and production of inflammatory cytokines, such as TNFα, IL1, and IL6 (**Figure 7**). [25,300] Global monocytes and macrophages depletion with clodronate-liposomes in infarcted mice decreased survival due to thromboembolic events, with decreased cardiac function and angiogenesis. [419] In the reparative phase, macrophages contribute to adaptive remodeling by releasing IL10 and TGFβ, which promote collagen production, fibrosis and angiogenesis. [420] Another paper corroborate the notion that macrophage contribute to cardiac fibrosis and scar formation. [421] Indeed, macrophages at Day7 after cardiac injury express gene related to collagen deposition, such as *Ctgf*, *Tgfβ3*, and *Serpine1*, and also express genes encoding collagen fibrillar isoforms (*Col1a1*, *Col3a1*), suggesting that they both indirectly and directly contribute to collagen synthesis in mice and zebrafish hearts. [421] Alternatively activated M2-like macrophages with a reparative role are described in mouse heart after myocardial infarction. [420] In this study, TRIB1-deficient mice showed selective depletion of M2-like macrophages, associated with reduced collagen deposition, fibroblast activation and increase cardiac rupture. [420]

A study performed RNA-seq in macrophages isolated at different time points after MI to assess changes in macrophage transcriptomic signatures. [422] According to their results, Day1 macrophages are enriched in pro-inflammatory and extracellular matrix degradation signature, Day3 macrophages displayed higher genes involved in proliferation, phagocytosis and mitochondrial function, and lastly Day7 macrophages are enriched in extracellular matrix remodeling and scar formation gene signature. [422]

$GATA6^{+}$ pericardial macrophages are also invading the myocardium, losing GATA6 expression and performing an anti-fibrotic function. Indeed, loss of GATA6+ macrophages in experimental MI enhances fibrosis. [408]

IFNIC macrophages play a detrimental role in the healing after MI. In fact, knockout mice for various component of the IRF3-IFN pathway (including cyclic GMP-AMP synthase (cGAS), STING, IRF3 and type I IFN receptor (IFNAR)) showed improvement of left ventricle size, contractile function, and survival. [407]

In a model of abnormal electrical conduction after MI, macrophages depletion exacerbate ventricular tachycardia and fibrillation. [286] Moreover, in mice lacking CD36 and MerTk, known receptors involved in efferocytosis, higher arrhythmia and mortality were described, together with increased cardiomyocytes death and mitochondrial dysfunction, suggesting that macrophage-mediated phagocytosis protect against MI-induced abnormal electrical conduction. [286]

Macrophages efficiently clear apoptotic cells from the damaged tissue, a process essential for inflammation resolution and tissue repair. [300,423–426] Indeed, blocking efferocytosis via MerTk deficiency in infarcted mice induced accumulation of apoptotic cardiomyocytes in the myocardium, delayed inflammation resolution, and reduced cardiac function and infarct size. [300,424] Other than MerTk, also milk fat globule epidermal growth factor-like factor 8 (Mfge8) is involved in the efferocytosis processes. [427] In fact, mice deficient for both MerTk and Mfge8 displayed accumulation of apoptotic cells with increased fibrosis, infarct size, and reduced angiogenesis. Moreover, MerTk and Mfge8-deficient bone marrow-derived macrophages have a lower efferocytosis capacity and VEGF-A production, a growth factor improving cardiac function and angiogenesis. [423] MerTk function is controlled by proteolytic cleavage via the generation of soluble MerTk. [428–430] Elevated serum levels of soluble MerTk were detected in mice and patients with

MI. In the same study, a mouse model in which MerTk is resistant to shedding showed improved cardiac function and reduced infarct size after MI. [424] Moreover, high expression of MerTk was observed in MHCII^{lo}CCR2^{-} cRTMs, which displayed increased pro-reparative cytokines production after efferocytosis. [424] Efferocytosis was also shown to promote macrophages IL10 production by enhancing mitochondrial β-oxidation thanks to apoptotic cell fatty acids availability. [425] Cardiac macrophages express high level of VEGF-C and apoptotic cell efferocytosis induces VEGF-C production in bone marrow-derived macrophages. [426] *Vegfc* deficiency specifically in murine macrophage led to increased inflammatory cells infiltration, such as neutrophils and Ly6C^{hi} monocytes, pro-inflammatory cytokines production, fibrosis, and reduced cardiac function after MI. [426]

The essential role of macrophages in cardiac remodeling after MI is highly demonstrated also in zebrafish and neonatal mice after cardiac injury. In fact, both zebrafish and neonatal mice are able to completely regenerate the injured heart with little or no fibrotic scar formation. [431,432] Cardiac cryoinjury in zebrafish induced massive cardiomyocytes death, transient fibrosis, followed by full regeneration of the heart. [433–435] Adoptive transfer of macrophages with *Col4a1* and *Col4a3bpa*-deficiency into zebrafish´s heart showed reduced scarring after cryoinjury, supporting the notion that macrophages actively contribute to collagen deposition and fibrotic processes. [421] The mouse neonatal heart can also fully regenerate after cardiac injury during the first 7 days after birth. Macrophage depletion in neonatal mice after cardiac injury induced fibrosis, reduced angiogenesis and cardiac function and impaired regeneration, suggesting that macrophages are essential to maintain a proper regenerative capacity in neonatal mice. [436] One study described the difference between neonatal and adult heart inflammation in response to injury, and demonstrated that neonatal heart injury generates minimal inflammation, with decreased recruitment of inflammatory cells and pro-inflammatory cytokines production, and promote cardiac recovery through cardiomyocyte proliferation and angiogenesis. [395] Moreover, injured neonatal heart show expansion of the embryonic-derived cardiac macrophage pool with small contribution from monocyte-derived macrophages compared to adult mice after cardiac injury. [395] Macrophages have a critical role in the heart regenerative processes also in other species. [437]

As I already mentioned, monocyte-derived macrophage heterogeneity is described in mouse heart after MI. [334,409] In particular, a macrophage subset highly expressing *Trem2* and displaying a “lipid-associated macrophage” signature populates the heart starting at Day3 after MI. [334,409] In this context, one focus of my thesis is to characterize the function of TREM2 in macrophages during adaptive remodeling after MI.

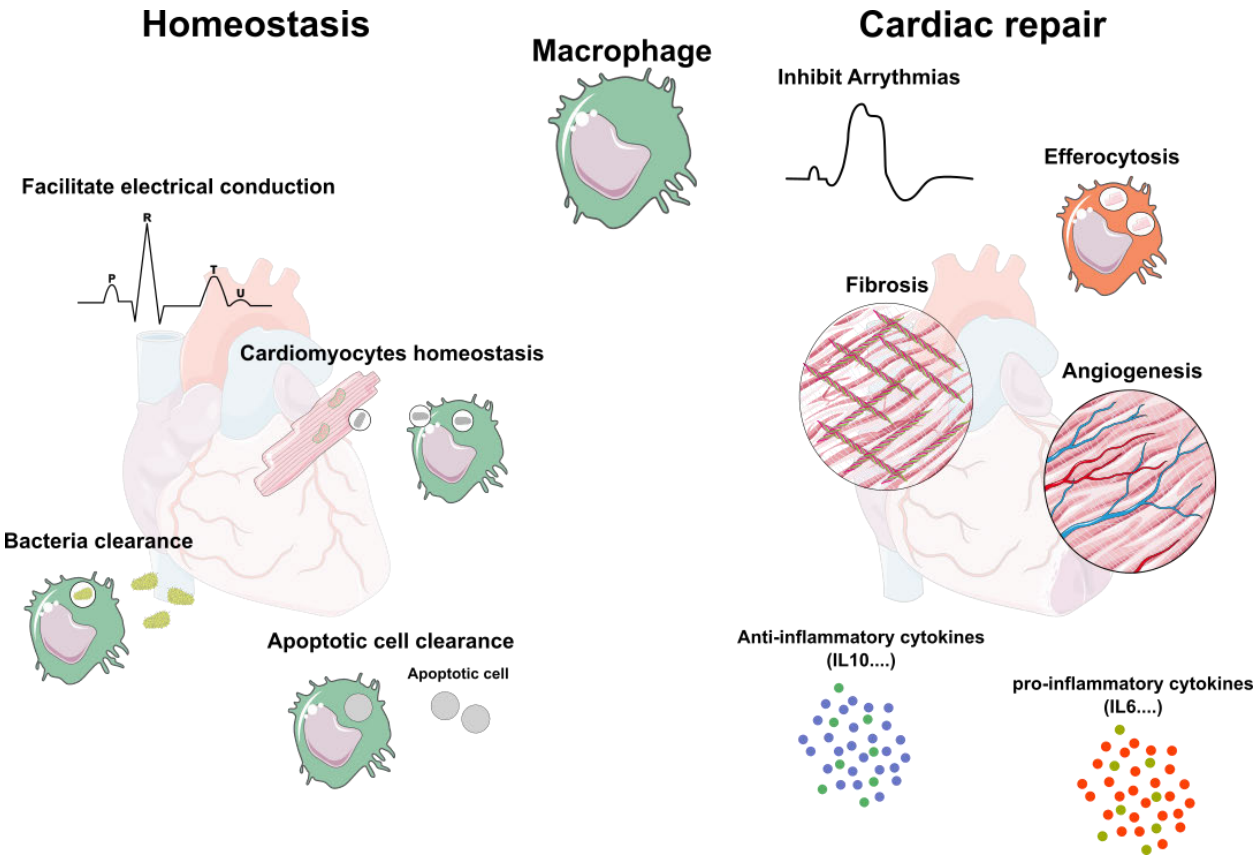

Figure 7: **Macrophage function in heart homeostasis and cardiac repair.** Macrophages play a crucial role in both cardiac homeostasis and repair after MI. In homeostatic conditions, macrophages actively contribute to tissue homeostasis by facilitating electrical conduction, maintaining cardiomyocytes homeostasis, and clearing bacteria and apoptotic cells. After MI, macrophages are involved in cardiac repair processes at different levels. They can both promote and shut down inflammation, prevent arrhythmia development after MI, clear dead cells from the microenvironment, and promote fibrosis and neovascularization. Images are taken from Servier Medical Art (smart.servier.com*)* and arranged with Inkscape.

2.3 Triggering receptor expressed on myeloid cells-2 (TREM2)

TREM2 is a transmembrane receptor of the immunoglobulin superfamily mainly expressed in macrophages. TREM2 ligands comprise a wide range of anionic molecules, such as bacterial products, DNA, lipoprotein, and phospholipids. [438] TREM2 receptor consists in four different parts: an extracellular domain with a V-type immunoglobulin domain, a short ectodomain, a single transmembrane helix, and a short cytosolic tail. Since the cytosolic tail lacks signal transduction motifs, TREM2 receptor is associated with two adaptor proteins, DNAX activation protein 12 (DAP12) and 10 (DAP10), via oppositely charged residues in their transmembrane domains. Upon TREM2 activation via receptor-ligand interaction, the co-receptors are phosphorylated inducing the intracellular signal transduction machinery recruitment. DAP12 induces activation of spleen tyrosine kinase (Syk), while DAP10 recruits phosphatidylinositol 3-kinase (PI3K). TREM2 can bind DAP12 or DAP10 and, in some cases, can build a TREM2-DAP12-DAP10 heterodimers. [439] Association with DAP12 and/or DAP10 is critical to determine the downstream signaling pathway. For example, *in vitro* studies in mouse macrophages have shown that DAP12 is required for Ca^{2+} mobilization, while DAP10 is necessary for activation of serine/threonine protein kinase (AKT1) and extracellular signal-regulated kinase (ERK) (**Figure 8**). [389,439,440]

Clinically, mutation and genetic variants of TREM2 leads to different neurodegenerative syndrome, such as Alzheimer's disease and Nasu-Hakola disease, and recent evidence also associated TREM2 with metabolic syndromes and cancer. [388,441,442]

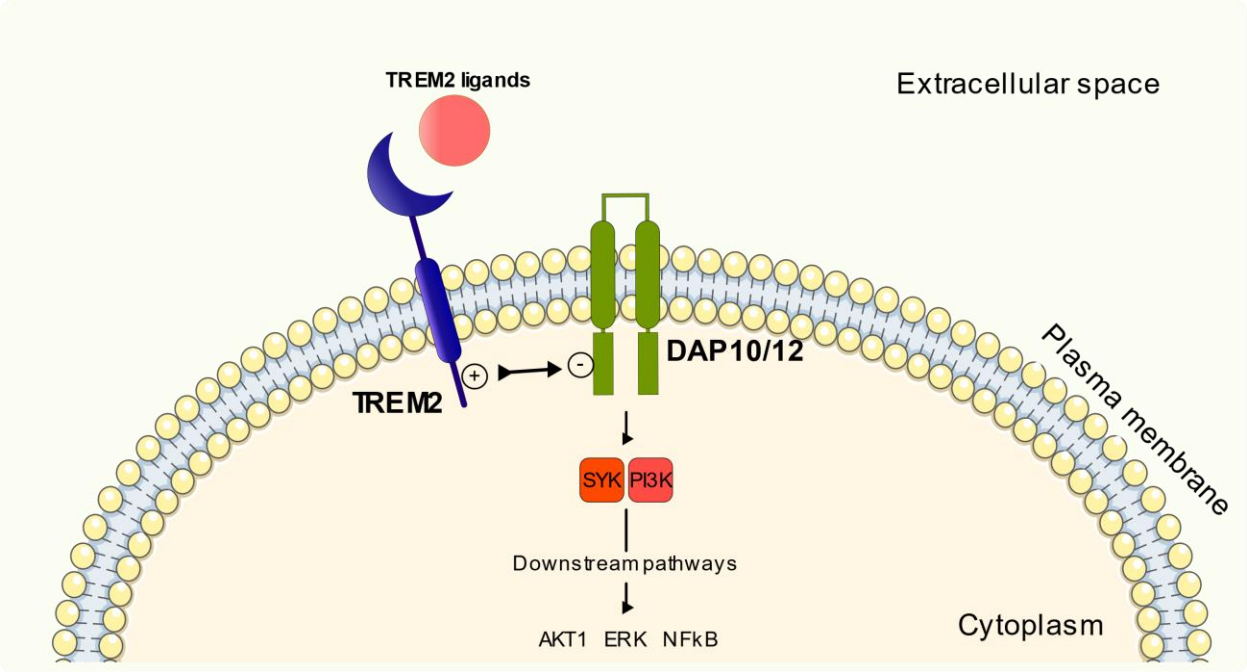

Figure 8: TREM2 signaling pathway. TREM2 interaction with its ligands induces activation of the protein kinases SYK and PI3K by the co-receptors DAP12 and DAP10 respectively, resulting in the activation of the downstream signaling pathways. Images are taken from Servier Medical Art (smart.servier.com) and arranged with Inkscape.

2.3.1 Regulatory mechanisms of the TREM2 signaling pathway

Since TREM2 is suggested to bind a wide range of molecules, the interaction with different ligands can modulate TREM2 signaling strength and direction. [438,439] For example, the immune receptor tyrosine-based activation motif (ITAM) of DAP12 is known to be activating signals, but studies in mice have shown that low-affinity/avidity ligands can promote partial DAP12 phosphorylation with recruitment of SH2 domain-containing protein tyrosine phosphatase SHP-1, which dephosphorylates downstream targets of Syk kinase resulting in cellular inhibition. [439] Moreover, the wide range of ligands complicates to predict which activation signal is activated. Some of these ligands are physiologically present in the body, such as lipoproteins and apolipoproteins, suggesting a constant activation of TREM2. After tissue damage or cell death additional molecules that interact

with TREM2 are released, such as LPS during bacterial infection or β-amyloid oligomers during Alzheimer's disease. [438,443,444] In a mouse model of Alzheimer's disease it was shown that microglia upregulate apolipoprotein E (APOE), a ligand of TREM2, resulting in its activation. [445] TREM2-deficient microglia have reduced expression of APOE. [445,446] In a similar way, in high-fat-diet induced obesity mouse adipose tissue, APOE expression increases in a TREM2-dependent manner. [388] These findings suggest a mechanism in which TREM2 activation promotes production of TREM2 ligands that sustain TREM2-dependent activation. [389,447]

The TREM2 signaling pathway might have parallel cellular processes responsible for its activation and regulation. For instance, TREM2 downstream signaling is influenced by the presence and availability of DAP12 and DAP10 that may change based on the cell type and activation state. [439,448–450] Moreover, the ITAM motif of DAP12 is also phosphorylated by activation of CSF1 receptor (CSF1R), suggesting that CSF1R activity might modulate TREM2 signaling pathway activation. [451,452] Supporting this idea, humans with a genetic background causing partial CSF1R activity show symptoms resembling to Nasu-Hakola disease, suggesting synergy between the TREM2 and CSF1R pathways. [453–455]

TREM2 signaling via DAP12 counteracts inflammatory cytokine production following TLR activation in cultured mouse macrophages, and, contrarily, LPS or IFNγ stimulation abrogate TREM2 expression. [456–459]

α-secretases-disintegrin, metalloproteinase domain-containing protein 17 (ADAM17) and ADAM10 are others regulator of TREM2, acting by cleaving TREM2 at the H157-S158 peptide and leading to the release of soluble TREM2 (sTREM2), resulting in a decrease of membrane TREM2 levels and thus blocking the TREM2 signaling pathway. [460–463]

Another TREM2 regulation mechanism is through controlling its expression levels. TREM2 expression is upregulated in a mouse model of Alzheimer's disease after PPARγ, PPARδ, liver X receptor (LXR) and retinoid X receptor (RXR) stimulation. [464,465] Moreover, TREM2 protein expression in mice has been suggested to be regulated also at post-transcriptional level by the microRNA mir-34a, which is expressed following NF-kB activation and is present at high levels in the brain of Alzheimer's disease patients.[466,467]

2.3.2 TREM2 and cellular mechanisms

Absence of TREM2 in mice or *in vitro* macrophages negatively impact phagocytosis of apoptotic cells, cellular debris, β-amyloid and bacteria. [468–470] On the same line, TREM2 overexpression in non-phagocytic cells induced bacterial, lipoprotein and cellular debris phagocytosis. [469,471] Phagocytosis via TREM2 seems to require membrane presence of its full-length form. Indeed, inhibition of TREM2 shedding boosted bacterial uptake in a model of microglia cell line. [468] Although several *in vitro* experiments suggested that TREM2 is involved in macrophage phagocytosis, another work showed that TREM2-deficient and wild-type microglia engulf apoptotic debris equally *in vitro*. [447] In an *in vivo* mouse model of demyelination, phagocytosis of myelin debris is not impaired in TREM2-deficient microglia, but lipid processing after phagocytosis in affected leading to cholesteryl ester and oxidized cholesteryl ester accumulation. [472] Accumulation of these molecules are found in Alzheimer's disease brain and in atherosclerotic plaques, two diseases in which TREM2 was suggested to play a critical role. [374,473,474] These findings suggest that TREM2 is definitely involved in phagocytosis processes, but the exact mechanisms remain poorly understood.

As mentioned earlier, TREM2 activation antagonize pro-inflammatory signals. [456–458] Indeed, several anti-inflammatory genes are expressed in macrophages in a TREM2-dependent manner, including Galectin-1, Galectin-3, IL1R antagonist (*Il1rn*), pro-granulin (*Grn*). [390,445] TREM2 is also counteracting immune-activation sensors of bacterial signals, like TLRs, by not only producing anti-inflammatory factors, but also shutting down pro-inflammatory signals. [456–459]

TREM2 promotes survival of cultured macrophages deprived of CSF-1 *in vitro*, and *in vivo* under stress condition. [447,448,475] Microglia deficient for TREM2 or expressing its dysfunctional variant T66M showed reduced glycolysis and low ATP level, suggesting that low survival might be caused by metabolic defects.[389,468] Confirming this hypothesis, reconstitution of ATP level in microglia under β-amyloid-mediated toxicity improved survival. [468]

TREM2 signaling is essential for osteoclast maturation. Indeed, TREM2-deficient mice showed reduced number of osteoclasts, and *in vitro* osteoclast precursors required TREM2 to maturate upon M-CSF treatment. [476] This finding could also explain why bone function is impaired in Nasu-Hakola disease patients. [450–452]

TREM2 is required for the induction of a specific gene expression pattern called disease-associated microglia (DAMs), a subset of microglia that occurs in several neurodegenerative diseases in mouse and is characterized by increase in phagocytic capacity and lipid metabolism-related pathways. [445,477] Similar gene expression pattern was described in TREM2 lipid-associated macrophages (LAMs) in obese mice adipose tissue, which form crown-like structure around adipocytes and this gene expression signature is also TREM2-dependent. [390] Computational analysis predicted that DAM program requires four transcription factors: basic-helix-loop-helix family member E40 (BHLHE40), RXR gamma (RXRG), HIF1α and microphthalmia-associated transcription factor (MITF). Between these, HIF1α is expressed in DAMs in a TREM2-dependent manner in a mouse model of Alzheimer's disease. [389,445]

2.3.3 Physiological role of TREM2

The role of TREM2 is widely studied in association with diseases, but its physiological role still needs to be fully investigated (**Figure 9**). As previously mentioned, TREM2 genetic variants in human develop diseases in which the most studied are the Nasu-Hakola disease and the Alzheimer's disease. The fact that these variants, especially in the Nasu-Hakola disease patients, develop a consistent variant-dependent phenotype, suggest that TREM2 might play an important role also in physiological conditions. Analysis of the Human Cell Atlas showed Trem2 expression in restricted niches, including microglia, osteoclast, adrenal gland and placenta macrophages. [478] While the role of TREM2 in adrenal gland and placenta is still unclear, extensive studies showed the role of TREM2 in microglia and osteoclasts.

TREM2 is important for myeloid cells survival and differentiation, as shown in osteoclasts isolated from Nasu-Hakola patients. [450–452] TREM2 in mice is also involved in synaptic pruning, a process of neuronal development in which microglia and astrocytes remove excessive synapsis via phagocytosis. [479] Additionally, TREM2 deficiency induces reduced synapses in 4-week-old mice, although later in life this defect is normalized. [480]

A TREM2+ macrophages subset is also found in the hair follicle niche, in which they promote quiescence of the hair follicle stem cells in an oncostatin-M (OSM)-dependent way. [481]

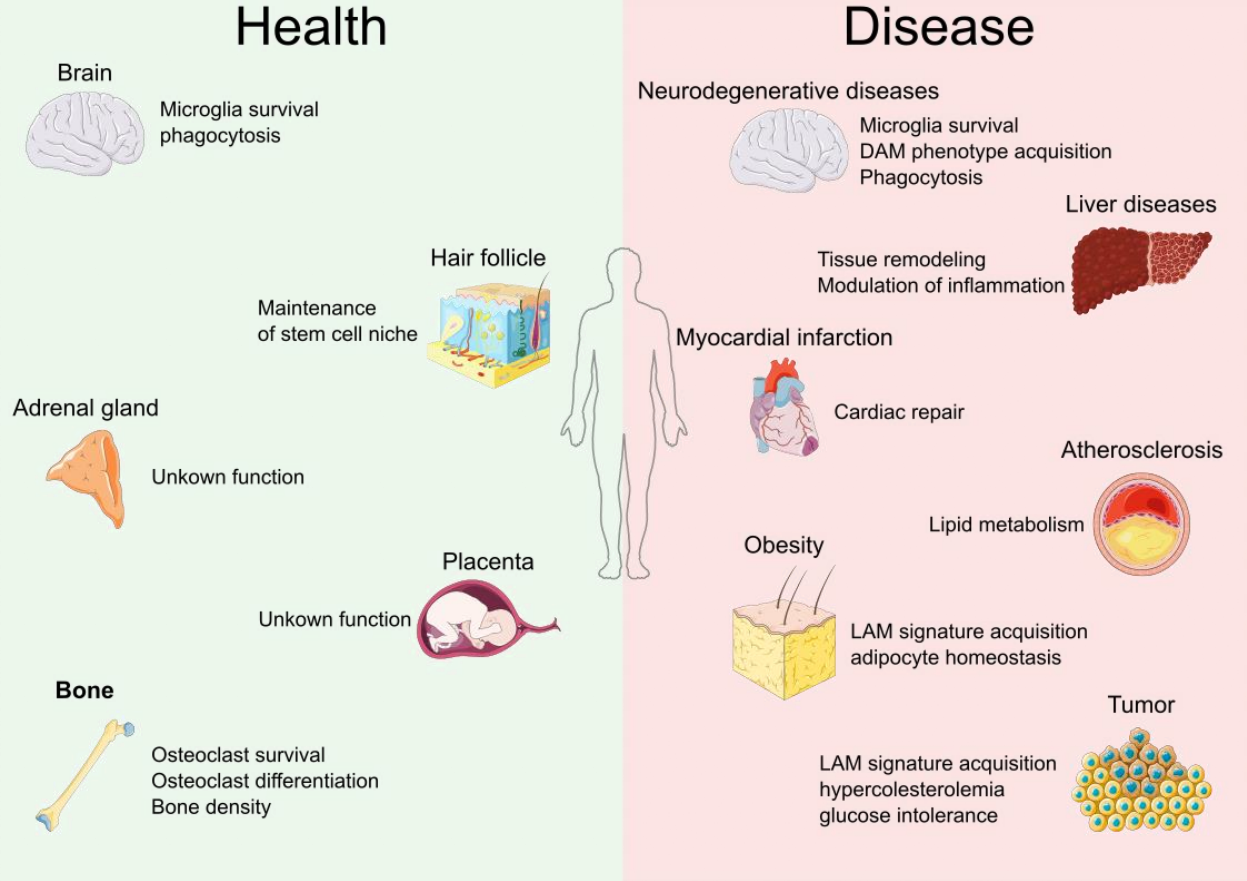

Figure 9: TREM2 function in health and disease. In homeostatic conditions, TREM2 macrophages are restricted in specific compartments, such as the brain, hair follicles, adrenal glands, placenta, and bones. On the contrary, TREM2 plays an important role in different diseases context: neurodegenerative diseases, metabolic diseases such as obesity, fatty liver, and atherosclerosis, tumor, and myocardial infarction. Images are taken from Servier Medical Art (smart.servier.com) and arranged with Inkscape. Figure re-adapted from Deczkowska A. et al., 2020. [478]

2.3.4 Pathological role of TREM2

TREM2 and DAP12 dysfunction was first described in Nasu-Hakola disease, a lipomembranous osteodysplasia with sclerosing leukoencephalopathy characterized by bone cysts followed by bone fractures and progressive dementia. [482] In particular, TREM2 is required in microglia for proper phagocytosis of apoptotic neuronal debris and resolution of inflammation. [483] Moreover, TREM2-deficiency negatively affects osteoclast differentiation. [450]

Different genetic variants of TREM2 are linked with late onset of Alzheimer's disease. [484] The most common TREM2 variant associated with Alzheimer's disease is R47H, in which TREM2 loses the binding ability to its ligands and, therefore, the capability to phagocyte TREM2-interacting ligands, such as β-amyloid, APOE and plaque-associated lipids. [447,485,486] Moreover, TREM2 is required for microglial survival and the acquisition of the DAM phenotype. [389,445] Presence of microglia with the DAMs in human is still debated. Studies performing scRNA-seq and single nucleus RNA-seq (snRNA-seq) showed three different results: no differences in microglia between control and patient with Alzheimer's disease, presence of DAMs in brain of Alzheimer's disease patient, or a completely different signature in Alzheimer's disease brain. [487–489] The technical challenges derived by the isolation of single cells and nuclei from postmortem brain tissue can explain why the presence of DAMs in human brain is inconsistent between different publications. [490,491] DAMs were also found in other models of neurodegenerative disease, such as experimental autoimmune encephalomyelitis (AEA), multiple sclerosis (MS), amyotrophic lateral sclerosis (ALS) and natural aging. [445,477,492]

TREM2 LAMs are detected in obese human and mice visceral adipose tissue. TREM2 deficiency in obese mice revealed that its signaling pathway is crucial for the LAM phenotype acquisition. In the same study, TREM2 deficiency in obese mice induced

adipocyte hypertrophy, systemic hypercholesterolemia, body fat accumulation and glucose intolerance, suggesting a beneficial role of the LAMs in obesity. [388]

LAMs are also detected in atherosclerotic plaque, and they have been proposed to correspond to foam cells. Gene expression analysis revealed that foamy macrophages express low inflammatory genes but many lipid processing genes, typical of the TREM2^{+} LAMs signature pattern. [387,391] Although their presence is well established, the function of TREM2 in the context of atherosclerosis still need to be clarified.

In the liver, LAMs were identified in fatty livers of mice fed with a high-fat diet, in other models of acute and chronic liver injury and human liver cirrhosis. [392,493,494] In a model of liver injury, TREM2 promotes re-population of Kupffer cells, controls endothelial phenotype and support the transition from pro-inflammatory to tissue repair phenotype in macrophages. [495]

Additional evidence suggested a role TREM2 in tumor-associated macrophages (TAMs). TREM2 was detected in blood monocytes and in TAMs in lung from cancer patients and in a mouse model of lung cancer, and it was also shown to positively correlate with tumor progression.[496] ScRNA-seq studies revealed expression of TREM2 in several subsets of myeloid cells that in the tumor environment are termed myeloid-derived suppressor cells. [497] In a mouse model of lung cancer, TREM2 deletion or treatment with anti-TREM2 antibody improved cancer therapy, suggesting that TREM2 expressed in TAMs support tumor growth.[441] More in depth analysis of TREM2 TAM revealed enrichment in lipid metabolism genes, extracellular matrix remodeling and immunosuppression.

TREM2 expression in microglia is modulating inflammation in a model of ischemia/reperfusion injury.[498] Indeed, in both *in vivo* and *in vitro* TREM2 gene silencing intensify the inflammatory response and neuronal apoptosis. [498] In a contrary approach, TREM2 overexpression suppresses inflammation and neuronal apoptosis. [498]

TREM2-expressing macrophages are also described in the heart after myocardial infarction. [334,409] I will extensively discuss the role of TREM2 in macrophages in the context of MI in **Chapter 4** and **Chapter 5**.

2.3.5 Soluble TREM2

sTREM2 is generated by cleavage of TREM2 by ADAM10/17 or by alternative splicing. [463,499–501] High levels of sTREM2 are detected in cerebrospinal fluids of patients with various neurological conditions, such as multiple sclerosis, Alzheimer's disease, Parkinson's disease, frontotemporal dementia, natural aging and in plasma of Down syndrome patients. [502–510] Moreover, sTREM2 is identified as a genetic Alzheimer's disease risk status. [506,507,511] Studies of patients with Alzheimer's disease showed that sTREM2 levels in cerebrospinal fluid are low during the asymptomatic phase, increase during the early symptomatic stage and decrease slightly in the dementia phase. [505,506,512,513] These findings correlate sTREM2 level in cerebrospinal fluid with changes in microglia activation status, suggesting that sTREM2 concentration might be used as a biomarker of neuronal injury. [505,507]

Other than being a biomarker, some studies showed that sTREM2 might also have a biological role. Indeed, sTREM2 treatment of bone marrow-derived macrophages and cultured human microglia deprived of CSF1 and GM-CSF respectively, showed increase in macrophage survival, activation of NF-kB signaling pathway, production of inflammatory cytokines and morphological changes in microglia. [514,515] The same effect was described in *in vivo* injection of sTREM2 in the hippocampus of WT and TREM2ko mice. [515] In a mouse model of Alzheimer's disease, sTREM2 injection or sTREM2 overexpression resulted in β-amyloid plaque reduction and rescue of the memory abilities. [516] These findings suggest a potential therapeutic role of sTREM2, but further studies are necessary since the pro-inflammatory activation may lead to negative side effect.

sTREM2 injection in the heart after MI ameliorates cardiac healing outcome by increasing cardiac function, survival and reducing infarct size. [409]

3 Chapter 2: Materials and Methods

3.1 Mice

C57BL6/J male mice were purchased from Janvier Lab (France), TREM2 knock-out mice were kindly provided by Marco Colonna (Washington, USA) and bred in the ZEMM (Centre for Experimental and Molecular Medicine) animal facility (Wuerzburg, Germany). [517]Mice were exposed to 12 hours light cycle with lights turning on at 7:00 and switched off at 19:00. All animal studies conform to the Directive 2010/63/EU of the European Parliament and have been approved by the appropriate local authorities (Regierung von Unterfranken, Wuerzburg, Germany, Akt.-Z. 55.2-DMS-2532-2-743 and Akt.-Z. 55.2-DMS-2532-2-865).

3.2 Myocardial Infarction

C57BL6/J and TREM2 knock-out male mice of matched age between 8- and 12-week-old underwent Left Anterior Descending (LAD) coronary artery ligation to induce myocardial infarction. Before surgery, mice received an injection of analgesic (Buprenorphine, 0.1mg/Kg, i.p.). After 30 minutes, deep anesthesia was induced with 5% isoflurane and mice were intubated with endotracheal canula (B/Braun, 4269098S-01) and placed under mechanical ventilation on a heating pad (Physitemp Instruments inc., TCAT-2LV). For echocardiography experiments the ventilator VentElite from Harvard apparatus was used, otherwise the SAR-830/AP from CWE incorporated was used. Deep anesthesia was checked by absence of paw withdrawal reflex and maintained between 2.0-2.5% isoflurane during surgery. After skin incision, thoracotomy at fourth intercostal space was performed to expose the heart. LAD coronary artery ligation was made with a 7/0 non-resorbable nylon suture thread (Serapren, CP05341A). The rib cage was closed with three independent sutures and skin was closed with a continuous suture using a 6/0

non-resorbable nylon suture thread (Serapren, CP07281A). For pain alleviation, mice were injected with two daily injections of analgesic (Buprenorphine, 0.1mg/Kg, i.p.) for two days after surgery. For neutrophil depletion experiment, mice were injected daily with anti-Ly6G (50µg, clone 1A8, BioXCell) or Isotype control antibody (50µg, clone 2A3, BioXCell) i.p. in 100µl of sterile PBS (Phosphate buffered Saline, Gibco, 14190-094). The first injection was performed the day before the induction of MI. For CCR2 depletion experiment, mice were injected one day before surgery with anti-CCR2 or Isotype control antibody (20µg, clone LTF-2, BioXcell) i.p. in 100µl of sterile PBS. Mice received daily injections starting from one day before the surgery. [517] Mice that died before the endpoint and with small infarct (with infarct size less than 30%) were excluded from the analysis.

3.3 Echocardiography measurements

Echocardiography was performed using Vevo 2100 System (FUJIFILM Visualsonics) and a MS400 transducer (FUJIFILM Visualsonics). C57BL6/J and Trem2 knock-out mice were kept in light anesthesia with 1% of Isoflurane, and echocardiography was recorded at day 0, 7, 14 and 28 after permanent coronary artery ligation. Long and Short axis of the heart were acquired at apical, middle and base levels of the left ventricle. Simpson´s analysis was performed to the long and short axis to calculate left ventricle volume and wall deepness. M-mode of short-axis at the middle and apical levels were used to calculate fractional shortening, ejection fraction and cardiac output. Only animal with heart rate (HR) between 450 and 600 b/m were included in the analysis. Analysis were performed using Vevo LAB software version 3.2.6 (FUJIFILM Visualsonics).

3.4 Heart processing for histology

Mice without and with MI were killed by cervical dislocation under isoflurane anesthesia. The heart was injected with KCl to arrest the heart in diastole before perfusing it with ice-cold PBS. Then, the heart was dissected and frozen in liquid nitrogen-cold Isopentane (Carl Roth, 3927.1) and stored at -80°C. Sections of the heart were made with Cryostat (Leica, CM3050 S) at 7µm thickness, placed onto SuperFrost slide (Langenbrick GmbH, 03-0060) and stored at -80°C.

3.5 Histology

For immunofluorescence, heart sections were blocked with Normal Serum goat (Biolegend, 927503) for 30 minutes to prevent unspecific staining of the secondary antibody. Then, they were incubated with rat anti-mouse CD68 (Biolegend, clone FA-11, 137001), rat anti-mouse CD31 (Invitrogen, clone 390, 14-0311-85), Wheat Germ Agglutinin (Vector laboratories, RL-1022-5), anti-αSmooth-muscle actin (Sigma-Aldrich, clone 1A4, C6198), rat anti-SiglecF (ThermoFisher, clone 1RNM44N, 14-1702-82), anti-Ly6G (BD Biosciences, 551459) or rabbit anti-GPNMB (Abcam, clone EPR18226-147, ab188222) overnight. After washing with PBS (Sigma-Aldrich, P3813), sections were stained with goat α-rat Alexa 488 (Invitrogen, A11006) or goat α-rabbit AlexaFluor555 (Invitrogen, A21429). Finally, the slides were mounted in Vectashield containing DAPI (Vectashield, H-1200). For Sirius red staining, fresh frozen sections were processed according to manufacturer's instruction. Briefly, sections were passed in Xylene (VWR, 28975360) and decreasing concentrations of ethanol (CARL-ROTH, T913.3). After rinsing the sections twice with distilled water, the sections were incubated with Pikosirius red (Sigma, Direct Red 80, 365548-5G) for 1 hour. Following 2 passages in acidified water (0.5% glacial Acetic Acid (Sigma-Aldrich, 33209) in water), the sections were dehydrated in increasing ethanol concentrations and xylene. The slides were mounted with Vectashield (Vectashield, H-5000). Images were acquired with Leica DM 4000 B LED microscope. Analysis was performed with ImageJ software (Fiji).

3.6 Apoptotic cells generation

Apoptotic cells were generated by stimulating thymocytes with Staurosporine. Briefly, thymus was extracted from young C57BL6/J mice and cells were isolated by crushing the thymus on a 70µm cell strainer with a syringe plunger. After washing the strainer with PBS, the cell suspension was spined down at 400g for 5 minutes at 4°C. The pellet was resuspended with DC medium (RPMI (Gibco, 21875-034) supplemented with 10% FCS, 100 U/ml penicillin and streptomycin (Sigma-Aldrich, P4333), and 50µM of β-Mercaptoethanol(Gibco, 31350-010)) and $1X10^6$cells/ml were stimulated with 1µM of Staurosporine (Sigma Aldrich, S6942) at 37°C for 17 hours. After stimulation, apoptotic thymocytes were washed twice to remove completely the Staurosporine and resuspended in DC medium supplemented with in 0.5% FCS. Apoptosis was then evaluated with Annexin V/ 7-AAD staining kit (ThermoFisher, 00-0055-56). Apoptotic thymocytes were then ready to use.

3.7 LAM-signature analysis of bone marrow-derived macrophages treated with apoptotic cells.

Bone marrow cells were isolated from femur and tibia of two hindlimbs of C57BL6/J and TREM2ko mice. Briefly, tibia and femur were dissected, bone marrow was exposed, and they were both placed in a 0.5ml Eppendorf tube with a hole on the bottom of the tube made with a 12G needle. The 0.5ml Eppendorf tube was then placed in a 1.5ml Eppendorf tube and centrifuged at 10000g for 15 seconds. The bone marrow was collected in the 1.5ml Eppendorf tube. The cells were then resuspended in DC medium (RPMI (Gibco, 21875-034) supplemented with 10% FCS, 100 U/ml penicillin and streptomycin (Sigma-Aldrich, P4333), and 50µM of β-Mercaptoethanol(Gibco, 31350-010)), filtered with a

70µm cell strainer, and centrifuged at 400g for 5 minutes at 4°C. After washing, cell suspension was resuspended in DC medium supplemented with 15% of L929 medium, cells were counted, and a concentration of $2X10^6$/ml was plated in a $10cm^2$ cell culture dish (SARSTEDT, 83.3902). Medium was changed at day 3 and 5 after the start of the culture. At day7, attached macrophages were collected with Accutase (Sigma-Aldrich, A6964), washed, resuspended in DC medium, and $0.4X10^6$ macrophages were plated in a 12 well plate (SARSTEDT, 83.3921). The day after, macrophages were incubated with starving medium (RPMI supplemented with 0.5% FCS). After 4 hours resting, macrophages were stimulated with apoptotic thymocytes in a ratio 1:5 (1 macrophages to 5 apoptotic thymocytes) for 17 hours. Cells were then washed with PBS and resuspended in RA1 lysis buffer of the Nucleo Spin RNA extraction kit (Macherey-Nagel, 740955.50). RNA was extracted according to manufacturer's instructions. Equal amounts of RNA were used for cDNA synthesis using random hexamer primer of the First Strand cDNA Synthesis kit (Thermofisher, K1612). Quantitative Real-Time Polymerase Chain Reaction was performed using SYBR-green (Applied Biosystems, A25742) and acquired on an Applied Biosystems™ QuantStudio™ 6 Flex Real-Time PCR System. Fold-change expression was determined using the ΔCT method and using *Hprt* as housekeeping gene. Primer sequences used were: *Hprt* forward (TCCTCCTCAGACCGCTTTT), *Hprt* reverse (CCTGGTTCATCATCGCTAATC); *Trem2* forward (CTGGAACCGTCACCATCACTC), *Trem2* reverse (CGAAACTCGATGACTCCTCGG); *Gdf15* forward (GCTGTCCGGATACTCAG), *Gdf15* reverse (TCAGGGGCCTAGTGATGTCC); *Fabp5* forward (AAGCCACGGCTTTGAGGAGT), *Fabp5* reverse (TTCACTGTGCTCTCGGTTTTG); *Gpnmb* forward(GGGCCATGAACAGTATCCCG), *Gpnmb* reverse (CCTTCTGGCATCTGGGGAAC); *Lipa* forward (TGTTCGTTTTCACCATTGGGA), *Lipa* reverse (CGCATGATTATCTCGGTCACA); *Spp1* forward (ATCTCACCATTCGGATGAGTCT), *Spp1* reverse (TGTAGGGACGATTGGAGTGAAA); *Mertk* forward, (CAGGGCCTTTACCAGGGAGA), *Mertk* reverse (TGTGTGCTGGATGTGATCTTC); *Abca1* forward (AGTGATAATCAAAGTCAAAGGGACAC), *Abca1* reverse

(AGCAACTTGGCACTAGTAACTCTG); *Il10* forward (ATTTGAATTCCCTGGGTGAGAAG), *Il10* reverse (CACAGGGGAGAAATCGATGACA).

3.8 Quantitative Real-Time Polymerase Chain Reaction analysis of sorted bone marrow monocytes

Bone marrow cells were isolated from femur and tibia of two hindlimbs of C57BL6/J mice as described above (see **LAM-signature analysis of bone marrow-derived macrophages treated with apoptotic cells**). After the centrifugation step, the cell were then resuspended in PBS enriched with 1%FCS, filtered with a 70µm cell strainer, and washed once more. Cells were then resuspended in TruStain FcX (Biolegend, 101320) and incubated for 10 minutes at 4°C to block unspecific staining. After blocking, cells were labeled with Fixable Viability dye e780 (ThermoFisher, 65-0865-14), CD45.2 BV421 (Biolegend, clone 104, 109832), CD11b PercpCy5.5 (Biolegend, clone M1/70, 101228), CD115 APC (Biolegend, clone AFS98, 135510), Ly6G Alexa488 (Biolegend, clone 1A8, 127626), Ly6C BV510 (Biolegend, clone HK1.4, 128033), Ter119 (Biolegend, clone TER-119, 116222), CD3 PECy7 (Biolegend, clone 145-2C11, 100320), CD19 PECy7(ThermoFisher, 25-0193-82), NK1.1 PECy7 (ThermoFisher, clone PK136, 25-5941-82). 50,000 Viable $CD45^{+}/CD11b^{+}/(Ter119/CD3/CD19/NK1.1)^{-}/CD115^{+}/Ly6G^{-}/Ly6C^{hi}$ monocytes were sorted and collected directly in RA1 lysis buffer of the Nucleo Spin RNA extraction kit (Macherey-Nagel, 740955.50). RNA was extracted according to manufacturer's instructions. Equal amounts of RNA were used for cDNA synthesis using random hexamer primer of the First Strand cDNA Synthesis kit (Thermofisher, K1612). Quantitative Real-Time Polymerase Chain Reaction was performed using SYBR-green (Applied Biosystems, A25742) and acquired on an Applied Biosystems™ QuantStudio™ 6 Flex Real-Time PCR System. Fold-change expression was determined using the ΔCT method and using *Hprt* as housekeeping gene. Primer sequences used were: *Hprt* forward (TCCTCCTCAGACCGCTTTT), *Hprt* reverse (CCTGGTTCATCATCGCTAATC); *Prtn3* forward

(CCAGACTTCCGGAGCGATCA), *Prtn3* reverse (CTGCTGGGGCAGAGAA); Socs3 forward 5'-ATTTCGCTTCGGGACTAGC-3', *Socs3* reverse 5'-AACTTGCTGTGGGTGACCAT-3'; *Lcn2* forward (CCAGACTTCCGGAGCGATCA), *Lcn2* reverse (TGTTCTGATCCAGTAGCGACA); *Mmp8* forward (CCATGCCTTCCCAGTACCT), *Mmp8* reverse (GCACTCCACATCGAGGCATT); *Chil3* forward (ATGGAAGTTTGGACCTGCCC), *Chil3* reverse (CCTTGGAATGTCTTTCTCCACAG).

3.9 Heart processing for flow cytometry analysis

After killing mice via cervical dislocation under isoflurane anesthesia, the heart from non-infarcted and infarcted mice was exposed and flushed with ice-cold PBS. Then the heart was excised, right ventricle was removed, the heart was weighed and minced with a scissor in 500µl of RPMI. The solution with minced heart was incubated with a digestion mix containing Collagenase I (450 U/ml, Sigma-Aldrich, C0130), Collagenase XI (125 U/ml, Sigma-Aldrich, C7657), Hyaluronidase (60 U/ml, Sigma-Aldrich, H3506) and DNase I (60 U/ml, Sigma-Aldrich, DN25) in agitation for 1 hour at 37°C using a thermomixer (Eppendorf, Thermomixer C). After digestion, the digested heart was filtered with a 70µm cell strainer (Greiner bio-one, 542070) and the remaining pieces were crushed with a syringe plunger. The cell suspension was then centrifuged at 400g for 5 minutes at 4°C and resuspended in PBS enriched with 1% of Fetal Calf Serum (FCS)(Sigma-Aldrich, S0615). Cells were ready for further processing.

3.10 Flow cytometry staining

Single cell suspension was plated in 96 round-bottom well plate (Sarstedt, 82.1582) and centrifuged at 400g for 5 minutes at 4°C. The pellet was resuspended in TruStain FcX (Biolegend, 101320) and incubated for 10 minutes at 4°C to block unspecific staining. Then, cells were stained with CD11b BV510 (Biolegend, clone M1/70, 101263), CD11b PercpCy5.5 (Biolegend, clone M1/70, 101228), CD11b PE (ThermoFisher, clone M1/70, 10-0112-81), CD11b BV785 (Biolegend, clone M1/70, 101243), CXCR4 Biotin (Miltenyi biotec, clone REA107, 130-112-171), SiglecF PE (ThermoFisher, clone 1RNM44N, 12-1702-82), Ly6G v450 (BD Biosciences, clone 1A8, 560603), Ly6G Pacific Blue (Biolegend, clone 1A8, 127612), Ly6G BV785 (Biolegend, clone 1A8, 127645), CD115 PE (ThermoFisher, clone AFS98, 12-1152-81), CD115 APC (Biolegend, AFS98, 135510), CD64 APC (Biolegend, clone X54-5/7.1, 139306), CD64 AlexaFluor647 (BD Biosciences, clone X54-5/7.1, 558539), CD62L BV605 (Biolegend, clone MEL-14, 104438), CXCR2 PECy7 (Biolegend, clone SA044G4, 149316), ICAM1 PercpCy5.5 (Biolegend, clone YN1/1.7.4, 116124), Ly6C PECy7 (ThermoFisher, clone HK1.4, 25-593-80), Ly6C BV510 (Biolegend, clone HK1.4, 128033), Ly6C Alexa488 (Biolegend, clone HK1.4, 128022), CD45 PE (ThermoFisher, clone 30-F11, 12-0451-82), CD45 Alexa700 (Biolegend, clone 30-F11, 103128), F4/80 PECy7 (Biolegend, BM8, 123114), Fixable Viability dye e780 (ThermoFisher, 65-0865-14) for 30 minutes in the dark at 4°C. After washing, cells were resuspended in PBS enriched with 1% FCS and ready for FACS measurement. For heart sample, 100µl of counting beads (Biolegend, 424902) were added and cell counts were calculated based on manufacturer's instruction. Cells were read by BD FACS Celesta (BD biosciences) and analyzed with Flowjo v10.

3.11 Heart protein Isolation for TREM2 and sTREM2 measurement

Non-infarcted and infarcted heart were perfused with ice-cold PBS, excised and frozen in liquid nitrogen. The heart was then stored at -80°C until further processing.

3.12 Plasma Isolation for sTREM2 measurements

Deep anesthesia was induced in C57BL6/J mice. Blood was collected retro-orbitally in EDTA tube (Sarstedt, 411.504.005). The blood was centrifuged at 2000g for 15 minutes at 4°C and supernatant was collected and stored at -80°C until further processing.

3.13 TREM2 and sTREM2 protein measurements

TREM2 and s TREM2 protein levels were measured in frozen heart as described here ([518]) and using a MSD ELISA assay ([519]).

3.14 Heart cell isolation with Hashtag and Cellular indexing of Transcriptomes and Epitopes by sequencing (CITE-seq): **Chapter 3 Figure 10**

C57BL6/J at Day1 (n=5), Day3 (n=5) and Day5 (n=3) after MI were used for this experiment. Mice were anesthetized and received an intravenous injection of 5µg of anti-CD45.2 APC (Biolegend, clone 104, 109814) to label all circulating leukocytes 5 minutes before sacrifice. The heart was flushed with ice-cold PBS, excised and right ventricle was removed. The heart was weighed and minced with a scissor in 500µl of RPMI. The solution with minced heart was incubated with digestion mix containing Collagenase I

(450 U/ml, Sigma-Aldrich, C0130), Collagenase XI (125 U/ml, Sigma-Aldrich, C7657), Hyaluronidase (60 U/ml, Sigma-Aldrich, H3506) and DNase I (60 U/ml, Sigma-Aldrich, DN25) in a thermomixer (Eppendorf, Thermomixer C) for 1 hour at 37°C. The cell suspension was filtered through a 70µm cell strainer and remaining undigested pieces were crushed with a syringe plunger. Cells were then washed in 50ml ice-cold PBS enriched with 1% FCS and centrifuged at 300g for 8 minutes at 4°C.

Isolated cells were firstly incubated with TruStain FcX and then stained with Fixable Viability dye e780, CD11b BV510 (for Day1 cells, BD Biosciences, clone M1/70, 562950), CD11b PercpCy5.5 (for Day 3 cells, Biolegend, clone M1/70, 101228), CD11b PE (for Day5 cells, Invitrogen, clone M1/70, 557397) for 25 minutes at 4°C in the dark. Cells where then washed once, resuspended in PBS/1%FCS, pooled, and centrifuged once more at 350g for 8 minutes at 4°C. Viable CD11b BV510, CD11b PercpCy5.5, CD11b PE cells were separately sorted using FACS Aria III (BD Biosciences).

After sorting, each time point was stained with different hashtag antibodies (Hashtag 1 for Day1 cells, Hashtag 2 for Day2 cells, Hashtag 3 for Day 3 cells) and CITE-Seq antibodies (1,5µg of Ly6C, Ly6G, CD64, F4/80, CD11c, MSR1, IA/IE, TIM4, CX3CR1 and CCR2) for 30 minutes at 4°C. The complete list of Hashtag and CITE-seq antibodies are listed in **Table1-2**. Then, cells were centrifuged at 350g for 8 minutes, resuspended with PBS enriched with 0.04% BSA (Bovine Serum Albumin, Sigma Aldrich, SRE0036), pooled and centrifuged again at 350g for 8 minutes. Cells were resuspended in 150µl of PBS/0.04% BSA, filtered through 40µm cell strainer and counted before loading in the 10x Genomics Chromium. Cells were loaded at a concentration of 1,300 cell/µl.

3.15 Mechanical isolation of heart cells

Since enzymatic digestion failed to preserve some epitopes (CXCR2 and CD62L), we employed mechanical digestion of cardiac tissue to obtain fresh neutrophils to label these

surface markers. This method was also used to collect neutrophils for functional assays (ROS-production and phagocytosis assay). Shortly, hearts were collected as described previously, minced and mechanically dissociated using a 12-Well Tissue Disaggregator plate (ScienceWare, Bel-Art Product). Cells were washed, filtered with a 70µm cell strainer and processed for flow cytometry.

3.16 ROS production assay

Heart cells from MI Day1 and Day3 were mechanically isolated and processed by flow cytometry as described above. After cytometry staining, cells were incubated for 30 minutes at 37°C with Dihydrorhodamine-123 (DHR123, final concentration 1/200, ThermoFisher, D23806), while control cells were incubated at 4°C. Cells were then acquired with FACS Celesta (BD Biosciences) and analyzed with Flowjo v10.

3.17 Phagocytosis assay

Heart cells from MI Day1 and Day3 were mechanically isolated and processed by flow cytometry as described above. After flow cytometry staining, cells were incubated for 30 minutes at 37°C with fluorescent *E. Coli* bioparticles (10µg/ml, ThermoFisher, P35366). Cells were then acquired with FACS Celesta (BD biosciences) and analyzed with Flowjo v10.

3.18 Blood and heart cells solation for CITE-seq experiment: **Chapter 3 Figure 13 and Chapter 4 Figure 5**

The following experimental conditions were applied for this experiment: no surgery mice (n=3), sham surgery Day1 (n=3), sham surgery Day3 (N=3), MI Day1 (n=5), MI Day3 (N=5). Blood and heart cells were isolated from these mice and processed for scRNA-seq. Blood was collected retro-orbitally with heparin-coated capillaries and kept on ice in agitation until blood was collected from all mice. Red blood cells were lysed in ACK buffer for 5 minutes on ice twice. Heart was dissected and cells were isolated with mechanical digestion as previously described. Blood and heart cells were labeled with Hashtag antibodies, Fixable Viability dye e780 (ThermoFisher, 65-0865-14), B220 PECy7 (ThermoFisher, clone RA3-6B2, 25-0452-82), NK1.1 PECy7 (ThermoFisher, clone PK136, 25-5941-82), Ter119 PECy7 (Biolegend, clone Ter119, 116222), CD11b PercpCy5.5 (Biolegend, clone M1/70, 101228), Ly6G PacificBlue (Biolegend, clone 1A8, 127645), SiglecF Biotin (Miltenyi Biotech, clone REA798, 130-112-171). Viable $Ter119^{-}$ $B220^{-}Nk1.1^{-}CD11b^{+}$ cells were sorted using FACS Aria III (BD Biosciences). Ly6G+ and Ly6G- cells were adjusted roughly to 1:1 proportion. After sorting, cells were washed and each sample were pulled together. Pooled cells were stained with CITE-seq antibodies (5µg/ml of CD64, CD54/ICAM1, CD49d, Fcer1a, CCR3 and CXCR4; 2.5µg/ml of anti-biotin and CD115; 1.67µg/ml of CD62L; 1.25µg/ml of IA-IE; 1µg/ml of Ly6C). After CITE-seq staining, cells were washed twice in PBS enriched with 0.04% of BSA and then loaded in the 10x Genomics Chromium at a concentration of 1700 cells/µl.

3.19 CCR2-depletion and CITE-seq: **Chapter 5 Figure 4**

The following experimental condition were used for this experiment: No MI (n=3), MI Day5 Isotype control (n=4), MI Day5 anti-CCR2 (n=5). Mice were anesthetized and received an intravenous injection of 5µg of anti-CD45.2 APC (Biolegend, clone 104, 109814) to label all circulating leukocytes. Blood was collected retro-orbitally and red blood cells were lysed in ACK buffer for 5 minutes on ice. Blood was then processed for flow cytometry to validate Ly6C^{hi} monocyte depletion. Heart cells were enzymatically isolated as described above. Around 10% of the cells were processed for flow cytometry analysis to determine cell counts, while the remaining were processed for sorting. Cells were washed twice in MACS buffer (PBS supplemented with 0,5% BSA + 2mM EDTA) incubated for 5 minutes at 4°C with TruStain FcX to remove unspecific staining. Cells were then incubated with anti-VSIG4 PE (ThermoFisher, clone NLA-14, 12-5752-82), mouse CD45 microbeads (Milteny Biotec, 130-052-301), anti-LYVE1 Biotin (ThermoFisher, clone ALY7, 14-0443-82), anti-mouse CD45.2 eFluor506 (steady state heart samples, ThermoFisher, clone 104, 69-0454-82), anti-mouse CD45.2-Alexa488 (MI Day5 Isotype samples, Biolegend, clone 104, 109816) and anti-mouse CD45.2 BV421 (MI Day5 anti-CCR2, Biolegend, clone 104, 109832) for 10 minutes at 4°C. Afterwards, Hashtag antibodies were added as follow: No MI (Hashtag 1 to 3), MI Day5 Isotype (Hashtag 4 to 7), MI Day5 anti-CCR2 (Hashtag 8-12). Cells were additionally incubated for 15 minutes at 4°C, washed twice with MACS buffer, pooled, and magnetic selection was performed using LS Columns (Miltenyi Biotech, 130-042-401) and MidiMACS separators (Miltenyi Biotech, 130-042-302). Of note, prior experiments confirmed that labeling with the anti-CD45microbeads, anti-CD45 Hashtags antibodies (clone 30-F11) and anti-CD45.2 antibodies (clone 104) did not interfere with each other. To avoid column clogging, MACS selection was performed on six separated LS columns and the positive cell fraction was pooled together. CD45+ cells were washed with PBS supplemented with 0.04% of BSA (Sigma-Aldrich, A1595) and incubated with Fixable Viability dye eFluor780 (ThermoFisher, 65-0865-14) and CITE-seq mix (list provided in **Table 2**) for 25 minutes at 4°C. Cells were washed with PBS/0.04% FCS, resuspended and Viable CD45iv-CD45+ cells were sorted using

FACS Aria III (BD biosciences) with a 10µm nozzle. Number of sorted cells were adjusted to have: 20% of the cells from No MI group, 40% of the cells from MI Day5 Isotype group, and 40% of the cells from MI Day5 anti-CCR2 group. Cells were resuspended, counted and 20,000 cells were loaded in 10X Genomics Chromium in duplicate.

3.20 Wild type and TREM2ko heart cells isolation for scRNA-seq: **Chapter 4 Figure 1 and Chapter 5 Figure 15**

The following experimental condition were used in this experiment: wild type no MI (n=2), wild type MI Day5 (n=5), TREM2ko no MI (n=3), TREM2ko MI Day5 (N=5). Wild type data were used for analysis in Chapter 4 Figure 15, while wild type and TREM2 knock-out data were used for analysis in Chapter 5 Figure 21. Mice were anesthetized and received an intravenous injection of 5µg of anti-CD45.2 APC (Biolegend, clone 104, 109814) to label all circulating leukocytes. Heart cells were enzymatically isolated as previously described. Around 10% of the cells were processed for flow cytometry analysis to determine to cell counts, while the remaining were processed for sorting. Briefly, cells were incubated with TruStain FcX to remove unspecific staining. After washing with MACS buffer, cell were incubated with anti-VSIG4 PE (ThermoFisher, clone NLA-14, 12-5752-82), mouse CD45 microbeads (Miltenyi Biotec, 130-052-301), anti-LYVE1 Biotin (ThermoFisher, clone ALY7, 14-0443-82), anti-mouse CD45.2 AlexaFluor488 (for wild type sample, Biolegend, clone 104, 109815) or anti-mouse CD45.2 AlexaFluor700 (for Trem2 knock-out samples, Biolegend, clone 104, 109822) and incubated for 10 minutes at 4°C. Hashtag antibodies were added as follow: wild type no MI (Hashtag 1-2), wild type MI Day5 (Hashtag 5 to 9), TREM2ko no MI (Hashtag 2-3-15), TREM2ko MI Day5 (Hashtag 10 to 14). Cells were incubated for 15 minutes at 4°C, washed twice with MACS buffer, pooled, and CD45 magnetic selection was performed LS column as described above (see **CCR2-depletion and CITE-seq: Figure 18**). The positive cell fraction was pooled together and incubated with CITE-seq mix (list provided in **Table 2**) and Fixable Viability Dye eFluor780

(ThermoFisher, 65-0865-14) for 25 minutes at 4°C. Cells were washed with PBS/0.04% FCS, resuspended and Viable CD45iv-CD45+ cells were sorted using FACS Aria III (BD biosciences) with a 100µm nozzle. Cells from steady state and infarcted heart were sorted separately in order to reach ~50% of cells from wild type mice and ~50% of cells from TREM2ko mice in each experimental condition. Cells were then pooled post-sorting to have ~30% of the cells from steady state heart and ~70% of the cells from MI Day5 of the total cell pool. 20,000.25,000 cells were loaded in 10X Genomics Chromium in duplicate.

3.21 scRNA-seq data analysis

3.21.1 Pre-processing

10x Genomics data, HTO and ADT libraries were demultiplexed using Cell Ranger software (version 3.0.1). Alignment and counting steps were performed with Mouse GRCm38 reference genome. The –feature-ref flag of Cell Ranger software was used to generate a gene expression matrix counts alongside the expression of cell surface proteins. The obtained gene-barcode matrix was further analyzed using Seurat v3. [520]

3.21.2 Demultiplexing

Demultiplex was done in the experiments where Hashtag antibodies were used. Demultiplexing was performed in Seurat v3 to identify sample of origin, multiplet exclusion, and cells with undetectable hashtag signal. Hashtag demultiplexing was executed according to instructions provided by software developers.

Analysis of cell surface epitopes with CITE-seq was performed using a standard Seurat workflow.

3.21.3 Clustering analysis

Clustering analysis was performed based on RNA levels using a standard Seurat workflow. Shortly, low quality cells were removed (with more than 5% unique molecular identifiers (UMIs) mapping to mitochondrial transcripts), data were normalized and “vst” method was used to identify 2000 variable features. Moreover, the “ScaleData” function was applied, Principal Component Analysis (PCA) was performed, and significant principal component (PC) were determined using the JackStraw method. 20 PCs were used to perform clustering analysis and Uniform Manifold Approximation and Projection (UMAP) dimensional reduction. Immune cell population were identified combining transcript and CITE-seq surface marker expression of canonical markers. For monocyte/macrophages and neutrophils sub-clustering, they were subseted in a new Seurat Object and new clustering analysis was performed. 2000 variable genes and 20 PCs were used to perform the latter analysis.

To assign the IEG (immediate Early Genes) expression score we used the “AddModuleScore” function in Seurat v3 using the following selected gene as a feature: *Jun*, *Junb*, *Jund*, *FosbI*, *Atf3*, *Hsp90aa1*, Hsp90ab1, *Hspa8*, *Zfp36*, *Cebpb*, *Cebpd*, *Socs3*, *Hspe1*, *Dusp1*. We employed the same “AddModuleScore” function to assign the “Bone marrow proximity score” using the following genes as a feature: *Mmp8*, *Ifitm6*, *Mmp25*, *Retnlg*, *Lcn2*, *Olfm4*, *Chil3*, *Itgb2*, *Fpr1*, *Ltf*, *Camp*, *Lyz2*, *Lyz1*. We employed again the “AddModuleScore” function to assign the “LAM signature score” using the following genes as a feature: *Spp1*, *Gpnmb*, *Ctsd*, *Cd9*, *Fam20c*, *Lgals3*, *Anxa4*, *Cd63*, *Ftl1*, *Fth1*, *Clec4d*, *Psap*, *Emp1*, *Fabp5*, *Lgals1*, *Syngr1*, *Cyba*, *Capg*, *Vat1*, *Plin2*, *Pgam1*, *Gapdh*, *Aldoa*, *Lat2*, *Pkm*, *Mmp14*, *Anpep*, *Rnh1*, *Ctsz*, *Anxa5*, *Anxa1*, *Adam8, Fam129b*, *Aprt*, *Esd*, *Trem2*, *Alcam*, *Cd68*, *Vim*, *Prdx1*, *Kcnn4*, *Glipr1*, *Ctss*, *Atox1*, *Uap1/1*, *Bcl2a1b*,

Il7r, *Lilr4b*, *Pld3*, *Nceh1*, *Gpr137b*, *Gsn*, *Anxa2*, *Lmna*, *Ctsd*, *Itgax*, *Dpep2*, *Lipa*, *Lilrb4a*, *Fabp4*, *Basp1*, *Ptms*, *Ctsb*, *Atp6v1a*, *Lpl*, *Sgk1*.

3.21.4 Pseudotime analysis

Monocle's differentialGeneTest function was used to determine differentially expressed genes. [521] In the neutrophils chapter, the blood/heart differentially expressed genes were determined according to Seurat clusters and 503 ordering genes were used. In the monocyte/macrophage chapter, MI Day1-3-5 dataset differentially expressed genes were determined according to Seurat clusters and 1,071 ordering genes were used. For blood/heart dataset 1,076 ordering genes were used. The "ReduceDimension" function and "DDRTree" method were used for dimensional reduction, and "oderCells" function was employed for pseudotime ordering.

3.21.5 Absolute cell counts for scRNA-seq analysis: **Chapter 4 Figure 4** and **Chapter 5 Figure 15**

Absolute cell counts of viable cardiac immune cells were obtained by processing 10% of the post-digested cell suspension for FACS analysis (see above). Briefly, cells were labeled with Fixable Viability dye eFluor780 (ThermoFisher, 65-0865-4) and fluorochrome couple anti-CD45 for 30 minutes at 4°C. Cells were washed and resuspended with PBS enriched with 1%FCS. Absolute cell counts were determined using Precision Count Beads (Biolegend, 424902) following manufacturer´s instruction using BD FACS Celesta (BD biosciences) and analyzed with Flowjo v10. $CD45^+$ cells were then normalized to the heart weight, obtaining $CD45^+$ cells/mg of tissue. The proportion of each cells population defined by the processed scRNA-seq dataset was

calculated in percentage of $CD45^+$ for each individual replicate was then multiplied by the $CD45^+$ cells/mg obtained by the FACS analysis.

TotalSeq Antibody	Catalog Number	Company
Hashtag 1	155801	Biolegend
Hashtag 2	155803	Biolegend
Hashtag 3	155805	Biolegend
Hashtag 4	155807	Biolegend
Hashtag 5	155809	Biolegend
Hashtag 6	155811	Biolegend
Hashtag 7	155813	Biolegend
Hashtag 8	155815	Biolegend
Hashtag 9	155817	Biolegend
Hashtag 10	155819	Biolegend
Hashtag 11	155821	Biolegend
Hashtag 12	155823	Biolegend
Hashtag 13	155825	Biolegend
Hashtag 14	155827	Biolegend
Hashtag 15	155829	Biolegend

Table 1: Hashtag antibodies list with catalog numbers and company.

CITE-seq Antibody	Catalog Number	Company
Ly6G	127655	Biolegend
CD11b	101265	Biolegend
CD62L	104451	Biolegend
IAIE	107653	Biolegend
ICAM1	116127	Biolegend
Ly6C	128047	Biolegend
CXCR4	146520	Biolegend
MSR1	154703	Biolegend
CD64	139325	Biolegend
MAR1	134333	Biolegend
CCR3	144523	Biolegend
CD80	104745	Biolegend
CD117	105843	Biolegend
Sca1	108147	Biolegend
CD11c	117355	Biolegend
TIMD4	130011	Biolegend
CX3CR1	149041	Biolegend
XCR1	148227	Biolegend
F4/80	123153	Biolegend
CD86	105047	Biolegend
CD135	135316	Biolegend
CD103	121437	Biolegend
CD169	142425	Biolegend
CD8a	100773	Biolegend
SiglecH	129615	Biolegend
CD19	115559	Biolegend
CD3	100251	Biolegend
CD63	143915	Biolegend
CD9	124819	Biolegend

CD163	155303	Biolegend
NK1.1	108755	Biolegend
CD279	109123	Biolegend
CD127	135045	Biolegend
CD68	137031	Biolegend
Sirpa	144033	Biolegend
CD274	153604	Biolegend
ITGB7	321227	Biolegend
CD4	100569	Biolegend
TCRgd	118137	Biolegend
MGL2	146817	Biolegend
CD26	137811	Biolegend

Table 2: CITE-seq antibodies list with catalog numbers and company.

4 Chapter 3: Neutrophils dynamics after Myocardial Infarction

In this Chapter we used scRNA-seq analysis to explore neutrophil heterogeneity in the heart after myocardial infarction. **Chapter 3** was published as a research article (Vafadarnejad E.*, Rizzo G.*, Krampert L.*, Arampatzi P., Arias-Loza A., Nazzal Y., Rizakou A., Knochenhauer T., Bandi S., Nugroho V., Schulz D., Roesch M., Alayrac P., Vilar J., Silvestre J., Zernecke A., Saliba A., Cochain C. “Dynamics of Cardiac Neutrophil Diversity in Murine Myocardial Infarction”) published in “*Circulation Research”* (2020), doi: https://doi.org/10.1161/CIRCRESAHA.120.317200. The journal copyright does not allow the re-use of the paper for non-commercial purpose. The original paper is re-adapted and figures were changed in order to use the data as part of this thesis to avoid conflict with the journal copyright.

* Equal contributions

4.1 ScRNA-seq reveals a time-dependent cluster of *SiglecF^{hi}* neutrophils populating the infarcted heart

We performed scRNA-seq combined with CITE-seq and hashing of CD45+CD11b+ cells isolated from the heart of C57BL/J mice at Day1, 3 and 5 after MI (**Figure 10A**). Monocytes and macrophages were identified by expression of common surface markers for monocyte/macrophages (CD64, Ly6C) and related transcript (*Fcgr1*, *Ly6c2*), while neutrophils were discriminated by expression of Ly6G surface marker and *S100a8* transcript level (**Figure 10B**). To better resolve neutrophils transcriptional heterogeneity after MI, we subsetted neutrophil population from **Figure 10B** and re-clustered according to Seurat analysis (**Figure 10C-D)**. We identified six neutrophil clusters with distinct kinetics: at Day1 Neutro4 cluster was predominant together with Neutro2; at Day3 the most abundant population was Neutro1, followed by Neutro2,3 and 5 while Neutro4 population disappeared; at Day5 Neutro3 and Neutro2 proportion were increased, while Neutro1 and Neutro5 proportion decreased (**Figure 10C-E**). Differential gene expression analysis revealed a time-dependent *Siglecf* enrichment in neutrophils, peaking at Day3 after MI and decreasing at Day5 after MI (**Figure 10F**). To validate the presence of SiglecF^{hi} neutrophils in the infarcted heart, we mechanically dissociated infarcted heart at Day1 and 3 after MI and performed flow cytometry analysis showing presence of SiglecF expression in neutrophils at Day3 after MI, confirming the scRNA-seq data (**Figure 11A**). Immunohistology staining of heart cryosections further confirm infiltration of SiglecF expressing neutrophils in day 3 infarcted hearts, while no SiglecF staining was detected at Day1 post-MI (**Figure 11C**). SiglecF is a marker widely used to label eosinophil. To verify that our gating strategy does not include eosinophil contamination, we checked side scatter property of Ly6G^{-}SiglecF^{hi} cell (gating for eosinophils), Ly6G^{+}SiglecF^{lo} cells, and Ly6G^{+}SiglecF^{hi} cells via flow cytometry. Ly6G^{+}SiglecF^{lo} and Ly6G^{+}SiglecF^{hi} cells are defined by low side scatter, representing neutrophils, while Ly6G^{-}SiglecF^{hi} are characterized by intermediate side scatter, representing eosinophils, suggesting that Ly6G+SiglecFhi cells are indeed neutrophils (**Figure 11B**).

We then assessed differences in phagocytosis ability and ROS production between SiglecF^{hi} and SiglecF^{lo} neutrophils at Day3 after MI. SiglecF^{hi} neutrophils displays higher phagocytosis of *E. coli* bioparticles and higher ROS production as shown by DHR123 fluorescence labeling (**Figure 11D-E**). Neutrophils at Day1 showed level of phagocytosis and ROS similar to the SiglecF^{hi} at Day3 after MI (**Figure 11D-E**). Overall, we showed a new neutrophil state present in the heart at Day3 after MI with increased phagocytosis activity and ROS production.

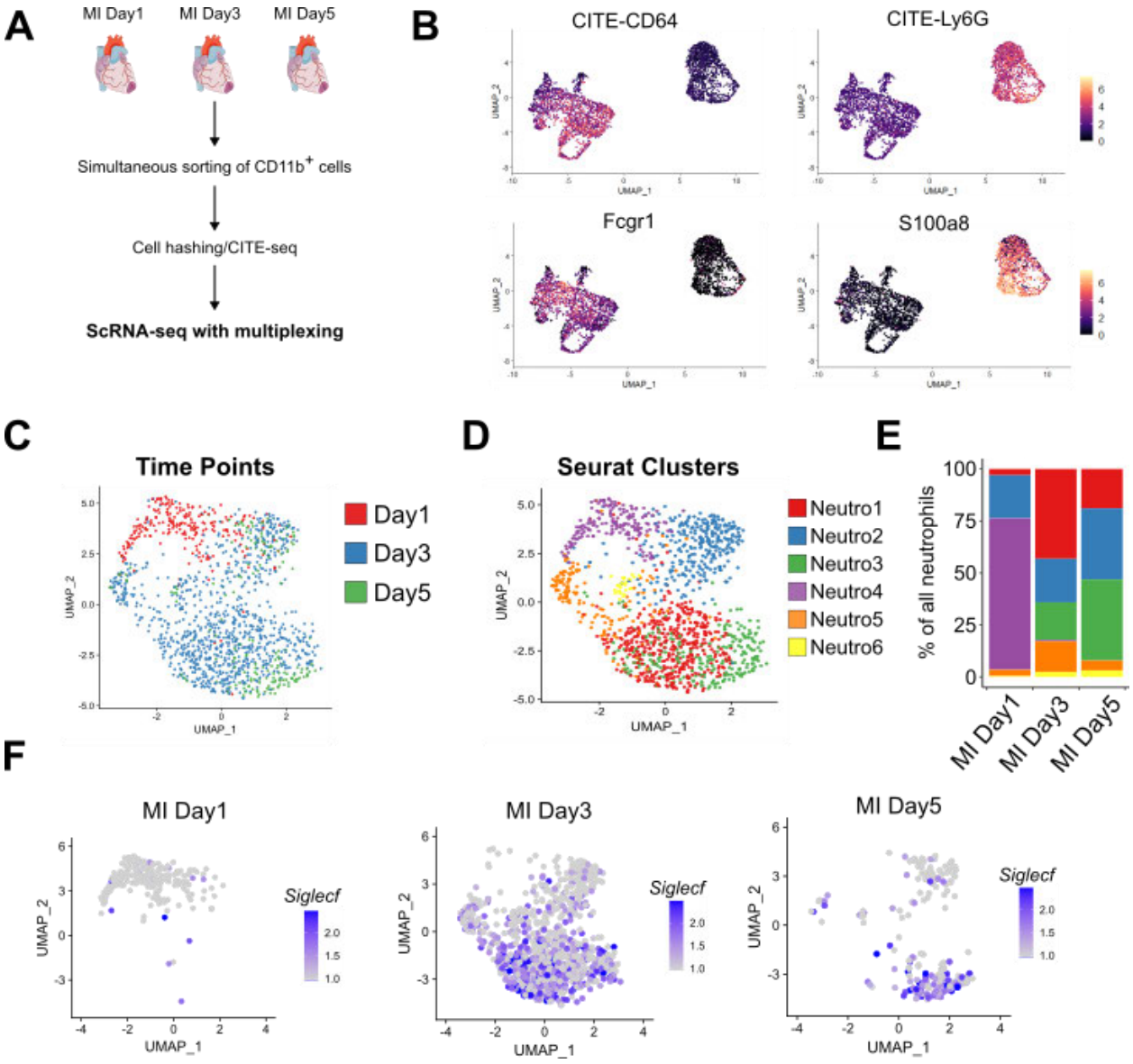

Figure 10: **scRNA-seq of cardiac leukocytes reveals neutrophil transcriptional heterogeneity after MI**. **A**, Graphical representation of the experimental design; **B**, CITE-seq (above) and transcriptional level (below) of the indicate markers in the UMAP plot of scRNA-seq data of total CD11b⁺ cells; **C and D,** UMAP representation of 1334 neutrophil with time points in **C** and Seurat clusters in **D**; **E,** Proportion of each cluster showed in **D** in total neutrophils at each time point; **F**, *SiglecF* transcript level projected in the UMAP plot split according to time points. Images are taken from Servier Medical Art (smart.servier.com*)* and arranged with Inkscape.

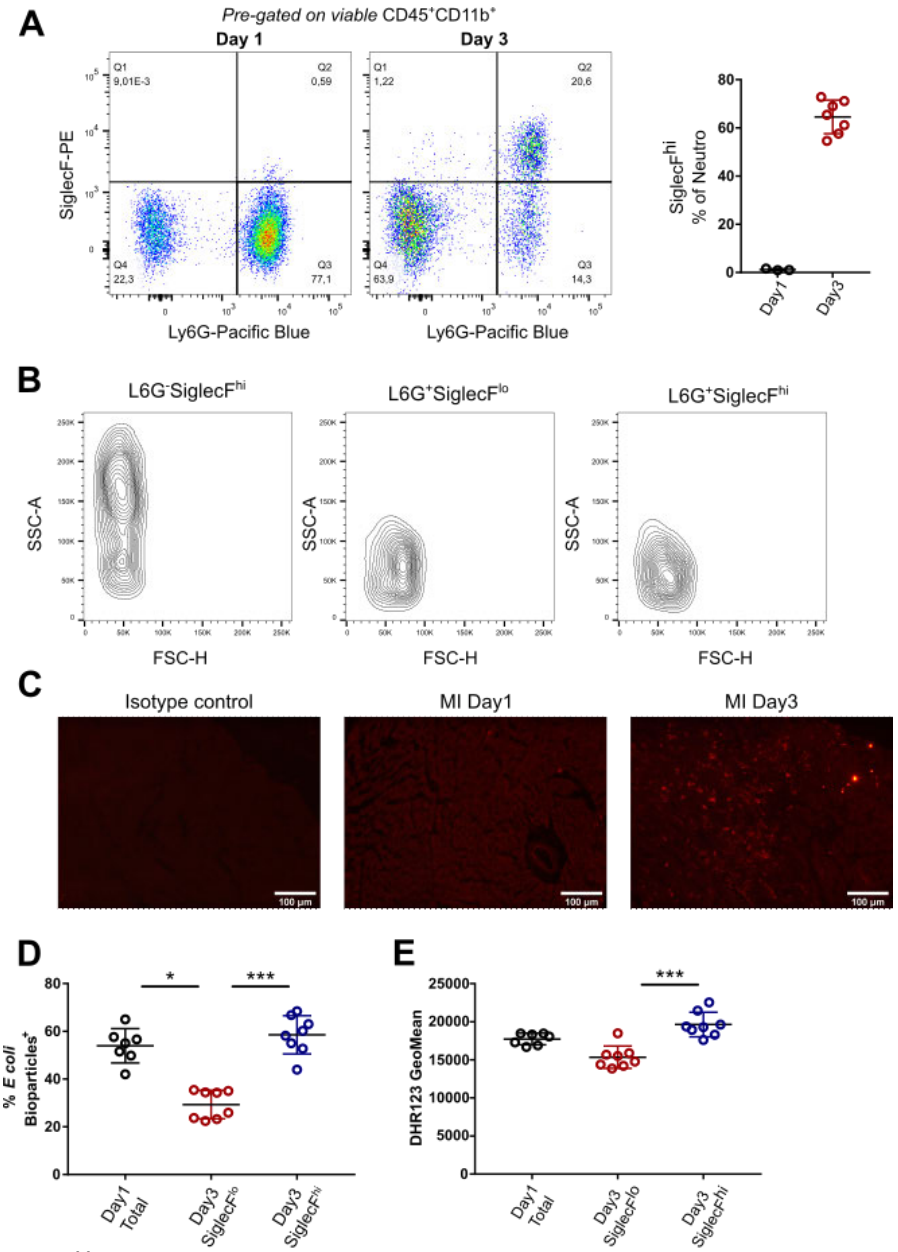

Figure 11: SiglecF^{hi} neutrophils populate the heart at day 3 after MI and have increased phagocytosis capacity and ROS production. A, SiglecF/Ly6G flow cytometry plot of cardiac leukocytes at day 1 and 3 post MI (right) and proportion of SiglecF^{hi} neutrophils at day 1 and 3 after MI (right) (Day1 n=7; Day3 n=7); **B**, SSC-A/FSC-A flow cytometry representative plot of gated Ly6G^{-}SiglecF^{hi} eosinophils, Ly6G^{+}SiglecF^{lo} neutrophils, and Ly6G^{+}SiglecF^{hi}; **C**, SiglecF immunofluorescence staining in cryosections of heart at day1 and 3 after MI, x200, scale bar 100µm; **D**, phagocytosis of *E.coli* bioparticles (left) (Day1 Total n=7, Day3 SiglecF^{lo} n=8, Day3 SiglecF^{hi} n=8) and reactive oxygen species production measured with DHR123 (right)) (Day1 Total n=7, Day3 SiglecF^{lo} n=8, Day3 SiglecF^{hi} n=8). Statistical analysis was performed using Mann-Whitney U test for panel **A** and Kruskall-Wallis test with Dunn multiple comparison test for panel **D** and **E**. Images are arranged with Inkscape.

4.2 SiglecF^{hi} neutrophils express aging markers

Based on the scRNA-seq neutrophil data (**Figure 10C-D**), *Siglecf* enriched neutrophils co-express aging markers of "old" neutrophil signature genes, such as *Icam1* (Intracellular adhesion molecule 1; ICAM1/CD54), *Itga4* (CD49d), *Cxcr4* (CXCR4), while the marker of "young" neutrophils *Sell* (CD62L) was expressed specifically in neutrophils at Day1 time point (**Figure 12A**). We also checked surface marker expression of the "old" and "young" neutrophils via flow cytometry. As suggested from our scRNA-seq data, SiglecF^{hi} neutrophils at Day3 after MI expressed the aging marker ICAM1, CD49d and CXCR4. On the contrary, total neutrophils at Day1 and SiglecF^{lo} neutrophils at Day3 after MI are enriched in CD62L (**Figure 12B-C**). *Cxcr2* transcript level was higher at Day1 and Day3 time points, but decreased at the later time points (**Figure 12A**). On the contrary, neutrophils at Day1 and Day3 after MI express similar level of surface CXCR2 markers analyzed by flow cytometry (**Figure 12B-C**).

To summarize, we could see enrichment of aging markers in SiglecF^{hi} neutrophils compared to SiglecF^{lo} and Day1 neutrophils, confirmed also by flow cytometry analysis.

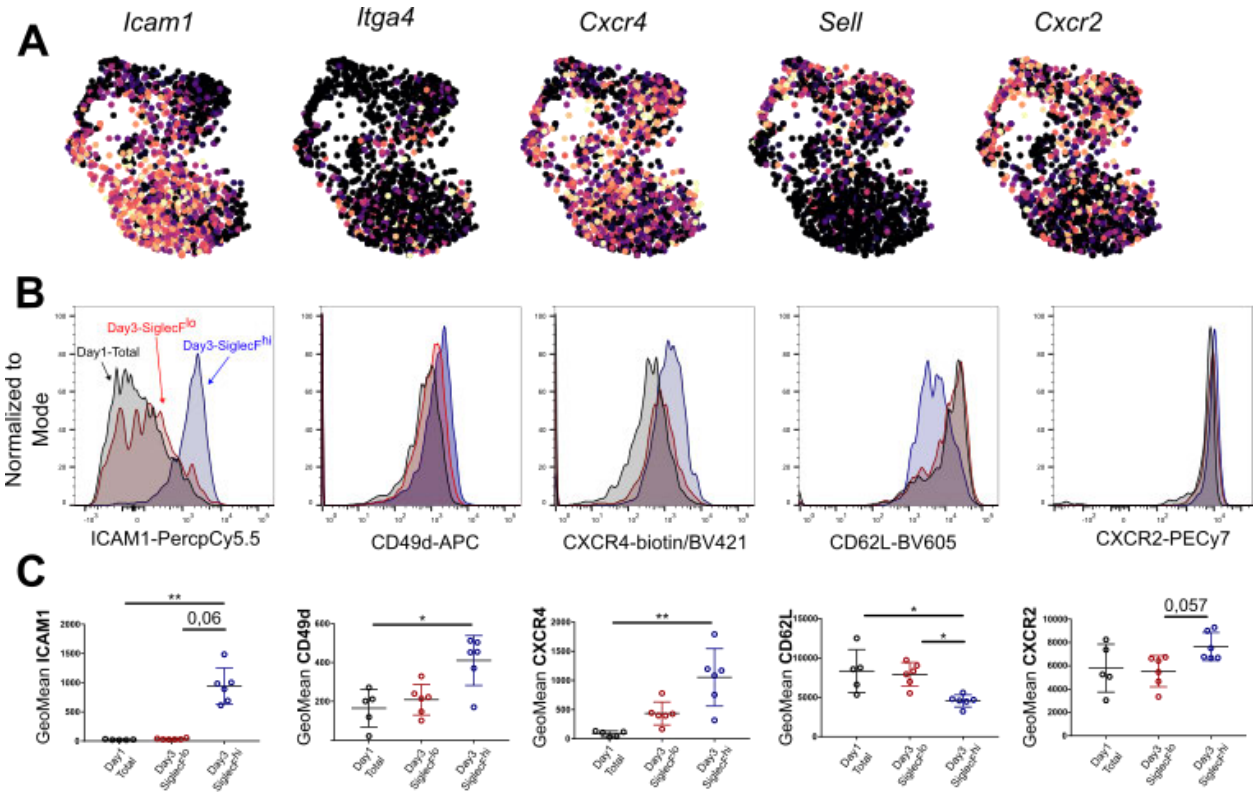

Figure 12: SiglecF^{hi} neutrophils express aging markers. A, log normalized level of the indicated transcripts projected in the UMAP plot; **B**, representative flow cytometry plot of the indicated surface markers in total neutrophils at day 1, SiglecF^{lo} and SiglecF^{hi} neutrophils at day 3 after MI; **C**, quantitative analysis of the indicated surface markers in total neutrophils at day 1 (n=5), SiglecF^{lo} (n=6) and SiglecF^{hi} (n=6) neutrophils at day 3 after MI. Statistical analysis in panel C was performed using Kruskall-Wallis test with Dunn multiple comparison. Images are arranged with Inkscape.

4.3 SiglecF^{hi} neutrophils age in the infarcted heart

After ischemic injury, neutrophils mobilize from the bone marrow, enter the circulation, and infiltrate the infarcted heart. Based on our data, we showed increase in aging markers in SiglecF^{hi} neutrophils at Day3 after MI, but whether this state is acquired by aging process of newly infiltrating neutrophils or by infiltration of already aged SiglecF^{hi} neutrophils remain to be determined. To address this question, we performed scRNA-seq of blood and heart immune cells isolated from non-operated mice, sham-operated and

MI-operated mice after 1 and 3 days after MI to perform a combined analysis of blood and heart neutrophils (**Figure 13A**). We defined neutrophils as $Ly6G^{+}CD115^{-}$ using CITE-seq surface markers expression and subsetted neutrophil population alone for more in-depth analysis (**Figure 13B-C**). Sample demultiplexing helped to discriminate blood and heart cells (**Figure 13C**). Based on gene expression analysis we identified 4 different blood neutrophil clusters: “young” neutrophils ($CD62L^{hi}$, low *Cxcr4*), “old” neutrophils ($CD62L^{lo}$, high *Cxcr4*), neutrophils with a type I IFN response signature (Neu-IFN), and a minor cluster most likely comprising neutrophil/platelet aggregates (**Figure 13D**). Supporting our previous scRNA-seq data analysis (**Figure 10**), we could distinguish in the infarcted heart $SiglecF^{lo}$ neutrophils at Day1 and $SiglecF^{hi}$ neutrophils at Day3 after MI (**Figure 13D**). Moreover, we detected neutrophils with a $SiglecF^{hi}$ signature just in the infarcted heart at Day3 time point, supporting the hypothesis that SiglecF neutrophils state is acquired in the infarcted heart and not upstream during neutrophils mobilization from the bone marrow (**Figure 13E**). To further confirm the hypothesis that SiglecF state is acquired by aging neutrophils in the infarcted heart, we applied a bone marrow (BM) proximity score to the neutrophils cluster in **Figure 12C** based on a set of genes previously identified in neutrophils at different developmental stage. [208,522] Blood “young” neutrophils and heart $SiglecF^{lo}$ neutrophils had a high BM proximity score, in line with the idea that they are mobilized from the bone marrow and infiltrating the infarcted heart (**Figure 13F**). On the contrary, blood “old” neutrophils and $SiglecF^{hi}$ neutrophils had a low BM proximity score, suggesting that they are aging in the circulation and in the heart, respectively (**Figure 13F**). Moreover, $SiglecF^{hi}$ neutrophils also expressed high ribosomal genes as well as blood “old” neutrophils, corroborating the idea that the $SiglecF^{hi}$ state is acquired by aging of “young” $SiglecF^{lo}$ neutrophils in the infarcted heart (**Figure 13F**).

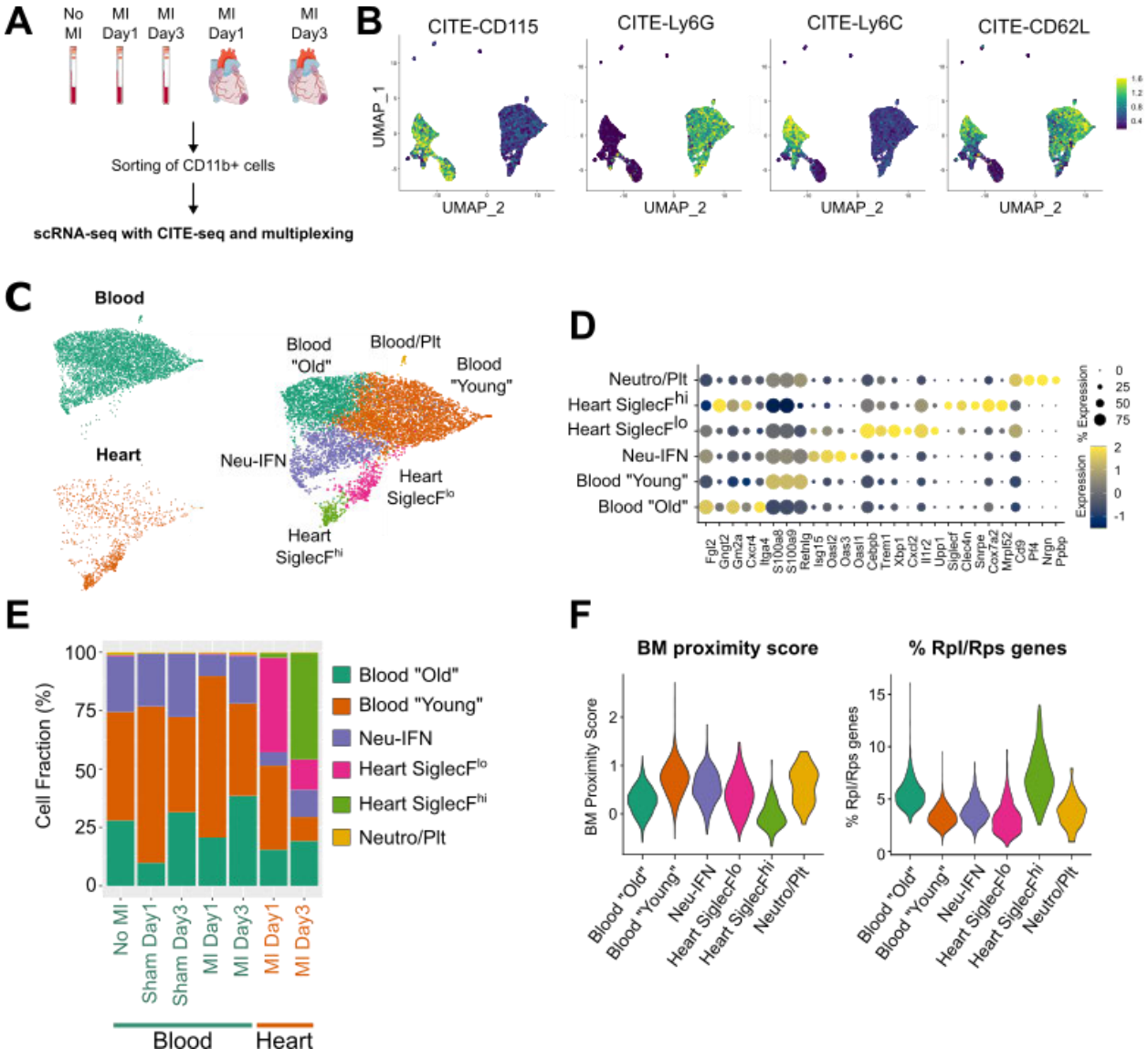

Figure 13: SiglecF^{hi} neutrophils acquire aging markers in the infarcted heart. A, graphical representation of the experimental setup; **B**, UMAP of the indicated CITE-seq signal projected in the UMAP plot of isolated viable Ter119^{-}CD3^{-}B220^{-}CD11b^{+} cells; **C**, UMAP plot of neutrophil subclustering indicating sample of origin (left) and Seurat clusters (right); **D**, expression of the indicated transcripts in neutrophil clusters; **E**, proportion of each cluster showed in **C** in total neutrophils in the different experimental conditions; **F**, BM proximity score (left) and percentage of Rpl/Rps genes (right) in total neutrophil. Images are taken from Servier Medical Art (smart.servier.com*)* and arranged with Inkscape.

4.4 Anti-Ly6G depletion shifts the neutrophils proportion toward SiglecF^{hi} state

To further investigate neutrophils time-dependent heterogeneity in the infarcted heart, we employed a neutrophil depletion approach previously used in the literature to investigate neutrophils function in the heart after MI. [299] We intraperitoneally injected C57BL6/J mice with 50µg of anti-Ly6G antibody or isotype control one day before the surgery and one daily injection to keep neutrophils at low level. The mice got sacrificed at Day3 after MI and heart and blood were dissected and processed for FACS analysis (**Figure 14A**). To exclude Ly6G antigen masking by the depletion antibody, we established a gating strategy for neutrophils defined in the heart as CD11b^{+}CD64^{-}CXCR2^{+} and in the blood as CD11b^{+}CD115^{-}CXCR2^{+} (**Figure 14B-C**). This gating strategy showed that more than 90% of CD11b^{+}CD64^{-}CXCR2^{+} in the heart and CD11b^{+}CD115^{-}CXCR2^{+} in the blood were Ly6G^{+}, suggesting that CXCR2 gating was defining neutrophils as efficiently as Ly6G (**Figure 14B-C**). Anti-Ly6G treatment failed to completely deplete neutrophils from the circulation and in the infarcted heart as shown in the alternative CXCR2 gating strategy (**Figure 14D and E**). Neutrophils were drastically reduced in the blood after Ly6G treatment, and the reduction was less efficient in the heart in which neutrophils were reduced around 50% (**Figure 14D-F**). These data indicate that anti-Ly6G treatment failed to completely deplete neutrophil input in the infarcted heart, probably due to the massive neutrophil mobilization caused by the ischemic injury. Interestingly, although SiglecF^{hi} and SiglecF^{lo} neutrophils numbers were reduced after treatment, the SiglecF^{hi} proportion was higher in the anti-Ly6G treated group compared to control (**Figure 14F**). Since blood neutrophils are efficiently depleted at Day3 after MI, the shift in proportion of the SiglecF^{hi} and SiglecF^{lo} neutrophils corroborates the hypothesis that the SiglecF^{hi} state in the heart might be acquired by aging processes.

Overall, anti-Ly6G treatment failed to completely deplete neutrophils but instead induced a shift towards SiglecF^{hi} neutrophils, corroborating the notion that the SiglecF^{hi} state is acquired in the infarcted tissue.

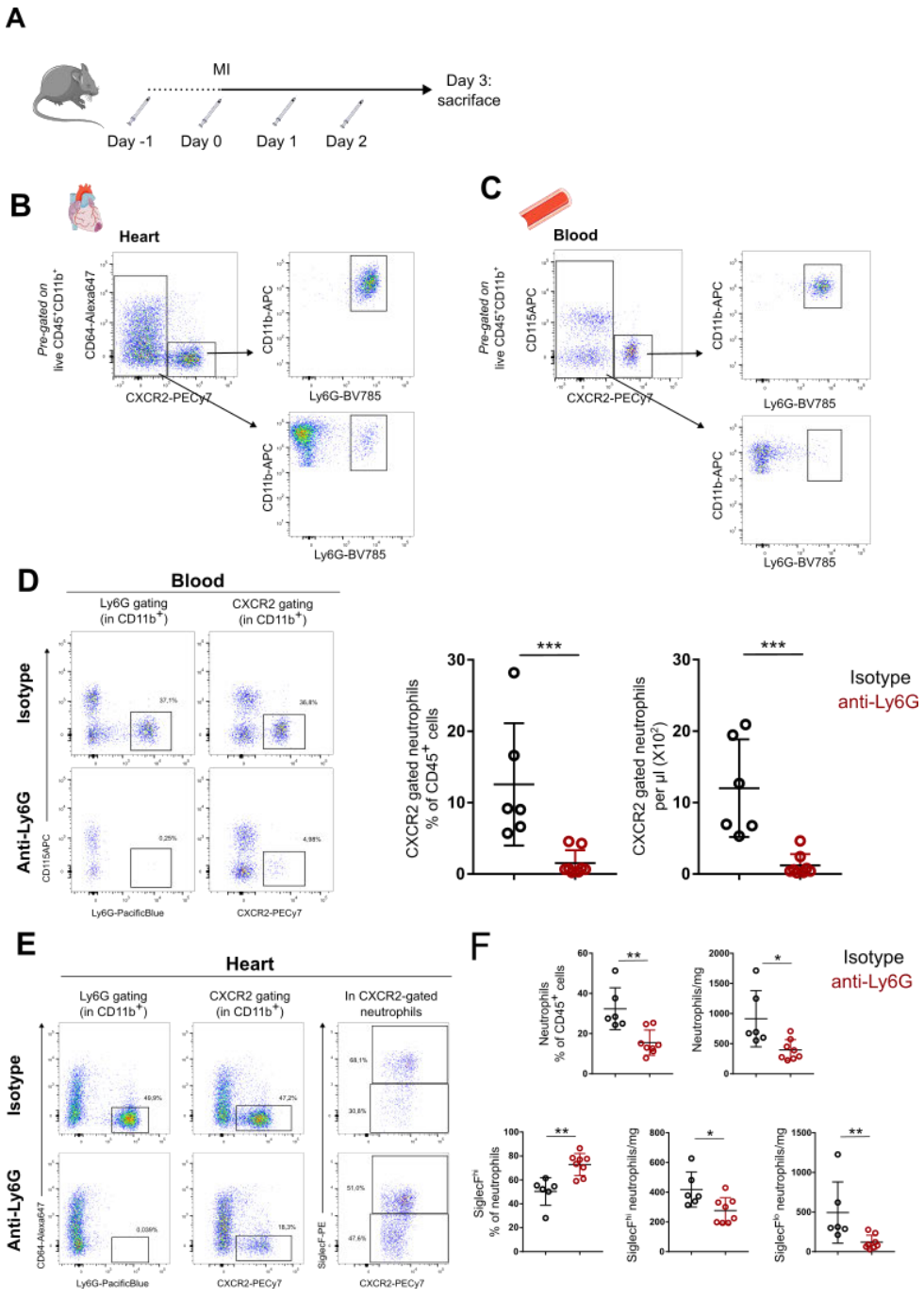

Figure 14: anti-Ly6G treatment induces partial neutrophils depletion and a shift towards SiglecF^{hi} in the infarcted heart. A, graphical representation of the experimental plan; **B**, representative flow cytometry plots of heart CD64/CXCR2 and CD11b/Ly6G cells; **C**, representative flow cytometry plots of heart CD115/CXCR2 and CD11b/Ly6G cells; **D**, representative flow cytometry plot of blood CD115/Ly6G

and CD115/CXCR2 cells (left) and quantitative analysis of the indicated cells (right) (Isotype group n=6; anti-Ly6G group n=8); **E**, representative flow cytometry plots of heart CD64/Ly6G and CD64/CXCR2 cells pre-gated in viable $CD45^{+}CD11b^{+}$ cells; **F**, quantitative analysis of the indicated cells ((Isotype group n=6; anti-Ly6G group n=8). Statistical analysis in panel **D** (right) and **F** was performed using Mann-Whitney U test. Images are taken from Servier Medical Art (smart.servier.com*)* and arranged with Inkscape.

5 Chapter 4: Dynamics of monocyte-derived macrophage diversity in experimental myocardial infarction

Here we used scRNA-seq analysis to explore monocytes and macrophage diversity in the heart after myocardial infarction. **Chapter 4** was published as a research article (Rizzo G., Gropper J., Piollet M., Vafadarnejad E., Rizakou A., Bandi S, Arampatzi P., Krammer T., DiFabion N., Dietrich O., Arias-Loza A., Prinz M., Mack M., Schlepckow K., Haass C., Silvestre J., Zernecke A., Saliba A., Cochain C. “Dynamic of monocyte-derived macrophage diversity in experimental myocardial infarction”) in the Journal “*Cardiovascular Research”* (2022), doi: https://doi.org/10.1093/cvr/cvac113. This is an Open Access article distributed under the terms of the Creative Commons Attribution-NonCommercial License (https://creativecommons.org/licenses/by-nc/4.0/), which permits non-commercial re-use, distribution, and reproduction in any medium, provided the original work is properly cited (CC-BY-NC open access license).

ESC European Society of Cardiology

Cardiovascular Research (2022) **00**, 1–14
https://doi.org/10.1093/cvr/cvac113

Dynamics of monocyte-derived macrophage diversity in experimental myocardial infarction

Giuseppe Rizzo[1,2], Julius Gropper[1,2], Marie Piollet[1,2], Ehsan Vafadarnejad[3], Anna Rizakou[2], Sourish Reddy Bandi[1,2], Panagiota Arampatzi [4], Tobias Krammer[3], Nina DiFabion[3], Oliver Dietrich[3], Anahi-Paula Arias-Loza[1], Marco Prinz [5,6,7], Matthias Mack[8], Kai Schlepckow[9], Christian Haass[9,10,11], Jean-Sébastien Silvestre [12], Alma Zernecke[2], Antoine-Emmanuel Saliba [3], and Clément Cochain [1,2]*

[1]Comprehensive Heart Failure Center, University Hospital Würzburg, Am Schwarzenberg 15, A15, 97078 Würzburg, Germany; [2]Institute of Experimental Biomedicine, University Hospital Würzburg, Josef-Schneider-Str. 2, D16, 97080 Würzburg, Germany; [3]Helmholtz Institute for RNA-based Infection Research (HIRI), Helmholtz-Center for Infection Research (HZI), Josef-Schneider-Str. 2, D15, 97080 Würzburg, Germany; [4]Core Unit Systems Medicine, University Hospital Würzburg, Josef-Schneider-Str. 2, D15, 97080 Würzburg, Germany; [5]Institute of Neuropathology, Faculty of Medicine, University of Freiburg, Freiburg, Germany; [6]Signalling Research Centres BIOSS and CIBSS, University of Freiburg, Freiburg, Germany; [7]Center for Basics in NeuroModulation (NeuroModulBasics), Faculty of Medicine, University of Freiburg, Freiburg, Germany; [8]Department of Internal Medicine II, Nephrology, Franz-Josef-Strauss Allee 11, University Hospital Regensburg, 93053 Regensburg, Germany; [9]German Center for Neurodegenerative Diseases (DZNE) Munich, 81377 Munich, Germany; [10]Division of Metabolic Biochemistry, Faculty of Medicine, Biomedical Center (BMC), Ludwig-Maximilians-Universität München, 81377 Munich, Germany; [11]Munich Cluster for Systems Neurology (SyNergy), 81377 Munich, Germany; and [12]Université de Paris, PARCC, INSERM, F-75015 Paris, France

Received 12 March 2022; revised 7 June 2022; accepted 26 June 2022

Time for primary review: 20 days

Aims Macrophages have a critical and dual role in post-ischaemic cardiac repair, as they can foster both tissue healing and damage. Multiple subsets of tissue resident and monocyte-derived macrophages coexist in the infarcted heart, but their precise identity, temporal dynamics, and the mechanisms regulating their acquisition of discrete states are not fully understood. To address this, we used multi-modal single-cell immune profiling, combined with targeted cell depletion and macrophage fate mapping, to precisely map monocyte/macrophage transitions after experimental myocardial infarction.

Methods and results We performed single-cell transcriptomic and cell-surface marker profiling of circulating and cardiac immune cells in mice challenged with acute myocardial infarction, and integrated single-cell transcriptomes obtained before and at 1, 3, 5, 7, and 11 days after infarction. Using complementary strategies of $CCR2^{+}$ monocyte depletion and fate mapping of tissue resident macrophages, we determined the origin of cardiac macrophage populations. The macrophage landscape of the infarcted heart was dominated by monocyte-derived cells comprising two pro-inflammatory populations defined as $Isg15^{hi}$ and $MHCII^{+}Il1b^{+}$, alongside non-inflammatory $Trem2^{hi}$ cells. $Trem2^{hi}$ macrophages were observed in the ischaemic area, but not in the remote viable myocardium, and comprised two subpopulations sequentially populating the heart defined as $Trem2^{hi}Spp1^{hi}$ monocyte-to-macrophage intermediates, and fully differentiated $Trem2^{hi}Gdf15^{hi}$ macrophages. Cardiac $Trem2^{hi}$ macrophages showed similarities to 'lipid-associated macrophages' found in mouse models of metabolic diseases and were observed in the human heart, indicating conserved features of this macrophage state across diseases and species. Ischaemic injury induced a shift of circulating $Ly6C^{hi}$ monocytes towards a $Chil3^{hi}$ state with granulocyte-like features, but the acquisition of the $Trem2^{hi}$ macrophage signature occurred in the ischaemic tissue. *In vitro*, macrophages acquired features of the $Trem2^{hi}$ signature following apoptotic-cell efferocytosis.

Conclusion Our work provides a comprehensive map of monocyte/macrophage transitions in the ischaemic heart, constituting a valuable resource for further investigating how these cells may be harnessed and modulated to promote post-ischaemic heart repair.

* Corresponding author. Tel: +49 931 201-48335; Fax: +49 931 201-648341, E-mail: cochain_c@ukw.de

Graphical Abstract

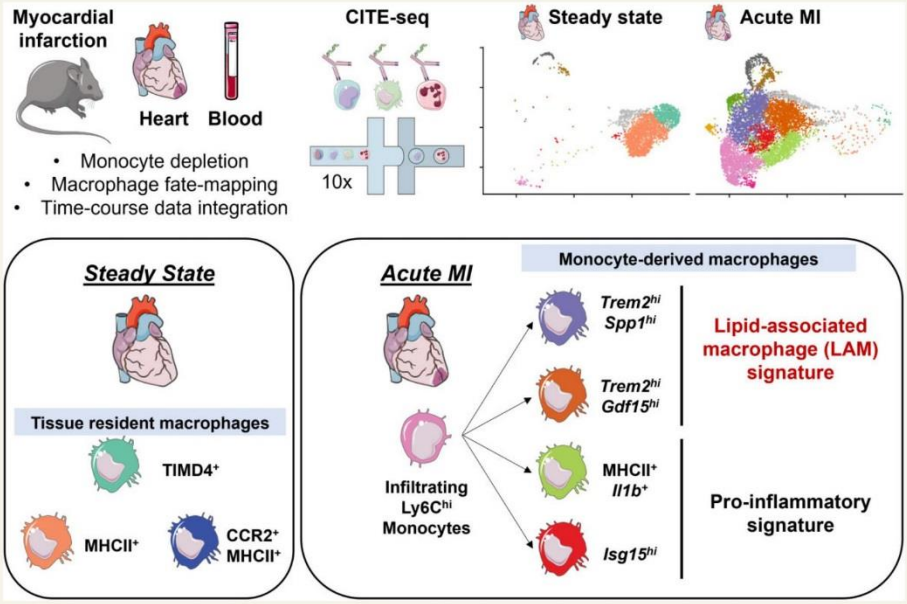

Keywords Monocyte • Macrophage • Inflammation • Myocardial infarction • Single-cell RNA-seq

1. Introduction

Macrophages are critically involved in cardiac repair after myocardial infarction (MI), where they have a dual role as they can either promote tissue repair or precipitate myocardial damage.[1] In the infarcted heart, cardiac macrophages form a large group of cells with different ontogenies,[2] temporal dynamics and states, and delineating the contribution of each macrophage subtype to post-MI cardiac repair remains a major challenge.[3] On one hand, resident tissue macrophages (RTMs) that self-renew independently of circulating monocyte input have cardioprotective functions.[4,5] On the other hand, recruited monocyte-derived macrophages that numerically predominate during the acute post-MI phase adopt more heterogeneous phenotypes, and can either drive tissue repair or damage.[3] Fundamental work investigating the kinetics of monocyte/macrophage transitions in the infarcted heart based on flow cytometry or bulk transcriptomics has established the notion that functionally distinct subsets of monocytes and monocyte-derived cells are present in the heart with specific temporal dynamics.[6–8] More recent advances based on single-cell transcriptomic profiling have highlighted a substantial heterogeneity of monocyte-derived macrophages in various disease contexts.[9] Although single-cell analysis has provided new insights into cardiac resident macrophage diversity[4] or the Type I interferon (IFN) response in macrophages after ischaemic injury,[10,11] a detailed analysis of the monocyte-to-macrophage transition after acute MI has not been performed previously, and the identity of monocyte-derived macrophage subsets, their dynamics, and the mechanisms regulating their acquisition of discrete states associated with specific functional capacities remain to be precisely characterized. The recent introduction of multi-modal single-cell analysis, and in particular, the simultaneous measurement of transcript expression and cell-surface markers in single cells via cellular indexing of transcriptomes and epitopes by sequencing (CITE-seq),[12] offers a unique opportunity to refine our understanding of monocyte-derived macrophage heterogeneity in the infarcted myocardium.

Here, we used CITE-seq,[12] combined with targeted depletion of circulating CCR2$^+$ monocytes and fate-mapping analysis of tissue resident macrophages, to precisely characterize circulating and cardiac monocyte-derived cell states after experimental MI. We identified monocyte-derived macrophage subsets with discrete gene expression signatures and analysed their dynamics in the infarcted heart. Notably, we identified macrophages presenting a *Trem2*^{hi} lipid-associated gene expression signature acquired in the ischaemic heart, and reminiscent of a lipid-associated macrophage (LAM) signature found in other tissues in metabolic disease contexts. Altogether, our work presents a refined time-resolved map of monocyte/macrophage transitions after experimental MI, providing a valuable resource for further understanding the multifaceted roles of monocytes and macrophages in ischaemic heart repair.

2. Methods

Detailed experimental methods are available with Supplementary material online. Single-cell RNA-seq and CITE-seq data shown in this report can be browsed in a web-accessible interface: https://infection-atlas.org/Rizzo2022/.

All animal studies and numbers of animals used conform to the Directive 2010/63/EU of the European Parliament and have been approved by the appropriate local authorities (Regierung von Unterfranken, Würzburg, Germany, Akt.-Z. 55.2-DMS-2532-2-743 and 2-865). Illustrations were created using Servier Medical Art (smart.servier.com). In all experiments, animals were killed by cervical dislocation under isoflurane anaesthesia (induced by isoflurane inhalation 4.0%).

3. Results

3.1 Single-cell CITE-seq analysis of macrophages in the healthy and infarcted heart

Myocardial infarction is characterized by rapid and massive infiltration of inflammatory monocytes and a shift in the cardiac monocyte/macrophage landscape.[6,7] To obtain a high-dimensional characterization of monocyte/macrophage shifts in the ischaemic heart based on transcriptomic profiling and analysis of cell-surface marker expression, we performed CITE-seq analysis of cardiac CD45$^+$ cells encompassing 45 epitopes defining all the main immune lineages and discrete subsets of innate and adaptive immune cells (see Section 2). We analysed CD45$^+$ cells extracted from the heart of male wild-type C57BL6/J mice in the steady state ($n = 5$) and at 5 days after MI ($n = 9$), comprising a total of 13 805 cells (*Figure 1A and B*). We performed our main analysis at Day 5 after MI, as it represents a time point where differentiated macrophages are abundant, but active Ly6C^{hi} monocyte recruitment is still ongoing,[7] which allows capturing unsynchronized cells at various stages of the monocyte-to-macrophage transition in a single data set. Immune cell lineages were identified using canonical surface markers of T cells (CD3), NK cells (NK1.1), γδT cells (γδTCR), B cells (CD19), dendritic cells (DCs: MHCII, CD11c) including XCR1$^+$ cDC1, plasmacytoid DCs (SiglecH), neutrophils (Ly6G), F4/80$^+$CD64$^+$CX3CR1$^+$Ly6C^{lo} macrophages comprising steady-state RTMs and macrophages appearing after MI (MI Mac), and monocytes (Ly6C$^+$; *Figure 1C*, see Supplementary material online, *Figure S1A*). Cellular identities, including small clusters of contaminating endothelial cells and fibroblasts, were confirmed by examination of enriched transcripts (see Supplementary material online, *Figure S1B*). Monocytes/macrophages ($n = 10\,365$ cells) were extracted and reclustered *in silico* to precisely delineate subpopulations and their distribution in the healthy and infarcted heart (*Figure 1D and E*). Based on differentially expressed cell-surface markers and transcripts (*Figure 1F–H*, see Supplementary material online, *Figure S1C and D*), we annotated 13 populations of monocytes/macrophages and their relative abundance in the steady-state and ischaemic heart (*Figure 1D and E*, see Supplementary material online, *Figure S1E and F*).

At the steady state, we found two RTM populations, the first one represented 23.40 ± 2.28% of all steady-state macrophages and was defined as TIMD4$^+$LYVE1$^+$MHCII^{low}*Folr2*^{hi}, corresponding to previously described cardiac RTM defined as Lyve1$^+$,[13] TIMD4$^+$,[4] or more recently 'TLF' (TIMD4$^+$LYVE1$^+$Folr2$^+$).[14] Here, we termed this population RTM-TIMD4 (*Figure 1D–F*). The second RTM population was MHCII$^+$ with low expression of RTM-TIMD4 surface markers and transcripts, called RTM-MHCII (60.33 ± 1.52% of all steady-state macrophages) (*Figure 1D–H* and see Supplementary material online, *Figure S1C, E and F*). We identified surface markers differentially expressed by RTM subsets: compared with MI-associated macrophages, RTM-TIMD4 and RTM-MHCII expressed higher surface MGL2 (*Figure 1H*). RTM-TIMD4 additionally expressed high CD163, and part of this cluster expressed VSIG4 (*Figure 1H*). While RTM-TIMD4 and RTM-MHCII were mostly negative for *Ccr2* expression (*Figure 1I and J*), previous reports have identified a third cardiac RTM subset defined as CCR2$^+$MHCII$^+$,[4] and it was recently proposed that three RTM subsets populate mouse tissues, namely 'TLF', MHCII$^+$, and CCR2$^+$ macrophages, each presenting a specific core gene expression signature conserved across organs.[14] To better resolve steady-state populations of cardiac monocyte/macrophages, we reclustered cells from the steady state alone, which recovered similar populations (see Supplementary material online, *Figure S2A–C*). *Ccr2* expression was observed in Ly6C^{hi} monocytes (which represent monocytes within the tissue, as ensured by exclusion of intravenous leucocytes during sorting, see Supplementary Methods). *Ccr2* was also detected within the RTM-MHCII$^+$ cluster, which is in line with the existence of resident CCR2$^+$MHCII$^+$ macrophages in the heart.[4,14] However, in our hands, CCR2$^+$MHCII$^+$ RTM did not form a separate cluster as proposed in Dick *et al.*[4,14] We manually gated *Ccr2*$^+$ cells within the RTM-MHCII$^+$ population (see Supplementary material online, *Figure S2D and E*) and analysed expression of 'core signature genes' of the three RTMs conserved across organs (including the heart) as defined in Dick *et al.*[14] Within these three bona fide RTM alone, relative expression of the core signature genes appeared mostly consistent with the distribution recently proposed in Dick *et al.*[14] When considering all steady-state cardiac populations, relative expression of the genes of the 'CCR2$^+$ RTM' signature was highest in monocytes, excepted for MHCII encoding transcripts (see Supplementary material online, *Figure S2F and G*).

At Day 5 post-MI, the monocyte/macrophage compartment was dominated by Ly6C^{hi} monocytes (17.56 ± 6.58% of monocytes/macrophages at Day 5 post-MI), pro-inflammatory macrophages expressing MHCII and enriched in *Il1b*, *Tnip3*, *Tlr2*, or *Tnfsf9* (MHCII$^+$*Il1b*$^+$; 14.51 ± 3.70% of monocytes/macrophages), and Type I IFN signature cells enriched for *Isg15* (previously termed IFNIC: IFN-inducible cells[10]; *Isg15*^{hi}, 6.25 ± 1.91%; *Figure 1D–G*). We also delineated three clusters sharing enrichment for *Trem2* (*Trem2*^{hi}; *Figure 1D and G*). A first *Trem2*^{hi} population had high expression of *Spp1* encoding osteopontin (*Trem2*^{hi}*Spp1*^{hi}, 21.20 ± 4.63% of monocytes/macrophages), a second cluster was enriched for *Gdf15* (*Trem2*^{hi}*Gdf15*^{hi}, 20.74 ± 5.01% of monocytes/macrophages), while a third cluster was characterized by enrichment for *Prdx1* (*Trem2*^{hi}*Prdx1*^{hi}; 2.51 ± 1.24% of monocytes/macrophages; *Figure 1D and G*). Low levels of Ly6C^{low} monocytes and a population defined as *Fn1*^{hi}*Ltc4s*^{hi} were observed. Finally, we recovered a minor population characterized by mixed expression of tissue resident and MI-associated macrophage markers, found at similar levels in both experimental conditions, showing low transcript variety and a low RNA content ('low RNA' cluster, see Supplementary material online, *Figure S1C and D*). We interpret these cells as low-quality cells damaged during sample preparation, and did not consider them further in subsequent analyses.

As the data presented in *Figure 1*, results from computational integration of two independent CITE-seq experiments where samples were pooled using cell hashing[15] (see Section 2), we ensured reproducibility of our observations by analysing both experiments independently with similar analysis parameters as those used initially in *Figure 1*. The result of the analysis is presented in Supplementary material online, *Figure S3*. In each separate experiment, similar populations of monocytes/macrophages were recovered, although some small populations (*Trem2*^{hi}*Prdx1*^{hi} and Ly6C^{lo} monocytes enriched in, e.g. *Ace* or *Ear2*) were not resolved at the clustering resolution used (see

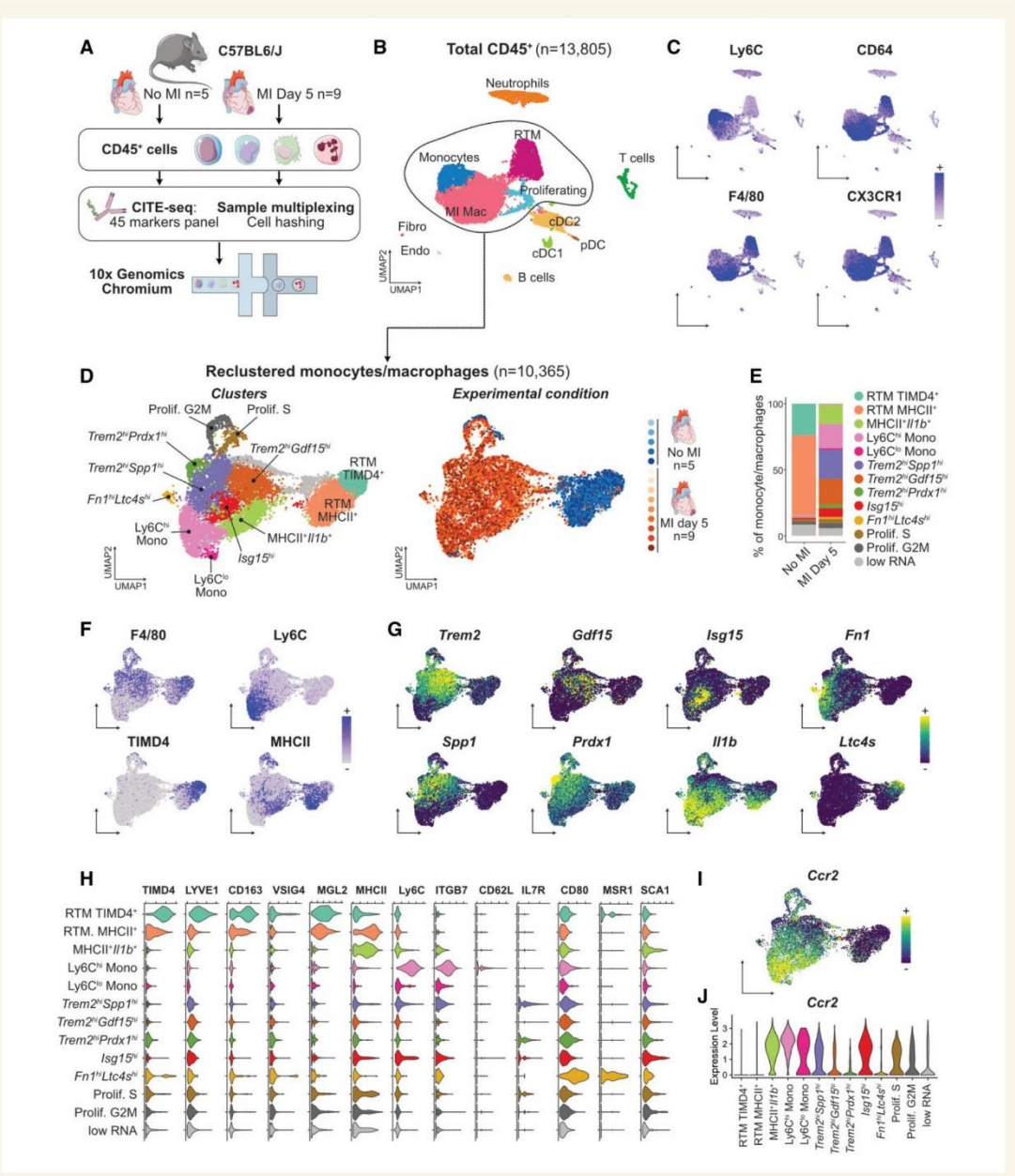

Figure 1 CITE-seq analysis of the monocyte/macrophage landscape in the steady-state and infarcted heart. For all graphs in this figure, cells were obtained from $n = 5$ mice without MI, and $n = 9$ mice with MI, pooled from two independent experiments (see Section 2). (*A*) Experimental design summary; (*B*) UMAP representation of transcriptome-based clustering of $n = 13\,805$ total cardiac CD45$^+$ cells; (*C*) CITE-seq signal for the indicated monocyte/macrophage surface markers projected onto the total CD45$^+$ cells UMAP plot; (*D*) $n = 10\,365$ cells corresponding to monocytes and macrophages (including proliferating macrophages) were extracted for clustering and UMAP dimensional reduction analysis with annotated cell clusters (left) and sample of origin colour coded on the UMAP plot (right); (*E*) average proportions of each cluster according to experimental condition; (*F*) surface markers and (*G*) transcript expression projected onto the UMAP plot for selected markers used to identify and annotate clusters; (*H*) expression of the indicated surface markers in each monocyte/macrophage cluster; (*I* and *J*) expression of *Ccr2* projected on the UMAP plot of monocyte/macrophages (*I*) and shown across clusters (*J*). RTM, resident tissue macrophages; MI Mac, MI-associated macrophages; (p)DC, (plasmacytoid) dendritic cell; Endo, endothelial cells; Fibro, fibroblasts.

Supplementary material online, *Figure S3A–J*). We also observed variability in distribution of RTM to the RTM-TIMD4^{+} or RTM-MHCII^{+} clusters, which we attribute to 'intermediate' TIMD4^{int}MHCII^{int} cells, also observed by flow cytometry (see Supplementary material online, *Figure S3L*), distributing preferentially to the RTM-MHCII^{+} (Experiment 1) or RTM-TIMD4^{+} (Experiment 2) clusters in different experiments (see Supplementary material online, *Figure S3B, G and K*). Clustering analysis of each biological replicate independently also provided consistent results, although the analysis of much lower cell numbers in each single replicate overall yielded a lower clustering granularity (see Supplementary Analysis R Notebook).

3.2 *Trem2^{hi}* macrophage subsets have a LAM transcriptional signature conserved in humans

Trem2 expression is characteristic of a LAM (lipid-associated macrophage) signature previously defined by single-cell RNA-seq in metabolic disease contexts, such as in the obese adipose tissue,[16] in atherosclerotic lesions,[17,18] and in the liver in experimental models of NAFLD[19] and NASH.[20] At first glance, cardiac *Trem2^{hi}* macrophage populations appeared enriched for some characteristic LAM transcripts (e.g. *Gpnmb*, *Spp1*, *Ctsd*, *Cd63*, *Psap*; see Supplementary material online, *Figure S1C*). To further explore gene expression similarities across tissues, we first extracted a list of 66 commonly enriched transcripts (see Section 2) in Foamy/*Trem2^{hi}* macrophages in atherosclerotic lesions,[18] and LAMs in the NASH liver,[20] two lipid driven pathologies, and used these to calculate a 'LAM gene signature' score in cardiac macrophages. The LAM signature was highest in *Trem2^{hi}Spp1^{hi}* and *Trem2^{hi}Prdx1^{hi}* macrophages, followed by the *Trem2^{hi}Gdf15^{hi}* cluster (*Figure 2A*). Gene ontology analysis revealed putatively enriched biological processes relevant to a LAM state, for example, 'positive regulation of macrophage foam cell formation' in *Trem2^{hi}Spp1^{hi}*, and 'positive regulation of cholesterol efflux' in *Trem2^{hi}Gdf15^{hi}* macrophages (*Figure 2B*). LAM-signature transcripts (e.g. *Gpnmb*, *Pld3*, *Nceh1*, *Psap*) showed a clear and specific enrichment in *Trem2^{hi}* macrophage populations (*Figure 2C*). When directly integrating scRNA-seq data obtained from the infarcted heart, NASH liver, and atherosclerotic aortas, *Trem2^{hi}* MI-associated cardiac macrophage populations clustered together with Foamy/*Trem2^{hi}* macrophages from atherosclerotic vessels[18] and LAMs from NASH liver[20] (see Supplementary material online, *Figure S4A–C*). *Gpnmb* has previously been associated with the LAM signature[19–21] and appeared specifically enriched in *Trem2^{hi}* MI-associated cardiac macrophages with a LAM signature (*Figure 2C*). At Day 5 after MI, GPNMB expressing CD68^{+} macrophages were observed specifically in the infarcted area of the myocardium (*Figure 2D*, see Supplementary material online, *Figure S5*), indicating that LAM-signature macrophages accumulate in the infarcted area. TREM2 protein levels were increased in the heart of infarcted mice compared with sham controls at Day 5 (*Figure 2E*), further confirming cardiac accumulation of TREM2 expressing cells after MI.

The macrophage LAM signature is conserved across species in various disease contexts.[16,18,22] To evaluate whether the LAM signature was also found in the diseased human heart, we analysed recently published data from human ischaemic cardiomyopathy patients ($n = 3$ samples ischaemic left ventricle, 1 sample remote non-ischaemic left ventricle, and 1 sample control myocardium).[23] A population of macrophages enriched for characteristic genes of the LAM signature (e.g. *TREM2*, *SPP1*, *CTSD*, *FABP5*) was readily observed (see Supplementary material online, *Figure S4D and E*).

We further analysed the gene expression signature of the major *Trem2^{hi}Spp1^{hi}* and *Trem2^{hi}Gdf15^{hi}* populations, relative to other abundant MI-associated macrophages, that is MHCII^{+}*Il1b*$^{+}$ and *Isg15^{hi}* clusters, with a focus on experimentally validated effectors (*Figure 2F*). MHCII^{+}*Il1b*$^{+}$ macrophages were enriched in transcripts associated with a pro-inflammatory and pathogenic profile (e.g. *Axl*,[24] *Nlrp3*[25]), while *Isg15^{hi}* highly expressed *Il18*[26] in addition to their typical Type I IFN response signature (*Isg15*, *Irf7*, *Cxcl10*).[10,11] In contrast, *Trem2*-enriched populations highly expressed genes involved in immune modulation, tissue repair and efferocytosis (*Trem2^{hi}Spp1^{hi}*: *Hmox1*,[27] *Arg1*,[28] *Anxa1*[29]; *Trem2^{hi}Gdf15^{hi}*: *Igf1*,[30] *Gdf15*,[31] *Mertk*,[32] *Timp2*,[33] *Apoe*[34]). Both *Trem2^{hi}* populations were enriched for expression of the profibrotic, LAM-signature transcript[19] *Spp1* (with highest levels observed in *Trem2^{hi}Spp1^{hi}*). *Trem2^{hi}Spp1^{hi}* were additionally enriched for profibrotic *Mmp14* (encoding MT1-MMP)[35] (*Figure 2F*). Altogether, our data show the accumulation of two populations of *Trem2^{hi}* macrophages in the ischaemic heart harbouring a LAM signature also identified in other organs and disease contexts and in the diseased human heart.

3.3 Dynamics of monocyte/macrophage populations in the infarcted heart

To resolve the kinetics of MI-associated macrophage accumulation, we integrated our data with existing scRNA-seq data sets of cardiac macrophages from the steady state and at 1, 3, 5, 7, and 11 days after MI[4,36,37] (*Figure 3A* and see Supplementary material online, *Figure S6A and B*), representing a total of 24 637 cells. Similar MI-associated populations were recovered, although the minute *Trem2^{hi}Prdx1^{hi}* population grouped with *Trem2^{hi}Spp1^{hi}* macrophages at this clustering resolution (see Supplementary material online, *Figure S6C*). We observed dynamic transitions within the monocyte/macrophage compartment (*Figure 3A and B*). *Trem2^{hi}Spp1^{hi}* cells peaked at Days 3–5 post-MI, while *Trem2^{hi}Gdf15^{hi}* cells peaked at Days 5–7 (*Figure 3A and B*). Infiltration of MHCII^{+}*Il1b*$^{+}$ and *Isg15^{hi}* macrophages also peaked at Days 3–7. At Days 7 and 11, partial recovery of RTM subsets was observed (*Figure 3A and B*). To better resituate our observations relative to previous analyses of monocyte/macrophage dynamics in the infarcted heart performed using flow cytometry,[6] we analysed the expression of Ly6C, a monocyte surface marker, vs. expression of macrophage differentiation markers (CD64, CX3CR1, and F4/80) on monocytes and the major MI-associated macrophage populations (*Figure 3C and D*, see Supplementary material online, *Figure S6D*). Ly6C^{hi} monocytes where Ly6C^{hi}CD64^{low}CX3CR1^{low}F4/80^{low} and *Trem2^{hi}Gdf15^{hi}* cells appeared as fully differentiated macrophages (Ly6C^{low}CD64^{hi}CX3CR1^{hi}F4/80^{hi}), while *Trem2^{hi}Spp1^{hi}* had a Ly6C^{int}CD64^{int}CX3CR1^{int}F4/80^{int} profile suggestive of a monocyte-to-macrophage intermediate state (*Figure 3C and D*, see Supplementary material online, *Figure S6D*). Altogether, these data suggest that the *Trem2^{hi}Spp1^{hi}* population represents a monocyte-to-macrophage intermediate state while *Trem2^{hi}Gdf15^{hi}* cells are differentiated macrophages, and that these populations sequentially peak in the infarcted heart.

3.4 *Trem2^{hi}* macrophage populations originate from recruited monocytes

Macrophage origin (i.e. self-renewing tissue resident macrophage vs. monocyte-derived macrophage) has been proposed as a major driver of cardiac macrophage function.[3] We thus investigated the origin of the major MI-associated macrophage populations. High *Ccr2* expression in MHCII^{+}*Il1b*$^{+}$ and *Isg15^{hi}* clusters (*Figure 1I and J*), clearly indicates a

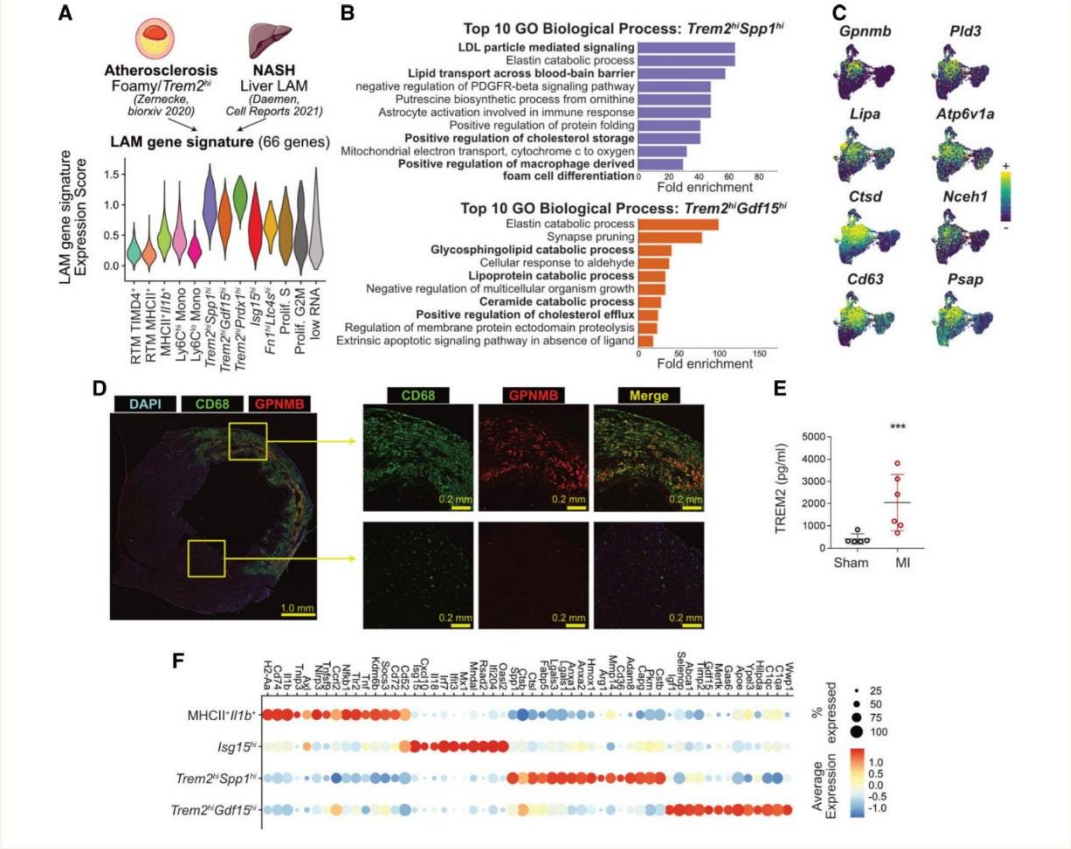

Figure 2 Identification of *Trem2*^{hi} macrophages with a LAM signature in the ischaemic myocardium. (*A*) Sixty-six LAM-signature genes were extracted from the indicated data sets and a gene expression score was applied to cardiac macrophages (LAM-signature expression score), represented here as a violin plot. The atherosclerosis data set consists of a pool of $n = 12$ scRNA-seq data sets (see Zernecke *et al.*[18]); the NASH data set of one scRNA-seq library (Daemen *et al.*[20]); the LAM-signature expression score was applied to cardiac macrophages ($n = 10\,365$ cells; cells were obtained from $n = 5$ mice without MI, and $n = 9$ mice with MI, pooled from two independent experiments, see *Figure 1*, see Section 2). (*B*) Fold enrichment for the top 10 enriched Gene Ontology (GO) Biological Processes in the indicated cardiac macrophage cluster (all with adjusted *P*-value <0.05); macrophage clusters were determined in analysis shown in *Figure 1D* from $n = 10\,365$ cells; cells were obtained from $n = 5$ mice without MI, and $n = 9$ mice with MI, pooled from two independent experiments. (*C*) Expression of selected LAM-signature transcripts projected on the UMAP plot of monocytes/macrophages as detailed in *Figure 1D* ($n = 10\,365$ cells; cells were obtained from $n = 5$ mice without MI, and $n = 9$ mice with MI, pooled from two independent experiments). (*D*) Immunofluorescence labelling of CD68 and GPNMB in Day 5 infarcts with overview of a full myocardial section and high magnification images of the infarcted area and remote non-ischaemic myocardium (representative pictures shown for $n = 1$ heart). (*E*) Total levels of TREM2 detected by ELISA in extracts from the hearts of mice after sham operation ($n = 5$ mice) or permanent MI (Day 5; $n = 6$ mice). (*F*) Dot plot showing expression of the selected transcripts in the indicated cardiac macrophage clusters (all the transcripts shown significantly enriched in the relevant clusters with adjusted *P*-value <0.05); macrophage clusters were determined in analysis shown in *Figure 1D* from $n = 10\,365$ cells; cells were obtained from $n = 5$ mice without MI, and $n = 9$ mice with MI, pooled from two independent experiments. NASH, non-alcoholic steatohepatitis.

monocytic origin. *Trem2*^{hi}*Spp1*^{hi} and *Trem2*^{hi}*Gdf15*^{hi} macrophages expressed intermediate and low levels of *Ccr2*, respectively (*Figure 1I*), and lacked expression of surface markers associated with RTM subsets (CD163, TIMD4, LYVE1, VSIG4, MHCII; *Figure 1*), suggesting a monocytic origin. We hypothesized that *Trem2*^{hi} macrophages originate from Ly6C^{hi}*Ccr2*$^{+}$ monocytes that lose *Ccr2* expression upon differentiation in the heart.

To test this hypothesis, we first depleted circulating Ly6C^{hi} monocytes in mice using the anti-CCR2 monoclonal antibody MC-21.[38] Twenty-four hours after a single injection, Ly6C^{hi} monocytes were efficiently depleted from the bloodstream as previously described[38] (see Supplementary material online, *Figure S7A*), and MI was induced. Monocyte depletion was maintained by daily i.p. injections of anti-CCR2 until Day 5 after MI (see Supplementary material online,

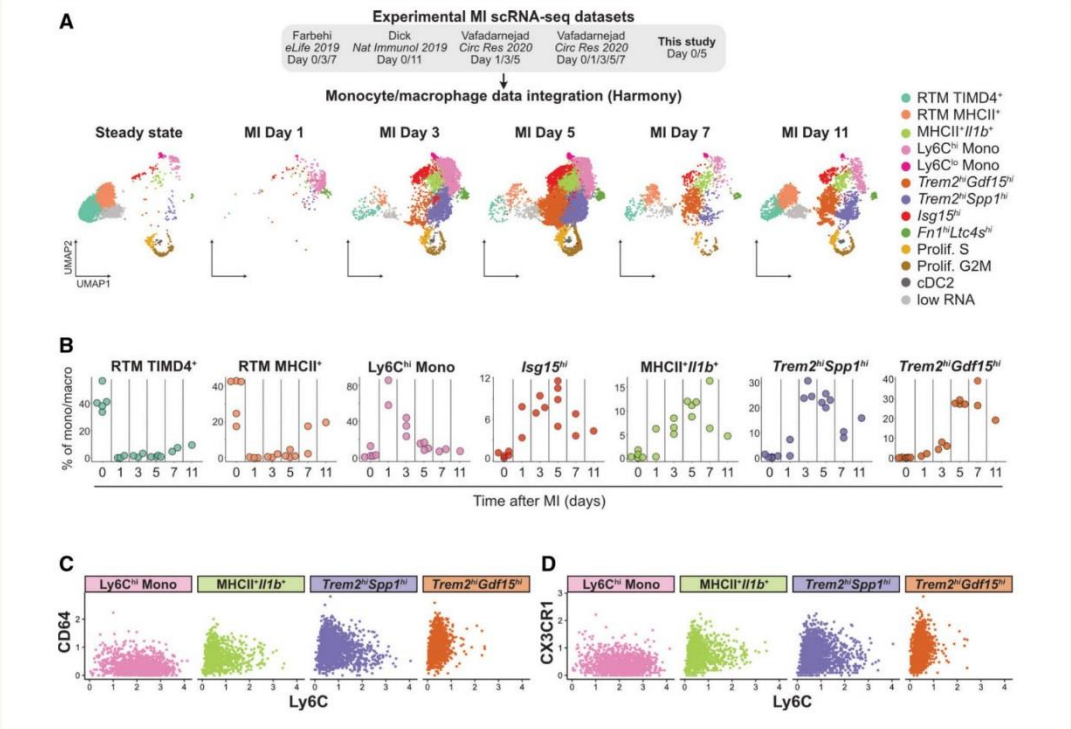

Figure 3 Monocyte/macrophage dynamics in the infarcted heart. (*A*) The indicated MI data sets were integrated using Harmony and monocyte/macrophage population identified; the resulting clustering analysis and UMAP plot are shown split according to time point after MI with monocyte/macrophage clusters colour coded; $n = 24\,637$ total cells from $n = 6$ independent scRNA-seq data sets. (*B*) Proportion of the indicated clusters within total monocyte/macrophage over the post-MI time continuum, calculated from the integrated data set. Each data point represents proportion of the indicated cluster at the indicated time point in independent scRNA-seq libraries (see also Supplementary material online, *Figure S5*). (*C*) CITE-seq signal for Ly6C vs. CD64 and (*D*) Ly6C vs. CX3CR1 in the indicated cell populations (analysis in *C* and *D* performed on monocyte/macrophage clusters determined in analysis shown in *Figure 1D* from $n = 10\,365$ cells; cells were obtained from $n = 5$ mice without MI, and $n = 9$ mice with MI, pooled from two independent experiments).

Figure S7B), where cardiac CD45$^+$ cells were sampled for CITE-seq analysis (*Figure 4A–C*). Analysis of CITE-seq data identified the main CD45$^+$ cell populations and monocyte/macrophage subsets (*Figure 4C*) similar to those described above (*Figure 1*). While levels of RTM subsets were not affected by CCR2$^+$ cell depletion, known circulating monocyte-derived populations (Ly6C^{hi} monocytes, MHCII$^+$*Il1b*$^+$ macrophages, *Isg15*^{hi}) were strongly reduced in the infarcted heart at Day 5. The *Fn1*^{hi}*Ltc4s*^{hi} population was not affected, indicating that it is independent of CCR2$^+$ monocyte recruitment. We furthermore noted a drastic reduction of *Trem2*^{hi}*Spp1*^{hi} and *Trem2*^{hi}*Gdf15*^{hi} macrophages counts, indicating that accumulation of these cells is dependent on circulating monocyte infiltration (*Figure 4D*). Additionally, cDC1[39] and cDC2, proposed to be *Ccr2* dependent in inflammatory contexts[40] were reduced (see Supplementary material online, *Figure S7D*). Cardiac neutrophils, T cells, NK cells, and pDC numbers were not affected by anti-CCR2 (see Supplementary material online, *Figure S7C*).

To further confirm that *Trem2*^{hi} macrophage populations derive from monocytes, we then analysed the expression of *TdTomato* transcripts that mark RTM in pulse-labelled Cx3cr1^{CreERT2} mice in Dick *et al.*[4] from our integrated analysis (*Figure 4E and F*). *TdTomato* transcripts mapped preferentially to tissue resident and proliferating macrophages, while only scattered cells were observed in *Trem2*^{hi} subsets and MHCII$^+$*Il1b*$^+$ cells (*Figure 4E and F*). We additionally performed fate-mapping analysis of RTM and MI-associated macrophages by flow cytometry in tamoxifen-pulsed *Cx3cr1*^{creERT2}-*Rosa26*^{EYFP} mice[41] after a 4-week washout period (*Figure 4G*), when circulating Ly6C^{hi} monocytes had lost YFP expression while microglia were >90% YFP$^+$ (*Figure 4H*). Only partial recombination was observed in long living macrophages such as TIMD4$^+$MHCII$^-$ RTM ($40.35 \pm 4.45\%$) in the steady state, which remained stable after MI ($41.63 \pm 7.65\%$ YFP+ in TIMD4$^+$MHCII$^-$ RTM; *Figure 4I and J*). At 7 days after MI TIMD4$^-$MHCII$^-$ macrophages, most MI-associated macrophage populations including *Trem2*^{hi} subsets, as defined by CITE-seq (*Figure 1*), were overwhelmingly YFP^{neg} ($93.47 \pm 2.25\%$; *Figure 4I and J*). Although partial tamoxifen-induced recombination in RTM represents a limitation of our analysis, these data nevertheless suggest that pre-existing RTM do not represent a major source of MI-associated TIMD4$^-$MHCII$^-$ macrophages (*Figure 4I and J*). Altogether, our complementary approaches of circulating CCR2$^+$

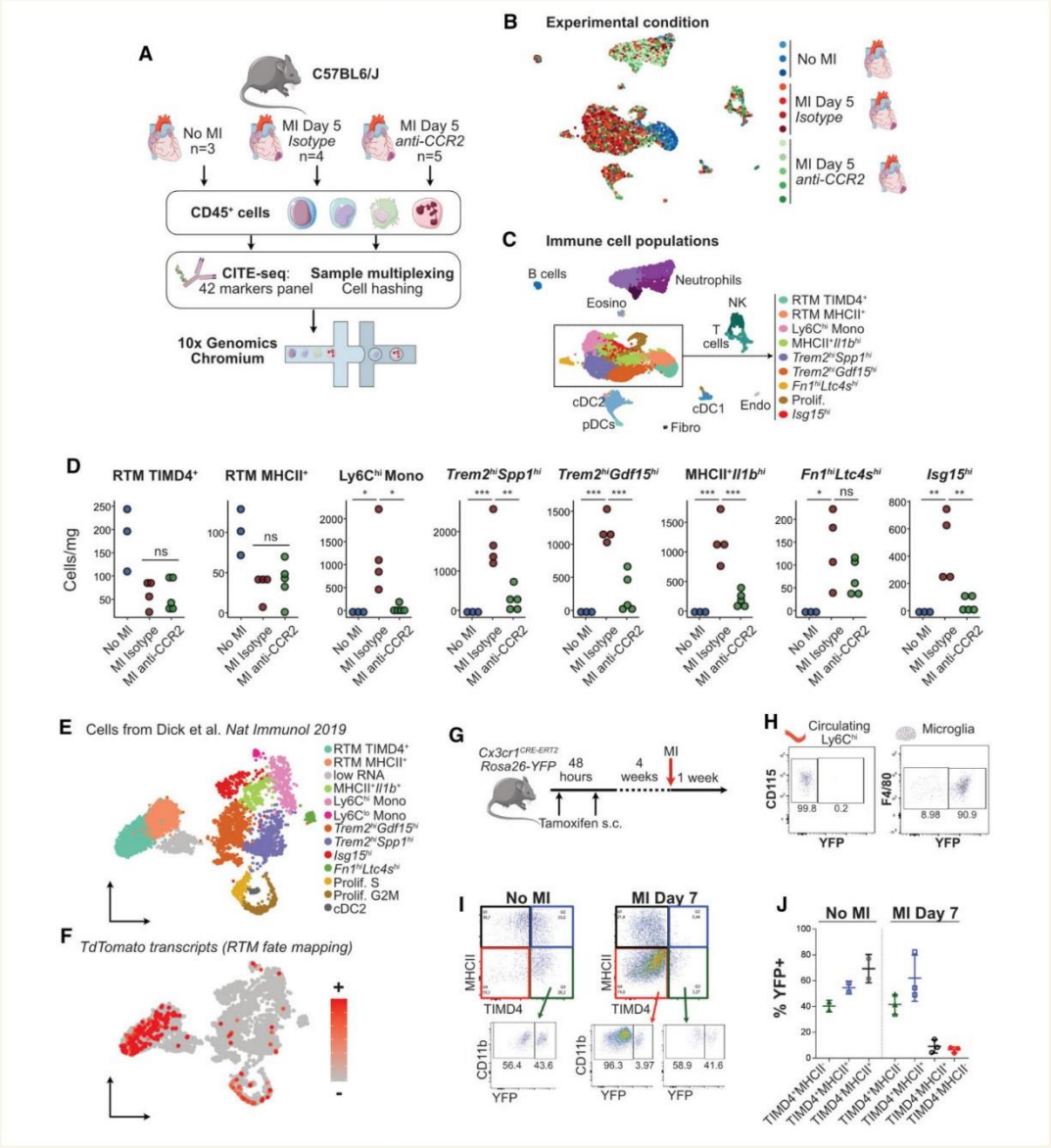

Figure 4 MI-associated macrophage populations originate from recruited CCR2^{+} monocytes. (*A*) Schematic representation of the experimental design; (*B* and *C*) UMAP representation of scRNA-seq analysis ($n = 10\,831$ cells) with (*B*) sample of origin and (*C*) biological identity of cell clusters colour coded on the UMAP plot; (*D*) absolute counts of the indicated cell clusters (per mg of cardiac tissue); data shown in *A–D* were obtained from one experiment with $n = 3$ mice without MI, $n = 4$ mice at Day 5 after MI treated with isotype control; $n = 5$ mice at Day 5 after MI treated with anti-CCR2; (*E*) annotated UMAP plot of cells from Dick *et al.*[4] ($n = 5802$ cells from $n = 1$ scRNA-seq data set from mice without MI and $n = 1$ scRNA-seq data sets from mice at 11 days after MI) extracted from integrated data analysis shown in *Figure 3* and (*F*) identification of TdTomato^{+} fate mapped RTMs, cells ordered according to transcript detection, that is, cells with detectable transcripts moved to front of the plot; (*G*) experimental setup for CX3CR1-based fate mapping of tissue resident macrophages; (*H*) recombination controls in Ly6C^{hi} monocytes and microglia after the 4 weeks washout period; (*I* and *J*) fate mapping of cardiac macrophages before and at 7 days post-MI, pre-gated on live CD45^{+}CD11b^{+}F4/80^{hi}Ly6C^{low}. Data shown in *G–J* were obtained in one experiment with $n = 2$ mice without MI and $n = 3$ mice at Day 7 after MI.

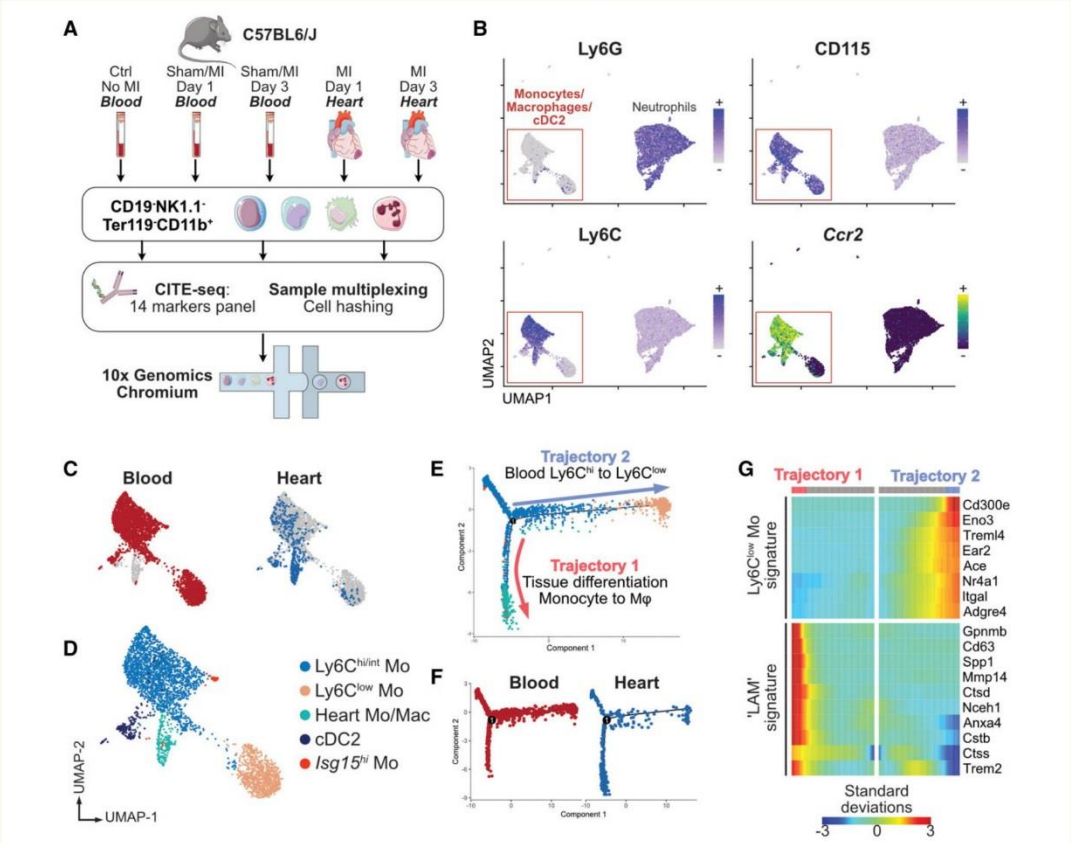

Figure 5 Monocytes/macrophages acquire the *Trem2*^{hi} LAM signature in the ischaemic heart. (*A*) Experimental design overview; (*B*) *Ccr2* transcript expression and CITE-seq signal for the indicated surface markers in blood and heart CD19^{-}NK1.1^{-}Ter119^{-}CD11b^{+} cells projected on the UMAP plot (n = 9848 cells); (*C*) tissue of origin of single cells corresponding to monocytes/macrophages/cDC2 (n = 3378 cells) projected on the UMAP plot; (*D*) clustering analysis and annotation of cell clusters; (*E*) pseudotime analysis of monocytes/macrophages in Monocle, cell identity colour-code identical to *D* (n = 3378 cells); (*F*) pseudotime analysis split according to tissue origin; (*G*) heatmap of pseudotime gene expression variation for selected genes on branches of the pseudotime tree (as indicated on *E*; n = 3378 cells; all indicated genes show statistically significant variation). All data shown in *Figure 5* were obtained from n = 1 pooled cell preparation per experimental condition, grouped in a single (n = 1) multiplexed scRNA-seq data set.

monocyte depletion, fate mapping of RTM in previously published scRNA-seq data, and fate mapping of RTM by flow cytometry indicate that *Trem2*-enriched, MI-associated macrophage subsets originate from recruited monocytes.

3.5 The macrophage *Trem2*^{hi}/LAM signature is acquired in the ischaemic heart

We next investigated whether MI-associated cardiac monocyte/macrophage states could be acquired remotely, notably via the production of ischaemic injury-associated atypical monocytes arising from emergency myelopoiesis,[42] that would transit in the bloodstream before infiltrating the myocardium. We performed CITE-seq analysis of CD19^{-}NK1.1^{-}Ter119^{-}CD11b^{+} cells from the blood of control mice, sham-operated animals at 1 and 3 days post-surgery, and mice with MI at 1 and 3 days. Cardiac cells from the ischaemic heart at 1 and 3 days post-MI were also included[37] (*Figure 5A*).

We first investigated remote priming of blood monocytes by MI by separately reclustering cells obtained from the peripheral blood. This revealed expansion of injury-associated Ly6C^{hi} monocytes enriched for *Chil3* (encoding Chitinase-like protein 3 also known as Ym1) and granulocyte marker genes (*Lcn2*, *Prtn3*) induced by MI, and also sham surgery at 1 day after MI (*Chil3*^{hi} monocytes, see Supplementary material online, *Figure S8A–E*). Bulk-sorted bone marrow Ly6C^{hi} monocytes also showed increased levels of *Chil3*, *Lcn2*, and *Prtn3* at 3 days after MI (see Supplementary material online, *Figure S8F*). These results are consistent with the emergence of Ym1^{+} monocytes enriched in granulocyte marker transcripts induced by tissue injury[43] or during emergency

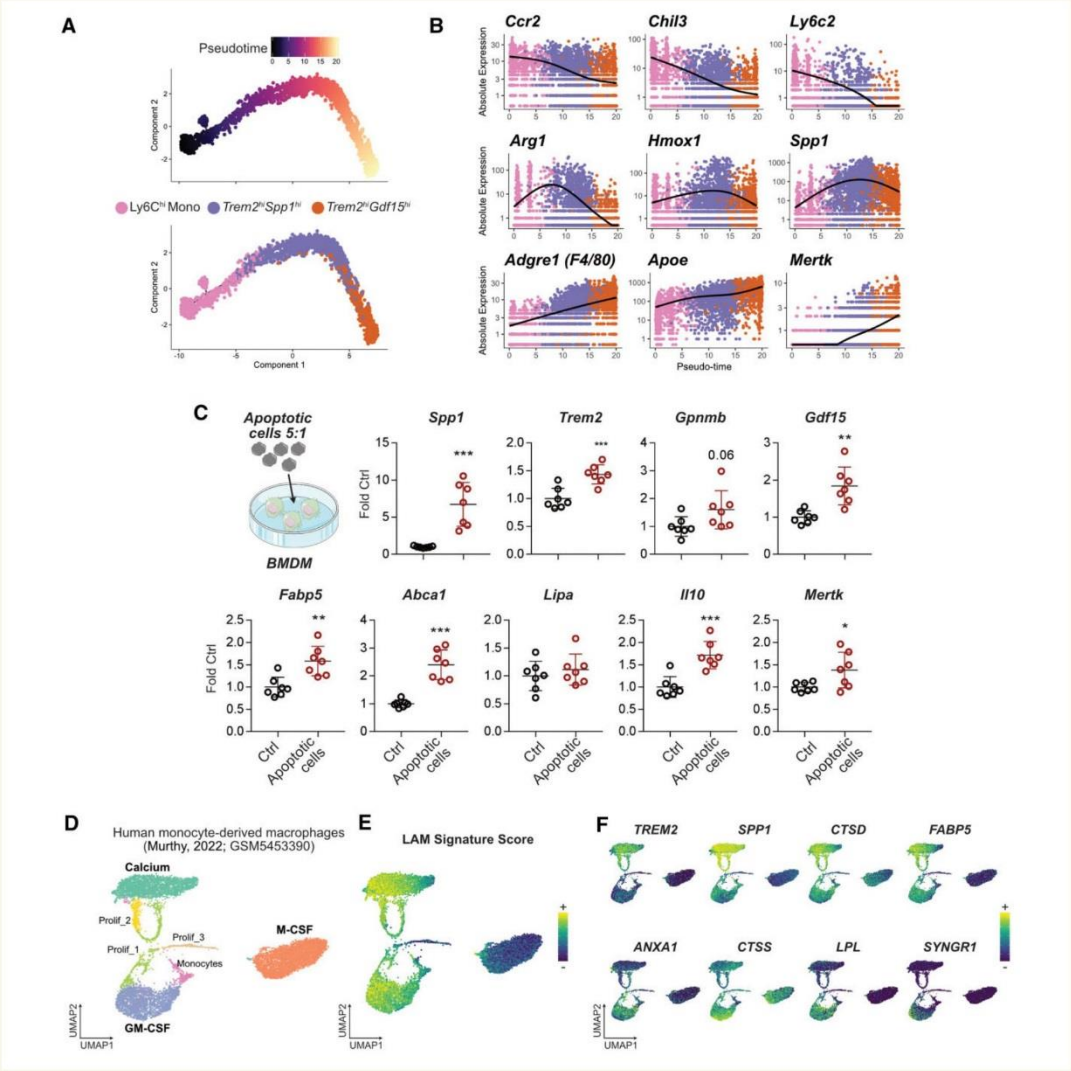

Figure 6 Monocyte transition to *Trem2*^{hi} macrophages and potential inducers of the LAM signature. (*A*) Pseudotime trajectory analysis of Ly6C^{hi} monocytes, *Trem2*^{hi}*Spp1*^{hi} and *Trem2*^{hi}*Gdf15*^{hi} macrophages. (*B*) Expression of the indicated transcripts according to pseudotime and colour coded by cell population of origin. In *A* and *B*, cells belonging to the indicated clusters ($n = 4633$ total cells) were extracted from the analysis shown in *Figure 1D* ($n = 10\,365$ cells obtained from $n = 5$ mice without MI, and $n = 9$ mice with MI, pooled from two independent experiments). (*C*) Expression of the indicated transcripts in mouse bone marrow–derived macrophages (BMDM) in control condition or after overnight exposure to apoptotic cells (Apo = apoptotic thymocyte at a 5:1 apoptotic cell:macrophage ratio). Each data point represents macrophages from one mouse assayed in technical duplicates, total $n = 7$ per condition, pooled from two independent experiments (*$P < 0.05$; **$P < 0.01$; ***$P < 0.001$). (*D*) Reanalysis of data from Murthy *et al.*[48] with UMAP of *in vitro* human monocyte-derived macrophages differentiated in the presence of calcium, GM-CSF or M-CSF. (*E*) LAM-signature score projected on the UMAP plot. (*F*) Expression of the indicated LAM-signature transcripts induced by calcium (top) or GM-CSF (bottom).

myelopoiesis.[44] Although we noted a slight increase of the LAM-signature expression score in *Chil3*^{hi} monocytes compared with baseline Ly6C^{hi} monocytes, most LAM-signature transcripts were expressed at low levels and only two genes (*Gapdh*, *Lpl*) were significantly enriched in *Chil3*^{hi} monocytes compared with baseline Ly6C^{hi} monocytes (see Supplementary material online, *Figure S8G*).

To analyse the acquisition of the LAM signature by monocytes infiltrating the ischaemic heart, we analysed blood and cardiac

CD115^{+}Ly6G^{-} cells together (3378 cells; *Figure 5*). One cell cluster contained almost only cells extracted from the ischaemic heart and expressed *Ccr2* indicating an infiltrating monocyte origin (Heart Mo/Mac, *Figure 5A–D*). Pseudotime ordering of monocytes/macrophages in Monocle[45] delineated two major trajectories (*Figure 5E and F*), with blood cells expectedly following a Ly6C^{hi} to Ly6C^{low} trajectory with the acquisition of Ly6C^{low} monocyte marker genes (*Ace*, *Treml4*, *Nr4a1*, *Itgal*; *Figure 5G*), while cells infiltrated in the heart acquired expression of *Trem2* and transcripts associated with the LAM signature (*Figure 5G*). These data indicate that MI induces a peripheral shift of Ly6C^{hi} monocytes towards a *Chil3*^{hi} granulocyte-like state in the blood, while in the ischaemic heart monocyte-derived macrophages acquire the full *Trem2*^{hi} LAM signature.

3.6 Monocyte-to-*Trem2*^{hi} macrophage transition in the heart and potential inducers of the macrophage LAM signature

Based on our observations that (i) *Trem2*^{hi}*Spp1*^{hi} and *Trem2*^{hi}*Gdf15*^{hi} macrophages sequentially peak in the heart, (ii) *Trem2*^{hi}*Spp1*^{hi} likely represents monocyte-to-macrophage differentiation intermediates, while *Trem2*^{hi}*Gdf15*^{hi} is differentiated macrophages, (iii) *Trem2*^{hi}*Spp1*^{hi} and *Trem2*^{hi}*Gdf15*^{hi} macrophages share features of a LAM gene expression signature, (iv) cells corresponding to *Trem2*^{hi}*Spp1*^{hi} and *Trem2*^{hi}*Gdf15*^{hi} macrophages are not observed in the bloodstream (i.e. they acquire their gene expression signature in the injured tissue), and (v) *Trem2*^{hi}*Spp1*^{hi} and *Trem2*^{hi}*Gdf15*^{hi} macrophages are lost upon depletion of circulating monocytes, we performed pseudotime analysis in Monocle,[45] following the assumption that *Trem2*^{hi}*Spp1*^{hi} and *Trem2*^{hi}*Gdf15*^{hi} macrophages originate from Ly6C^{hi} monocytes, and might represent different states along a monocyte-to-macrophage differentiation trajectory (*Figure 6A*). This analysis yielded a putative trajectory with Ly6C^{hi} monocytes at its beginning, and *Trem2*^{hi}*Gdf15*^{hi} macrophages at its end, with progressive loss of monocyte marker genes (*Ccr2*, *Chil3*, *Ly6c2*) and acquisition of macrophage differentiation markers (*Adgre1*, *Mertk*, *Apoe*), while *Spp1* and genes involved in the differentiation of monocytes to alternatively activated macrophages (e.g. *Hmox1*, *Arg1*) were transiently increased (*Figure 6B*). These results suggest that *Trem2*^{hi}*Spp1*^{hi} cells are monocyte/macrophage intermediates that may represent a transitional state towards fully differentiated *Trem2*^{hi}*Gdf15*^{hi} macrophages.

We next investigated potential inducers of the LAM signature. Based on the gene expression profile of cardiac *Trem2*^{hi} macrophages enriched for phagocytic genes and with low expression of pro-inflammatory cytokines, we hypothesized that efferocytosis, a major regulator of macrophage anti-inflammatory gene expression in the ischaemic heart,[46] might be involved in acquisition of the LAM signature. Expression of *Spp1*, *Trem2*, *Gdf15*, and *Fabp5* was increased in mouse bone marrow–derived macrophages after exposure to apoptotic cells, alongside previously documented efferocytosis-induced genes such as *Mertk*, *Abca1*, or *Il10*[46,47] (*Figure 6C*). A recent report[48] showed that exposing human monocyte to calcium, which is released from necrotic cells to activate macrophages,[49] leads to their differentiation into macrophages producing high levels of *SPP1*, a marker of *Trem2*^{hi} macrophages. Reanalysing data from Murthy *et al.*,[48] we observed that exposure to calcium was associated with high expression of not only *SPP1*, but also many characteristic genes of the LAM signature such as *TREM2*, *CTSD*, and *FABP5*, while monocyte-derived macrophages exposed to GM-CSF also acquired some markers of the LAM signature (*Figure 6D–F*). Altogether, these data suggest that phagocytosis of dead cells, and exposure to damage associated molecular patterns released by dead cells, might be involved in macrophage acquisition of the *Trem2*^{hi} LAM signature.

4. Discussion

Using single-cell CITE-seq analysis of circulating and cardiac monocytes/macrophages, combined with fate mapping and CCR2^{+} monocyte depletion, we mapped monocyte/macrophage dynamics and characterized monocyte-derived macrophage heterogeneity in experimental MI. This allowed us to precisely delineate MI-associated monocyte-derived macrophage populations in the ischaemic heart, including *Trem2*^{hi} macrophage subsets with a tissue-acquired LAM gene expression signature.

We identified previously described populations of TIMD4^{+}, MHCII^{+}, and CCR2^{+} RTMs,[4,14] and could confirm CD163[50] or identify novel surface markers (MGL2, VSIG4) of these populations, that may be useful for cardiac macrophage characterization by flow cytometry or targeting of specific resident macrophage subsets. Consistent with previous reports, these populations almost entirely vanished from the infarcted heart immediately after MI.[4,51]

Rapid shifts in monocyte/macrophage populations after acute MI had previously been characterized by flow cytometric analyses (e.g. Nahrendorf *et al.*[6] or Weinberger *et al.*[52]). Our CITE-seq and time-dependent scRNA-seq characterization of cardiac monocytes/macrophages provide a refined and accurate picture of these shifts and identify previously unrecognized MI-associated macrophage states. Notably, we confirm that bona fide Ly6C^{low} monocytes only infiltrate the heart in low numbers,[53] and identified a population of *Fn1*^{hi}*Ltc4s*^{hi} macrophages with a discrete gene expression signature and surface expression of some RTM markers (TIMD4 and VSIG4). The origin, localization, and function of these macrophages remain to be determined. The major populations of MI-associated macrophages comprised two pro-inflammatory populations (*Isg15*^{hi} and MHCII^{+}*Il1b*$^{+}$), and three *Trem2*^{hi} macrophage populations with low inflammatory gene expression. All the major MI-associated macrophage populations originate from infiltrating monocytes as determined by CCR2^{+} cell depletion and fate-mapping analysis.

Trem2^{hi} macrophages comprised three subpopulations (two large populations termed *Trem2*^{hi}*Spp1*^{hi} and *Trem2*^{hi}*Gdf15*^{hi}, and a smaller *Trem2*^{hi}*Prdx1*^{hi} subset), and showed gene expression features reminiscent of a LAM signature previously observed in obese adipose tissue,[16] atherosclerotic lesions,[17,18] and the liver in models of NAFLD[19] and NASH.[20] Cardiac *Trem2*^{hi} LAM-signature macrophages were derived from monocytes, similar to previous observations in the liver,[19,20] and adipose tissue.[16] However, the LAM signature is also shared by TREM2-dependent disease-associated microglia,[54] indicating that its acquisition does not depend on macrophage origin and is mostly driven by the local tissue environment. Features of the LAM transcriptional signature may not only be induced by pathological lipid loading but rather more generally induced in contexts of tissue damage. In line, our data indicate that *Trem2*^{hi} LAM-signature macrophage populations likely differentiate from monocytes in injured areas of the myocardium, as GPNMB, a highly specific marker of the LAM signature, was exclusively seen on CD68^{+} macrophages within the infarcted area of the heart, but not in the infarct border zone or remote non-affected tissue. Major transcriptional hubs involved in the regulation of lipid homeostasis are activated also in response to efferocytosis of dead cells, such as the liver-X-receptor pathway[47] which was recently implicated in microglial

acquisition of the LAM gene expression in response to chronic phagocytic challenge.[55] This raises the possibility that macrophages with high efferocytosis activity, and lipid loading from dead cell engulfment, acquire a LAM signature. In line, exposure of bone marrow–derived macrophages to apoptotic cells *in vitro* induced expression of several characteristic LAM transcripts. More recently, the LAM signature was also observed in steady-state bile-duct macrophages, and LAM genes were induced by lipids during *in vitro* monocyte-to-macrophage differentiation,[21] indicating that also homeostatic exposure to high lipid loads may drive acquisition of a LAM signature. Acquisition of the LAM signature might not only depend on lipid-related pathways, but also be driven by other microenvironmental cues. Exposure to calcium, a damage associated molecular pattern released by necrotic cells,[48] strongly induced expression of characteristic LAM markers in human monocyte-derived macrophages. Specific inflammatory cytokines might dictate the monocyte-to-macrophage transition in the heart, as recently shown for IFN-γ and GM-CSF in the context of neuro-inflammation.[56] *In vitro*, our data indicate that some features of the LAM signature can be driven by GM-CSF. Importantly, macrophages with a LAM signature were observed in human ischaemic cardiomyopathy samples. While this represents a different pathological context compared with acute cardiac ischaemia in our mouse model, this provides proof-of-concept that the TREM2$^+$ LAM signature can be observed in the disease human heart, consistent with the LAM signature also being observed in humans in atherosclerosis,[18] adipose tissue,[16] and in the steatotic human liver,[21] indicating conservation of this macrophage state across species and disease contexts.

In the ischaemic mouse heart, features of the *Trem2^{hi}* LAM signature were shared by three macrophage subpopulations. A small population was highly enriched for *Prdx1* and genes involved in iron handling (*Ftl1*, *Fth1*, *Slc40a1*, *Slc48a1*). Two other *Trem2^{hi}* populations represented the most abundant MI-associated macrophages and were characterized as *Trem2^{hi}Spp1^{hi}* and *Trem2^{hi}Gdf15^{hi}*. Their sequential presence in the ischaemic heart, as well as expression patterns of *Ccr2* and monocyte/macrophage differentiation markers, suggest that *Trem2^{hi}Spp1^{hi}* cells are a monocyte/macrophage intermediate giving rise to fully differentiated *Trem2^{hi}Gdf15^{hi}* macrophages. However, our data do not exclude that pro-inflammatory macrophage populations (*Isg15^{hi}* and MHCII$^+$*Il1b*$^+$) could also shift towards a non-inflammatory *Trem2^{hi}Gdf15^{hi}* state overtime after MI.

Our analysis of circulating monocytes indicates that ischaemic injury induces a shift towards monocytes enriched for the expression of *Chil3* (encoding Ym1) and several granulocyte-associated genes (e.g. *Prtn3*, *Lcn2*). Recent reports proposed that mature monocytes arise from two distinct pathways in the steady state, with monocyte-dendritic progenitors and granulocyte-monocyte progenitors differentiating to monocytes with a 'DC-like' state or a 'neutrophil-like' state, respectively.[57] Our results are thus consistent with an MI-induced shift towards the production of 'granulocyte-like' monocytes, which appear similar to Ym1$^+$Ly6C^{hi} monocytes that emerge after tissue injury.[43] Bulk transcriptome analysis of human monocytes sampled 48 h after acute MI showed upregulation of *LCN2*, a prototypical marker of the granulocyte-like signature, as well as other granulocyte-associated transcripts (*IL1RN*, *CXCR1*),[58] indicating that a similar shift in circulating monocyte transcriptome might occur in patients with MI. While our data indicate that the macrophage LAM signature is acquired in the ischaemic heart, and not directly induced in blood monocytes by MI, it remains to be determined whether injury-associated *Chil3^{hi}* monocytes are primed towards acquiring the LAM signature once infiltrated in the infarcted myocardium.

5. Conclusion

In conclusion, our work provides a novel high-resolution view of the heterogeneity and dynamics of monocyte/macrophage transitions during the acute post-MI inflammation phase and constitutes a valuable resource for further investigating how these cells may be harnessed and modulated to promote post-ischaemic heart repair.

Supplementary material

Supplementary material is available at *Cardiovascular Research* online.

Authors' contributions

Performed experiments: G.R., J.G., M.Pi, E.V., A.R., S.R.B., P.A., T.K., N.D., A.P.A.L., K.S., C.C.; Analysed and interpreted data: G.R., J.G., M.Pi, E.V., A.R., S.R.B., P.A., T.K., N.D., A.P.A.L., K.S., C.H., J.S.S., A.Z., A.E.S., C.C.; Created the web-based interface: O.D.; Provided critical mouse lines, assays, and reagents: M.Pr., M.M., K.S., C.H.; Revised and edited the manuscript: J.S.S., M.Pr., M.M., C.H., A.Z.; Designed the study: G.R., A.E.S., C.C.; Wrote the manuscript: G.R., A.E.S., C.C.

Conflict of interest: C.H. collaborates with Denali Therapeutics, participated on one advisory board meeting of Biogen, and received a speaker honorarium from Novartis and Roche. C.H. is chief advisor of ISAR Bioscience and a member of the advisory board of AviadoBio.

Funding

This work was supported by the Interdisciplinary Center for Clinical Research (Interdisziplinäres Zentrum für Klinische Forschung, IZKF), University Hospital Würzburg (E-352 and A-384 to A.Z., E-353 to C.C.), the Deutsche Forschungsgemeinschaft (DFG; German Research Foundation, Projects 374031971-TRR 240, 324392634-TR221, ZE827/13-1, 14-1, project numbers 396923792 to A.Z., 432915089 to A.Z. and C.C., 458539578 and 471705758 to C.C.), the SFB1525 project number 453989101 (projects A1 and B3 to A.Z., project PS2 to A.E.S. and C.C., project A6 to C.C.), and the BMBF within the Comprehensive Heart Failure Centre Würzburg (BMBF 01EO1504 to C.C. and A.E.S.). A.E.S. is supported by the EMBO Young Investigator Program. This work was supported by grants from the Deutsche Forschungsgemeinschaft under Germany's Excellence Strategy within the framework of the Munich Cluster for Systems Neurology (EXC 2145 SyNergy, ID 390857198 to C.H.) and the Helmholtz-Gemeinschaft Zukunftsthema 'Immunology and Inflammation' (ZT-0027 to C.H.).

Data availability

Single-cell RNA-sequencing data generated for this report has been deposited in Gene Expression Omnibus (GSE135310, GSE197441, GSE197853).

References

1. Frodermann V, Nahrendorf M. Macrophages and cardiovascular health. *Physiol Rev* 2018; **98**:2523–2569.
2. Molawi K, Wolf Y, Kandalla PK, Favret J, Hagemeyer N, Frenzel K, Pinto AR, Klapproth K, Henri S, Malissen B, Rodewald HR, Rosenthal NA, Bajenoff M, Prinz M, Jung S, Sieweke MH. Progressive replacement of embryo-derived cardiac macrophages with age. *J Exp Med* 2014;**211**:2151–2158.
3. Zaman R, Hamidzada H, Epelman S. Exploring cardiac macrophage heterogeneity in the healthy and diseased myocardium. *Curr Opin Immunol* 2020;**68**:54–63.

4. Dick SA, Macklin JA, Nejat S, Momen A, Clemente-Casares X, Althagafi MG, Chen J, Kantores C, Hosseinzadeh S, Aronoff L, Wong A, Zaman R, Barbu I, Besla R, Lavine KJ, Razani B, Ginhoux F, Husain M, Cybulsky MI, Robbins CS, Epelman S. Self-renewing resident cardiac macrophages limit adverse remodeling following myocardial infarction. *Nat Immunol* 2019;**20**:29–39.
5. Bajpai G, Bredemeyer A, Li W, Zaitsev K, Koenig AL, Lokshina I, Mohan J, Ivey B, Hsiao HM, Weinheimer C, Kovacs A, Epelman S, Artyomov M, Kreisel D, Lavine KJ. Tissue resident CCR2− and CCR2+ cardiac macrophages differentially orchestrate monocyte recruitment and fate specification following myocardial injury. *Circ Res* 2019;**124**:263–278.
6. Nahrendorf M, Swirski FK, Aikawa E, Stangenberg L, Wurdinger T, Figueiredo JL, Libby P, Weissleder R, Pittet MJ. The healing myocardium sequentially mobilizes two monocyte subsets with divergent and complementary functions. *J Exp Med* 2007;**204**:3037–3047.
7. Leuschner F, Rauch PJ, Ueno T, Gorbatov R, Marinelli B, Lee WW, Dutta P, Wei Y, Robbins C, Iwamoto Y, Sena B, Chudnovskiy A, Panizzi P, Keliher E, Higgins JM, Libby P, Moskowitz MA, Pittet MJ, Swirski FK, Weissleder R, Nahrendorf M. Rapid monocyte kinetics in acute myocardial infarction are sustained by extramedullary monocytopoiesis. *J Exp Med* 2012;**209**:123–137.
8. Mouton AJ, DeLeon-Pennell KY, Rivera Gonzalez OJ, Flynn ER, Freeman TC, Saucerman JJ, Garrett MR, Ma Y, Harmancey R, Lindsey ML. Mapping macrophage polarization over the myocardial infarction time continuum. *Basic Res Cardiol* 2018;**113**:26.
9. Gessain G, Bleriot C, Ginhoux F. Non-genetic heterogeneity of macrophages in diseases—a medical perspective. *Front Cell Dev Biol* 2020;**8**:613116.
10. King KR, Aguirre AD, Ye YX, Sun Y, Roh JD, Ng RP Jr, Kohler RH, Arlauckas SP, Iwamoto Y, Savol A, Sadreyev RI, Kelly M, Fitzgibbons TP, Fitzgerald KA, Mitchison T, Libby P, Nahrendorf M, Weissleder R. IRF3 and type I interferons fuel a fatal response to myocardial infarction. *Nat Med* 2017;**23**:1481–1487.
11. Calcagno DM, Ng RP, Jr., Toomu A, Zhang C, Huang K, Aguirre AD, Weissleder R, Daniels LB, Fu Z, King KR. The myeloid type I interferon response to myocardial infarction begins in bone marrow and is regulated by Nrf2-activated macrophages. *Sci Immunol* 2020;**5**:eaaz1974.
12. Stoeckius M, Hafemeister C, Stephenson W, Houck-Loomis B, Chattopadhyay PK, Swerdlow H, Satija R, Smibert P. Simultaneous epitope and transcriptome measurement in single cells. *Nat Methods* 2017;**14**:865–868.
13. Chakarov S, Lim HY, Tan L, Lim SY, See P, Lum J, Zhang XM, Foo S, Nakamizo S, Duan K, Kong WT, Gentek R, Balachander A, Carbajo D, Bleriot C, Malleret B, Tam JKC, Baig S, Shabeer M, Toh SES, Schlitzer A, Larbi A, Marichal T, Malissen B, Chen J, Poidinger M, Kabashima K, Bajenoff M, Ng LG, Angeli V, Ginhoux F. Two distinct interstitial macrophage populations coexist across tissues in specific subtissular niches. *Science* 2019;**363**:eaau0964.
14. Dick SA, Wong A, Hamidzada H, Nejat S, Nechanitzky R, Vohra S, Mueller B, Zaman R, Kantores C, Aronoff L, Momen A, Nechanitzky D, Li WY, Ramachandran P, Crome SQ, Becher B, Cybulsky MI, Billia F, Keshavjee S, Mital S, Robbins CS, Mak TW, Epelman S. Three tissue resident macrophage subsets coexist across organs with conserved origins and life cycles. *Sci Immunol* 2022;**7**:eabf7777.
15. Stoeckius M, Zheng S, Houck-Loomis B, Hao S, Yeung BZ, Mauck WM 3rd, Smibert P, Satija R. Cell Hashing with barcoded antibodies enables multiplexing and doublet detection for single cell genomics. *Genome Biol* 2018;**19**:224.
16. Jaitin DA, Adlung L, Thaiss CA, Weiner A, Li B, Descamps H, Lundgren P, Bleriot C, Liu Z, Deczkowska A, Keren-Shaul H, David E, Zmora N, Eldar SM, Lubezky N, Shibolet O, Hill DA, Lazar MA, Colonna M, Ginhoux F, Shapiro H, Elinav E, Amit I. Lipid-associated macrophages control metabolic homeostasis in a Trem2-dependent manner. *Cell* 2019;**178**:686–98.e14.
17. Cochain C, Vafadarnejad E, Arampatzi P, Pelisek J, Winkels H, Ley K, Wolf D, Saliba AE, Zernecke A. Single-cell RNA-Seq reveals the transcriptional landscape and heterogeneity of aortic macrophages in murine atherosclerosis. *Circ Res* 2018;**122**:1661–1674.
18. Zernecke A, Erhard F, Weinberger T, Schulz C, Ley K, Saliba A-E, Cochain C. Integrated scRNA-seq analysis identifies conserved transcriptomic features of mononuclear phagocytes in mouse and human atherosclerosis. *bioRxiv* 2020. doi:10.1101/2020.12.09.417535.
19. Remmerie A, Martens L, Thone T, Castoldi A, Seurinck R, Pavie B, Roels J, Vanneste B, De Prijck S, Vanhockerhout M, Binte Abdul Latib M, Devisscher L, Hoorens A, Bonnardel J, Vandamme N, Kremer A, Borghgraef P, Van Vlierberghe H, Lippens S, Pearce E, Saeys Y, Scott CL. Osteopontin expression identifies a subset of recruited macrophages distinct from Kupffer cells in the fatty liver. *Immunity* 2020;**53**:641–57.e14.
20. Daemen S, Gainullina A, Kalugotla G, He L, Chan MM, Beals JW, Liss KH, Klein S, Feldstein AE, Finck BN, Artyomov MN, Schilling JD. Dynamic shifts in the composition of resident and recruited macrophages influence tissue remodeling in NASH. *Cell Rep* 2021;**34**:108626.
21. Guilliams M, Bonnardel J, Haest B, Vanderborght B, Bujko A, Martens L, Thoné T, Browaeys R, De Ponti FF, Remmerie A, Wagner C, Vanneste B, Zwicker C, Vanhalewyn T, Gonçalves A, Lippens S, Devriendt B, Cox E, Ferrero G, Wittamer V, Willaert A, Kaptein SJF, Neyts J, Dallmeier K, Geldhof P, Casaert S, Deplancke B, ten Dijke P, Hoorens A, Vanlander A, Berrevoet F, Van Nieuwenhove Y, Saeys Y, Saelens W, Van Vlierberghe H, Devisscher L, Scott CL. Spatial proteogenomics reveals distinct and evolutionarily-conserved hepatic macrophage niches. *Cell* 2022;**185**:379–396.e38.
22. Ramachandran P, Dobie R, Wilson-Kanamori JR, Dora EF, Henderson BEP, Luu NT, Portman JR, Matchett KP, Brice M, Marwick JA, Taylor RS, Efremova M, Vento-Tormo R, Carragher NO, Kendall TJ, Fallowfield JA, Harrison EM, Mole DJ, Wigmore SJ, Newsome PN, Weston CJ, Iredale JP, Tacke F, Pollard JW, Ponting CP, Marioni JC, Teichmann SA, Henderson NC. Resolving the fibrotic niche of human liver cirrhosis at single-cell level. *Nature* 2019;**575**:512–518.
23. Rao M, Wang X, Guo G, Wang L, Chen S, Yin P, Chen K, Chen L, Zhang Z, Chen X, Hu X, Hu S, Song J. Resolving the intertwining of inflammation and fibrosis in human heart failure at single-cell level. *Basic Res Cardiol* 2021;**116**:55.
24. DeBerge M, Glinton K, Subramanian M, Wilsbacher LD, Rothlin CV, Tabas I, Thorp EB. Macrophage AXL receptor tyrosine kinase inflames the heart after reperfused myocardial infarction. *J Clin Invest* 2021;**131**:e139576.
25. Louwe MC, Olsen MB, Kaasboll OJ, Yang K, Fosshaug LE, Alfsnes K, Ogaard JDS, Rashidi A, Skulberg VM, Yang M, de Miranda Fonseca D, Sharma A, Aronsen JM, Schrumpf E, Ahmed MS, Dahl CP, Nyman TA, Ueland T, Melum E, Halvorsen BE, Bjoras M, Attramadal H, Sjaastad I, Aukrust P, Yndestad A. Absence of NLRP3 inflammasome in hematopoietic cells reduces adverse remodeling after experimental myocardial infarction. *JACC Basic Transl Sci* 2020;**5**:1210–1224.
26. Xiao H, Li H, Wang J-J, Zhang J-S, Shen J, An X-B, Zhang C-C, Wu J-M, Song Y, Wang X-Y, Yu H-Y, Deng X-N, Li Z-J, Xu M, Lu Z-Z, Du J, Gao W, Zhang A-H, Feng Y, Zhang Y-Y. IL-18 cleavage triggers cardiac inflammation and fibrosis upon beta-adrenergic insult. *Eur Heart J* 2018;**39**:60–69.
27. Vijayan V, Wagener F, Immenschuh S. The macrophage heme-heme oxygenase-1 system and its role in inflammation. *Biochem Pharmacol* 2018;**153**:159–167.
28. Yang Z, Ming XF. Functions of arginase isoforms in macrophage inflammatory responses: impact on cardiovascular diseases and metabolic disorders. *Front Immunol* 2014;**5**:533.
29. Ferraro B, Leoni G, Hinkel R, Ormanns S, Paulin N, Ortega-Gomez A, Viola JR, de Jong R, Bongiovanni D, Bozoglu T, Maas SL, D'Amico M, Kessler T, Zeller T, Hristov M, Reutelingsperger C, Sager HB, Doring Y, Nahrendorf M, Kupatt C, Soehnlein O. Pro-angiogenic macrophage phenotype to promote myocardial repair. *J Am Coll Cardiol* 2019;**73**:2990–3002.
30. Zaman R, Hamidzada H, Kantores C, Wong A, Dick SA, Wang Y, Momen A, Aronoff L, Lin J, Razani B, Mital S, Billia F, Lavine KJ, Nejat S, Epelman S. Selective loss of resident macrophage-derived insulin-like growth factor-1 abolishes adaptive cardiac growth to stress. *Immunity* 2021;**54**:2057–2071.e6.
31. Kempf T, Zarbock A, Widera C, Butz S, Stadtmann A, Rossaint J, Bolomini-Vittori M, Korf-Klingebiel M, Napp LC, Hansen B, Kanwischer A, Bavendiek U, Beutel G, Hapke M, Sauer MG, Laudanna C, Hogg N, Vestweber D, Wollert KC. GDF-15 is an inhibitor of leukocyte integrin activation required for survival after myocardial infarction in mice. *Nat Med* 2011;**17**:581–588.
32. Wan E, Yeap XY, Dehn S, Terry R, Novak M, Zhang S, Iwata S, Han X, Homma S, Drosatos K, Lomasney J, Engman DM, Miller SD, Vaughan DE, Morrow JP, Kishore R, Thorp EB. Enhanced efferocytosis of apoptotic cardiomyocytes through myeloid-epithelial-reproductive tyrosine kinase links acute inflammation resolution to cardiac repair after infarction. *Circ Res* 2013;**113**:1004–1012.
33. Kandalam V, Basu R, Abraham T, Wang X, Soloway PD, Jaworski DM, Oudit GY, Kassiri Z. TIMP2 deficiency accelerates adverse post-myocardial infarction remodeling because of enhanced MT1-MMP activity despite lack of MMP2 activation. *Circ Res* 2010;**106**:796–808.
34. Ali K, Middleton M, Pure E, Rader DJ. Apolipoprotein E suppresses the type I inflammatory response in vivo. *Circ Res* 2005;**97**:922–927.
35. Alonso-Herranz L, Sahun-Espanol A, Paredes A, Gonzalo P, Gkontra P, Nunez V, Clemente C, Cedenilla M, Villalba-Orero M, Inserte J, Garcia-Dorado D, Arroyo AG, Ricote M. Macrophages promote endothelial-to-mesenchymal transition via MT1-MMP/TGFbeta1 after myocardial infarction. *Elife* 2020;**9**:e57920.
36. Farbehi N, Patrick R, Dorison A, Xaymardan M, Janbandhu V, Wystub-Lis K, Ho JW, Nordon RE, Harvey RP. Single-cell expression profiling reveals dynamic flux of cardiac stromal, vascular and immune cells in health and injury. *Elife* 2019;**8**:e43882.
37. Vafadarnejad E, Rizzo G, Krampert L, Arampatzi P, Arias-Loza PA, Nazzal Y, Rizakou A, Knochenhauer T, Reddy Bandi S, Nugroho VA, Schulz DJ, Roesch M, Alayrac P, Vilar J, Silvestre JS, Zernecke A, Saliba AE, Cochain C. Dynamics of cardiac neutrophil diversity in murine myocardial infarction. *Circ Res* 2020;**127**:e232–e249.
38. Mack M, Cihak J, Simonis C, Luckow B, Proudfoot AE, Plachy J, Bruhl H, Frink M, Anders HJ, Vielhauer V, Pfirstinger J, Stangassinger M, Schlondorff D. Expression and characterization of the chemokine receptors CCR2 and CCR5 in mice. *J Immunol* 2001;**166**:4697–4704.
39. Schlitzer A, Sivakamasundari V, Chen J, Sumatoh HR, Schreuder J, Lum J, Malleret B, Zhang S, Larbi A, Zolezzi F, Renia L, Poidinger M, Naik S, Newell EW, Robson P, Ginhoux F. Identification of cDC1- and cDC2-committed DC progenitors reveals early lineage priming at the common DC progenitor stage in the bone marrow. *Nat Immunol* 2015;**16**:718–728.
40. Bosteels C, Neyt K, Vanheerswynghels M, van Helden MJ, Sichien D, Debeuf N, De Prijck S, Bosteels V, Vandamme N, Martens L, Saeys Y, Louagie E, Lesage M, Williams DL, Tang SC, Mayer JU, Ronchese F, Scott CL, Hammad H, Guilliams M, Lambrecht BN. Inflammatory type 2 cDCs acquire features of cDC1s and macrophages to orchestrate immunity to respiratory virus infection. *Immunity* 2020;**52**:1039–1056.e9.
41. Goldmann T, Wieghofer P, Muller PF, Wolf Y, Varol D, Yona S, Brendecke SM, Kierdorf K, Staszewski O, Datta M, Luedde T, Heikenwalder M, Jung S, Prinz M. A new type of microglia gene targeting shows TAK1 to be pivotal in CNS autoimmune inflammation. *Nat Neurosci* 2013;**16**:1618–1626.

42. Schultze JL, Mass E, Schlitzer A. Emerging principles in myelopoiesis at homeostasis and during infection and inflammation. *Immunity* 2019;**50**:288–301.
43. Ikeda N, Asano K, Kikuchi K, Uchida Y, Ikegami H, Takagi R, Yotsumoto S, Shibuya T, Makino-Okamura C, Fukuyama H, Watanabe T, Ohmuraya M, Araki K, Nishitai G, Tanaka M. Emergence of immunoregulatory Ym1(+)Ly6C(hi) monocytes during recovery phase of tissue injury. *Sci Immunol* 2018;**3**:eaat0207.
44. Yanez A, Coetzee SG, Olsson A, Muench DE, Berman BP, Hazelett DJ, Salomonis N, Grimes HL, Goodridge HS. Granulocyte-monocyte progenitors and monocyte-dendritic cell progenitors independently produce functionally distinct monocytes. *Immunity* 2017;**47**:890–902.e4.
45. Trapnell C, Cacchiarelli D, Grimsby J, Pokharel P, Li S, Morse M, Lennon NJ, Livak KJ, Mikkelsen TS, Rinn JL. The dynamics and regulators of cell fate decisions are revealed by pseudotemporal ordering of single cells. *Nat Biotechnol* 2014;**32**:381–386.
46. Zhang S, Weinberg S, DeBerge M, Gainullina A, Schipma M, Kinchen JM, Ben-Sahra I, Gius DR, Yvan-Charvet L, Chandel NS, Schumacker PT, Thorp EB. Efferocytosis fuels requirements of fatty acid oxidation and the electron transport chain to polarize macrophages for tissue repair. *Cell Metab* 2019;**29**:443–456.e5.
47. A-Gonzalez N, Bensinger SJ, Hong C, Beceiro S, Bradley MN, Zelcer N, Deniz J, Ramirez C, Diaz M, Gallardo G, de Galarreta CR, Salazar J, Lopez F, Edwards P, Parks J, Andujar M, Tontonoz P, Castrillo A. Apoptotic cells promote their own clearance and immune tolerance through activation of the nuclear receptor LXR. *Immunity* 2009;**31**:245–258.
48. Murthy S, Karkossa I, Schmidt C, Hoffmann A, Hagemann T, Rothe K, Seifert O, Anderegg U, von Bergen M, Schubert K, Rossol M. Danger signal extracellular calcium initiates differentiation of monocytes into SPP1/osteopontin-producing macrophages. *Cell Death Dis* 2022;**13**:53.
49. Rossol M, Pierer M, Raulien N, Quandt D, Meusch U, Rothe K, Schubert K, Schoneberg T, Schaefer M, Krugel U, Smajilovic S, Brauner-Osborne H, Baerwald C, Wagner U. Extracellular Ca2+ is a danger signal activating the NLRP3 inflammasome through G protein-coupled calcium sensing receptors. *Nat Commun* 2012;**3**:1329.
50. Pinto AR, Paolicelli R, Salimova E, Gospocic J, Slonimsky E, Bilbao-Cortes D, Godwin JW, Rosenthal NA. An abundant tissue macrophage population in the adult murine heart with a distinct alternatively-activated macrophage profile. *PLoS One* 2012;**7**:e36814.
51. Heidt T, Courties G, Dutta P, Sager HB, Sebas M, Iwamoto Y, Sun Y, Da Silva N, Panizzi P, van der Laan AM, Swirski FK, Weissleder R, Nahrendorf M. Differential contribution of monocytes to heart macrophages in steady-state and after myocardial infarction. *Circ Res* 2014;**115**:284–295.
52. Weinberger T, Rauber S, Schneider V, Messerer D, Fischer M, Rudi WS, Kobayashi Y, Schulz C. Differential MHC-II expression and phagocytic functions of embryo-derived cardiac macrophages in the course of myocardial infarction in mice. *Eur J Immunol* 2021;**51**:250–252.
53. Hilgendorf I, Gerhardt LM, Tan TC, Winter C, Holderried TA, Chousterman BG, Iwamoto Y, Liao R, Zirlik A, Scherer-Crosbie M, Hedrick CC, Libby P, Nahrendorf M, Weissleder R, Swirski FK. Ly-6Chigh monocytes depend on Nr4a1 to balance both inflammatory and reparative phases in the infarcted myocardium. *Circ Res* 2014;**114**:1611–1622.
54. Keren-Shaul H, Spinrad A, Weiner A, Matcovitch-Natan O, Dvir-Szternfeld R, Ulland TK, David E, Baruch K, Lara-Astaiso D, Toth B, Itzkovitz S, Colonna M, Schwartz M, Amit I. A unique microglia type associated with restricting development of Alzheimer's disease. *Cell* 2017;**169**:1276–1290.e17.
55. Nugent AA, Lin K, van Lengerich B, Lianoglou S, Przybyla L, Davis SS, Llapashtica C, Wang J, Kim DJ, Xia D, Lucas A, Baskaran S, Haddick PCG, Lenser M, Earr TK, Shi J, Dugas JC, Andreone BJ, Logan T, Solanoy HO, Chen H, Srivastava A, Poda SB, Sanchez PE, Watts RJ, Sandmann T, Astarita G, Lewcock JW, Monroe KM, Di Paolo G. TREM2 regulates microglial cholesterol metabolism upon chronic phagocytic challenge. *Neuron* 2020;**105**:837–854.e9.
56. Amorim A, De Feo D, Friebel E, Ingelfinger F, Anderfuhren CD, Krishnarajah S, Andreadou M, Welsh CA, Liu Z, Ginhoux F, Greter M, Becher B. IFNgamma and GM-CSF control complementary differentiation programs in the monocyte-to-phagocyte transition during neuroinflammation. *Nat Immunol* 2022;**23**:217–228.
57. Weinreb C, Rodriguez-Fraticelli A, Camargo FD, Klein AM. Lineage tracing on transcriptional landscapes links state to fate during differentiation. *Science* 2020;**367**:eaaw3381.
58. Ruparelia N, Godec J, Lee R, Chai JT, Dall'Armellina E, McAndrew D, Digby JE, Forfar JC, Prendergast BD, Kharbanda RK, Banning AP, Neubauer S, Lygate CA, Channon KM, Haining NW, Choudhury RP. Acute myocardial infarction activates distinct inflammation and proliferation pathways in circulating monocytes, prior to recruitment, and identified through conserved transcriptional responses in mice and humans. *Eur Heart J* 2015;**36**:1923–1934.

5.1 Supplementary figures

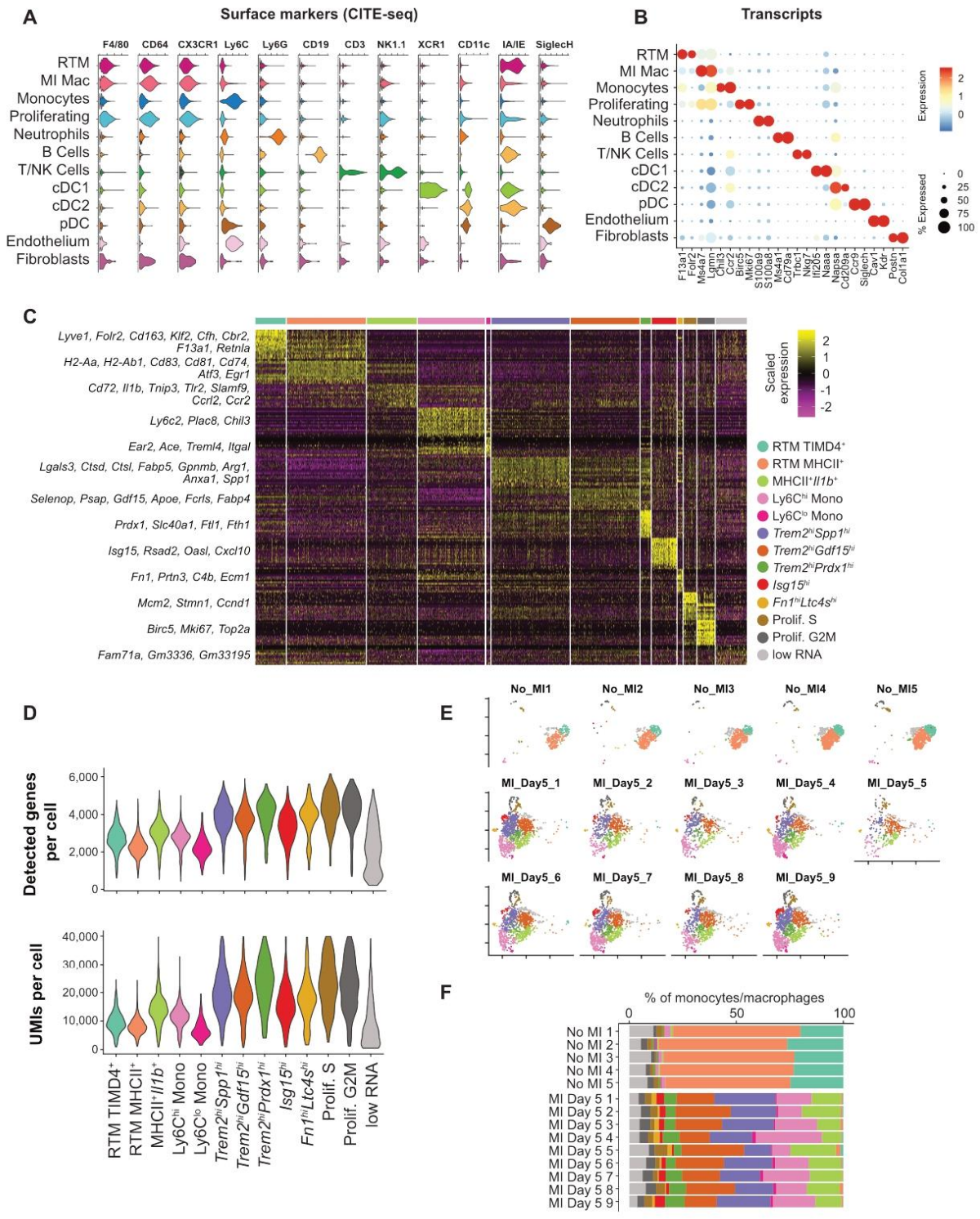

Supplementary Figure I: additional data related to Figure 1. For all data shown in Figure SI, cells were obtained from n=5 mice without MI, and n=9 mice with MI, pooled from 2 independent experiments (see methods). **A-B)** Identification of immune lineages in total cardiac CD45⁺ cells (n=13,805) based on expression of known markers with **A)** cell surface CITE-seq signal for selected markers and **B)** selected enriched transcripts; **C)** heatmap of scaled expression of the top 20 enriched genes (ranked by Log2 fold change) in the 13 monocyte/macrophage clusters (n=10,365 cells). Representative genes associated to each cluster are indicated; **D)** number of genes and UMIs (unique molecular identifiers) detected in the monocyte/macrophage clusters (cells with >40,000 UMIs were excluded during quality control filtering) (n=10,365 cells). **E)** UMAP from Figure 1D split according to sample of origin; **F)** proportion of each cluster among total monocytes/macrophages in each sample.

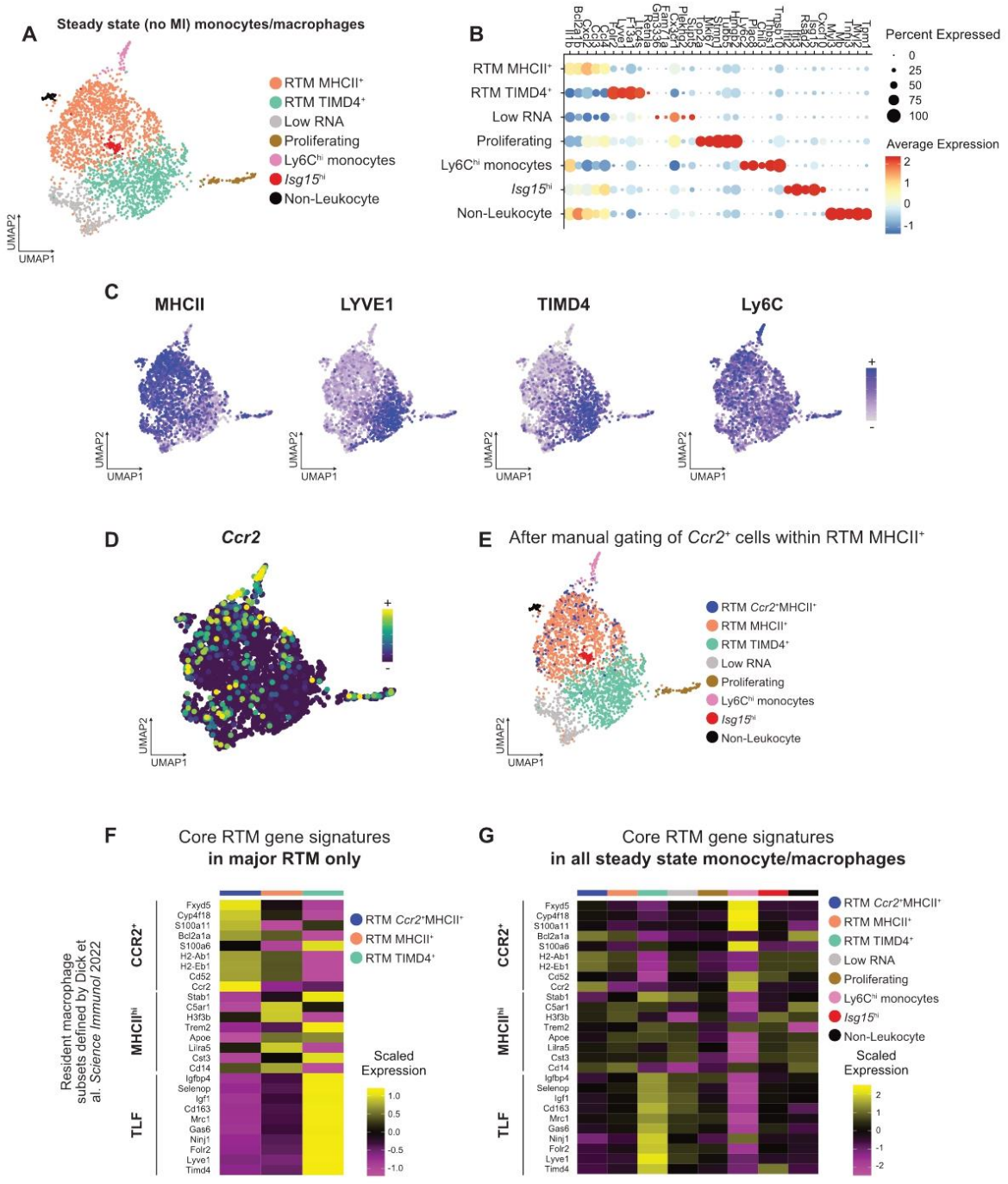

Supplementary Figure II (related to Figure 1): Analysis of cardiac monocytes/macrophages in the steady state alone. For all graphs in Figure 1, cells were obtained from n=5 mice without MI, pooled from 2 independent experiments (see methods). **A)** UMAP representation of transcriptome-based clustering of steady state monocyte/macrophages; n=2,730 cells; **B)** expression of the top 5 differentially expressed genes (ranked by log fold change) per cluster; **C)** CITE-seq signal of the indicated surface markers projected onto the UMAP plot; **D)** transcript expression of *Ccr2* projected onto the UMAP plot; **E)** UMAP plot after manual selection of *Ccr2*$^{+}$ cells within the 'RTM MHCII+' cluster; **F-G)** heatmap showing average relative expression of transcripts assigned to 'core resident tissue macrophage gene expression signatures' in three resident tissue macrophage (RTM) subsets as defined by Dick et al. Science Immunology 2022: 'TLF' resident macrophages (i.e 'Timd4^{+}Lyve1^{+}Folr2^{+}), MHCII^{+} resident macrophages and CCR2^{+} resident macrophages. The heatmap in **F)** shows relative levels of these transcripts in the major RTM populations, while in **G)** the relative expression for all steady state monocyte/macrophage populations is shown.

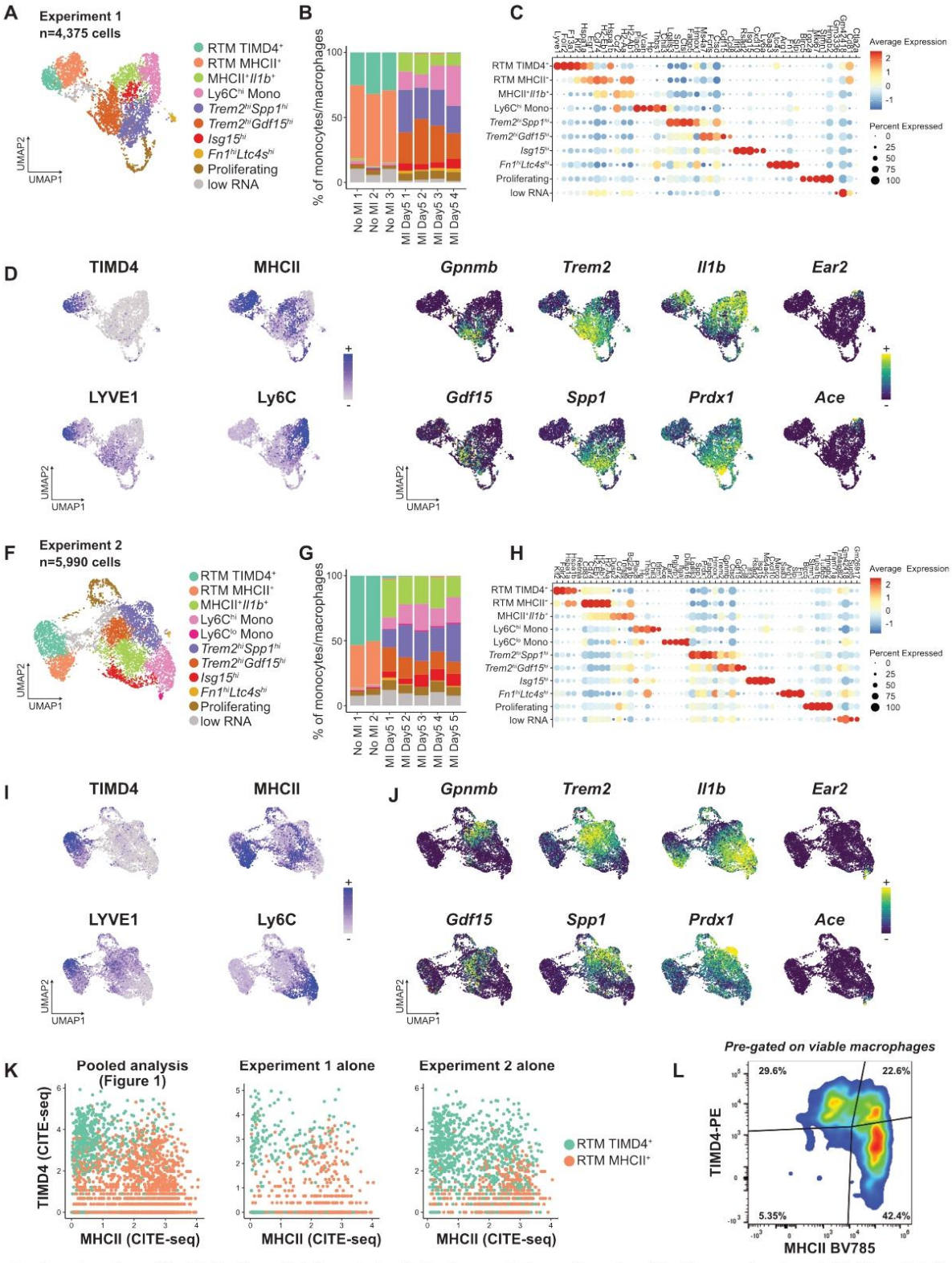

Supplementary Figure III (related to Figure 1): independent analysis of monocytes/macrophages in cell hashing experiments pooled in Figure 1. A-E) Experiment 1 comprising n=4,375 monocytes macrophages from n=3 mice without MI and n=4 mice with MI at Day 5; **F-J)** Experiment 2 comprising n=5,990 monocytes/macrophages from n=2 mice without MI and n=5 mice with MI at Day 5. **A and F**) UMAP plot and clustering analysis; **B and G**) proportion of each cluster across individual samples; **C and H**) dotplot showing average expression of the top5 differentially expressed genes in each cluster (ranked according to fold change); **D and I)** CITE-seq signal of the indicated surface markers projected onto the UMAP plot; **E and J)** expression of the indicated transcripts projected onto the UMAP plot. **K)** CITE-seq signal for TIMD4 and MHCII in cardiac RTM subset in the pooled analysis from Figure 1 and in each experiment alone. **L)** Flow cytometry analysis of TIMD4 and MHCII in cardiac RTM from a control C57BL6/J mouse, pre-gated on viable macrophages (viable CD45+CD11b+Ly6G-F4/80+Ly6Clow).

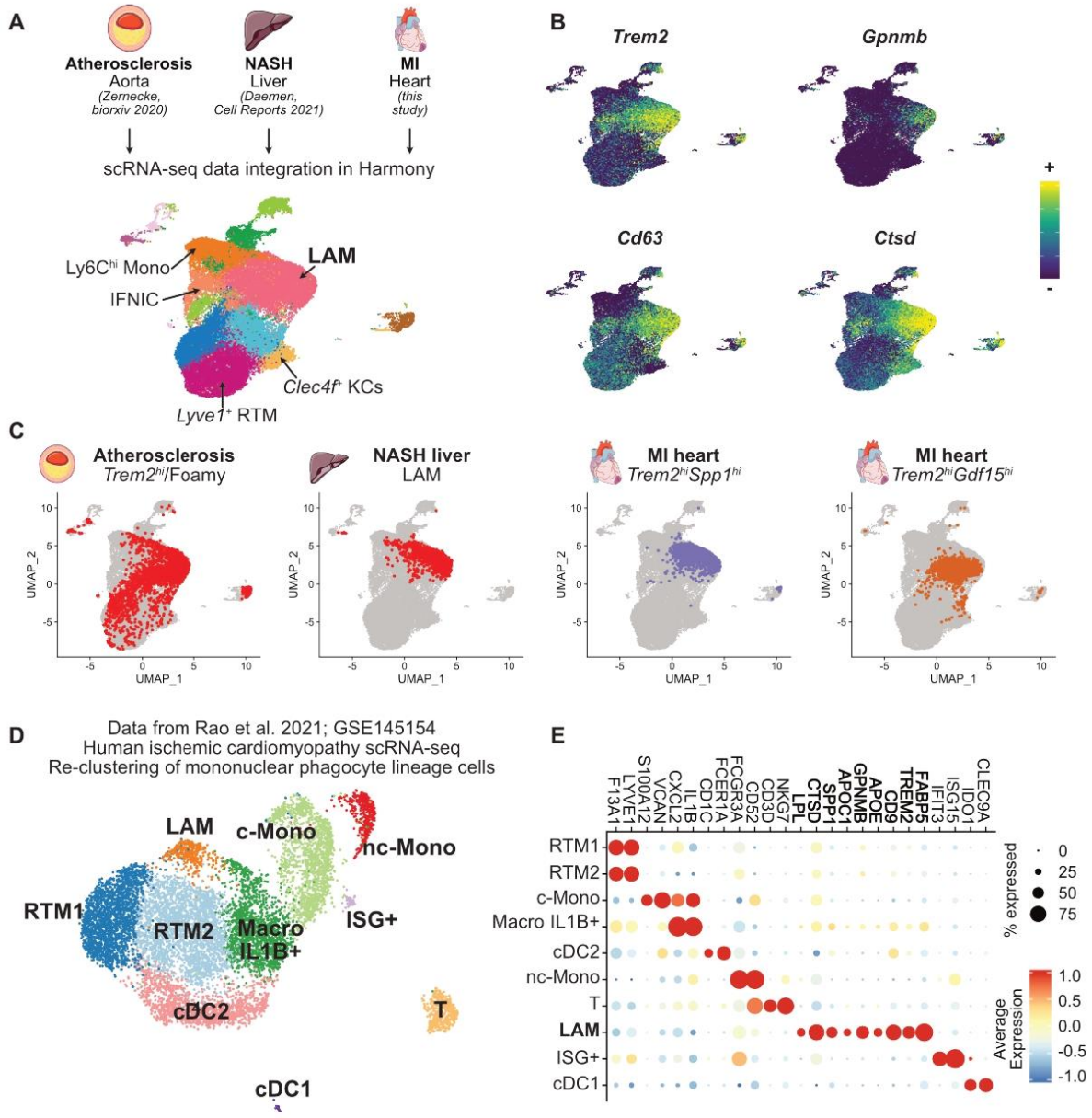

Supplementary Figure IV: Inter-organ and cross-species identification of the *Trem2^hi^* lipid-associated macrophage signature. A) Single-cell gene expression data from mouse healthy and atherosclerotic aorta, non-alcoholic steatophepatitis (NASH)-liver and healthy/infarcted heart were integrated using Harmony. Common populations (Ly6C^hi^ monocytes, IFNIC, lipid associated macrophage (LAM)-signature macrophages), as well as tissue-specific populations (Lyve1+ RTM in the aorta and heart, *Clec4f*+ Kupffer Cells (KCs) in the liver were identified; **B)** expression of LAM-signature transcripts projected on the UMAP plot; **C)** localization of LAM-signature populations from the indicated organs on the UMAP plot; for panels A to C: n=34,847 cells; the atherosclerosis dataset consists of a pool of n=12 scRNA-seq datasets (see Zernecke, biorxiv 2020), the NASH dataset of one scRNA-seq library (Daemen, Cell Reports 2021), for the heart dataset cells were obtained from n=5 mice without MI, and n=9 mice with MI, pooled from 2 independent experiments(see Figure 1). **D)** UMAP plot of re-clustered cells corresponding to human mononuclear phagocyte lineage cells from Rao et al. GSE145154 and **E)** dot plot showing average expression of selected significant marker genes in the identified cell populations. RTM: resident tissue macrophage, c-Mono: classical monocytes, nc-Mono: non-classical monocytes, cDC: conventional Dendritic Cell, LAM: lipid associated macrophage. For panel C-D: cells were obtained from n=3 samples ischemic left ventricle, n=1 sample remote non-ischemic left ventricle, n=1 sample control myocardium; total n cells=10,076.

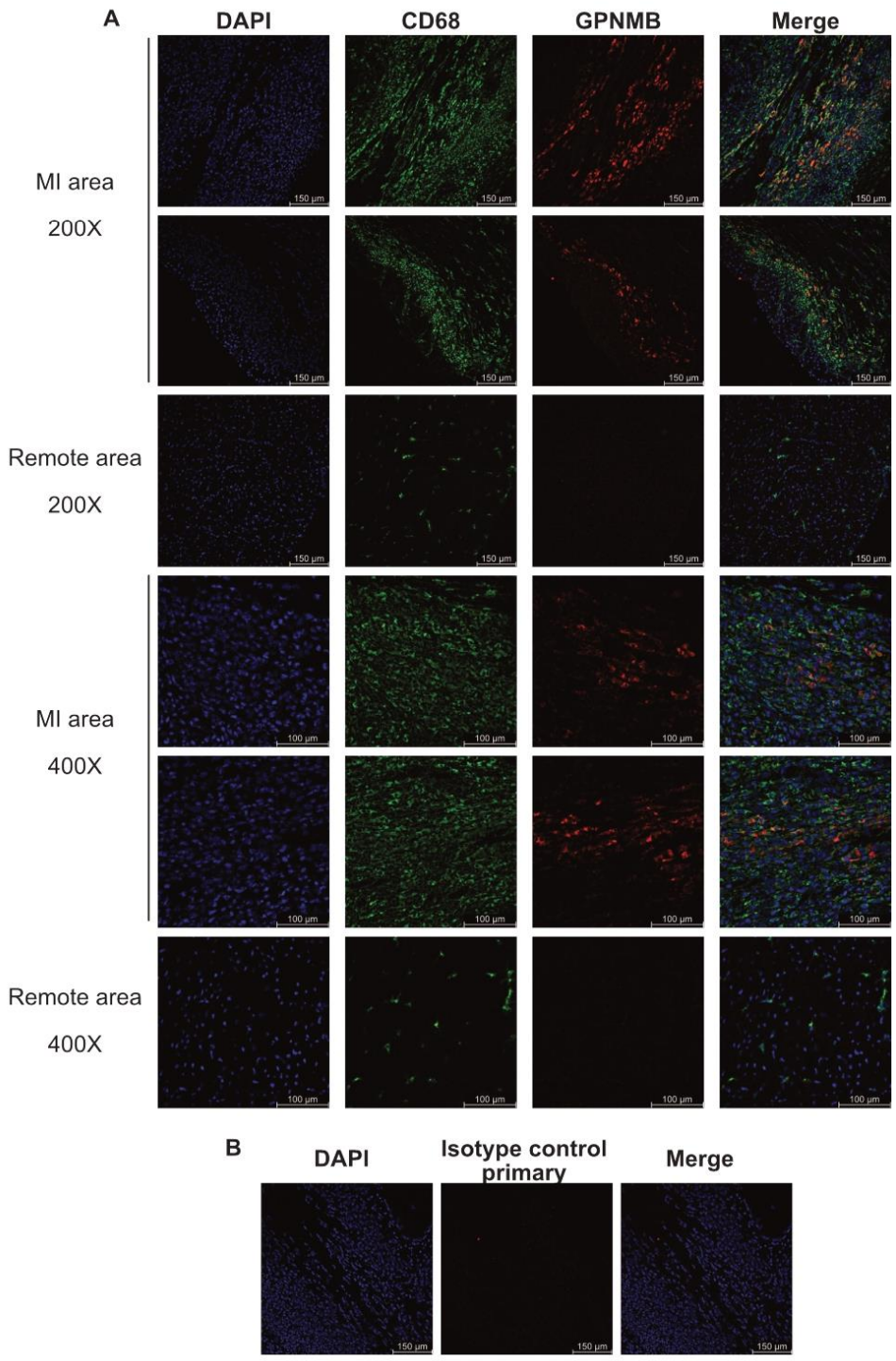

Supplementary Figure V (related to Figure 2): Additional GPNMB immunostainings. A) Immunofluorescence labeling of CD68 and GPNMB in day 5 infarcts at the indicated magnification, in the infarcted area and in the remote non-ischemic area. **B)** control immunostaining with an isotype control antibody (rabbit IgG) used as a primary antibody instead of the anti-GPNMB antibody. Picture is from the macrophage-rich infarcted area.

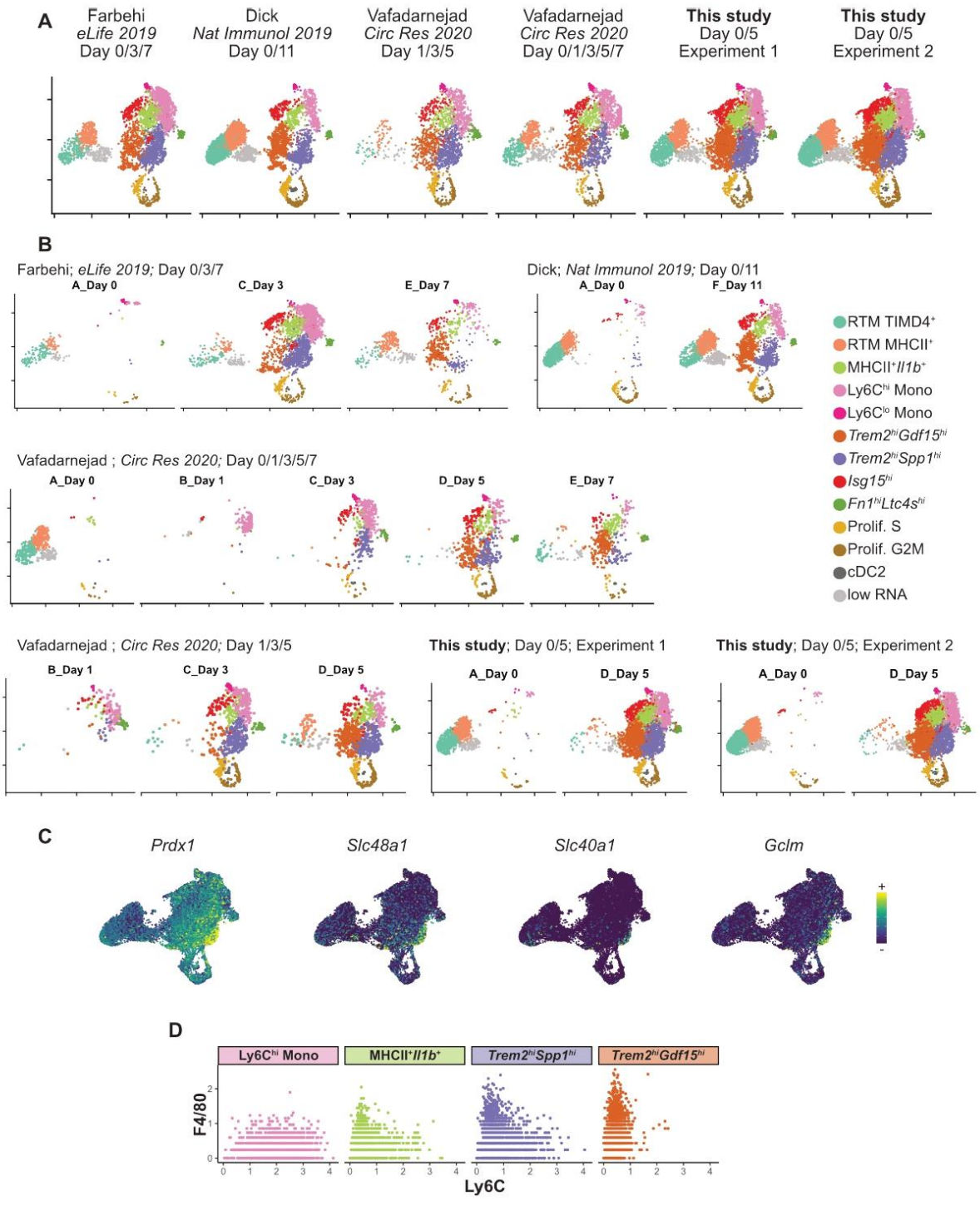

Supplementary Figure VI (related to Figure 3): integration of single-cell RNA-seq data from different MI studies. A) The indicated MI datasets were integrated using Harmony and monocyte/macrophage population identified (see Figure 2G); the resulting clustering analysis and UMAP visualization are shown split according to dataset of origin with monocyte/macrophage clusters color coded; in **B)** the UMAP for each dataset is further split according to time point; **C)** expression of transcripts of the *Trem2*^{hi}*Prdx1*^{hi} signature projected onto the UMAP plot. In panel A and B: n=24,637 total cells from n=6 independent scRNA-seq datasets. **D)** CITE-seq signal for Ly6C vs. F4/80 in the indicated cell populations.

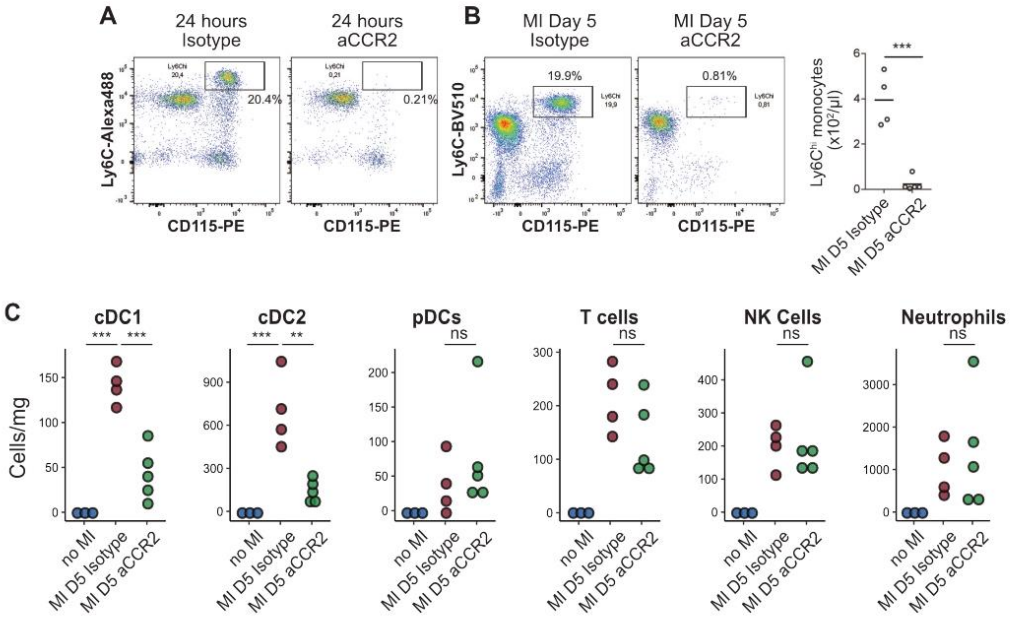

Supplementary Figure VII (related to Figure 4): CCR2^{+} cell depletion: additional data. A-B) Flow cytometry analysis shows efficient depletion of circulating CD115^{+}Ly6C^{hi} monocytes (pre-gated on CD11b^{+} myeloid cells) **A)** 24 hours after a single injection of anti-CCR2 antibody clone MC-21 (representative FACS plot for one experiment with n=2 per condition) and **B)** at 5 days after myocardial infarction following daily injection of anti-CCR2 starting 1 day before the onset of surgery (n=4 mice with MI at day 5 treated with Isotype control; n=5 mice with MI at day 5 treated with anti-CCR2); **C)** absolute counts of the indicated cell clusters (per mg of cardiac tissue; n=3 mice without myocardial infarction, n=4 mice at day 5 after myocardial infarction treated with Isotype Control; n=5 mice at day 5 after myocardial infarction treated with anti-CCR2). ***p<0.001; **p<0.01; ns: not significant.

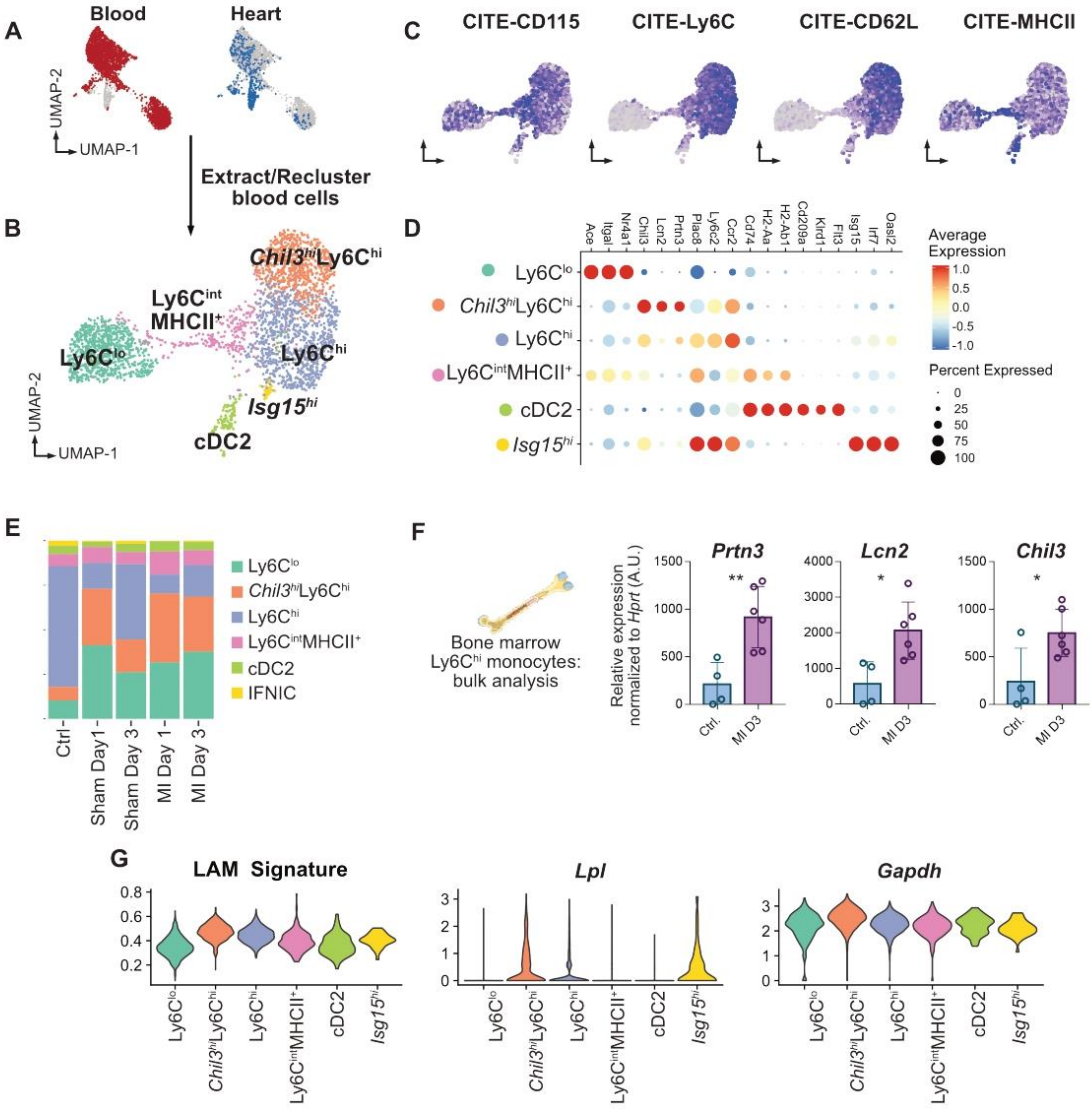

Supplementary Figure VIII: Myocardial infarction shifts circulating Ly6C^{hi} monocytes towards a *Chil3^{hi}* granulocyte-like transcriptional state. For data shown in panel A-E and G: n=2,695 cells, obtained from n=1 pooled cell preparation per experimental condition, grouped in a single (n=1) multiplexed scRNA-seq dataset. **A)** Experimental design overview and clustering analysis of blood monocytes/cDC2; **B)** clustering analysis; **C)** CITE-seq signal for the indicated surface markers in blood monocytes/cDC2 projected on the UMAP plot; **D)** Dot Plot showing average expression of selected markers in the different clusters; **E)** proportion of the indicated clusters among total monocytes according to sample of origin; **F)** expression of the indicated transcripts as measured by qPCR in sorted bone marrow Ly6C^{hi} monocytes (A.U.=arbitrary units); *p<0.05; **p<0.01; unpaired t test; one experiment with n=4 Control mice, n=6 mice at day 3 after MI. **G)** expression of the indicated metrics/transcripts in the clusters.

6 Chapter 5: Role of *Trem2^{hi}* LAM macrophages after Myocardial Infarction

In **Chapter 4** we identified **Trem2^{hi}** LAM macrophages with a pro-fibrotic gene signature populating the infarcted heart. In this chapter we analyzed the role of *Trem2* in controlling macrophage response and cardiac repair after myocardial infarction.

6.1 *Trem2* is required for LAM macrophage response in the infarcted heart

TREM2 is known to be involved in macrophage survival in different contexts. [348,349] We performed CD68 staining in heart tissue sections at Day5 after MI from wild type and Trem2ko mice to evaluate macrophage content in the tissue. Measurements of macrophage in the infarcted heart showed a 50% reduction of $CD68^{+}$ area in Trem2ko mice compared to wild type control, in line with the notion that TREM2 is necessary for macrophage survival *in vivo* (**Figure 15A**). Due to lack of markers to identify histologically and by flow cytometry the different MI-associated macrophages described in **Chapter 4**, we employed scRNA-seq of leukocytes isolated from infarcted and non-infarcted heart of wild type and Trem2ko mice to resolve MI-associated macrophage functional heterogeneity in *Trem2*-deficiency condition (**Figure 15B**). In our dataset we could resolve 14,194 leukocytes in which 10,948 cells were defined as monocyte/macrophages that we subsetted and re-clustered to deeply analyze macrophage heterogeneity (**Figure 15C-D**). We identified monocyte/macrophage populations similar to those described in **Chapter 4**. Cell number analysis of the different monocyte/macrophage clusters showed a specific reduction of the LAM macrophages and $Ly6C^{hi}$ monocytes in Trem2ko mice compared to wild type control, while the number of the tissue resident macrophages and the other MI-associated macrophages were unaffected (**Figure 15E**).

Trem2 is known to be required for the LAM signature upregulation in macrophages. [388,445,477] To corroborate this notion, we checked whether *Trem2* is required for the LAM signature acquisition in the context of MI. We applied the LAM signature score (see **Chapter 4**) to the *Trem2*^{hi} LAM macrophage clusters in our scRNA-seq dataset and observed a reduction in the LAM signature score in Trem2ko mice compared to wild type control (**Figure 15F**).

Overall, our data suggests that *Trem2* is required for LAM macrophages accumulation and LAM signature acquisition in macrophages in the heart after MI.

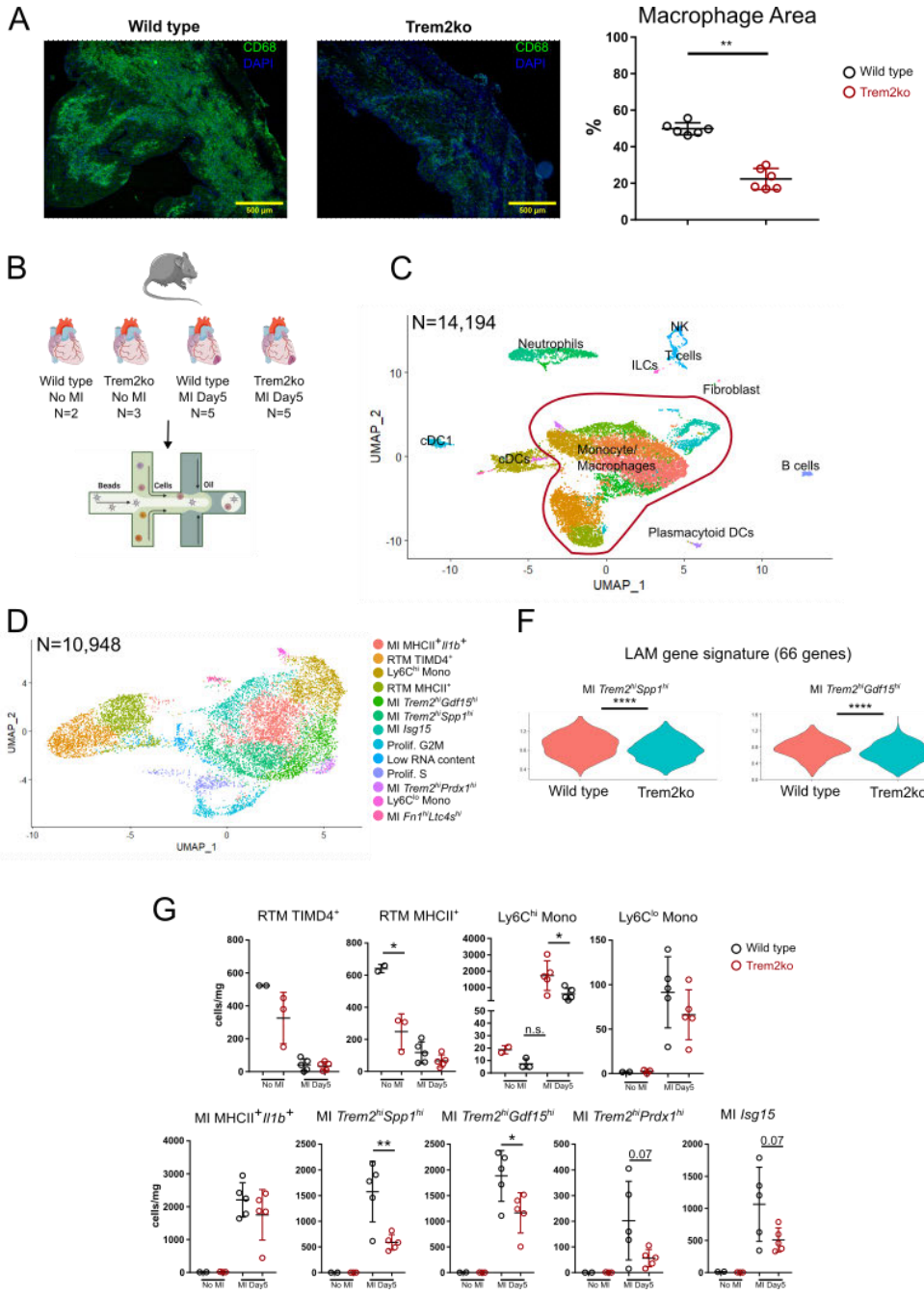

Figure 15: TREM2 is required for LAM macrophages accumulation in the infarcted heart. A, representative immunofluorescence pictures of CD68 staining in wild type and Trem2ko mice (left) and quantitative analysis of CD68^{+} area in wild type (n=6) and Trem2ko (n=6) mice; **B**, graphical representation of the experimental layout; **C**, UMAP plot of total viable CD45+ cells; **D**, UMAP plot and Seurat clusters of macrophage subclustering; **F**, LAM signature score applied in MI *Trem2^{hi}Spp1^{hi}* and MI *Trem2^{hi}Gdf15^{hi}* in wild type and Trem2ko mice; **G**, quantitative analysis of the indicated cell types in Wild type No MI (n=2), Trem2ko no MI (n=3), WT MI Day5 (n=5), and Trem2ko No MI (n=5). Statistical analysis was performed using Mann-Whitney U test for panel **A** and Kruskall-Wallis test with Dunn

multiple comparison for panel **E**. Images are taken from Servier Medical Art (smart.servier.com*)* and arranged with Inkscape.

6.2 *Trem2^{hi}* LAM macrophages promote fibrosis after MI

To elucidate *Trem2^{hi}* LAM macrophage function, we performed MI in wild type and Trem2ko mice and measured different functional readouts parameters after 28 Days (**Figure 16A**). Over 28 days, we could not observe changes in survival between wild type and Trem2ko mice (**Figure 16B**). We recorded echocardiography at Day0 (no MI), Day7, Day14, and Day28 after MI and measured ejection fraction and fractional shortening to evaluate cardiac function. No differences were observed in ejection fraction and fractional shortening, at the apex and mid ventricle level, between wild type and Trem2ko mice at any of the time points analyzed (**Figure 16C-D**). We then evaluated morphological changes in the heart at histology level. Infarct size was unchanged between wild type and Trem2ko mice (**Figure 16E**). Staining with Wheat Germ Agglutinin (WGA) and CD31 was performed to investigate hypertrophy by measuring cardiomyocyte's cross-sectional area (CSA) and angiogenesis respectively. In line with the other results, hypertrophy and angiogenesis was not affected in Trem2ko mice compared to wild type control mice (**Figure 16F-G**). We already showed (**Chapter 4**) that *Trem2^{hi}* LAM macrophages are enriched in a pro-fibrotic gene expression signature (e.g., *Spp1, Mmp14*), suggesting a role in fibrosis. To confirm that, we performed Sirius red staining in heart section at Day28 after MI to measure collagen deposition in the border zone. In line with our hypothesis, we observed reduced collagen deposition in the border zone of Trem2ko mice hearts compared to control (**Figure 16G**). Although we have seen less collagen at Day28 after MI, fibroblast area at Day5 after MI was not changed between wild type and Trem2ko mice (**Figure 16H**).

Overall, our data highlight the role of *Trem2* in fibrotic processes in myocardial healing.

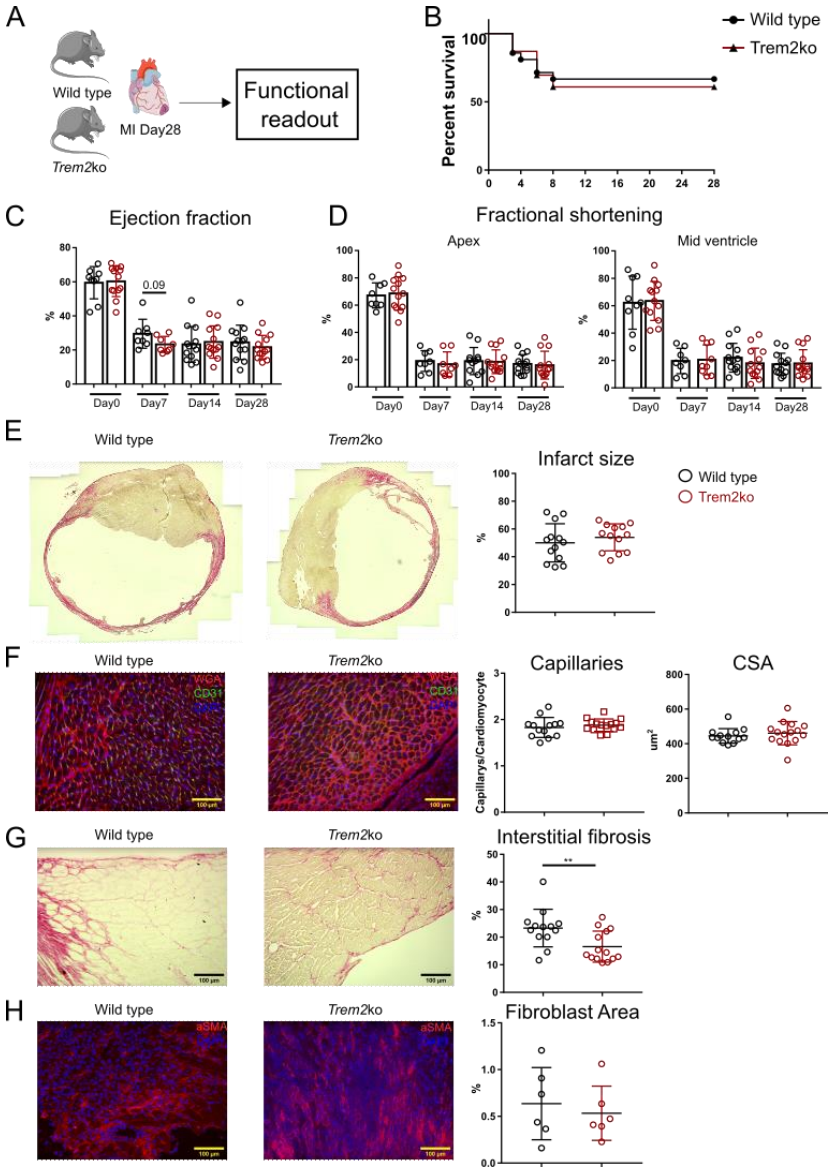

Figure 16: *Trem2*-deficiency reduced collagen deposition and does not influence cardiac function in the infarcted heart. A, graphical representation of the experimental layout; **B**, survival plot of wild type (n=21) and Trem2ko (n=23) mice over 28 days after MI; **C**, ejection fraction expressed in percentage of wild type (Day0 n=9, Day7 n=7, Day14 and Day28 n=13) and Trem2ko (Day0 n=13, Day7 n=8, Day14 and 28 n=13) mice; **D**, fractional shortening expressed in percentage at the apex and mid ventricle level of wild type (Day0 n=9, Day7 n=7, Day14 and Day28 n=13) and Trem2ko (Day0 n=13, Day7 n=8, Day14 and 28 n=13) mice; **E**, representative heart staining of Sirius red staining (left) and quantitative analysis of infarct size (right) in wild type (n=13) and Trem2ko (n=13) mice at Day28 after MI; **F**, representative heart immunofluorescece staining of CD31 and WGA (left) and quantitative analysis of capillaries counts and WGA area (right) in wild type (n=13) and Trem2ko (n=13) mice at Day28 after MI; **G**, representative heart staining of Sirius red staining (left) and quantitative analysis of red positive staining in the border zone (right) in wild type (n=13) and Trem2ko (n=13) mice at Day28 after MI; **H**, representative heart immunofluorescence staining of αSMA (left) and quantitative analysis of αSMA positive area in wild type (n=6) and Trem2ko (n=5) mice at Day5 after MI. Statistical analysis was performed using Log-Rank (Mantel-

Cox) for panel **B**, one-way ANOVA with multiple comparison for panel **C** and **D**, and unpaired t test for panel **E**, **F**, **G**, and **H**. Images are taken from Servier Medical Art (smart.servier.com*)* and arranged with Inkscape.

6.3 *Trem2* is required for LAM signature genes upregulation *in vitro*

In **Chapter 4** we hypothesized and showed that efferocytosis, a process highly exerted by macrophages during myocardial healing processes, is one of the stimuli that drives the acquisition of the LAM signature in BMDM. To corroborate the notion that Trem2 is required for the LAM signature acquisition, we generated wild-type and Trem2ko BMDM and treated them with apoptotic cells in a ratio 1:5 (1 macrophage to 5 apoptotic cells) (**Figure 17A**). We observed that the upregulation of the LAM genes in BMDM after stimulation with apoptotic cell was reverted in some of the signatures genes in Trem2-deficiency condition (e.g. *Gpnmb, Abca1, Fabp5*) (**Figure 17B**). However, the expression of a key LAM-signature gene, *Spp1* encoding osteopontin, was similarly upregulated in Trem2-deficient macrophages. This data suggest that Trem2 is partially required for the LAM signature acquisition in BMDM challenged with apoptotic cells.

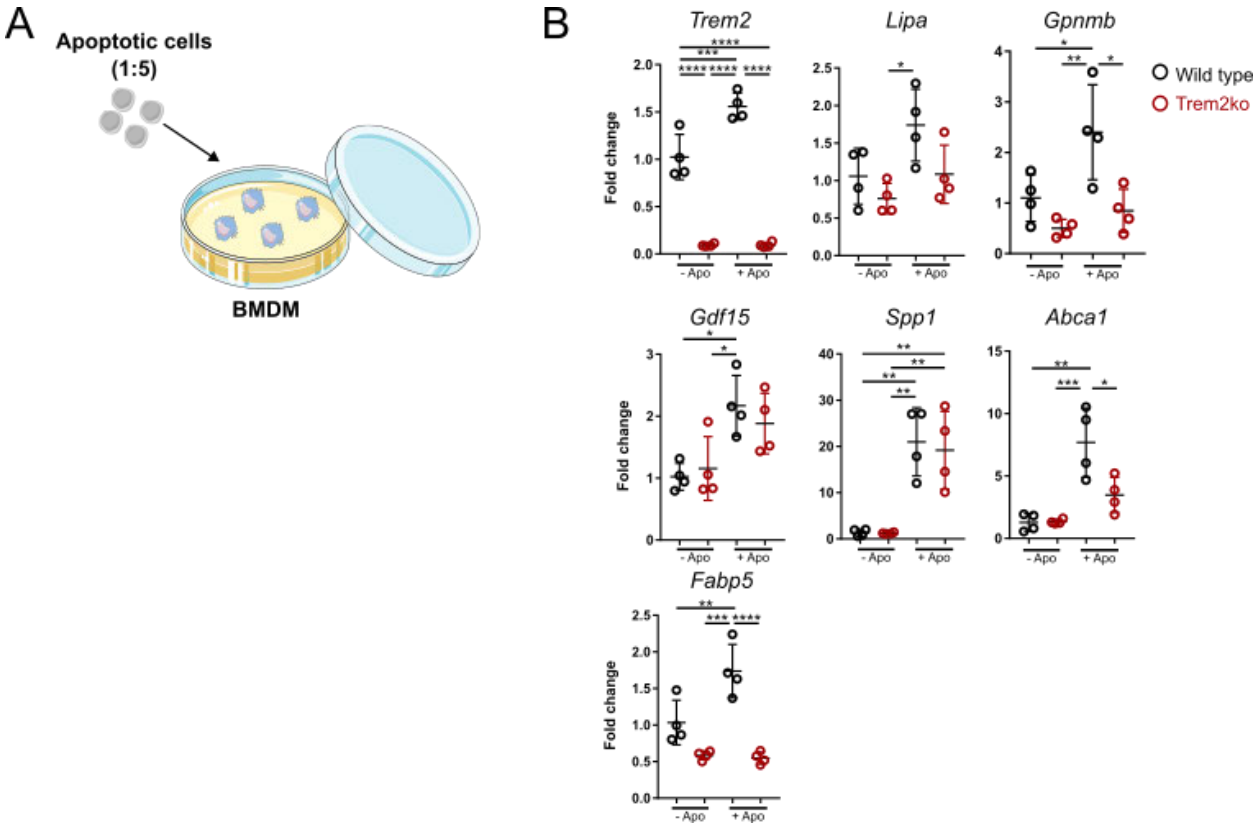

Figure 17: *Trem2* is required for LAM signature acquisition in apoptotic cell-stimulated bone marrow-derived macrophages. A, graphical representation of the experimental setup; **B**, quantitative PCR analysis of the indicated transcripts in wild type (-Apo n=4; +Apo n=4) and Trem2ko (-Apo n=4; +Apo n=4) mice. Statistical analysis in panel **B** was performed using one-way ANOVA with multiple comparison. Images are taken from Servier Medical Art (smart.servier.com) and arranged with Inkscape.

7 Chapter 6: Discussion

Using single-cell CITE-seq analysis of circulating and cardiac leukocytes at different time points after MI we explored the dynamics of neutrophils and monocytes/macrophages heterogeneity in experimental myocardial infarction. We could identify a new SiglecF^{hi} neutrophils state and heterogeneous population of monocyte-derived macrophages with specific gene-expression signature in the infarct area. We also identified three *Trem2^{hi}* macrophage subsets enriched in a LAM signature and potentially involved in cardiac fibrosis, and analyzed the function of TREM2 in macrophage responses in the infarcted heart.

Neutrophil heterogeneity in myocardial infarction

Neutrophils rapidly infiltrate the ischemic heart and are known to play both deleterious and protective role. [262]

From Day1 to Day5 after MI, we observed diverse neutrophils transcriptional states infiltrating the heart in a time-dependent manner. In particular, we described a neutrophil population characterized by SiglecF^{hi} expression starting at Day3 after MI. A similar state was also described in tumor-infiltrating neutrophils and, more recently, they have been identified in different inflammatory contexts, such as renal inflammation, inflamed olfactory neuroepithelium and asthma. [258,524–527] We also observed a neutrophil population with a type I IFN response (enriched in *Isg15*, *Irf7*) previously described during bacterial infection. [246] Although these neutrophils were abundant in the blood, neutrophils with a type I IFN response are not increasing after MI, in contrast to a study showing their expansion after cardiac ischemic injury. [528] RNA sequencing and proteomics of bulk-sorted neutrophils already described a temporal dynamic neutrophils response in the infarcted heart, supporting inflammation in the early stages to then support scar formation during the reparative phase. [259] Although these studies described a shift in neutrophils response over time, their heterogeneity was not elucidated. N1 and N2 neutrophils classification was suggested using markers defining M1/M2 macrophage population, a classification known to be insufficient to describe macrophage heterogeneity *in vivo*. [260,353]

Our scRNA-seq analysis of cardiac neutrophils described diverse transcriptional state populating the heart at different time points, characterizing a more complex response compared to the one previously described.

SiglecF^{hi} neutrophil state expressed markers related to aging neutrophils, such as low CD62L and high CXCR4 expression. On the contrary, cardiac SiglecF^{lo} neutrophils expressed young neutrophil markers genes (e.g. CD62L) as the one described in the blood, suggesting that SiglecF^{lo} state represents newly infiltrating neutrophils. Although SiglecF^{hi} neutrophils expressed aging genes shared with "aged" neutrophils in the blood, they are characterized by upregulation of SiglecF and ICAM1, suggesting that neutrophils aging in the infarcted heart follow a different direction compared to the one in the blood, probably induced by the tissue microenvironment. However, our data cannot exclude that events of pre-commitment towards the SiglecF^{hi} state might be upregulated prior infiltration in the infarcted heart. To address this question, in depth transcriptional analysis of blood and bone marrow neutrophils are necessary to detect changes during granulopoiesis induced by MI. For instance, by using metabolic RNA labeling to analyze newly synthetized and old RNA, such as SLAM-seq, or changes in chromatin accessibility, such as ATAC-seq.

In the context of MI, neutrophils perform diverse functions. SiglecF^{hi} neutrophils described in lung cancer displayed augmented ROS production compared to SiglecF^{lo} neutrophils.[258] At Day3 after MI, SiglecF^{hi} exhibited higher ROS production and phagocytosis ability in comparison to the SiglecF^{lo} counterpart. Instead, Day1 neutrophils and SiglecF^{hi} had similar ROS production and phagocytosis capacity. Production of ROS is known to promote tissue injury and release of pro-inflammatory cytokines, while phagocytosis is essential for removal of necrotic myocardial cells and debris.[272–274,287]Although SiglecF^{hi} neutrophils showed an increase in both processes, in which function they are specialized still needs to be determined. Neutrophils are also able to produce NETs, a process shown to promote cardiac events in patients with acute MI, but we did not check for NETs production in SiglecF^{hi} neutrophils.[277–280] The functional role of SiglecF expression in neutrophils remains still unknown. SiglecF engagement has been described to induce apoptosis in eosinophils.[529,530] Since SiglecF^{hi} neutrophils appear when neutrophils infiltration starts to decline, SiglecF acquisition in neutrophils might be associated with

induction of apoptotic processes and inflammation resolution. However, cardiac SiglecF^{hi} neutrophils are enriched in anti-apoptotic genes (e.g. *Bcl2a1a*, *Bcl2a1b*, *Bcl2a1d*) and they also exhibited activation of the NFkB signaling pathway, a known program that support survival and resistance to apoptosis, supporting our hypothesis that SiglecF^{hi} state describe a long-live neutrophil population within the infarct. [531] SiglecF^{hi} neutrophils expressed ICAM1 at both transcript and protein level. ICAM1 was shown to be induced in neutrophils by LPS, TNFα and zymosan, and it was associated with enhanced phagocytosis and ROS production. [532] Siglec8 is the human functional paralog of SiglecF. [533] Siglec8 in human is expressed mainly in circulating eosinophils, but it is also expressed in basophils and mast cells. [533] Although Siglec8 expression in neutrophils is not yet documented, SiglecF might represent a useful marker to track tissue-neutrophil heterogeneity in different diseases in mice. [524–527,531]

To address the functional role of SiglecF^{hi} neutrophils after MI we employed a widely used model of neutrophil depletion, in which mice were injected i.p. with the α-Ly6G 1A8 monoclonal antibody. [534] Using a gating strategy adopting CXCR2 as a surrogate marker to detect neutrophils by flow cytometry, we determined that α-Ly6G treatment efficiently depleted circulating neutrophils but failed to prevent neutrophils input in the infarcted heart. Nevertheless, we saw a shift in higher proportion of SiglecF^{hi} neutrophils, supporting our hypothesis that this state is acquired in the infarcted tissue. These findings also suggest that the effect of α-Ly6G antibody in infarcted mice may be caused by not only reduced neutrophils infiltration, but also by a shift in the different neutrophils population. [299] Employment of better model of neutrophils depletion, such as the Ly6G-DTR, or murine model to target specific pathways in neutrophils, like the *Ly6G*-cre or *S100A8*-cre mice, will be useful to better understand the role of neutrophils and their heterogeneity after MI. [535]

Neutrophils can interact with macrophages and polarize them towards a reparative phenotype via LCN2. [299] Although in this work they employed a neutrophils depletion using the same α-Ly6G 1A8 that, in our hand, did not efficiently deplete neutrophils, the neutrophils/macrophage interaction hypothesis remain relevant. In our published paper

we perform NicheNet analysis to predict ligand/receptor interaction between neutrophils and macrophages. We identified C3/C3ar1, Sema4d/Plxnd2 and Csf1/Csf1r as potential ligand/receptor interactions between neutrophils and macrophages. [536] Although the paper from Horckmanns et al. described LCN2 as neutrophil-released molecule that influence macrophage phenotype, in our dataset LCN2 receptor (SCL22A17) expression in macrophages was barely detectable. The analysis of ligand/receptor interaction is biased by the efficiency of transcripts detection by the sequencing. For this reason, the inefficient detection of SCL22A17 might be due by a technical detection problem rather than a real biological effect.

Neutrophils heterogeneity is also described in humans. Zilionis et al. performed neutrophils cross-species analysis in healthy and tumor lung describing six neutrophil subsets in mouse and five subsets in human using scRNA-seq. [537] Comparing human and murine neutrophils, just three neutrophil subsets were conserved between mouse and human sample, suggesting that neutrophils are very different across species. In the same paper, they also identified three subsets of SiglecF^{hi} neutrophils in mouse lung cancer, of which just one subset was similar in human lung cancer, suggesting that part of the SiglecF^{hi} neutrophil signature might be conserved also in human. [537] Although neutrophils are different across species, our data on SiglecF^{hi} neutrophils might still have translational relevance in the context of myocardial infarction. To address this point, cross-species scRNA-seq data integration of human and mouse neutrophils in the ischemic heart are needed. For instance, by integrating our scRNA-seq mouse dataset with the recently published human multi-omic dataset from patients with myocardial infarction. [538]

Monocyte-derived macrophage dynamics in myocardial infarction

It is widely demonstrated that monocytes and macrophages play a crucial role in cardiac repair after MI, supporting both tissue damage and tissue healing. Nevertheless, their real heterogeneity is not very well understood. For this reason, we employed CITE-seq

of cardiac monocytes/macrophages at different time points after MI to analyze monocytes and macrophages dynamics and heterogeneity.

We identified three previously described cRTMs: a TIMD4^{+} self-renewing population, a MHCII^{+} population partially replenished by monocytes, and a CCR2^{+} population completely replenished by monocytes.[375,376] We also identified new cRTM surface markers, such as MGL2 and VSIG4, and confirmed CD163 as markers for cRTMs. [539] After MI the cRTM rapidly disappeared. [375,376]

Ischemic injury drastically changed the macrophage compartment as previously described. [540,541] Our integrated scRNA-seq analysis characterized heterogeneous population of monocytes and macrophages. We could confirm low number of Ly6C^{lo} monocytes infiltrating the heart and massive infiltration of Ly6C^{hi} monocytes during the acute inflammatory phase. [542] Moreover, we described a small macrophage population with unknown function enriched in *Fn1* and *Ltc4s* and surface expression of some cRTM markers, such as TIMD4 and VSIG4. We identified four major MI-associated population including two pro-inflammatory macrophages (*Isg15*^{hi} and MHCII^{+}*Il1b*$^{+}$) and three *Trem2*^{hi} macrophage population. According to our CCR2-depletion approach and fate mapping analysis, all the major MI-associated macrophage populations originated from infiltrating monocytes. In our data, *Ccr2* transcript was detected at low level in the *Trem2*^{hi} macrophage populations, suggesting that during monocyte-to-macrophage differentiation they might downregulate CCR2. Although we were not able to stain CCR2 at protein level to validate if *Ccr2* transcript levels correlate its protein expression, this result suggest that using CCR2 as a marker for monocyte-derived macrophages might be insufficient.

Trem2^{hi} macrophages comprise three subpopulations: two large populations labeled *Trem2*^{hi}*Spp1*^{hi} and *Trem2*^{hi}*Gdf15*^{hi}, and one small population labeled *Trem2*^{hi}*Prdx1*^{hi}. These macrophage subsets are enriched in a LAM signature already described in different disease contexts, such as obesity, atherosclerosis and liver injury (NAFLD and NASH). [388,391,543–545] In obese mice and liver injury model, *Trem2*^{hi} LAM macrophages originated from monocyte as we also described in our MI model. [388,544,545] The same LAM

signature is also expressed in DAM microglia, the resident macrophage population in the brain known to self-renew by proliferation with no monocyte contribution, suggesting that the *Trem2^{hi}* LAM signature state is not restricted to monocyte-derived macrophages, but instead it may be influenced by the tissue microenvironment. [445] Indeed, immunohistology staining for GPNMB, a marker highly expressed in *Trem2^{hi}* LAM macrophages, and CD68 co-localized within the infarct area, suggesting that the infarct microenvironment might induce the LAM signature expression.

One of the main drivers of the LAM signature are lipids. [546] Indeed, LAM signature acquisition in macrophages is described in many lipid-driven diseases. [388,391,543,544] In the context of MI, in which there is not lipid accumulation in the myocardium, we hypothesized that the ischemic tissue microenvironment induces LAM signature acquisition. In human and mouse atherosclerotic plaque the Liver-X-Receptor pathway is upregulated. [547] The Liver-X-Receptor pathway is also upregulated in response to efferocytosis and seems to be important for the LAM signature acquisition, as shown in microglia under phagocytic challenge. [472] Since one of the main role of macrophages in MI is efferocytosis, we hypothesized that this process may induce the LAM signature expression. Indeed, *in vitro* bone marrow-derived macrophages treated with apoptotic cells upregulated genes related to the LAM signature, including *Trem2*, *Gpnmb*, *Spp1*, *Fabp5*, and *Lipa*. LAM signature is also induced in human monocyte-derived macrophages challenged with calcium, a DAMP released by necrotic cells. [546] Moreover, GM-CSF can also induce LAM signature acquisition *in vitro*, suggesting that a wide range of molecules, depending on the tissue microenvironment, can induce LAM signature acquisition in macrophages.

Several evidences demonstrated that TREM2 is required for DAM and LAM signature acquisition. [388,389] Also in our efferocytosis model we could confirm that *Trem2*-deficiency in bone marrow-derived macrophages negatively affect the expression of some of the LAM signature genes, such as *Gpnmb*, *Abca1* and *Fabp5*. These evidences highlight the role of TREM2 in controlling the LAM signature genes expression in different disease contexts.

In the infarcted heart we described three subpopulation of *Trem2^{hi}* LAM signature macrophages that are distinct from each other. The small subpopulation of *Trem2^{hi} Prdx1^{hi}* is enriched in iron handling genes, such has *Ftl1*, *Fth1*, *Slc40a1*, *Slc48a1*, suggesting a putative interaction with tissue iron. The role of *Trem2^{hi}Prdx1^{hi}* macrophages needs to be further characterized. *Trem2^{hi}Spp1^{hi}* and *Trem2^{hi}Gdf15^{hi}* were the most abundant LAM signature macrophages in the ischemic heart. Based on the pseudotime analysis and on the temporal loss of monocyte markers and acquisition of macrophage markers, we hypothesized that *Trem2^{hi}Spp1^{hi}* represents an intermediate state toward the *Trem2^{hi}Gdf15^{hi}* state. Nevertheless, our data does not exclude that other macrophage populations, like *Isg15^{hi}* and MHCII^{+}*Il1b*$^{+}$, could differentiate towards the *Trem2^{hi}Gdf15^{hi}* non-inflammatory subset.

During inflammation, high monocyte demand leads to their production via two distinct ways: one from the MDP progenitors giving rise to a “DC-like monocytes”, and a second one from the GMP progenitors that give rise to a “neutrophil-like monocytes” state. [304,546] Moreover, tissue injury and inflammatory events lead to a reprogramming of bone marrow monocytes. Indeed, recurrent MI decrease the number of monocytes in the bone marrow correlating with reduced leukocytes infiltration into the ischemic heart. [548] Furthermore, MI reprogram bone marrow Ly6C^{hi} monocytes towards an immunosuppressive phenotype, supporting breast cancer growth in both human and mice. [549] Our analysis of combined blood and heart leukocytes described enrichment in *Chil3* and granulocyte-associated genes, such as *Prtn3* and *Lcn2*, in circulating monocytes after MI. Bone marrow Ly6C^{hi} monocytes displayed upregulation of *Prtn3*, *Lcn2* and *Chil3* after MI, corroborating the notion that ischemic heart damage reprograms bone marrow-monocytes towards a “neutrophil-like” state. Bulk-sequencing of human blood monocytes after MI showed upregulation of *LCN2*, a marker of neutrophil-like state, suggesting that similar state is occurring also in human patients. [550] Our data indicate that the LAM signature is acquired in the infarcted myocardium and not upregulated in blood monocytes. Nevertheless, we cannot exclude that *Chil3^{hi}* monocytes are primed to differentiate in *Trem2^{hi}* LAM macrophages after infiltrating the infarcted heart.

Trem2^{hi} LAM macrophages are conserved across species and diseases as they were observed in human atherosclerosis, adipose tissue and in steatotic human liver. [390,543,546] Re-analysis of available scRNA-seq dataset revealed the presence of a macrophage subset with a LAM signature in human ischemic cardiomyopathy sample. A recent paper described SPP1+*TREM2+^{i}* macrophages also in human ischemic heart and validated their presence in the heart tissue via immunofluorescence. [538] *Trem2^{hi}* macrophages were also described in human genetic cardiomyopathy, pointing out that this macrophage state is not just present during ischemic injury but might be involved in different cardiac diseases. [551] These data demonstrate that *Trem2^{hi}* LAM macrophages could be observed also in diseased human heart, indicating conservation of this macrophage state across species and diseases. Their presence in ischemic and non-ischemic heart suggest a potential role not only during cardiac ischemic remodeling but also in genetic heart diseases.

Trem2 control LAM macrophage response in the heart after myocardial-infarction

In depth analysis of the gene expression signature of the *Trem2^{hi}* macrophage subsets revealed enrichment of genes involved in immune modulation, tissue repair, and fibrosis, such as *Il10*, *Spp1*, *Mmp14*, *Timp2*. According to their gene expression signature, we hypothesized that *Trem2^{hi}* macrophages play a crucial role in cardiac remodeling after MI. *Trem2* was shown to not only be important for the LAM signature acquisition, but also to be necessary for the LAM macrophages function, as shown in obese mice. [390] *Trem2*-deficient mice exhibited reduced number of *Trem2^{hi}* LAM signature macrophages in the infarcted heart, as well as reduced expression of the LAM signature transcripts. Several reports showed that TREM2 is involved in macrophage survival, in line with reduced number of LAM macrophages in *Trem2*-deficient mice after MI. [450,451,476] Nevertheless we cannot exclude that TREM2 might be involved during monocyte-to-macrophage differentiation in specific monocytes subsets. Moreover, Ly6C^{hi} monocyte numbers were reduced in *Trem2*-defcient mice after MI, suggesting a putative role of TREM2 in bone marrow monocytes production and/or mobilization.

Trem2^{hi} LAM macrophages are also promoting liver fibrosis in a model of NASH. [544] In line with this finding and with pro-fibrotic genes expression in *Trem2^{hi}* LAM signature

macrophage subsets, we observed reduced collagen deposition in the border zone in *Trem2*-deficient mice. Although *Trem2* deficiency was not affecting cardiac function and survival over 28 days after MI, we cannot exclude a long-term deleterious effect. To better understand how *Trem2* expression in macrophages influences heart failure development, evaluation of cardiac function and survival over more than 4 weeks is needed. Overall, our *Trem2* knock-out mice data didn´t show a strong change in phenotype compared to wild type mice and this could be explained in different ways. The infarcted remodeling heart is full of proteolytic enzymes needed to digest the extracellular matrix. These enzymes might also be responsible for TREM2 cleavage, as we detected increase in soluble TREM2 in both heart and blood, suggesting reduced TREM2 levels on the macrophage surface and impaired TREM2 function. One possible approach would be to treat mice withTREM2-stabilizing reagents to prevent TREM2 shedding and boost its signaling pathway in macrophages. On the other side, we cannot exclude that sTREM2 might be involved in cardiac remodeling process. Indeed, in the recent work of Jung SH. et al. , sTREM2 treatment immediately after MI improved cardiac function, infarct size and survival over 28 days, pointing out that blocking completely sTREM2 formation might promote adverse remodeling. [409] Extensive cell death and fibrosis induced by permanent coronary artery ligation might hide functional changes that cannot be appreciated in such model. [552] For this reason, employing a model of Ischemia/Reperfusion, in which tissue damage is less drastic, might be better suitable to study *Trem2^{hi}* LAM macrophage function during cardiac remodeling. Employment of time-dependent TREM2 deletion using Trem2-flox mice crossed with mice expressing inducible Cre in macrophages (e.g. Cx3cr1-CreERT2) might better explore *Trem2^{hi}* LAM macrophage function in the different phases of cardiac remodeling after MI.

The phenotypic differences that we described in our mouse model might be influenced by the effect of TREM2 in the monocytes compartment. To better define how TREM2 is controlling macrophage response, employment of TREM2 deletion specifically in mature macrophages, using the CD64-cre mouse model, might be necessary.

Overall, our data provides a high-resolution characterization of neutrophils and monocytes/macrophages heterogeneity in cardiac repair after myocardial infarction, in

which we described a novel SiglecF^{hi} neutrophils state with still unknown function and high transcriptional macrophage heterogeneity, in particular two main *Trem2^{hi}* LAM signature subsets involved in cardiac fibrosis.

8 Summary

Current therapeutic strategies efficiently improve survival in patients after myocardial infarction (MI). Nevertheless, long-term consequences such as heart failure development, are still one of the leading causes of death worldwide. Inflammation is critically involved in the cardiac healing process after MI and has a dual role, contributing to both tissue healing and tissue damage. In the last decade, a lot of attention was given to targeting inflammation as a potential therapeutic approach in MI, but the poor understanding of inflammatory cell heterogeneity and function is a limit to the development of immune modulatory strategies. The recent development of tools to profile immune cells with high resolution has provided a unique opportunity to better understand immune cell heterogeneity and dynamics in the ischemic heart.

In this thesis, we employed single-cell RNA-sequencing combined with detection of epitopes by sequencing (CITE-seq) to refine our understanding of neutrophils and monocytes/macrophages heterogeneity and dynamic after experimental myocardial infarction.

Neutrophils rapidly invade the infarcted heart shortly after ischemic damage and have previously been proposed to display time-dependent functional heterogeneity. At the single-cell level, we observed dynamic transcriptional heterogeneity in neutrophil populations during the acute post-MI phase and defined previously unknown cardiac neutrophil states. In particular, we identified a locally acquired SiglecF^{hi} neutrophil state that displayed higher ROS production and phagocytic ability compared to newly recruited neutrophils, suggesting the acquisition of specific function in the infarcted heart. These findings highlight the importance of the tissue microenvironment in shaping neutrophil response.

From the macrophage perspective, we characterized MI-associated monocyte-derived macrophage subsets, two with a pro-inflammatory gene signature (MHCII^{hi}*Il1β*^{hi}) and

three *Trem2^{hi}* macrophage populations with a lipid associated macrophage (LAM) signature, also expressing pro-fibrotic and tissue repair genes. Combined analysis of blood monocytes and cardiac monocyte/macrophages indicated that the *Trem2^{hi}* LAM signature is acquired in the infarcted heart.

We furthermore characterized the role of TREM2, a surface protein expressed mainly in macrophages and involved in macrophage survival and function, in the post-MI macrophage response and cardiac repair. Using TREM2 deficient mice, we demonstrate that acquisition of the LAM signature in cardiac macrophages after MI is partially dependent on TREM2. While their cardiac function was not affected, TREM2 deficient mice showed reduced collagen deposition in the heart after MI. Thus, our data in *Trem2*-deficient mice highlight the role of TREM2 in promoting a macrophage pro-fibrotic phenotype, in line with the pro-fibrotic/tissue repair gene signature of the *Trem2^{hi}* LAM-signature genes.

Overall, our data provide a high-resolution characterization of neutrophils and macrophage heterogeneity and dynamics in the ischemic heart and can be used as a valuable resource to investigate how these cells modulate the healing processes after MI. Furthermore, our work identified TREM2 as a regulator of macrophage phenotype in the infarcted heart

9 Zusammenfassung

Die derzeitigen therapeutischen Ansätze verbessern die Überlebenschancen von Patienten nach einem Myokardinfarkt wirksam, dennoch sind Langzeitfolgen wie die Entwicklung einer Herzinsuffizienz immer noch eine der häufigsten Todesursachen weltweit. An den Heilungsprozessen nach einem Herzinfarkt sind Entzündungreaktionen beteiligt, die sowohl zur Gewebeheilung als auch zur Gewebeschädigung beitragen. In den letzten zehn Jahren wurde besondere Aufmerksamkeit auf die gezielte Beeinflussung von Entzündungen als potenzieller therapeutischer Ansatz gewidmet, allerdings stellt die Komplexität der Entzündungszellen bezüglich Heterogenität und Funktion eine Herausforderung für die Entwicklung von Strategien zur Immunmodulation dar. Aus diesem Grund ist die Entwicklung von Methoden, mit denen Immunzellen mit hoher Auflösung charakterisiert werden können, für ein besseres Verständnis der Heterogenität und Dynamik von Immunzellen im ischämischen Herzen unerlässlich.
In dieser Arbeit haben wir scRNA-seq eingesetzt, um die Heterogenität und Dynamik von Neutrophilen und Monozyten/Makrophagen nach einem experimentell-induzierten Myokardinfarkt zu bestimmen.

Neutrophile dringen unmittelbar nach der ischämischen Schädigung in das infarzierte Herz ein wo ihre Zahl innerhalb der ersten Tage abnimmt. Zudem konnten wir eine transkriptionelle Heterogenität in neutrophilen Populationen während der akuten Entzündungsphase beobachten. Insbesondere konnten wir ab dem 3. Tag nach Infarkt einen SiglecF^{hi}-Neutrophilenstatus identifizieren, der sich unseren Daten zufolge im betroffenen Gewebe entwickelt hat. SiglecF^{hi}-Neutrophile zeigten im Vergleich zu neu rekrutierten Neutrophilen eine höhere ROS-Produktion und phagozytische Fähigkeit, was auf den Erwerb einer spezifischen Funktion im infarzierten Herzen hindeutet. Diese Ergebnisse unterstreichen die Wichtigkeit der unmittelbaren Umgebung des Gewebes für die Reaktion der Neutrophilen.

Weiterhin zeigten unsere scRNA-seq-Daten eine erhebliche Heterogenität in der Monozyten-/Makrophagenpopulation. Durch die Kombination der scRNA-seq-Analyse von kardialen und zirkulierenden Leukozyten, konnten wir eine durch ischämische

Verletzungen induzierte Monozytenpopulation mit einer "neutrophilenähnlichen" Gensignatur identifizieren.

Aus der Makrophagenperspektive beobachteten wir verschiedene MI-assoziierte Makrophagenuntergruppen, zwei mit einer pro-inflammatorischen Gensignatur ($MHCII^{hi}Il1\beta^{hi}$) und drei $Trem2^{hi}$-Makrophagenpopulationen mit einer Lipid-assoziierten Makrophagensignatur (LAM), welche auch pro-fibrotische/Gewebereparaturgene exprimieren. Darüber hinaus entdeckten wir eine kleine Population von $Fn1^{hi}Ltc4s^{hi}$-Makrophagen mit unbekannter Funktion, die mit einigen cRTMs-Markern angereichert sind. CCR2-Depletion und Fate-Mapping-Studien zeigten einen eindeutigen monozytären Ursprung der MI-assoziierten Makrophagen-Untergruppen.

TREM2 ist ein Oberflächenprotein, das hauptsächlich in Makrophagen exprimiert wird und an der Makrophagenfunktion beteiligt ist. Die Funktion von TREM2 in Makrophagen wird in verschiedenen Krankheitskontexten (z. B. Alzheimer-Krankheit, Fettleibigkeit, Atherosklerose usw.) eingehend untersucht, und ist für den Erwerb der LAM-Signatur wesentlich. In unserem Herzinfarkt-Mausmodell beobachteten wir die Expression von Genen der LAM-Signatur im infarzierten Herzen und dass TREM2 für diese Hochregulation der LAM-Gene in vivo erforderlich ist.

Unsere vorläufigen Daten in Trem2-defizienten Mäusen unterstreichen die Rolle von TREM2 zur Förderung eines pro-fibrotischen Makrophagen-Phänotyps und dementsprechend für die pro-fibrotischen/Gewebereparatur-Gensignatur der Trem2-LAM-Signaturgene.

Insgesamt liefern unsere Daten eine hochauflösende Charakterisierung der Heterogenität und Dynamik von Neutrophilen und Makrophagen im ischämischen Herzen und können als wertvolle Grundlage für die Untersuchung der Frage dienen, wie diese Zellen die Heilungsprozesse nach einem Herzinfarkt modulieren.

10 References

1. Cardiovascular diseases. Accessed September 22, 2022. https://www.who.int/health-topics/cardiovascular-diseases#tab=tab_1

2. Cardiovascular diseases (CVDs). Accessed September 22, 2022. https://www.who.int/news-room/fact-sheets/detail/cardiovascular-diseases-(cvds)

3. Prabhu SD, Frangogiannis NG. The Biological Basis for Cardiac Repair After Myocardial Infarction: From Inflammation to Fibrosis. *Circ Res*. 2016;119(1):91-112. doi:10.1161/CIRCRESAHA.116.303577

4. Tanai E, Frantz S. Pathophysiology of Heart Failure. *Compr Physiol*. 2016;6(1):187-214. doi:10.1002/CPHY.C140055

5. Left Ventricular Rupture - StatPearls - NCBI Bookshelf. Accessed August 4, 2022. https://www.ncbi.nlm.nih.gov/books/NBK559271/

6. Frangogiannis NG. Pathophysiology of Myocardial Infarction. *Compr Physiol*. 2015;5(4):1841-1875. doi:10.1002/CPHY.C150006

7. Kobayashl S, Tadokoro H, Ryd~n L, Sfisquist P-O, Haendchen R V, Corday E. *Local Beta-Adrenergic Blockade Does Not Reduce Infarct Size After Coronary Occlusion and Reperfusion: A Study of Coronary Venous Retroinfusion of Metoprolol*. Vol 7.; 1993.

8. Friedman LM. A randomized trial of propranolol in patients with acute myocardial infarction. I. Mortality results. *JAMA*. 1982;247(12):1707-1714. doi:10.1001/JAMA.1982.03320370021023

9. Reynolds RD, Burmeister WE, Gorczynski RJ, Dickerson DD, Mathews MP, Lee RJ. Effects of propranolol on myocardial infarct size with and without coronary artery reperfusion in the dog. *Cardiovasc Res*. 1981;15(7):411-420. doi:10.1093/CVR/15.7.411

10. Waagstein F, Hjalmarson ÅC. Effect of cardioselective beta-blockade on heart

function and chest pain in acute myocardial infarction. *Acta Med Scand Suppl*. 1976;587(587 S):193-200. doi:10.1111/J.0954-6820.1976.TB05881.X

11. Braunwald E, Muller JE, Kloner RA, Maroko PR. Role of beta-adrenergic blockade in the therapy of patients with myocardial infarction. *Am J Med*. 1983;74(1):113-123. doi:10.1016/0002-9343(83)91127-0

12. Pfeffer MA, Braunwald E, Moyé LA, et al. Effect of captopril on mortality and morbidity in patients with left ventricular dysfunction after myocardial infarction. Results of the survival and ventricular enlargement trial. The SAVE Investigators. *N Engl J Med*. 1992;327(10):669-677. doi:10.1056/NEJM199209033271001

13. Liu YH, Yang XP, Sharov VG, et al. Effects of angiotensin-converting enzyme inhibitors and angiotensin II type 1 receptor antagonists in rats with heart failure. Role of kinins and angiotensin II type 2 receptors. *J Clin Invest*. 1997;99(8):1926-1935. doi:10.1172/JCI119360

14. Pharmacological modification of arrhythmias after experimentally induced acute myocardial infarction. Drugs acting on the nervous system - PubMed. Accessed December 30, 2021. https://pubmed.ncbi.nlm.nih.gov/1182977/

15. Leuschner F, Panizzi P, Chico-Calero I, et al. Angiotensin-converting enzyme inhibition prevents the release of monocytes from their splenic reservoir in mice with myocardial infarction. *Circ Res*. 2010;107(11):1364-1373. doi:10.1161/CIRCRESAHA.110.227454

16. Leri A, Fiordaliso F, Setoguchi M, et al. Inhibition of p53 function prevents renin-angiotensin system activation and stretch-mediated myocyte apoptosis. *Am J Pathol*. 2000;157(3):843-857. doi:10.1016/S0002-9440(10)64598-1

17. Tang XL, Sanganalmath SK, Sato H, et al. Atorvastatin therapy during the peri-infarct period attenuates left ventricular dysfunction and remodeling after myocardial infarction. *PLoS One*. 2011;6(9). doi:10.1371/JOURNAL.PONE.0025320

18. Nakaya R, Uzui H, Shimizu H, et al. Pravastatin suppresses the increase in matrix

metalloproteinase-2 levels after acute myocardial infarction. *Int J Cardiol*. 2005;105(1):67-73. doi:10.1016/J.IJCARD.2004.12.024

19. Hayashidani S, Tsutsui H, Shiomi T, et al. Fluvastatin, a 3-hydroxy-3-methylglutaryl coenzyme a reductase inhibitor, attenuates left ventricular remodeling and failure after experimental myocardial infarction. *Circulation*. 2002;105(7):868-873. doi:10.1161/HC0702.104164

20. Chen J, Mehta JL. Angiotensin II-mediated oxidative stress and procollagen-1 expression in cardiac fibroblasts: blockade by pravastatin and pioglitazone. *Am J Physiol Heart Circ Physiol*. 2006;291(4). doi:10.1152/AJPHEART.00341.2006

21. Saxena A, Russo I, Frangogiannis NG. Inflammation as a therapeutic target in myocardial infarction: learning from past failures to meet future challenges. *Transl Res*. 2016;167(1):152-166. doi:10.1016/J.TRSL.2015.07.002

22. Tardif J-C, Kouz S, Waters DD, et al. Efficacy and Safety of Low-Dose Colchicine after Myocardial Infarction. *N Engl J Med*. 2019;381(26):2497-2505. doi:10.1056/NEJMOA1912388/SUPPL_FILE/NEJMOA1912388_DATA-SHARING.PDF

23. Ridker PM, Everett BM, Thuren T, et al. Antiinflammatory Therapy with Canakinumab for Atherosclerotic Disease. *N Engl J Med*. 2017;377(12):1119-1131. doi:10.1056/NEJMOA1707914/SUPPL_FILE/NEJMOA1707914_DISCLOSURES.PDF

24. Abbate A, Wohlford GF, Del Buono MG, et al. Interleukin-1 blockade with anakinra and heart failure following ST-segment elevation myocardial infarction: results from a pooled analysis of the VCUART clinical trials. *Eur Hear J - Cardiovasc Pharmacother*. 2022;8(5):503-510. doi:10.1093/EHJCVP/PVAB075

25. Nian M, Lee P, Khaper N, Liu P. Inflammatory Cytokines and Postmyocardial Infarction Remodeling. *Circ Res*. 2004;94(12):1543-1553. doi:10.1161/01.RES.0000130526.20854.FA

26. Mann DL. Inflammatory mediators and the failing heart: past, present, and the foreseeable future. *Circ Res*. 2002;91(11):988-998. doi:10.1161/01.RES.0000043825.01705.1B

27. Prabhu SD. Cytokine-induced modulation of cardiac function. *Circ Res*. 2004;95(12):1140-1153. doi:10.1161/01.RES.0000150734.79804.92

28. Cavalera M, Frangogiannis N. Targeting the chemokines in cardiac repair. *Curr Pharm Des*. 2014;20(12):1971-1979. doi:10.2174/13816128113199990449

29. Newton K, Dixit VM. Signaling in innate immunity and inflammation. *Cold Spring Harb Perspect Biol*. 2012;4(3). doi:10.1101/CSHPERSPECT.A006049

30. Mann DL. THE EMERGING ROLE OF INNATE IMMUNITY IN THE HEART AND VASCULAR SYSTEM: FOR WHOM THE CELL TOLLS. *Circ Res*. 2011;108(9):1133. doi:10.1161/CIRCRESAHA.110.226936

31. Ghigo A, Franco I, Morello F, Hirsch E. Myocyte signalling in leucocyte recruitment to the heart. *Cardiovasc Res*. 2014;102(2):270-280. doi:10.1093/CVR/CVU030

32. De Haan JJ, Smeets MB, Pasterkamp G, Arslan F. Danger signals in the initiation of the inflammatory response after myocardial infarction. *Mediators Inflamm*. 2013;2013. doi:10.1155/2013/206039

33. Arslan F, De Kleijn DP, Pasterkamp G. Innate immune signaling in cardiac ischemia. *Nat Rev Cardiol*. 2011;8(5):292-300. doi:10.1038/NRCARDIO.2011.38

34. Timmers L, Pasterkamp G, De Hoog VC, Arslan F, Appelman Y, De Kleijn DPV. The innate immune response in reperfused myocardium. *Cardiovasc Res*. 2012;94(2):276-283. doi:10.1093/CVR/CVS018

35. Loukili N, Rosenblatt-Velin N, Li J, et al. Peroxynitrite induces HMGB1 release by cardiac cells in vitro and HMGB1 upregulation in the infarcted myocardium in vivo. *Cardiovasc Res*. 2011;89(3):586-594. doi:10.1093/CVR/CVQ373

36. Andrassy M, Volz HC, Igwe JC, et al. High-mobility group box-1 in ischemia-

reperfusion injury of the heart. *Circulation*. 2008;117(25):3216-3226. doi:10.1161/CIRCULATIONAHA.108.769331

37. Park JS, Svetkauskaite D, He Q, et al. Involvement of toll-like receptors 2 and 4 in cellular activation by high mobility group box 1 protein. *J Biol Chem*. 2004;279(9):7370-7377. doi:10.1074/JBC.M306793200

38. Tian J, Avalos AM, Mao SY, et al. Toll-like receptor 9-dependent activation by DNA-containing immune complexes is mediated by HMGB1 and RAGE. *Nat Immunol*. 2007;8(5):487-496. doi:10.1038/NI1457

39. Volz HC, Laohachewin D, Seidel C, et al. S100A8/A9 aggravates post-ischemic heart failure through activation of RAGE-dependent NF-κB signaling. *Basic Res Cardiol*. 2012;107(2). doi:10.1007/S00395-012-0250-Z

40. Katashima T, Naruko T, Terasaki F, et al. Enhanced expression of the S100A8/A9 complex in acute myocardial infarction patients. *Circ J*. 2010;74(4):741-748. doi:10.1253/CIRCJ.CJ-09-0564

41. Morrow DA, Wang Y, Croce K, et al. Myeloid-related protein 8/14 and the risk of cardiovascular death or myocardial infarction after an acute coronary syndrome in the Pravastatin or Atorvastatin Evaluation and Infection Therapy: Thrombolysis in Myocardial Infarction (PROVE IT-TIMI 22) trial. *Am Heart J*. 2008;155(1):49-55. doi:10.1016/J.AHJ.2007.08.018

42. Rohde D, Schön C, Boerries M, et al. S100A1 is released from ischemic cardiomyocytes and signals myocardial damage via Toll-like receptor 4. *EMBO Mol Med*. 2014;6(6):778-794. doi:10.15252/EMMM.201303498

43. Reddy VS, Harskamp RE, Van Ginkel MW, et al. Interleukin-18 stimulates fibronectin expression in primary human cardiac fibroblasts via PI3K-Akt-dependent NF-kappaB activation. *J Cell Physiol*. 2008;215(3):697-707. doi:10.1002/JCP.21348

44. Gondokaryono SP, Ushio H, Niyonsaba F, et al. The extra domain A of fibronectin stimulates murine mast cells via toll-like receptor 4. *J Leukoc Biol*.

2007;82(3):657-665. doi:10.1189/JLB.1206730

45. Arslan F, Smeets MB, Riem Vis PW, et al. Lack of fibronectin-EDA promotes survival and prevents adverse remodeling and heart function deterioration after myocardial infarction. *Circ Res*. 2011;108(5):582-592. doi:10.1161/CIRCRESAHA.110.224428

46. Amarante-Mendes GP, Adjemian S, Branco LM, Zanetti LC, Weinlich R, Bortoluci KR. Pattern recognition receptors and the host cell death molecular machinery. *Front Immunol*. 2018;9(OCT):2379. doi:10.3389/FIMMU.2018.02379/BIBTEX

47. Newton K, Dixit VM. Signaling in Innate Immunity and Inflammation. *Cold Spring Harb Perspect Biol*. 2012;4(3):a006049. doi:10.1101/CSHPERSPECT.A006049

48. Mann DL. THE EMERGING ROLE OF INNATE IMMUNITY IN THE HEART AND VASCULAR SYSTEM: FOR WHOM THE CELL TOLLS. *Circ Res*. 2011;108(9):1133. doi:10.1161/CIRCRESAHA.110.226936

49. Methe H, Kim JO, Kofler S, Weis M, Nabauer M, Koglin J. Expansion of circulating toll-like receptor 4-positive monocytes in patients with acute coronary syndrome. *Circulation*. 2005;111(20):2654-2661. doi:10.1161/CIRCULATIONAHA.104.498865

50. Satoh M, Shimoda Y, Maesawa C, et al. Activated toll-like receptor 4 in monocytes is associated with heart failure after acute myocardial infarction. *Int J Cardiol*. 2006;109(2):226-234. doi:10.1016/J.IJCARD.2005.06.023

51. Van Der Pouw Kraan TCTM, Bernink FJP, Yildirim C, et al. Systemic toll-like receptor and interleukin-18 pathway activation in patients with acute ST elevation myocardial infarction. *J Mol Cell Cardiol*. 2014;67:94-102. doi:10.1016/J.YJMCC.2013.12.021

52. Selejan S, Pss J, Walter F, et al. Ischaemia-induced up-regulation of Toll-like receptor 2 in circulating monocytes in cardiogenic shock. *Eur Heart J*. 2012;33(9):1085-1094. doi:10.1093/EURHEARTJ/EHR377

53. Kim SC, Ghanem A, Stapel H, et al. Toll-like receptor 4 deficiency: smaller

infarcts, but no gain in function. *BMC Physiol*. 2007;7. doi:10.1186/1472-6793-7-5

54. Arslan F, Smeets MB, O'Neill LAJ, et al. Myocardial ischemia/reperfusion injury is mediated by leukocytic toll-like receptor-2 and reduced by systemic administration of a novel anti-toll-like receptor-2 antibody. *Circulation*. 2010;121(1):80-90. doi:10.1161/CIRCULATIONAHA.109.880187

55. Favre J, Musette P, Douin-Echinard V, et al. Toll-like receptors 2-deficient mice are protected against postischemic coronary endothelial dysfunction. *Arterioscler Thromb Vasc Biol*. 2007;27(5):1064-1071. doi:10.1161/ATVBAHA.107.140723

56. Feng Y, Zhao H, Xu X, et al. Innate immune adaptor MyD88 mediates neutrophil recruitment and myocardial injury after ischemia-reperfusion in mice. *Am J Physiol Heart Circ Physiol*. 2008;295(3). doi:10.1152/AJPHEART.00119.2008

57. Lu C, Ren D, Wang X, et al. Toll-like receptor 3 plays a role in myocardial infarction and ischemia/reperfusion injury. *Biochim Biophys Acta - Mol Basis Dis*. 2014;1842(1):22-31. doi:10.1016/J.BBADIS.2013.10.006

58. Shimamoto A, Chong AJ, Yada M, et al. Inhibition of Toll-like receptor 4 with eritoran attenuates myocardial ischemia-reperfusion injury. *Circulation*. 2006;114(1 Suppl). doi:10.1161/CIRCULATIONAHA.105.000901

59. Arslan F, Houtgraaf JH, Keogh B, et al. Treatment with OPN-305, a humanized anti-toll-like receptor-2 antibody, reduces myocardial ischemia/reperfusion injury in pigs. *Circ Cardiovasc Interv*. 2012;5(2):279-287. doi:10.1161/CIRCINTERVENTIONS.111.967596

60. Parapanov R, Lugrin J, Rosenblatt-Velin N, et al. Toll-like receptor 5 deficiency exacerbates cardiac injury and inflammation induced by myocardial ischaemia-reperfusion in the mouse. *Clin Sci (Lond)*. 2015;129(2):187-198. doi:10.1042/CS20140444

61. Ha T, Hu Y, Liu L, et al. TLR2 ligands induce cardioprotection against ischaemia/reperfusion injury through a PI3K/Akt-dependent mechanism. *Cardiovasc Res*. 2010;87(4):694-703. doi:10.1093/CVR/CVQ116

62. Dong JW, Vallejo JG, Tzeng HP, Thomas JA, Mann DL. Innate immunity mediates myocardial preconditioning through Toll-like receptor 2 and TIRAP-dependent signaling pathways. *Am J Physiol Heart Circ Physiol*. 2010;298(3). doi:10.1152/AJPHEART.00306.2009

63. Chao W. Toll-like receptor signaling: A critical modulator of cell survival and ischemic injury in the heart. *Am J Physiol - Hear Circ Physiol*. 2009;296(1). doi:10.1152/AJPHEART.00995.2008/ASSET/IMAGES/LARGE/ZH400109864800 01.JPEG

64. Ha T, Hua F, Liu X, et al. Lipopolysaccharide-induced myocardial protection against ischaemia/reperfusion injury is mediated through a PI3K/Akt-dependent mechanism. *Cardiovasc Res*. 2008;78(3):546-553. doi:10.1093/CVR/CVN037

65. Cao Z, Ren D, Ha T, et al. CpG-ODN, the TLR9 agonist, attenuates myocardial ischemia/reperfusion injury: involving activation of PI3K/Akt signaling. *Biochim Biophys Acta*. 2013;1832(1):96-104. doi:10.1016/J.BBADIS.2012.08.008

66. Gordon JW, Shaw JA, Kirshenbaum LA. Multiple facets of NF-κB in the heart: to be or not to NF-κB. *Circ Res*. 2011;108(9):1122-1132. doi:10.1161/CIRCRESAHA.110.226928

67. Davidson SM, Selvaraj P, He D, et al. Remote ischaemic preconditioning involves signalling through the SDF-1α/CXCR4 signalling axis. *Basic Res Cardiol*. 2013;108(5). doi:10.1007/S00395-013-0377-6

68. Morimoto H, Hirose M, Takahashi M, et al. MCP-1 induces cardioprotection against ischaemia/reperfusion injury: role of reactive oxygen species. *Cardiovasc Res*. 2008;78(3):554-562. doi:10.1093/CVR/CVN035

69. Mann DL. Innate immunity and the failing heart: the cytokine hypothesis revisited. *Circ Res*. 2015;116(7):1254-1268. doi:10.1161/CIRCRESAHA.116.302317

70. Jaén RI, Val-Blasco A, Prieto P, et al. Innate Immune Receptors, Key Actors in Cardiovascular Diseases. *JACC Basic to Transl Sci*. 2020;5(7):735-749. doi:10.1016/J.JACBTS.2020.03.015

71. Mason DR, Beck PL, Muruve DA. Nucleotide-Binding Oligomerization Domain-Like Receptors and Inflammasomes in the Pathogenesis of Non-Microbial Inflammation and Diseases. *J Innate Immun*. 2012;4(1):16-30. doi:10.1159/000334247

72. Mechanism and Regulation of NLRP3 Inflammasome Activation | Elsevier Enhanced Reader. Accessed February 11, 2022. https://reader.elsevier.com/reader/sd/pii/S0968000416301487?token=6514554276309F2081F94AE1D71FEBC0FF093B643C4D5FF3C672C2DCFF5D57901B7C02F4EC25572E7674A95C3D282E31&originRegion=eu-west-1&originCreation=20220211111751

73. Ramos-Junior ES, Morandini AC. Gasdermin: A new player to the inflammasome game. *Biomed J*. 2017;40(6):313-316. doi:10.1016/J.BJ.2017.10.002

74. Wu X, Zhang K, Cheng M. Optimal control of constrained switched systems and application to electrical vehicle energy management. *Nonlinear Anal Hybrid Syst*. 2018;30:171-188. doi:10.1016/J.NAHS.2018.05.006

75. Van Tassell BW, Raleigh JMV, Abbate A. Targeting Interleukin-1 in Heart Failure and Inflammatory Heart Disease. *Curr Heart Fail Rep*. 2015;12(1):33-41. doi:10.1007/S11897-014-0231-7/TABLES/2

76. Yamaoka Tojo M, Tojo T, Inomata T, Machida Y, Osada K, Izumi T. Circulating levels of interleukin 18 reflect etiologies of heart failure: Th1/Th2 cytokine imbalance exaggerates the pathophysiology of advanced heart failure. *J Card Fail*. 2002;8(1):21-27. doi:10.1054/JCAF.2002.31628

77. Wang L, Qu P, Zhao J, Chang Y. NLRP3 and downstream cytokine expression elevated in the monocytes of patients with coronary artery disease. *Arch Med Sci*. 2014;10(4):791. doi:10.5114/AOMS.2014.44871

78. Van Hout GPJ, Bosch L, Ellenbroek GHJM, et al. The selective NLRP3-inflammasome inhibitor MCC950 reduces infarct size and preserves cardiac function in a pig model of myocardial infarction. *Eur Heart J*. 2017;38(11):828-

836. doi:10.1093/EURHEARTJ/EHW247

79. Liu Y, Lian K, Zhang L, et al. TXNIP mediates NLRP3 inflammasome activation in cardiac microvascular endothelial cells as a novel mechanism in myocardial ischemia/reperfusion injury. *Basic Res Cardiol*. 2014;109(5). doi:10.1007/S00395-014-0415-Z

80. Marchetti C, Chojnacki J, Toldo S, et al. A novel pharmacologic inhibitor of the NLRP3 inflammasome limits myocardial injury after ischemia-reperfusion in the mouse. *J Cardiovasc Pharmacol*. 2014;63(4):316-322. doi:10.1097/FJC.0000000000000053

81. Sun W, Lu H, Lyu L, et al. Gastrodin ameliorates microvascular reperfusion injury-induced pyroptosis by regulating the NLRP3/caspase-1 pathway. *J Physiol Biochem*. 2019;75(4):531-547. doi:10.1007/S13105-019-00702-7

82. Wang Y, Yan X, Mi S, et al. Naoxintong attenuates Ischaemia/reperfusion Injury through inhibiting NLRP3 inflammasome activation. *J Cell Mol Med*. 2017;21(1):4-12. doi:10.1111/JCMM.12915

83. Caruso R, Warner N, Inohara N, Núñez G. NOD1 and NOD2: Signaling, Host Defense, and Inflammatory Disease. *Immunity*. 2014;41(6):898-908. doi:10.1016/J.IMMUNI.2014.12.010

84. Yang H, Li N, Song LN, et al. Activation of NOD1 by DAP contributes to myocardial ischemia/reperfusion injury via multiple signaling pathways. *Apoptosis*. 2015;20(4):512-522. doi:10.1007/S10495-015-1089-1/FIGURES/7

85. Delgado C, Ruiz-Hurtado G, Gómez-Hurtado N, et al. NOD1, a new player in cardiac function and calcium handling. *Cardiovasc Res*. 2015;106(3):375-386. doi:10.1093/CVR/CVV118

86. Val-Blasco A, Navarro-García JA, Tamayo M, et al. Deficiency of NOD1 improves the β-adrenergic modulation of Ca2+ handling in a mouse model of heart failure. *Front Physiol*. 2018;9(JUN):702. doi:10.3389/FPHYS.2018.00702/BIBTEX

87. Prabhu SD, Frangogiannis NG. The Biological Basis for Cardiac Repair After

Myocardial Infarction: From Inflammation to Fibrosis. *Circ Res*. 2016;119(1):91-112. doi:10.1161/CIRCRESAHA.116.303577

88. Feldman AM, Combes A, Wagner D, et al. The role of tumor necrosis factor in the pathophysiology of heart failure. *J Am Coll Cardiol*. 2000;35(3):537-544. doi:10.1016/S0735-1097(99)00600-2

89. Rathi SS, Xu Y-J, Dhalla NS, Naranjan D, Dhalla S. Mechanism of cardioprotective action of TNF-α in the isolated rat heart. *Exp Clin Cardiol*. 2002;7(2-3):146. Accessed August 1, 2022. /pmc/articles/PMC2719167/

90. Yokoyama T, Vaca L, Rossen RD, Durante W, Hazarika P, Mann DL. Cellular Basis for the Negative Inotropic Effects of Tumor Necrosis Factor-a in the Adult Mammalian Heart.

91. Ahuja P, Sdek P, MacLellan WR. Cardiac myocyte cell cycle control in development, disease, and regeneration. *Physiol Rev*. 2007;87(2):521-544. doi:10.1152/PHYSREV.00032.2006

92. Chung ES, Packer M, Lo KH, Fasanmade AA, Willerson JT. Randomized, double-blind, placebo-controlled, pilot trial of infliximab, a chimeric monoclonal antibody to tumor necrosis factor-alpha, in patients with moderate-to-severe heart failure: results of the anti-TNF Therapy Against Congestive Heart Failure (ATTACH) trial. *Circulation*. 2003;107(25):3133-3140. doi:10.1161/01.CIR.0000077913.60364.D2

93. Mann DL, McMurray JJV, Packer M, et al. Targeted anticytokine therapy in patients with chronic heart failure: results of the Randomized Etanercept Worldwide Evaluation (RENEWAL). *Circulation*. 2004;109(13):1594-1602. doi:10.1161/01.CIR.0000124490.27666.B2

94. Padfield GJ, Din JN, Koushiappi E, et al. Cardiovascular effects of tumour necrosis factor α antagonism in patients with acute myocardial infarction: a first in human study. *Heart*. 2013;99(18):1330-1335. doi:10.1136/HEARTJNL-2013-303648

95. Bujak M, Dobaczewski M, Chatila K, et al. Interleukin-1 receptor type I signaling

critically regulates infarct healing and cardiac remodeling. *Am J Pathol*. 2008;173(1):57-67. doi:10.2353/AJPATH.2008.070974

96. Abbate A, Salloum FN, Vecile E, et al. Anakinra, a recombinant human interleukin-1 receptor antagonist, inhibits apoptosis in experimental acute myocardial infarction. *Circulation*. 2008;117(20):2670-2683. doi:10.1161/CIRCULATIONAHA.107.740233

97. Afonina IS, Müller C, Martin SJ, Beyaert R. Proteolytic Processing of Interleukin-1 Family Cytokines: Variations on a Common Theme. *Immunity*. 2015;42(6):991-1004. doi:10.1016/J.IMMUNI.2015.06.003

98. Heinrich PC, Behrmann I, Müller-Newen G, Schaper F, Graeve L. Interleukin-6-type cytokine signalling through the gp130/Jak/STAT pathway. *Biochem J*. 1998;334 (Pt 2)(Pt 2):297-314. doi:10.1042/BJ3340297

99. Hilfiker-Kleiner D, Shukla P, Klein G, et al. Continuous Glycoprotein-130–Mediated Signal Transducer and Activator of Transcription-3 Activation Promotes Inflammation, Left Ventricular Rupture, and Adverse Outcome in Subacute Myocardial Infarction. *Circulation*. 2010;122(2):145-155. doi:10.1161/CIRCULATIONAHA.109.933127

100. Smallie T, Ricchetti G, Horwood NJ, Feldmann M, Clark AR, Williams LM. IL-10 inhibits transcription elongation of the human TNF gene in primary macrophages. *J Exp Med*. 2010;207(10):2081-2088. doi:10.1084/JEM.20100414

101. Jung M, Ma Y, Iyer RP, et al. IL-10 improves cardiac remodeling after myocardial infarction by stimulating M2 macrophage polarization and fibroblast activation. *Basic Res Cardiol*. 2017;112(3). doi:10.1007/S00395-017-0622-5

102. Shirakawa K, Endo J, Kataoka M, et al. IL (Interleukin)-10-STAT3-Galectin-3 Axis Is Essential for Osteopontin-Producing Reparative Macrophage Polarization After Myocardial Infarction. *Circulation*. 2018;138(18):2021-2035. doi:10.1161/CIRCULATIONAHA.118.035047

103. Kubiczkova L, Sedlarikova L, Hajek R, Sevcikova S. TGF-β - an excellent servant

but a bad master. *J Transl Med*. 2012;10(1):1-24. doi:10.1186/1479-5876-10-183/FIGURES/4

104. Thompson NL, Flanders KC, Smith JM, Ellingsworth LR, Roberts AB, Sporn MB. Expression of transforming growth factor-beta 1 in specific cells and tissues of adult and neonatal mice. *J Cell Biol*. 1989;108(2):661-669. doi:10.1083/JCB.108.2.661

105. Bartram U, Molin DGM, Wisse LJ, et al. Double-outlet right ventricle and overriding tricuspid valve reflect disturbances of looping, myocardialization, endocardial cushion differentiation, and apoptosis in TGF-beta(2)-knockout mice. *Circulation*. 2001;103(22):2745-2752. doi:10.1161/01.CIR.103.22.2745

106. Heine UI, Munoz EF, Flanders KC, et al. Role of transforming growth factor-beta in the development of the mouse embryo. *J Cell Biol*. 1987;105(6 Pt 2):2861-2876. doi:10.1083/JCB.105.6.2861

107. Umbarkar P, Singh AP, Gupte M, et al. Cardiomyocyte SMAD4-Dependent TGF-β Signaling is Essential to Maintain Adult Heart Homeostasis. *JACC Basic to Transl Sci*. 2019;4(1):41-53. doi:10.1016/J.JACBTS.2018.10.003

108. Bujak M, Ren G, Kweon HJ, et al. Essential Role of Smad3 in Infarct Healing and in the Pathogenesis of Cardiac Remodeling. *Circulation*. 2007;116(19):2127-2138. doi:10.1161/CIRCULATIONAHA.107.704197

109. Birdsall HH, Green DM, Trial JA, et al. Complement C5a, TGF-beta 1, and MCP-1, in sequence, induce migration of monocytes into ischemic canine myocardium within the first one to five hours after reperfusion. *Circulation*. 1997;95(3):684-692. doi:10.1161/01.CIR.95.3.684

110. Bujak M, Frangogiannis NG. The role of TGF-beta signaling in myocardial infarction and cardiac remodeling. *Cardiovasc Res*. 2007;74(2):184-195. doi:10.1016/J.CARDIORES.2006.10.002

111. Vilahur G, Juan-Babot O, Peña E, Oñate B, Casaní L, Badimon L. Molecular and cellular mechanisms involved in cardiac remodeling after acute myocardial

infarction. *J Mol Cell Cardiol*. 2011;50(3):522-533. doi:10.1016/J.YJMCC.2010.12.021

112. Wünsch M, Sharma HS, Markert T, et al. In situ localization of transforming growth factor beta 1 in porcine heart: enhanced expression after chronic coronary artery constriction. *J Mol Cell Cardiol*. 1991;23(9):1051-1062. doi:10.1016/0022-2828(91)91640-D

113. Dewald O, Ren G, Duerr GD, et al. Of mice and dogs: species-specific differences in the inflammatory response following myocardial infarction. *Am J Pathol*. 2004;164(2):665-677. doi:10.1016/S0002-9440(10)63154-9

114. Robertson IB, Rifkin DB. Regulation of the Bioavailability of TGF-β and TGF-β-Related Proteins. *Cold Spring Harb Perspect Biol*. 2016;8(6):21907-21908. doi:10.1101/CSHPERSPECT.A021907

115. Gentry LE, Nash BW. The Pro Domain of Pre-Pro-Transforming Growth Factor β1 When Independently Expressed Is a Functional Binding Protein for the Mature Growth Factor. *Biochemistry*. 1990;29(29):6851-6857. doi:10.1021/BI00481A014/ASSET/BI00481A014.FP.PNG_V03

116. Annes JP, Munger JS, Rifkin DB. Making sense of latent TGFbeta activation. *J Cell Sci*. 2003;116(Pt 2):217-224. doi:10.1242/JCS.00229

117. Sarrazy V, Koehler A, Chow ML, et al. Integrins αvβ5 and αvβ3 promote latent TGF-β1 activation by human cardiac fibroblast contraction. *Cardiovasc Res*. 2014;102(3):407-417. doi:10.1093/CVR/CVU053

118. Liu CL, Guo J, Zhang X, Sukhova GK, Libby P, Shi GP. Cysteine protease cathepsins in cardiovascular disease: from basic research to clinical trials. *Nat Rev Cardiol*. 2018;15(6):351-370. doi:10.1038/S41569-018-0002-3

119. Villarreal F, Omens J, Dillmann W, Risteli J, Nguyen J, Covell J. Early degradation and serum appearance of type I collagen fragments after myocardial infarction. *J Mol Cell Cardiol*. 2004;36(4):597-601. doi:10.1016/j.yjmcc.2004.01.004

120. Spinale FG. Myocardial matrix remodeling and the matrix metalloproteinases: influence on cardiac form and function. *Physiol Rev*. 2007;87(4):1285-1342. doi:10.1152/PHYSREV.00012.2007

121. Murphy-Ullrich JE, Poczatek M. Activation of latent TGF-beta by thrombospondin-1: mechanisms and physiology. *Cytokine Growth Factor Rev*. 2000;11(1-2):59-69. doi:10.1016/S1359-6101(99)00029-5

122. Frangogiannis NG, Ren G, Dewald O, et al. Critical role of endogenous thrombospondin-1 in preventing expansion of healing myocardial infarcts. *Circulation*. 2005;111(22):2935-2942. doi:10.1161/CIRCULATIONAHA.104.510354

123. Van Amerongen MJ, Harmsen MC, Van Rooijen N, Petersen AH, Van Luyn MJA. Macrophage Depletion Impairs Wound Healing and Increases Left Ventricular Remodeling after Myocardial Injury in Mice. *Am J Pathol*. 2007;170(3):818. doi:10.2353/AJPATH.2007.060547

124. Dewald O, Zymek P, Winkelmann K, et al. CCL2/monocyte chemoattractant protein-1 regulates inflammatory responses critical to healing myocardial infarcts. *Circ Res*. 2005;96(8):881-889. doi:10.1161/01.RES.0000163017.13772.3a

125. Saxena A, Dobaczewski M, Rai V, et al. Regulatory T cells are recruited in the infarcted mouse myocardium and may modulate fibroblast phenotype and function. *Am J Physiol Heart Circ Physiol*. 2014;307(8):H1233-H1242. doi:10.1152/AJPHEART.00328.2014

126. Dobaczewski M, Xia Y, Bujak M, Gonzalez-Quesada C, Frangogiannis NG. CCR5 signaling suppresses inflammation and reduces adverse remodeling of the infarcted heart, mediating recruitment of regulatory T cells. *Am J Pathol*. 2010;176(5):2177-2187. doi:10.2353/AJPATH.2010.090759

127. Weirather J, Hofmann UDW, Beyersdorf N, et al. Foxp3+ CD4+ T cells improve healing after myocardial infarction by modulating monocyte/macrophage differentiation. *Circ Res*. 2014;115(1):55-67.

doi:10.1161/CIRCRESAHA.115.303895

128. Frangogiannis NG, Perrard JL, Mendoza LH, et al. Stem Cell Factor Induction Is Associated With Mast Cell Accumulation After Canine Myocardial Ischemia and Reperfusion. *Circulation*. 1998;98(7):687-698. doi:10.1161/01.CIR.98.7.687

129. Lefer AM, Ma XL, Weyrich AS, Scalia R. Mechanism of the cardioprotective effect of transforming growth factor beta 1 in feline myocardial ischemia and reperfusion. *Proc Natl Acad Sci U S A*. 1993;90(3):1018-1022. doi:10.1073/PNAS.90.3.1018

130. Schröder D, Heger J, Piper HM, Euler G. Angiotensin II stimulates apoptosis via TGF-β1 signaling in ventricular cardiomyocytes of rat. *J Mol Med*. 2006;84(11):975-983. doi:10.1007/S00109-006-0090-0/FIGURES/7

131. Rainer PP, Hao S, Vanhoutte D, et al. Cardiomyocyte-specific transforming growth factor β suppression blocks neutrophil infiltration, augments multiple cytoprotective cascades, and reduces early mortality after myocardial infarction. *Circ Res*. 2014;114(8):1246-1257. doi:10.1161/CIRCRESAHA.114.302653

132. Dobaczewski M, Bujak M, Li N, et al. Smad3 signaling critically regulates fibroblast phenotype and function in healing myocardial infarction. *Circ Res*. 2010;107(3):418-428. doi:10.1161/CIRCRESAHA.109.216101

133. Shinde A V., Humeres C, Frangogiannis NG. The role of α-smooth muscle actin in fibroblast-mediated matrix contraction and remodeling. *Biochim Biophys acta Mol basis Dis*. 2017;1863(1):298-309. doi:10.1016/J.BBADIS.2016.11.006

134. Cucoranu I, Clempus R, Dikalova A, et al. NAD(P)H oxidase 4 mediates transforming growth factor-beta1-induced differentiation of cardiac fibroblasts into myofibroblasts. *Circ Res*. 2005;97(9):900-907. doi:10.1161/01.RES.0000187457.24338.3D

135. Frantz S, Hu K, Adamek A, et al. Transforming growth factor beta inhibition increases mortality and left ventricular dilatation after myocardial infarction. *Basic Res Cardiol*. 2008;103(5):485-492. doi:10.1007/S00395-008-0739-7

136. Drake WT, Issekutz AC. Transforming growth factor-beta 1 enhances polymorphonuclear leucocyte accumulation in dermal inflammation and transendothelial migration by a priming action. *Immunology*. 1993;78(2):197. Accessed October 18, 2022. /pmc/articles/PMC1421793/?report=abstract

137. Wahl SM, Hunt DA, Wakefield LM, McCartney-Francis N, Roberts AB, Sporn MB. Transforming growth factor type beta induces monocyte chemotaxis and growth factor production. *Proc Natl Acad Sci U S A*. 1987;84(16):5788-5792. doi:10.1073/PNAS.84.16.5788

138. Letterio JJ, Roberts AB. Regulation of immune responses by TGF-beta. *Annu Rev Immunol*. 1998;16:137-161. doi:10.1146/ANNUREV.IMMUNOL.16.1.137

139. Ikeuchi M, Tsutsui H, Shiomi T, et al. Inhibition of TGF-beta signaling exacerbates early cardiac dysfunction but prevents late remodeling after infarction. *Cardiovasc Res*. 2004;64(3):526-535. doi:10.1016/J.CARDIORES.2004.07.017

140. Differential susceptibility of activated macrophage cytotoxic effector reactions to the suppressive effects of transforming growth factor-beta 1 - PubMed. Accessed October 18, 2022. https://pubmed.ncbi.nlm.nih.gov/1900875/

141. Macrophage deactivating factor and transforming growth factors-beta 1 -beta 2 and -beta 3 inhibit induction of macrophage nitrogen oxide synthesis by IFN-gamma - PubMed. Accessed October 18, 2022. https://pubmed.ncbi.nlm.nih.gov/2115549/

142. Transforming growth factor-beta enhances the M-CSF and GM-CSF-stimulated proliferation of macrophages - PubMed. Accessed October 18, 2022. https://pubmed.ncbi.nlm.nih.gov/1737928/

143. Xiao YQ, Freire-de-Lima CG, Janssen WJ, et al. Oxidants Selectively Reverse TGF-β Suppression of Proinflammatory Mediator Production. *J Immunol*. 2006;176(2):1209-1217. doi:10.4049/JIMMUNOL.176.2.1209

144. Zhang F, Wang H, Wang X, et al. TGF-β induces M2-like macrophage polarization via SNAIL-mediated suppression of a pro-inflammatory phenotype.

Oncotarget. 2016;7(32):52294-52306. doi:10.18632/ONCOTARGET.10561

145. Serbina N V., Pamer EG. Monocyte emigration from bone marrow during bacterial infection requires signals mediated by chemokine receptor CCR2. *Nat Immunol*. 2006;7(3):311-317. doi:10.1038/NI1309

146. Eash KJ, Greenbaum AM, Gopalan PK, Link DC. CXCR2 and CXCR4 antagonistically regulate neutrophil trafficking from murine bone marrow. *J Clin Invest*. 2010;120(7):2423-2431. doi:10.1172/JCI41649

147. Martin C, Burdon PCE, Bridger G, Gutierrez-Ramos JC, Williams TJ, Rankin SM. Chemokines acting via CXCR2 and CXCR4 control the release of neutrophils from the bone marrow and their return following senescence. *Immunity*. 2003;19(4):583-593. doi:10.1016/S1074-7613(03)00263-2

148. Hughes CE, Nibbs RJB. A guide to chemokines and their receptors. *FEBS J*. 2018;285(16):2944-2971. doi:10.1111/FEBS.14466

149. Nibbs RJB, Graham GJ. Immune regulation by atypical chemokine receptors. *Nat Rev Immunol 2013 1311*. 2013;13(11):815-829. doi:10.1038/nri3544

150. Lee JS, Frevert CW, Wurfel MM, et al. Duffy antigen facilitates movement of chemokine across the endothelium in vitro and promotes neutrophil transmigration in vitro and in vivo. *J Immunol*. 2003;170(10):5244-5251. doi:10.4049/JIMMUNOL.170.10.5244

151. Pruenster M, Mudde L, Bombosi P, et al. The Duffy antigen receptor for chemokines transports chemokines and supports their promigratory activity. *Nat Immunol*. 2009;10(1):101-108. doi:10.1038/NI.1675

152. Reich D, Nalls MA, Kao WHL, et al. Reduced neutrophil count in people of African descent is due to a regulatory variant in the Duffy antigen receptor for chemokines gene. *PLoS Genet*. 2009;5(1). doi:10.1371/JOURNAL.PGEN.1000360

153. Fra AM, Locati M, Otero K, et al. Cutting edge: scavenging of inflammatory CC chemokines by the promiscuous putatively silent chemokine receptor D6. *J Immunol*. 2003;170(5):2279-2282. doi:10.4049/JIMMUNOL.170.5.2279

154. Weber M, Blair E, Simpson C V., et al. The chemokine receptor D6 constitutively traffics to and from the cell surface to internalize and degrade chemokines. *Mol Biol Cell*. 2004;15(5):2492-2508. doi:10.1091/MBC.E03-09-0634

155. Cochain C, Auvynet C, Poupel L, et al. The chemokine decoy receptor D6 prevents excessive inflammation and adverse ventricular remodeling after myocardial infarction. *Arterioscler Thromb Vasc Biol*. 2012;32(9):2206-2213. doi:10.1161/ATVBAHA.112.254409

156. Pinto AR, Ilinykh A, Ivey MJ, et al. Revisiting cardiac cellular composition. *Circ Res*. 2016;118(3):400-409. doi:10.1161/CIRCRESAHA.115.307778/-/DC1

157. Gwechenberger M, Mendoza LH, Youker KA, et al. Cardiac Myocytes Produce Interleukin-6 in Culture and in Viable Border Zone of Reperfused Infarctions. *Circulation*. 1999;99(4):546-551. doi:10.1161/01.CIR.99.4.546

158. Tarzami ST, Cheng R, Miao W, Kitsis RN, Berman JW. Chemokine expression in myocardial ischemia: MIP-2 dependent MCP-1 expression protects cardiomyocytes from cell death. *J Mol Cell Cardiol*. 2002;34(2):209-221. doi:10.1006/JMCC.2001.1503

159. Kukielka GL, Hawkins HK, Michael L, et al. Regulation of intercellular adhesion molecule-1 (ICAM-1) in ischemic and reperfused canine myocardium. *J Clin Invest*. 1993;92(3):1504-1516. doi:10.1172/JCI116729

160. Xu M, Li XY, Song L, Tao C, Fang J, Tao L. miR-484 targeting of Yap1-induced LPS-inhibited proliferation, and promoted apoptosis and inflammation in cardiomyocyte. *Biosci Biotechnol Biochem*. 2021;85(2):378-385. doi:10.1093/BBB/ZBAA009

161. Weyrich AS, Ma XI, Lefer DJ, Albertine KH, Lefer AM. In vivo neutralization of P-selectin protects feline heart and endothelium in myocardial ischemia and reperfusion injury. *J Clin Invest*. 1993;91(6):2620-2629. doi:10.1172/JCI116501

162. Kolaczkowska E, Kubes P. Neutrophil recruitment and function in health and inflammation. *Nat Rev Immunol 2013 133*. 2013;13(3):159-175.

doi:10.1038/nri3399

163. Frangogiannis NG, Mendoza LH, Lewallen M, Michael LH, Smith CW, Entman ML. Induction and suppression of interferon-inducible protein 10 in reperfused myocardial infarcts may regulate angiogenesis. *FASEB J*. 2001;15(8):1428-1430. doi:10.1096/FJ.00-0745FJE

164. Kumar AG, Ballantyne CM, Michael LH, et al. Induction of monocyte chemoattractant protein-1 in the small veins of the ischemic and reperfused canine myocardium. *Circulation*. 1997;95(3):693-700. doi:10.1161/01.CIR.95.3.693

165. Vieira JM, Norman S, Del Campo CV, et al. The cardiac lymphatic system stimulates resolution of inflammation following myocardial infarction. *J Clin Invest*. 2018;128(8):3402-3412. doi:10.1172/JCI97192

166. Stevenson Keller IV TC, Lim L, Shewale S V., et al. Genetic blockade of lymphangiogenesis does not impair cardiac function after myocardial infarction. *J Clin Invest*. 2021;131(20). doi:10.1172/JCI147070

167. Shinde A V., Frangogiannis NG. Fibroblasts in myocardial infarction: a role in inflammation and repair. *J Mol Cell Cardiol*. 2014;70:74-82. doi:10.1016/J.YJMCC.2013.11.015

168. Saxena A, Chen W, Su Y, et al. IL-1 induces proinflammatory leukocyte infiltration and regulates fibroblast phenotype in the infarcted myocardium. *J Immunol*. 2013;191(9):4838-4848. doi:10.4049/JIMMUNOL.1300725

169. Abe H, Tanada Y, Omiya S, et al. NF-κB activation in cardiac fibroblasts results in the recruitment of inflammatory Ly6Chi monocytes in pressure-overloaded hearts. *Sci Signal*. 2021;14(704):4932. doi:10.1126/SCISIGNAL.ABE4932/SUPPL_FILE/SCISIGNAL.ABE4932_SM.PDF

170. Nakaya M, Watari K, Tajima M, et al. Cardiac myofibroblast engulfment of dead cells facilitates recovery after myocardial infarction. *J Clin Invest*. 2017;127(1):383-401. doi:10.1172/JCI83822

171. Patente TA, Pinho MP, Oliveira AA, Evangelista GCM, Bergami-Santos PC, Barbuto JAM. Human Dendritic Cells: Their Heterogeneity and Clinical Application Potential in Cancer Immunotherapy. *Front Immunol*. 2019;9(JAN). doi:10.3389/FIMMU.2018.03176

172. Musumeci A, Lutz K, Winheim E, Krug AB. What Makes a pDC: Recent Advances in Understanding Plasmacytoid DC Development and Heterogeneity. *Front Immunol*. 2019;10(MAY). doi:10.3389/FIMMU.2019.01222

173. Patente TA, Pinho MP, Oliveira AA, Evangelista GCM, Bergami-Santos PC, Barbuto JAM. Human dendritic cells: Their heterogeneity and clinical application potential in cancer immunotherapy. *Front Immunol*. 2019;10(JAN):3176. doi:10.3389/FIMMU.2018.03176/BIBTEX

174. Lee JS, Jeong S-J, Kim S, et al. Conventional Dendritic Cells Impair Recovery after Myocardial Infarction. *J Immunol*. 2018;201(6):1784-1798. doi:10.4049/JIMMUNOL.1800322

175. Van der Borght K, Scott CL, Nindl V, et al. Myocardial Infarction Primes Autoreactive T Cells through Activation of Dendritic Cells. *Cell Rep*. 2017;18(12):3005-3017. doi:10.1016/J.CELREP.2017.02.079

176. Choo EH, Lee JH, Park EH, et al. Infarcted Myocardium-Primed Dendritic Cells Improve Remodeling and Cardiac Function After Myocardial Infarction by Modulating the Regulatory T Cell and Macrophage Polarization. *Circulation*. 2017;135(15):1444-1457. doi:10.1161/CIRCULATIONAHA.116.023106

177. Sousa CR e. Sensing infection and tissue damage. *EMBO Mol Med*. 2017;9(3):285-288. doi:10.15252/EMMM.201607227

178. Forte E, Perkins B, Sintou A, et al. Cross-Priming Dendritic Cells Exacerbate Immunopathology After Ischemic Tissue Damage in the Heart. *Circulation*. 2021;143(8):821-836. doi:10.1161/CIRCULATIONAHA.120.044581

179. Nagai T, Honda S, Sugano Y, et al. Decreased myocardial dendritic cells is associated with impaired reparative fibrosis and development of cardiac rupture

after myocardial infarction in humans. *J Am Heart Assoc*. 2014;3(3). doi:10.1161/JAHA.114.000839

180. Chen L, Flies DB. Two-signal model Molecular mechanisms of T cell co-stimulation and co-inhibition. *Nat Rev | Immunol*. 2013;13. doi:10.1038/nri3405

181. Weirather J, Hofmann UDW, Beyersdorf N, et al. Foxp3+ CD4+ T cells improve healing after myocardial infarction by modulating monocyte/macrophage differentiation. *Circ Res*. 2014;115(1):55-67. doi:10.1161/CIRCRESAHA.115.303895

182. Hofmann U, Beyersdorf N, Weirather J, et al. Activation of CD4+ T lymphocytes improves wound healing and survival after experimental myocardial infarction in mice. *Circulation*. 2012;125(13):1652-1663. doi:10.1161/CIRCULATIONAHA.111.044164

183. Zouggari Y, Ait-Oufella H, Bonnin P, et al. B lymphocytes trigger monocyte mobilization and impair heart function after acute myocardial infarction. *Nat Med*. 2013;19(10):1273-1280. doi:10.1038/NM.3284

184. Yan X, Anzai A, Katsumata Y, et al. Temporal dynamics of cardiac immune cell accumulation following acute myocardial infarction. *J Mol Cell Cardiol*. 2013;62:24-35. doi:10.1016/J.YJMCC.2013.04.023

185. Yang Z, Day YJ, Toufektsian MC, et al. Myocardial infarct-sparing effect of adenosine A2A receptor activation is due to its action on CD4+ T lymphocytes. *Circulation*. 2006;114(19):2056-2064. doi:10.1161/CIRCULATIONAHA.106.649244

186. Hofmann U, Beyersdorf N, Weirather J, et al. Activation of CD4 + T lymphocytes improves wound healing and survival after experimental myocardial infarction in mice. *Circulation*. 2012;125(13):1652-1663. doi:10.1161/CIRCULATIONAHA.111.044164

187. Ilatovskaya D V., Pitts C, Clayton J, et al. CD8 + T-cells negatively regulate inflammation post-myocardial infarction. *Am J Physiol Heart Circ Physiol*.

2019;317(3):H581-H596. doi:10.1152/AJPHEART.00112.2019

188. Santos-Zas I, Lemarié J, Zlatanova I, et al. Cytotoxic CD8 + T cells promote granzyme B-dependent adverse post-ischemic cardiac remodeling. *Nat Commun*. 2021;12(1). doi:10.1038/S41467-021-21737-9

189. Goodchild TT, Robinson KA, Pang W, et al. Bone Marrow-Derived B Cells Preserve Ventricular Function After Acute Myocardial Infarction. *JACC Cardiovasc Interv*. 2009;2(10):1005-1016. doi:10.1016/J.JCIN.2009.08.010

190. Heinrichs M, Ashour DED, Siegel J, et al. The healing myocardium mobilizes a distinct B-cell subset through a CXCL13-CXCR5-dependent mechanism. *Cardiovasc Res*. 2021;117(13):2664-2676. doi:10.1093/CVR/CVAB181

191. Sun Y, Pinto C, Camus S, et al. Splenic Marginal Zone B Lymphocytes Regulate Cardiac Remodeling After Acute Myocardial Infarction in Mice. *J Am Coll Cardiol*. 2022;79(7):632-647. doi:10.1016/J.JACC.2021.11.051

192. Keppner L, Heinrichs M, Rieckmann M, et al. Antibodies aggravate the development of ischemic heart failure. *Am J Physiol Heart Circ Physiol*. 2018;315(5):H1358-H1367. doi:10.1152/AJPHEART.00144.2018

193. Sim G kee, Rajaserkar R, Dessing M, Augustin A. Homing and in situ differentiation of resident pulmonary lymphocytes. *Int Immunol*. 1994;6(9):1287-1295. doi:10.1093/INTIMM/6.9.1287

194. IL-4-producing gamma delta T cells that express a very restricted TCR repertoire are preferentially localized in liver and spleen - PubMed. Accessed August 8, 2022. https://pubmed.ncbi.nlm.nih.gov/10477572/

195. Takagaki Y, DeCloux A, Bonneville M, Tonegawa S. Diversity of gamma delta T-cell receptors on murine intestinal intra-epithelial lymphocytes. *Nature*. 1989;339(6227):712-714. doi:10.1038/339712A0

196. O'Brien RL, Born WK. Dermal γδ T cells--What have we learned? *Cell Immunol*. 2015;296(1):62-69. doi:10.1016/J.CELLIMM.2015.01.011

197. Chien YH, Meyer C, Bonneville M. γδ T cells: first line of defense and beyond. *Annu Rev Immunol*. 2014;32:121-155. doi:10.1146/ANNUREV-IMMUNOL-032713-120216

198. Godfrey DI, Uldrich AP, Mccluskey J, Rossjohn J, Moody DB. The burgeoning family of unconventional T cells. *Nat Immunol 2015 1611*. 2015;16(11):1114-1123. doi:10.1038/ni.3298

199. Yan X, Anzai A, Katsumata Y, et al. Temporal dynamics of cardiac immune cell accumulation following acute myocardial infarction. *J Mol Cell Cardiol*. 2013;62:24-35. doi:10.1016/J.YJMCC.2013.04.023

200. Yan X, Shichita T, Katsumata Y, et al. Deleterious effect of the IL-23/IL-17A axis and γδT cells on left ventricular remodeling after myocardial infarction. *J Am Heart Assoc*. 2012;1(5). doi:10.1161/JAHA.112.004408

201. Eberl G, Colonna M, Santo JPD, McKenzie ANJ. Innate lymphoid cells: A new paradigm in immunology. *Science (80-)*. 2015;348(6237). doi:10.1126/SCIENCE.AAA6566/ASSET/C3CFA811-5BF3-4336-AE73-7B4DC240460E/ASSETS/GRAPHIC/348_AAA6566_F4.JPEG

202. Yu X, Newland SA, Zhao TX, et al. Innate Lymphoid Cells Promote Recovery of Ventricular Function After Myocardial Infarction. *J Am Coll Cardiol*. 2021;78(11):1127-1142. doi:10.1016/J.JACC.2021.07.018

203. Kawamura S, Onai N, Miya F, et al. Identification of a Human Clonogenic Progenitor with Strict Monocyte Differentiation Potential: A Counterpart of Mouse cMoPs. *Immunity*. 2017;46(5):835-848.e4. doi:10.1016/J.IMMUNI.2017.04.019

204. Manz MG, Miyamoto T, Akashi K, Weissman IL. Prospective isolation of human clonogenic common myeloid progenitors. *Proc Natl Acad Sci U S A*. 2002;99(18):11872-11877. doi:10.1073/PNAS.172384399

205. Zhu YP, Padgett L, Dinh HQ, et al. Identification of an Early Unipotent Neutrophil Progenitor with Pro-tumoral Activity in Mouse and Human Bone Marrow. *Cell Rep*. 2018;24(9):2329-2341.e8. doi:10.1016/J.CELREP.2018.07.097

206. Ramírez C, Mendoza L. Phenotypic stability and plasticity in GMP-derived cells as determined by their underlying regulatory network. *Bioinformatics*. 2018;34(7):1174-1182. doi:10.1093/BIOINFORMATICS/BTX736

207. Kim MH, Yang D, Kim M, Kim SY, Kim D, Kang SJ. A late-lineage murine neutrophil precursor population exhibits dynamic changes during demand-adapted granulopoiesis. *Sci Reports 2017 71*. 2017;7(1):1-15. doi:10.1038/srep39804

208. Evrard M, Kwok IWH, Chong SZ, et al. Developmental Analysis of Bone Marrow Neutrophils Reveals Populations Specialized in Expansion, Trafficking, and Effector Functions. *Immunity*. 2018;48(2):364-379.e8. doi:10.1016/J.IMMUNI.2018.02.002

209. Bendall LJ, Bradstock KF. G-CSF: From granulopoietic stimulant to bone marrow stem cell mobilizing agent. *Cytokine Growth Factor Rev*. 2014;25(4):355-367. doi:10.1016/J.CYTOGFR.2014.07.011

210. Lapid K, Glait-Santar C, Gur-Cohen S, Canaani J, Kollet O, Lapidot T. Egress and Mobilization of Hematopoietic Stem and Progenitor Cells: A Dynamic Multi-facet Process. *StemBook*. Published online May 10, 2013. Accessed August 17, 2022. http://europepmc.org/books/NBK133261

211. Greenbaum AM, Link DC. Mechanisms of G-CSF-mediated hematopoietic stem and progenitor mobilization. *Leuk 2011 252*. 2010;25(2):211-217. doi:10.1038/leu.2010.248

212. Metcalf D. Hematopoietic cytokines. *Blood*. 2008;111(2):485-491. doi:10.1182/BLOOD-2007-03-079681

213. Ley K, Hoffman HM, Kubes P, et al. Neutrophils: New insights and open questions. *Sci Immunol*. 2018;3(30). doi:10.1126/SCIIMMUNOL.AAT4579

214. Ng LG, Ostuni R, Hidalgo A. Heterogeneity of neutrophils. *Nat Rev Immunol 2019 194*. 2019;19(4):255-265. doi:10.1038/s41577-019-0141-8

215. Jhunjhunwala S, Alvarez D, Aresta-DaSilva S, et al. Frontline Science: Splenic

progenitors aid in maintaining high neutrophil numbers at sites of sterile chronic inflammation. *J Leukoc Biol*. 2016;100(2):253. doi:10.1189/JLB.1HI0615-248RR

216. Eash KJ, Greenbaum AM, Gopalan PK, Link DC. CXCR2 and CXCR4 antagonistically regulate neutrophil trafficking from murine bone marrow. *J Clin Invest*. 2010;120(7):2423-2431. doi:10.1172/JCI41649

217. Manz MG, Boettcher S. Emergency granulopoiesis. *Nat Rev Immunol*. 2014;14(5):302-314. doi:10.1038/NRI3660

218. ATHENS JW, HAAB OP, RAAB SO, et al. LEUKOKINETIC STUDIES. IV. THE TOTAL BLOOD, CIRCULATING AND MARGINAL GRANULOCYTE POOLS AND THE GRANULOCYTE TURNOVER RATE IN NORMAL SUBJECTS. *J Clin Invest*. 1961;40(6):989-995. doi:10.1172/JCI104338

219. Ussov WY, Aktolun C, Myers MJ, Jamar F, Peters AM. Granulocyte margination in bone marrow: comparison with margination in the spleen and liver. *http://dx.doi.org/103109/00365519509075382*. 2009;55(1):87-96. doi:10.3109/00365519509075382

220. Pillay J, Den Braber I, Vrisekoop N, et al. In vivo labeling with 2H2O reveals a human neutrophil lifespan of 5.4 days. *Blood*. 2010;116(4):625-627. doi:10.1182/BLOOD-2010-01-259028

221. Dienz O, Rud JG, Eaton SM, et al. Essential role of IL-6 in protection against H1N1 influenza virus by promoting neutrophil survival in the lung. *Mucosal Immunol 2012 53*. 2012;5(3):258-266. doi:10.1038/mi.2012.2

222. Pocock JM, Storisteanu DML, Reeves MB, et al. Human Cytomegalovirus Delays Neutrophil Apoptosis and Stimulates the Release of a Prosurvival Secretome. *Front Immunol*. 2017;8(SEP):25. doi:10.3389/FIMMU.2017.01185

223. Lindemans CA, Coffer PJ, Schellens IMM, Graaff PMA de, Kimpen JLL, Koenderman L. Respiratory Syncytial Virus Inhibits Granulocyte Apoptosis through a Phosphatidylinositol 3-Kinase and NF-κB-Dependent Mechanism. *J Immunol*. 2006;176(9):5529-5537. doi:10.4049/JIMMUNOL.176.9.5529

224. Fox S, Leitch AE, Duffin R, Haslett C, Rossi AG. Neutrophil Apoptosis: Relevance to the Innate Immune Response and Inflammatory Disease. *J Innate Immun*. 2010;2(3):216-227. doi:10.1159/000284367

225. Walmsley SR, Print C, Farahi N, et al. Hypoxia-induced neutrophil survival is mediated by HIF-1α–dependent NF-κB activity. *J Exp Med*. 2005;201(1):105-115. doi:10.1084/JEM.20040624

226. Adrover JM, del Fresno C, Crainiciuc G, et al. A Neutrophil Timer Coordinates Immune Defense and Vascular Protection. *Immunity*. 2019;50(2):390-402.e10. doi:10.1016/J.IMMUNI.2019.01.002

227. Casanova-Acebes M, Pitaval C, Weiss LA, et al. Rhythmic modulation of the hematopoietic niche through neutrophil clearance. *Cell*. 2013;153(5):1025. doi:10.1016/J.CELL.2013.04.040

228. Uhl B, Vadlau Y, Zuchtriegel G, et al. Aged neutrophils contribute to the first line of defense in the acute inflammatory response. *Blood*. 2016;128(19):2327-2337. doi:10.1182/BLOOD-2016-05-718999

229. Reglero-Real N, Rolas L, Nourshargh S. Leukocyte Trafficking: Time to Take Time Seriously. *Immunity*. 2019;50(2):273-275. doi:10.1016/J.IMMUNI.2019.01.013

230. Casanova-Acebes M, Pitaval C, Weiss LA, et al. Rhythmic Modulation of the Hematopoietic Niche through Neutrophil Clearance. *Cell*. 2013;153(5):1025-1035. doi:10.1016/J.CELL.2013.04.040

231. Adrover JM, del Fresno C, Crainiciuc G, et al. A Neutrophil Timer Coordinates Immune Defense and Vascular Protection. *Immunity*. 2019;50(2):390-402.e10. doi:10.1016/J.IMMUNI.2019.01.002

232. Kolaczkowska E, Kubes P. Neutrophil recruitment and function in health and inflammation. *Nat Rev Immunol 2013 133*. 2013;13(3):159-175. doi:10.1038/nri3399

233. Pittman K, Kubes P. Damage-associated molecular patterns control neutrophil

recruitment. *J Innate Immun*. 2013;5(4):315-323. doi:10.1159/000347132

234. Nathan C. Neutrophils and immunity: challenges and opportunities. *Nat Rev Immunol 2006 63*. 2006;6(3):173-182. doi:10.1038/nri1785

235. Wang J. Neutrophils in tissue injury and repair. *Cell Tissue Res*. 2018;371(3):531. doi:10.1007/S00441-017-2785-7

236. Puellmann K, Kaminski WE, Vogel M, et al. A variable immunoreceptor in a subpopulation of human neutrophils. *Proc Natl Acad Sci U S A*. 2006;103(39):14441-14446. doi:10.1073/PNAS.0603406103

237. Fuchs T, Püellmann K, Scharfenstein O, et al. The neutrophil recombinatorial TCR-like immune receptor is expressed across the entire human life span but repertoire diversity declines in old age. *Biochem Biophys Res Commun*. 2012;419(2):309-315. doi:10.1016/J.BBRC.2012.02.017

238. Liu W, Yan M, Liu Y, McLeish KR, Coleman WG, Rodgers GP. Olfactomedin 4 inhibits cathepsin C-mediated protease activities, thereby modulating neutrophil killing of Staphylococcus aureus and Escherichia coli in mice. *J Immunol*. 2012;189(5):2460-2467. doi:10.4049/JIMMUNOL.1103179

239. Hu N, Mora-Jensen H, Theilgaard-Mönch K, et al. Differential expression of granulopoiesis related genes in neutrophil subsets distinguished by membrane expression of CD177. *PLoS One*. 2014;9(6). doi:10.1371/JOURNAL.PONE.0099671

240. Clemmensen SN, Bohr CT, Rørvig S, et al. Olfactomedin 4 defines a subset of human neutrophils. *J Leukoc Biol*. 2012;91(3):495-500. doi:10.1189/JLB.0811417

241. Bauer S, Abdgawad M, Gunnarsson L, Segelmark M, Tapper H, Hellmark T. Proteinase 3 and CD177 are expressed on the plasma membrane of the same subset of neutrophils. *J Leukoc Biol*. 2007;81(2):458-464. doi:10.1189/JLB.0806514

242. Silvestre-Roig C, Fridlender ZG, Glogauer M, Scapini P. Neutrophil Diversity in Health and Disease. *Trends Immunol*. 2019;40(7):565-583.

doi:10.1016/J.IT.2019.04.012

243. Kuckleburg CJ, Tilkens SM, Santoso S, Newman PJ. Proteinase 3 contributes to transendothelial migration of NB1-positive neutrophils. *J Immunol*. 2012;188(5):2419. doi:10.4049/JIMMUNOL.1102540

244. Massena S, Christoffersson G, Vågesjö E, et al. Identification and characterization of VEGF-A–responsive neutrophils expressing CD49d, VEGFR1, and CXCR4 in mice and humans. *Blood*. 2015;126(17):2016-2026. doi:10.1182/BLOOD-2015-03-631572

245. Puellmann K, Kaminski WE, Vogel M, et al. A variable immunoreceptor in a subpopulation of human neutrophils. *Proc Natl Acad Sci U S A*. 2006;103(39):14441-14446. doi:10.1073/PNAS.0603406103/SUPPL_FILE/03406FIG15.PDF

246. Xie X, Shi Q, Wu P, et al. Single-cell transcriptome profiling reveals neutrophil heterogeneity in homeostasis and infection. *Nat Immunol 2020 219*. 2020;21(9):1119-1133. doi:10.1038/s41590-020-0736-z

247. Scapini P, Marini O, Tecchio C, Cassatella MA. Human neutrophils in the saga of cellular heterogeneity: insights and open questions. *Immunol Rev*. 2016;273(1):48-60. doi:10.1111/IMR.12448

248. Carmona-Rivera C, Kaplan MJ. Low-density granulocytes: A distinct class of neutrophils in systemic autoimmunity. *Semin Immunopathol*. 2013;35(4):455-463. doi:10.1007/S00281-013-0375-7/FIGURES/4

249. Bronte V, Brandau S, Chen SH, et al. Recommendations for myeloid-derived suppressor cell nomenclature and characterization standards. *Nat Commun 2016 71*. 2016;7(1):1-10. doi:10.1038/ncomms12150

250. Moses K, Brandau S. Human neutrophils: Their role in cancer and relation to myeloid-derived suppressor cells. *Semin Immunol*. 2016;28(2):187-196. doi:10.1016/J.SMIM.2016.03.018

251. Veglia F, Perego M, Gabrilovich D. Myeloid-derived suppressor cells coming of

age. *Nat Immunol 2018 192*. 2018;19(2):108-119. doi:10.1038/s41590-017-0022-x

252. Hellebrekers P, Vrisekoop N, Koenderman L. Neutrophil phenotypes in health and disease. *Eur J Clin Invest*. 2018;48:e12943. doi:10.1111/ECI.12943

253. Bianchi ME. DAMPs, PAMPs and alarmins: all we need to know about danger. *J Leukoc Biol*. 2007;81(1):1-5. doi:10.1189/JLB.0306164

254. Pillay J, Ramakers BP, Kamp VM, et al. Functional heterogeneity and differential priming of circulating neutrophils in human experimental endotoxemia. *J Leukoc Biol*. 2010;88(1):211-220. doi:10.1189/JLB.1209793

255. Pillay J, Kamp VM, Van Hoffen E, et al. A subset of neutrophils in human systemic inflammation inhibits T cell responses through Mac-1. *J Clin Invest*. 2012;122(1):327-336. doi:10.1172/JCI57990

256. Pillay J, Tak T, Kamp VM, Koenderman L. Immune suppression by neutrophils and granulocytic myeloid-derived suppressor cells: similarities and differences. *Cell Mol Life Sci*. 2013;70(20):3813-3827. doi:10.1007/S00018-013-1286-4

257. Fridlender ZG, Sun J, Kim S, et al. Polarization of tumor-associated neutrophil phenotype by TGF-beta: “N1” versus “N2” TAN. *Cancer Cell*. 2009;16(3):183-194. doi:10.1016/J.CCR.2009.06.017

258. Engblom C, Pfirschke C, Zilionis R, et al. Osteoblasts remotely supply lung tumors with cancer-promotingSiglecFhigh neutrophils. *Science*. 2017;358(6367). doi:10.1126/SCIENCE.AAL5081

259. Daseke MJ, Valerio FM, Kalusche WJ, Ma Y, DeLeon-Pennell KY, Lindsey ML. Neutrophil proteome shifts over the myocardial infarction time continuum. *Basic Res Cardiol*. 2019;114(5). doi:10.1007/S00395-019-0746-X

260. Ma Y, Yabluchanskiy A, Iyer RP, et al. Temporal neutrophil polarization following myocardial infarction. *Cardiovasc Res*. 2016;110(1):51-61. doi:10.1093/CVR/CVW024

261. Daseke MJ, Tenkorang-Impraim MAA, Ma Y, et al. Exogenous IL-4 shuts off pro-inflammation in neutrophils while stimulating anti-inflammation in macrophages to induce neutrophil phagocytosis following myocardial infarction. *J Mol Cell Cardiol*. 2020;145:112-121. doi:10.1016/J.YJMCC.2020.06.006

262. Puhl SL, Steffens S. Neutrophils in Post-myocardial Infarction Inflammation: Damage vs. Resolution? *Front Cardiovasc Med*. 2019;6:25. doi:10.3389/FCVM.2019.00025/BIBTEX

263. Epelman S, Liu PP, Mann DL. Role of innate and adaptive immune mechanisms in cardiac injury and repair. *Nat Rev Immunol 2015 152*. 2015;15(2):117-129. doi:10.1038/nri3800

264. Peiseler M, Kubes P. More friend than foe: the emerging role of neutrophils in tissue repair. *J Clin Invest*. 2019;129(7):2629-2639. doi:10.1172/JCI124616

265. Guasti L, Dentali F, Castiglioni L, et al. Neutrophils and clinical outcomes in patients with acute coronary syndromes and/or cardiac revascularization: A systematic review on more than 34,000 subjects. *Thromb Haemost*. 2011;106(4):591-599. doi:10.1160/TH11-02-0096/ID/JR0096-10

266. Chia S, Nagurney JT, Brown DFM, et al. Association of Leukocyte and Neutrophil Counts With Infarct Size, Left Ventricular Function and Outcomes After Percutaneous Coronary Intervention for ST-Elevation Myocardial Infarction. *Am J Cardiol*. 2009;103(3):333-337. doi:10.1016/J.AMJCARD.2008.09.085

267. Phillipson M, Kubes P. The Healing Power of Neutrophils. *Trends Immunol*. 2019;40(7):635-647. doi:10.1016/J.IT.2019.05.001

268. Hiroi T, Wajima T, Negoro T, et al. Neutrophil TRPM2 channels are implicated in the exacerbation of myocardial ischaemia/reperfusion injury. *Cardiovasc Res*. 2013;97(2):271-281. doi:10.1093/CVR/CVS332

269. Carbone F, Crowe LA, Roth A, et al. Treatment with anti-RANKL antibody reduces infarct size and attenuates dysfunction impacting on neutrophil-mediated injury. *J Mol Cell Cardiol*. 2016;94:82-94. doi:10.1016/J.YJMCC.2016.03.013

270. Jolly SR, Kane WJ, Hook BG, Abrams GD, Kunkel SL, Lucchesi BR. Reduction of myocardial infarct size by neutrophil depletion: Effect of duration of occlusion. *Am Heart J*. 1986;112(4):682-690. doi:10.1016/0002-8703(86)90461-8

271. Romson JL, Hook BG, Kunkel SL, Abrams GD, Schork MA, Lucchesi BR. Reduction of the extent of ischemic myocardial injury by neutrophil depletion in the dog. *Circulation*. 1983;67(5):1016-1023. doi:10.1161/01.CIR.67.5.1016

272. Vinten-Johansen J. Involvement of neutrophils in the pathogenesis of lethal myocardial reperfusion injury. *Cardiovasc Res*. 2004;61(3):481-497. doi:10.1016/J.CARDIORES.2003.10.011/2/61-3-481-FIG2.GIF

273. Amulic B, Cazalet C, Hayes GL, Metzler KD, Zychlinsky A. Neutrophil Function: From Mechanisms to Disease. *https://doi.org/101146/annurev-immunol-020711-074942*. 2012;30:459-489. doi:10.1146/ANNUREV-IMMUNOL-020711-074942

274. Ma Y, Yabluchanskiy A, Lindsey ML. Neutrophil roles in left ventricular remodeling following myocardial infarction. *Fibrogenes Tissue Repair*. 2013;6(1):1-10. doi:10.1186/1755-1536-6-11/FIGURES/3

275. DiStasi MR, Ley K. Opening the flood-gates: how neutrophil-endothelial interactions regulate permeability. *Trends Immunol*. 2009;30(11):547-556. doi:10.1016/J.IT.2009.07.012

276. Ma Y, Yang X, Chatterjee V, Meegan JE, Beard RS, Yuan SY. Role of neutrophil extracellular traps and vesicles in regulating vascular endothelial permeability. *Front Immunol*. 2019;10(MAY):1037. doi:10.3389/FIMMU.2019.01037/BIBTEX

277. Liu J, Yang D, Wang X, et al. Neutrophil extracellular traps and dsDNA predict outcomes among patients with ST-elevation myocardial infarction. *Sci Reports 2019 91*. 2019;9(1):1-9. doi:10.1038/s41598-019-47853-7

278. Hofbauer TM, Mangold A, Scherz T, et al. Neutrophil extracellular traps and fibrocytes in ST-segment elevation myocardial infarction. *Basic Res Cardiol*. 2019;114(5):1-15. doi:10.1007/S00395-019-0740-3/FIGURES/8

279. Mangold A, Alias S, Scherz T, et al. Coronary neutrophil extracellular trap burden

and deoxyribonuclease activity in ST-elevation acute coronary syndrome are predictors of ST-segment resolution and infarct size. *Circ Res*. 2015;116(7):1182-1192. doi:10.1161/CIRCRESAHA.116.304944

280. Helseth R, Shetelig C, Andersen GØ, et al. Neutrophil Extracellular Trap Components Associate with Infarct Size, Ventricular Function, and Clinical Outcome in STEMI. *Mediators Inflamm*. 2019;2019. doi:10.1155/2019/7816491

281. Du M, Yang W, Schmull S, Gu J, Xue S. Inhibition of peptidyl arginine deiminase-4 protects against myocardial infarction induced cardiac dysfunction. *Int Immunopharmacol*. 2020;78:106055. doi:10.1016/J.INTIMP.2019.106055

282. Savchenko AS, Borissoff JI, Martinod K, et al. VWF-mediated leukocyte recruitment with chromatin decondensation by PAD4 increases myocardial ischemia/reperfusion injury in mice. *Blood*. 2014;123(1):141-148. doi:10.1182/BLOOD-2013-07-514992

283. Sreejit G, Abdel-Latif A, Athmanathan B, et al. Neutrophil-derived S100A8/A9 amplify granulopoiesis after myocardial infarction. *Circulation*. Published online March 31, 2020:1080-1094. doi:10.1161/CIRCULATIONAHA.119.043833

284. Manz MG, Boettcher S. Emergency granulopoiesis. *Nat Rev Immunol 2014 145*. 2014;14(5):302-314. doi:10.1038/nri3660

285. Sreejit G, Abdel Latif A, Murphy AJ, Nagareddy PR. Emerging roles of neutrophil-borne S100A8/A9 in cardiovascular inflammation. *Pharmacol Res*. 2020;161:105212. doi:10.1016/J.PHRS.2020.105212

286. Grune J, Lewis AJM, Yamazoe M, et al. Neutrophils incite and macrophages avert electrical storm after myocardial infarction. *Nat Cardiovasc Res 2022 17*. 2022;1(7):649-664. doi:10.1038/s44161-022-00094-w

287. Daseke MJ, Chalise U, Becirovic-Agic M, et al. Neutrophil signaling during myocardial infarction wound repair. *Cell Signal*. 2021;77:109816. doi:10.1016/J.CELLSIG.2020.109816

288. Kebir D El, Filep JG. Modulation of neutrophil apoptosis and the resolution of

inflammation through β2 integrins. *Front Immunol*. 2013;4(MAR):60. doi:10.3389/FIMMU.2013.00060/BIBTEX

289. Bratton DL, Henson PM. Neutrophil clearance: when the party is over, clean-up begins. *Trends Immunol*. 2011;32(8):350-357. doi:10.1016/J.IT.2011.04.009

290. El Kebir D, Filep JG. Targeting Neutrophil Apoptosis for Enhancing the Resolution of Inflammation. *Cells 2013, Vol 2, Pages 330-348*. 2013;2(2):330-348. doi:10.3390/CELLS2020330

291. Fox S, Leitch AE, Duffin R, Haslett C, Rossi AG. Neutrophil Apoptosis: Relevance to the Innate Immune Response and Inflammatory Disease. *J Innate Immun*. 2010;2(3):216-227. doi:10.1159/000284367

292. Elliott MR, Ravichandran KS. Clearance of apoptotic cells: implications in health and disease. *J Cell Biol*. 2010;189(7):1059-1070. doi:10.1083/JCB.201004096

293. Zhang Y, Kim HJ, Yamamoto S, Kang X, Ma X. Regulation of Interleukin-10 Gene Expression in Macrophages Engulfing Apoptotic Cells. *https://home.liebertpub.com/jir*. 2010;30(3):113-121. doi:10.1089/JIR.2010.0004

294. Huynh M-LN, Fadok VA, Henson PM. Phosphatidylserine-dependent ingestion of apoptotic cells promotes TGF-β1 secretion and the resolution of inflammation. *J Clin Invest*. 2002;109(1):41-50. doi:10.1172/JCI11638

295. Martin P, Palmer G, Vigne S, et al. Mouse neutrophils express the decoy type 2 interleukin-1 receptor (IL-1R2) constitutively and in acute inflammatory conditions. *J Leukoc Biol*. 2013;94(4):791-802. doi:10.1189/JLB.0113035

296. Crepaldi L, Silveri L, Calzetti F, Pinardi C, Cassatella MA. Molecular basis of the synergistic production of IL-1 receptor antagonist by human neutrophils stimulated with IL-4 and IL-10. *Int Immunol*. 2002;14(10):1145-1153. doi:10.1093/INTIMM/DXF079

297. Bourke E, Cassetti A, Villa A, Fadlon E, Colotta F, Mantovani A. IL-1 beta scavenging by the type II IL-1 decoy receptor in human neutrophils. *J Immunol*. 2003;170(12):5999-6005. doi:10.4049/JIMMUNOL.170.12.5999

298. Garlichs CD, Eskafi S, Cicha I, et al. Delay of neutrophil apoptosis in acute coronary syndromes. *J Leukoc Biol*. 2004;75(5):828-835. doi:10.1189/JLB.0703358

299. Horckmans M, Ring L, Duchene J, et al. Neutrophils orchestrate post-myocardial infarction healing by polarizing macrophages towards a reparative phenotype. *Eur Heart J*. 2017;38(3):187-197. doi:10.1093/EURHEARTJ/EHW002

300. Wan E, Yeap XY, Dehn S, et al. Enhanced efferocytosis of apoptotic cardiomyocytes through myeloid-epithelial-reproductive tyrosine kinase links acute inflammation resolution to cardiac repair after infarction. *Circ Res*. 2013;113(8):1004-1012. doi:10.1161/CIRCRESAHA.113.301198

301. Taichman NS, Young S, Cruchley AT, Taylor P, Paleolog E. Human neutrophils secrete vascular endothelial growth factor. *J Leukoc Biol*. 1997;62(3):397-400. doi:10.1002/JLB.62.3.397

302. Barletta KE, Ley K, Mehrad B. Regulation of neutrophil function by adenosine. *Arterioscler Thromb Vasc Biol*. 2012;32(4):856. doi:10.1161/ATVBAHA.111.226845

303. Guilliams M, Mildner A, Yona S. Developmental and Functional Heterogeneity of Monocytes. *Immunity*. 2018;49(4):595-613. doi:10.1016/J.IMMUNI.2018.10.005

304. Yáñez A, Coetzee SG, Olsson A, et al. Granulocyte-Monocyte Progenitors and Monocyte-Dendritic Cell Progenitors Independently Produce Functionally Distinct Monocytes. *Immunity*. 2017;47(5):890-902.e4. doi:10.1016/J.IMMUNI.2017.10.021

305. Ingersoll MA, Spanbroek R, Lottaz C, et al. Comparison of gene expression profiles between human and mouse monocyte subsets. *Blood*. 2010;115(3). doi:10.1182/BLOOD-2009-07-235028

306. Ziegler-Heitbrock HWL. Heterogeneity of human blood monocytes: the CD14+ CD16+ subpopulation. *Immunol Today*. 1996;17(9):424-428. doi:10.1016/0167-5699(96)10029-3

307. Jakubzick C, Gautier EL, Gibbings SL, et al. Minimal differentiation of classical monocytes as they survey steady-state tissues and transport antigen to lymph nodes. *Immunity*. 2013;39(3):599-610. doi:10.1016/J.IMMUNI.2013.08.007

308. Geissmann F, Jung S, Littman DR. Blood monocytes consist of two principal subsets with distinct migratory properties. *Immunity*. 2003;19(1):71-82. doi:10.1016/S1074-7613(03)00174-2

309. Identification and characterization of a novel monocyte subpopulation in human peripheral blood - PubMed. Accessed August 2, 2022. https://pubmed.ncbi.nlm.nih.gov/2478233/

310. Ancuta P, Rao R, Moses A, et al. Fractalkine preferentially mediates arrest and migration of CD16+ monocytes. *J Exp Med*. 2003;197(12):1701-1707. doi:10.1084/JEM.20022156

311. Landsman L, Liat BO, Zernecke A, et al. CX3CR1 is required for monocyte homeostasis and atherogenesis by promoting cell survival. *Blood*. 2009;113(4):963-972. doi:10.1182/BLOOD-2008-07-170787

312. Auffray C, Fogg D, Garfa M, et al. Monitoring of blood vessels and tissues by a population of monocytes with patrolling behavior. *Science*. 2007;317(5838):666-670. doi:10.1126/SCIENCE.1142883

313. Carlin LM, Stamatiades EG, Auffray C, et al. Nr4a1-dependent Ly6C(low) monocytes monitor endothelial cells and orchestrate their disposal. *Cell*. 2013;153(2):362-375. doi:10.1016/J.CELL.2013.03.010

314. Cros J, Cagnard N, Woollard K, et al. Human CD14dim Monocytes Patrol and Sense Nucleic Acids and Viruses via TLR7 and TLR8 Receptors. *Immunity*. 2010;33(3):375-386. doi:10.1016/J.IMMUNI.2010.08.012

315. Ingersoll MA, Spanbroek R, Lottaz C, et al. Comparison of gene expression profiles between human and mouse monocyte subsets. *Blood*. 2010;115(3):e10-e19. doi:10.1182/BLOOD-2009-07-235028

316. Patel AA, Zhang Y, Fullerton JN, et al. The fate and lifespan of human monocyte

subsets in steady state and systemic inflammation. *J Exp Med*. 2017;214(7):1913-1923. doi:10.1084/JEM.20170355

317. Mossadegh-Keller N, Gentek R, Gimenez G, Bigot S, Mailfert S, Sieweke MH. Developmental origin and maintenance of distinct testicular macrophage populations. *J Exp Med*. 2017;214(10):2829-2841. doi:10.1084/JEM.20170829

318. Calderon B, Carrero JA, Ferris ST, et al. The pancreas anatomy conditions the origin and properties of resident macrophages. *J Exp Med*. 2015;212(10):1497-1512. doi:10.1084/JEM.20150496

319. Molawi K, Wolf Y, Kandalla PK, et al. Progressive replacement of embryo-derived cardiac macrophages with age. *J Exp Med*. 2014;211(11):2151-2158. doi:10.1084/JEM.20140639

320. Zigmond E, Varol C, Farache J, et al. Ly6Chi Monocytes in the Inflamed Colon Give Rise to Proinflammatory Effector Cells and Migratory Antigen-Presenting Cells. *Immunity*. 2012;37(6):1076-1090. doi:10.1016/J.IMMUNI.2012.08.026

321. Tamoutounour S, Guilliams M, MontananaSanchis F, et al. Origins and Functional Specialization of Macrophages and of Conventional and Monocyte-Derived Dendritic Cells in Mouse Skin. *Immunity*. 2013;39(5):925-938. doi:10.1016/J.IMMUNI.2013.10.004

322. Tamoutounour S, Henri S, Lelouard H, et al. CD64 distinguishes macrophages from dendritic cells in the gut and reveals the Th1-inducing role of mesenteric lymph node macrophages during colitis. *Eur J Immunol*. 2012;42(12):3150-3166. doi:10.1002/EJI.201242847

323. Bain CC, Scott CL, Uronen-Hansson H, et al. Resident and pro-inflammatory macrophages in the colon represent alternative context-dependent fates of the same Ly6Chi monocyte precursors. *Mucosal Immunol 2013 63*. 2012;6(3):498-510. doi:10.1038/mi.2012.89

324. Epelman S, Lavine KJ, Beaudin AE, et al. Embryonic and Adult-Derived Resident Cardiac Macrophages Are Maintained through Distinct Mechanisms at Steady

State and during Inflammation. *Immunity*. 2014;40(1):91-104. doi:10.1016/J.IMMUNI.2013.11.019

325. Yona S, Kim KW, Wolf Y, et al. Fate Mapping Reveals Origins and Dynamics of Monocytes and Tissue Macrophages under Homeostasis. *Immunity*. 2013;38(1):79-91. doi:10.1016/J.IMMUNI.2012.12.001

326. Mildner A, Schmidt H, Nitsche M, et al. Microglia in the adult brain arise from Ly-6ChiCCR2+ monocytes only under defined host conditions. *Nat Neurosci 2007 1012*. 2007;10(12):1544-1553. doi:10.1038/nn2015

327. Ajami B, Bennett JL, Krieger C, Tetzlaff W, Rossi FMV. Local self-renewal can sustain CNS microglia maintenance and function throughout adult life. *Nat Neurosci 2007 1012*. 2007;10(12):1538-1543. doi:10.1038/nn2014

328. Chorro L, Sarde A, Li M, et al. Langerhans cell (LC) proliferation mediates neonatal development, homeostasis, and inflammation-associated expansion of the epidermal LC network. *J Exp Med*. 2009;206(13):3089-3100. doi:10.1084/JEM.20091586/VIDEO-5

329. Ginhoux F, Greter M, Leboeuf M, et al. Fate mapping analysis reveals that adult microglia derive from primitive macrophages. *Science (80-)*. 2010;330(6005):841-845. doi:10.1126/SCIENCE.1194637/SUPPL_FILE/GINHOUX.SOM.PDF

330. Guilliams M, De Kleer I, Henri S, et al. Alveolar macrophages develop from fetal monocytes that differentiate into long-lived cells in the first week of life via GM-CSF. *J Exp Med*. 2013;210(10):1977-1992. doi:10.1084/JEM.20131199

331. Hashimoto D, Chow A, Noizat C, et al. Tissue-Resident Macrophages Self-Maintain Locally throughout Adult Life with Minimal Contribution from Circulating Monocytes. *Immunity*. 2013;38(4):792-804. doi:10.1016/J.IMMUNI.2013.04.004

332. Tak T, Drylewicz J, Conemans L, et al. Circulatory and maturation kinetics of human monocyte subsets in vivo. *Blood*. 2017;130(12):1474-1477. doi:10.1182/BLOOD-2017-03-771261

333. Mildner A, Schönheit J, Giladi A, et al. Genomic Characterization of Murine

Monocytes Reveals C/EBPβ Transcription Factor Dependence of Ly6C− Cells. *Immunity*. 2017;46(5):849-862.e7. doi:10.1016/J.IMMUNI.2017.04.018

334. Rizzo G, Vafadarnejad E, Arampatzi P, et al. Single-cell transcriptomic profiling maps monocyte/macrophage transitions after myocardial infarction in mice. doi:10.1101/2020.04.14.040451

335. Tamura A, Hirai H, Yokota A, et al. C/EBPβ is required for survival of Ly6C - monocytes. *Blood*. 2017;130(16):1809-1818. doi:10.1182/BLOOD-2017-03-772962

336. Thomas GD, Hanna RN, Vasudevan NT, et al. Deleting an Nr4a1 Super-Enhancer Subdomain Ablates Ly6C low Monocytes while Preserving Macrophage Gene Function. *Immunity*. 2016;45(5):975-987. doi:10.1016/J.IMMUNI.2016.10.011

337. Hanna RN, Carlin LM, Hubbeling HG, et al. The transcription factor NR4A1 (Nur77) controls bone marrow differentiation and the survival of Ly6C− monocytes. *Nat Immunol 2011 128*. 2011;12(8):778-785. doi:10.1038/ni.2063

338. Buenrostro JD, Corces MR, Lareau CA, et al. Integrated Single-Cell Analysis Maps the Continuous Regulatory Landscape of Human Hematopoietic Differentiation. *Cell*. 2018;173(6):1535-1548.e16. doi:10.1016/J.CELL.2018.03.074

339. VARIETY Synonyms: 63 Synonyms & Antonyms for VARIETY | Thesaurus.com. Accessed August 10, 2022. https://www.thesaurus.com/browse/variety

340. Shi C, Pamer EG. Monocyte recruitment during infection and inflammation. *Nat Rev Immunol 2011 1111*. 2011;11(11):762-774. doi:10.1038/nri3070

341. Heimbeck I, Hofer TPJ, Eder C, et al. Standardized single-platform assay for human monocyte subpopulations: Lower CD14+CD16++ monocytes in females. *Cytom Part A*. 2010;77A(9):823-830. doi:10.1002/CYTO.A.20942

342. Seidler S, Zimmermann HW, Bartneck M, Trautwein C, Tacke F. Age-dependent alterations of monocyte subsets and monocyte-related chemokine pathways in

healthy adults. *BMC Immunol*. 2010;11. doi:10.1186/1471-2172-11-30

343. Satoh T, Nakagawa K, Sugihara F, et al. Identification of an atypical monocyte and committed progenitor involved in fibrosis. *Nat 2016 5417635*. 2016;541(7635):96-101. doi:10.1038/nature20611

344. Van Der Laan AM, Ter Horst EN, Delewi R, et al. Monocyte subset accumulation in the human heart following acute myocardial infarction and the role of the spleen as monocyte reservoir. *Eur Heart J*. 2014;35(6):376-385. doi:10.1093/EURHEARTJ/EHT331

345. Robbins CS, Chudnovskiy A, Rauch PJ, et al. Extramedullary hematopoiesis generates Ly-6C(high) monocytes that infiltrate atherosclerotic lesions. *Circulation*. 2012;125(2):364-374. doi:10.1161/CIRCULATIONAHA.111.061986

346. Swirski FK, Nahrendorf M, Etzrodt M, et al. Identification of splenic reservoir monocytes and their deployment to inflammatory sites. *Science (80-)*. 2009;325(5940):612-616. doi:10.1126/SCIENCE.1175202/SUPPL_FILE/SWIRSKI.SOM.PDF

347. Croxford AL, Lanzinger M, Hartmann FJ, et al. The Cytokine GM-CSF Drives the Inflammatory Signature of CCR2+ Monocytes and Licenses Autoimmunity. *Immunity*. 2015;43(3):502-514. doi:10.1016/J.IMMUNI.2015.08.010

348. Briseño CG, Haldar M, Kretzer NM, et al. Distinct Transcriptional Programs Control Cross-Priming in Classical and Monocyte-Derived Dendritic Cells. *Cell Rep*. 2016;15(11):2462-2474. doi:10.1016/J.CELREP.2016.05.025

349. Graubardt N, Vugman M, Mouhadeb O, et al. Ly6Chi monocytes and their macrophage descendants regulate neutrophil function and clearance in acetaminophen-induced liver injury. *Front Immunol*. 2017;8(JUN):626. doi:10.3389/FIMMU.2017.00626/BIBTEX

350. Zigmond E, Samia-Grinberg S, Pasmanik-Chor M, et al. Infiltrating Monocyte-Derived Macrophages and Resident Kupffer Cells Display Different Ontogeny and Functions in Acute Liver Injury. *J Immunol*. 2014;193(1):344-353.

doi:10.4049/JIMMUNOL.1400574/-/DCSUPPLEMENTAL

351. London A, Itskovich E, Benhar I, et al. Neuroprotection and progenitor cell renewal in the injured adult murine retina requires healing monocyte-derived macrophages. *J Exp Med*. 2011;208(1):23-39. doi:10.1084/JEM.20101202

352. Nobs SP, Kopf M. Tissue-resident macrophages: guardians of organ homeostasis. *Trends Immunol*. 2021;42(6):495-507. doi:10.1016/J.IT.2021.04.007

353. Shapouri-Moghaddam A, Mohammadian S, Vazini H, et al. Macrophage plasticity, polarization, and function in health and disease. *J Cell Physiol*. 2018;233(9):6425-6440. doi:10.1002/JCP.26429

354. Ginhoux F, Guilliams M. Tissue-Resident Macrophage Ontogeny and Homeostasis. *Immunity*. 2016;44(3):439-449. doi:10.1016/j.immuni.2016.02.024

355. Hoeffel G, Chen J, Lavin Y, et al. C-Myb+ Erythro-Myeloid Progenitor-Derived Fetal Monocytes Give Rise to Adult Tissue-Resident Macrophages. *Immunity*. 2015;42(4):665-678. doi:10.1016/J.IMMUNI.2015.03.011

356. Orkin SH, Zon LI. Hematopoiesis: An Evolving Paradigm for Stem Cell Biology. *Cell*. 2008;132(4):631-644. doi:10.1016/J.CELL.2008.01.025

357. Palis J, Robertson S, Kennedy M, Wall C, Keller G. Development of erythroid and myeloid progenitors in the yolk sac and embryo proper of the mouse. *Development*. 1999;126(22):5073-5084. doi:10.1242/DEV.126.22.5073

358. Tober J, Koniski A, McGrath KE, et al. The megakaryocyte lineage originates from hemangioblast precursors and is an integral component both of primitive and of definitive hematopoiesis. *Blood*. 2007;109(4):1433-1441. doi:10.1182/BLOOD-2006-06-031898

359. Frame JM, McGrath KE, Palis J. Erythro-myeloid progenitors: “Definitive” hematopoiesis in the conceptus prior to the emergence of hematopoietic stem cells. *Blood Cells, Mol Dis*. 2013;51(4):220-225. doi:10.1016/J.BCMD.2013.09.006

360. Palis J, Yoder MC. Yolk-sac hematopoiesis: The first blood cells of mouse and man. *Exp Hematol*. 2001;29(8):927-936. doi:10.1016/S0301-472X(01)00669-5

361. Bertrand JY, Jalil A, Klaine M, Jung S, Cumano A, Godin I. Three pathways to mature macrophages in the early mouse yolk sac. *Blood*. 2005;106(9):3004-3011. doi:10.1182/BLOOD-2005-02-0461

362. Cumano A, Godin I. Ontogeny of the Hematopoietic System. *http://dx.doi.org/101146/annurev.immunol25022106141538*. 2007;25:745-785. doi:10.1146/ANNUREV.IMMUNOL.25.022106.141538

363. Godin I, Cumano A. The hare and the tortoise: an embryonic haematopoietic race. *Nat Rev Immunol 2002 28*. 2002;2(8):593-604. doi:10.1038/nri857

364. Sica A, Mantovani A. Macrophage plasticity and polarization: in vivo veritas. *J Clin Invest*. 2012;122(3):787-795. doi:10.1172/JCI59643

365. Mantovani A, Sica A, Sozzani S, Allavena P, Vecchi A, Locati M. The chemokine system in diverse forms of macrophage activation and polarization. *Trends Immunol*. 2004;25(12):677-686. doi:10.1016/J.IT.2004.09.015

366. Sica A, Erreni M, Allavena P, Porta C. Macrophage polarization in pathology. *Cell Mol Life Sci*. 2015;72(21):4111-4126. doi:10.1007/S00018-015-1995-Y

367. Murray PJ. Macrophage Polarization. *Annu Rev Physiol*. 2017;79:541-566. doi:10.1146/ANNUREV-PHYSIOL-022516-034339

368. Locati M, Mantovani A, Sica A. Macrophage activation and polarization as an adaptive component of innate immunity. *Adv Immunol*. 2013;120:163-184. doi:10.1016/B978-0-12-417028-5.00006-5

369. Biswas SK, Chittezhath M, Shalova IN, Lim JY. Macrophage polarization and plasticity in health and disease. *Immunol Res*. 2012;53(1-3):11-24. doi:10.1007/S12026-012-8291-9

370. Cassetta L, Cassol E, Poli G. Macrophage polarization in health and disease. *ScientificWorldJournal*. 2011;11:2391-2402. doi:10.1100/2011/213962

371. Zhu L, Zhao Q, Yang T, Ding W, Zhao Y. Cellular metabolism and macrophage functional polarization. *Int Rev Immunol*. 2015;34(1):82-100. doi:10.3109/08830185.2014.969421

372. Wang N, Liang H, Zen K. Molecular mechanisms that influence the macrophage M1-M2 polarization balance. *Front Immunol*. 2014;5(NOV):614. doi:10.3389/FIMMU.2014.00614/BIBTEX

373. Porta C, Riboldi E, Ippolito A, Sica A. Molecular and epigenetic basis of macrophage polarized activation. *Semin Immunol*. 2015;27(4):237-248. doi:10.1016/J.SMIM.2015.10.003

374. Cochain C, Vafadarnejad E, Arampatzi P, et al. Single-cell RNA-seq reveals the transcriptional landscape and heterogeneity of aortic macrophages in murine atherosclerosis. *Circ Res*. 2018;122(12):1661-1674. doi:10.1161/CIRCRESAHA.117.312509/-/DC1

375. Dick SA, Macklin JA, Nejat S, et al. Self-renewing resident cardiac macrophages limit adverse remodeling following myocardial infarction. *Nat Immunol*. 2019;20(1):29-39. doi:10.1038/s41590-018-0272-2

376. Dick SA, Wong A, Hamidzada H, et al. Three tissue resident macrophage subsets coexist across organs with conserved origins and life cycles. *Sci Immunol*. 2022;7(67). doi:10.1126/SCIIMMUNOL.ABF7777

377. Nobs SP, Kopf M. Tissue-resident macrophages: guardians of organ homeostasis. *Trends Immunol*. 2021;42(6):495-507. doi:10.1016/j.it.2021.04.007

378. Shouval DS, Biswas A, Goettel JA, et al. Interleukin-10 Receptor Signaling in Innate Immune Cells Regulates Mucosal Immune Tolerance and Anti-Inflammatory Macrophage Function. *Immunity*. 2014;40(5):706-719. doi:10.1016/J.IMMUNI.2014.03.011

379. Schneider C, Nobs SP, Kurrer M, Rehrauer H, Thiele C, Kopf M. Induction of the nuclear receptor PPAR-γ by the cytokine GM-CSF is critical for the differentiation of fetal monocytes into alveolar macrophages. *Nat Immunol 2014 1511*.

2014;15(11):1026-1037. doi:10.1038/ni.3005

380. Sipe GO, Lowery RL, Tremblay M, Kelly EA, Lamantia CE, Majewska AK. Microglial P2Y12 is necessary for synaptic plasticity in mouse visual cortex. *Nat Commun 2016 71*. 2016;7(1):1-15. doi:10.1038/ncomms10905

381. Sierra A, Encinas JM, Deudero JJP, et al. Microglia Shape Adult Hippocampal Neurogenesis through Apoptosis-Coupled Phagocytosis. *Cell Stem Cell*. 2010;7(4):483-495. doi:10.1016/J.STEM.2010.08.014

382. Gabanyi I, Muller PA, Feighery L, Oliveira TY, Costa-Pinto FA, Mucida D. Neuro-immune Interactions Drive Tissue Programming in Intestinal Macrophages. *Cell*. 2016;164(3):378-391. doi:10.1016/J.CELL.2015.12.023

383. Ikarashi M, Nakashima H, Kinoshita M, et al. Distinct development and functions of resident and recruited liver Kupffer cells/macrophages. *J Leukoc Biol*. 2013;94(6):1325-1336. doi:10.1189/JLB.0313144

384. Nishiyama K, Nakashima H, Ikarashi M, et al. Mouse CD11b+Kupffer Cells Recruited from Bone Marrow Accelerate Liver Regeneration after Partial Hepatectomy. *PLoS One*. 2015;10(9):e0136774. doi:10.1371/JOURNAL.PONE.0136774

385. Zigmond E, Samia-Grinberg S, Pasmanik-Chor M, et al. Infiltrating Monocyte-Derived Macrophages and Resident Kupffer Cells Display Different Ontogeny and Functions in Acute Liver Injury. *J Immunol*. 2014;193(1):344-353. doi:10.4049/JIMMUNOL.1400574/-/DCSUPPLEMENTAL

386. Tran S, Baba I, Poupel L, et al. Impaired Kupffer Cell Self-Renewal Alters the Liver Response to Lipid Overload during Non-alcoholic Steatohepatitis. *Immunity*. 2020;53(3):627-640.e5. doi:10.1016/J.IMMUNI.2020.06.003

387. Kim K, Shim D, Lee JS, et al. Transcriptome Analysis Reveals Nonfoamy Rather Than Foamy Plaque Macrophages Are Proinflammatory in Atherosclerotic Murine Models. *Circ Res*. 2018;123(10):1127-1142. doi:10.1161/CIRCRESAHA.118.312804

388. Jaitin DA, Adlung L, Thaiss CA, et al. Lipid-Associated Macrophages Control Metabolic Homeostasis in a Trem2-Dependent Manner. *Cell*. 2019;178(3):686-698.e14. doi:10.1016/J.CELL.2019.05.054

389. Ulland TK, Song WM, Huang SCC, et al. TREM2 Maintains Microglial Metabolic Fitness in Alzheimer's Disease. *Cell*. 2017;170(4):649-663.e13. doi:10.1016/J.CELL.2017.07.023

390. Jaitin DA, Adlung L, Thaiss CA, et al. Lipid-Associated Macrophages Control Metabolic Homeostasis in a Trem2-Dependent Manner. *Cell*. 2019;178(3):686-698.e14. doi:10.1016/J.CELL.2019.05.054

391. Cochain C, Vafadarnejad E, Arampatzi P, et al. Single-cell RNA-seq reveals the transcriptional landscape and heterogeneity of aortic macrophages in murine atherosclerosis. *Circ Res*. 2018;122(12):1661-1674. doi:10.1161/CIRCRESAHA.117.312509

392. Xiong X, Kuang H, Ansari S, et al. Landscape of Intercellular Crosstalk in Healthy and NASH Liver Revealed by Single-Cell Secretome Gene Analysis. *Mol Cell*. 2019;75(3):644-660.e5. doi:10.1016/J.MOLCEL.2019.07.028

393. Heidt T, Courties G, Dutta P, et al. Differential Contribution of Monocytes to Heart Macrophages in Steady-State and after Myocardial Infarction. *Circ Res*. 2014;115(2):284. doi:10.1161/CIRCRESAHA.115.303567

394. Hulsmans M, Clauss S, Xiao L, et al. Macrophages Facilitate Electrical Conduction in the Heart. *Cell*. 2017;169(3):510-522.e20. doi:10.1016/J.CELL.2017.03.050

395. Lavine KJ, Epelman S, Uchida K, et al. Distinct macrophage lineages contribute to disparate patterns of cardiac recovery and remodeling in the neonatal and adult heart. *Proc Natl Acad Sci U S A*. 2014;111(45):16029-16034. doi:10.1073/PNAS.1406508111/SUPPL_FILE/PNAS.1406508111.SAPP.PDF

396. Leid J, Carrelha J, Boukarabila H, Epelman S, Jacobsen SEW, Lavine KJ. Primitive Embryonic Macrophages are Required for Coronary Development and

Maturation. *Circ Res*. 2016;118(10):1498-1511. doi:10.1161/CIRCRESAHA.115.308270

397. Nahrendorf M, Swirski FK, Aikawa E, et al. The healing myocardium sequentially mobilizes two monocyte subsets with divergent and complementary functions. *J Exp Med*. 2007;204(12):3037-3047. doi:10.1084/jem.20070885

398. Nahrendorf M, Swirski FK, Aikawa E, et al. The healing myocardium sequentially mobilizes two monocyte subsets with divergent and complementary functions. *J Exp Med*. 2007;204(12):3037-3047. doi:10.1084/JEM.20070885

399. Swirski FK, Nahrendorf M, Etzrodt M, Wildgruber M, Cortez-Retamozo V, Panizzi P, Figueiredo JL, Kohler RH, Chudnovskiy A, Waterman P, Aikawa E, Mempel TR, Libby P, Weissleder R PM. Identification of splenic reservoir monocytes and their deployment to inflammatory sites. Science. 2009; 325(5940):612-6. DOI: 10.1126/science.1175202. *Science (80-)*. 2010;325(5940):612-616. doi:10.1126/science.1175202.Identification

400. Heidt T, Sager HB, Courties G, et al. Chronic variable stress activates hematopoietic stem cells. *Nat Med*. 2014;20(7):754. doi:10.1038/NM.3589

401. Leuschner F, Rauch PJ, Ueno T, et al. Rapid monocyte kinetics in acute myocardial infarction are sustained by extramedullary monocytopoiesis. *J Exp Med*. 2012;209(1):123-137. doi:10.1084/JEM.20111009

402. Ismahil MA, Hamid T, Bansal SS, Patel B, Kingery JR, Prabhu SD. Remodeling of the mononuclear phagocyte network underlies chronic inflammation and disease progression in heart failure: critical importance of the cardiosplenic axis. *Circ Res*. 2014;114(2):266-282. doi:10.1161/CIRCRESAHA.113.301720

403. Nahrendorf M, Swirski FK, Aikawa E, et al. The healing myocardium sequentially mobilizes two monocyte subsets with divergent and complementary functions. *J Exp Med*. 2007;204(12):3037-3047. doi:10.1084/JEM.20070885

404. Hilgendorf I, Gerhardt LMS, Tan TC, et al. Ly-6 chigh monocytes depend on nr4a1 to balance both inflammatory and reparative phases in the infarcted

myocardium. *Circ Res*. 2014;114(10):1611-1622. doi:10.1161/CIRCRESAHA.114.303204/-/DC1

405. Anzai A, Choi JL, He S, et al. The infarcted myocardium solicits GM-CSF for the detrimental oversupply of inflammatory leukocytes. *J Exp Med*. 2017;214(11):3293-3310. doi:10.1084/JEM.20170689

406. Panizzi P, Swirski FK, Figueiredo JL, et al. Impaired infarct healing in atherosclerotic mice with Ly-6Chi monocytosis. *J Am Coll Cardiol*. 2010;55(15):1629. doi:10.1016/J.JACC.2009.08.089

407. King KR, Aguirre AD, Ye YX, et al. IRF3 and type I interferons fuel a fatal response to myocardial infarction. *Nat Med 2017 2312*. 2017;23(12):1481-1487. doi:10.1038/nm.4428

408. Deniset JF, Belke D, Lee WY, et al. Gata6 + Pericardial Cavity Macrophages Relocate to the Injured Heart and Prevent Cardiac Fibrosis. *Immunity*. 2019;51(1):131-140.e5. doi:10.1016/J.IMMUNI.2019.06.010

409. Jung S-H, Hwang B-H, Shin S, et al. Spatiotemporal dynamics of macrophage heterogeneity and a potential function of Trem2hi macrophages in infarcted hearts. *Nat Commun 2022 131*. 2022;13(1):1-15. doi:10.1038/s41467-022-32284-2

410. Lemke G. How macrophages deal with death. *Nat Rev Immunol 2019 199*. 2019;19(9):539-549. doi:10.1038/s41577-019-0167-y

411. Freeman SA, Grinstein S. Phagocytosis: receptors, signal integration, and the cytoskeleton. *Immunol Rev*. 2014;262(1):193-215. doi:10.1111/IMR.12212

412. Zent CS, Elliott MR. Maxed out macs: physiologic cell clearance as a function of macrophage phagocytic capacity. *FEBS J*. 2017;284(7):1021-1039. doi:10.1111/FEBS.13961

413. Nicolás-Ávila JA, Lechuga-Vieco A V., Esteban-Martínez L, et al. A Network of Macrophages Supports Mitochondrial Homeostasis in the Heart. *Cell*. 2020;183(1):94-109.e23. doi:10.1016/j.cell.2020.08.031

414. Sun Z, Zhou D, Xie X, et al. Cross-talk between macrophages and atrial myocytes in atrial fibrillation. *Basic Res Cardiol*. 2016;111(6):1-19. doi:10.1007/S00395-016-0584-Z/TABLES/1

415. Kostić T, Momčilović S, Perišić ZD, et al. Manifestations of Lyme carditis. *Int J Cardiol*. 2017;232:24-32. doi:10.1016/J.IJCARD.2016.12.169

416. Tschöpe C, Ammirati E, Bozkurt B, et al. Myocarditis and inflammatory cardiomyopathy: current evidence and future directions. *Nat Rev Cardiol 2020 183*. 2020;18(3):169-193. doi:10.1038/s41569-020-00435-x

417. Zaman R, Hamidzada H, Kantores C, et al. Selective loss of resident macrophage-derived insulin-like growth factor-1 abolishes adaptive cardiac growth to stress. *Immunity*. 2021;54(9):2057-2071.e6. doi:10.1016/j.immuni.2021.07.006

418. Wong NR, Mohan J, Kopecky BJ, et al. Resident cardiac macrophages mediate adaptive myocardial remodeling. *Immunity*. 2021;54(9):2072-2088.e7. doi:10.1016/j.immuni.2021.07.003

419. Frantz S, Hofmann U, Fraccarollo D, et al. Monocytes/macrophages prevent healing defects and left ventricular thrombus formation after myocardial infarction. *FASEB J*. 2013;27(3):871-881. doi:10.1096/FJ.12-214049

420. Shiraishi M, Shintani Y, Shintani Y, et al. Alternatively activated macrophages determine repair of the infarcted adult murine heart. *J Clin Invest*. 2016;126(6):2151-2166. doi:10.1172/JCI85782

421. Simões FC, Cahill TJ, Kenyon A, et al. Macrophages directly contribute collagen to scar formation during zebrafish heart regeneration and mouse heart repair. *Nat Commun*. 2020;11(1). doi:10.1038/S41467-019-14263-2

422. Mouton AJ, DeLeon-Pennell KY, Rivera Gonzalez OJ, et al. Mapping macrophage polarization over the myocardial infarction time continuum. *Basic Res Cardiol*. 2018;113(4). doi:10.1007/S00395-018-0686-X

423. Howangyin KY, Zlatanova I, Pinto C, et al. Myeloid-Epithelial-Reproductive

Receptor Tyrosine Kinase and Milk Fat Globule Epidermal Growth Factor 8 Coordinately Improve Remodeling After Myocardial Infarction via Local Delivery of Vascular Endothelial Growth Factor. *Circulation*. 2016;133(9):826-839. doi:10.1161/CIRCULATIONAHA.115.020857

424. DeBerge M, Yeap XY, Dehn S, et al. MerTK Cleavage on Resident Cardiac Macrophages Compromises Repair After Myocardial Ischemia Reperfusion Injury. *Circ Res*. 2017;121(8):930-940. doi:10.1161/CIRCRESAHA.117.311327

425. Zhang S, Weinberg S, DeBerge M, et al. Efferocytosis Fuels Requirements of Fatty Acid Oxidation and the Electron Transport Chain to Polarize Macrophages for Tissue Repair. *Cell Metab*. 2019;29(2):443-456.e5. doi:10.1016/J.CMET.2018.12.004

426. Glinton KE, Ma W, Lantz C, et al. Macrophage-produced VEGFC is induced by efferocytosis to ameliorate cardiac injury and inflammation. *J Clin Invest*. 2022;132(9). doi:10.1172/JCI140685

427. Hanayama R, Tanaka M, Miwa K, Shinohara A, Iwamatsu A, Nagata S. Identification of a factor that links apoptotic cells to phagocytes. *Nature*. 2002;417(6885):182-187. doi:10.1038/417182A

428. Thorp E, Vaisar T, Subramanian M, Mautner L, Blobel C, Tabas I. Shedding of the Mer Tyrosine Kinase Receptor Is Mediated by ADAM17 Protein through a Pathway Involving Reactive Oxygen Species, Protein Kinase Cδ, and p38 Mitogen-activated Protein Kinase (MAPK). *J Biol Chem*. 2011;286(38):33335-33344. doi:10.1074/JBC.M111.263020

429. Cai B, Thorp EB, Doran AC, et al. MerTK cleavage limits proresolving mediator biosynthesis and exacerbates tissue inflammation. *Proc Natl Acad Sci U S A*. 2016;113(23):6526-6531. doi:10.1073/PNAS.1524292113/SUPPL_FILE/PNAS.201524292SI.PDF

430. Sather S, Kenyon KD, Lefkowitz JB, et al. A soluble form of the Mer receptor tyrosine kinase inhibits macrophage clearance of apoptotic cells and platelet

aggregation. *Blood*. 2007;109(3):1026-1033. doi:10.1182/BLOOD-2006-05-021634

431. Porrello ER, Mahmoud AI, Simpson E, et al. Transient regenerative potential of the neonatal mouse heart. *Science*. 2011;331(6020):1078-1080. doi:10.1126/SCIENCE.1200708

432. Ryan R, Moyse BR, Richardson RJ. Zebrafish cardiac regeneration-looking beyond cardiomyocytes to a complex microenvironment. *Histochem Cell Biol*. 2020;154(5):533-548. doi:10.1007/S00418-020-01913-6

433. Chablais F, Veit J, Rainer G, Jawiska A. The zebrafish heart regenerates after cryoinjury-induced myocardial infarction. *BMC Dev Biol*. 2011;11. doi:10.1186/1471-213X-11-21

434. González-Rosa JM, Martín V, Peralta M, Torres M, Mercader N. Extensive scar formation and regression during heart regeneration after cryoinjury in zebrafish. *Development*. 2011;138(9):1663-1674. doi:10.1242/DEV.060897

435. Schnabel K, Wu CC, Kurth T, Weidinger G. Regeneration of cryoinjury induced necrotic heart lesions in zebrafish is associated with epicardial activation and cardiomyocyte proliferation. *PLoS One*. 2011;6(4). doi:10.1371/JOURNAL.PONE.0018503

436. Aurora AB, Porrello ER, Tan W, et al. Macrophages are required for neonatal heart regeneration. *J Clin Invest*. 2014;124(3):1382-1392. doi:10.1172/JCI72181

437. Godwin JW, Debuque R, Salimova E, Rosenthal NA. Heart regeneration in the salamander relies on macrophage-mediated control of fibroblast activation and the extracellular landscape. *npj Regen Med 2017 21*. 2017;2(1):1-11. doi:10.1038/s41536-017-0027-y

438. Kober DL, Brett TJ. TREM2-Ligand Interactions in Health and Disease. *J Mol Biol*. 2017;429(11):1607-1629. doi:10.1016/J.JMB.2017.04.004

439. Peng Q, Malhotra S, Torchia JA, Kerr WG, Coggeshall KM, Humphrey MB. TREM2- and DAP12-dependent activation of PI3K requires DAP10 and is

inhibited by SHIP1. *Sci Signal*. 2010;3(122). doi:10.1126/SCISIGNAL.2000500

440. Colonna Patrick Ross M, Teitelbaum SL, Takayanagi H, et al. Osteoclastogenesis Homeostasis by Controlling the Rate of-Catenin Regulate Bone β TREM2 and. Published online 2012. doi:10.4049/jimmunol.1102836

441. Molgora M, Esaulova E, Vermi W, et al. TREM2 Modulation Remodels the Tumor Myeloid Landscape Enhancing Anti-PD-1 Immunotherapy. *Cell*. 2020;182(4):886-900.e17. doi:10.1016/J.CELL.2020.07.013

442. Carmona S, Zahs K, Wu E, Dakin K, Bras J, Guerreiro R. The role of TREM2 in Alzheimer's disease and other neurodegenerative disorders. *Lancet Neurol*. 2018;17(8):721-730. doi:10.1016/S1474-4422(18)30232-1

443. Zhong L, Wang Z, Wang D, et al. Amyloid-beta modulates microglial responses by binding to the triggering receptor expressed on myeloid cells 2 (TREM2). *Mol Neurodegener*. 2018;13(1). doi:10.1186/S13024-018-0247-7

444. Hsieh CL, Koike M, Spusta SC, et al. A role for TREM2 ligands in the phagocytosis of apoptotic neuronal cells by microglia. *J Neurochem*. 2009;109(4):1144-1156. doi:10.1111/J.1471-4159.2009.06042.X

445. Keren-Shaul H, Spinrad A, Weiner A, et al. A Unique Microglia Type Associated with Restricting Development of Alzheimer's Disease. *Cell*. 2017;169(7):1276-1290.e17. doi:10.1016/J.CELL.2017.05.018

446. Parhizkar S, Arzberger T, Brendel M, et al. Loss of TREM2 function increases amyloid seeding but reduces plaque-associated ApoE. *Nat Neurosci 2019 222*. 2019;22(2):191-204. doi:10.1038/s41593-018-0296-9

447. Wang Y, Cella M, Mallinson K, et al. TREM2 Lipid Sensing Sustains the Microglial Response in an Alzheimer's Disease Model. *Cell*. 2015;160(6):1061-1071. doi:10.1016/J.CELL.2015.01.049

448. Ulland TK, Song WM, Huang SCC, et al. TREM2 Maintains Microglial Metabolic Fitness in Alzheimer's Disease. *Cell*. 2017;170(4):649-663.e13. doi:10.1016/J.CELL.2017.07.023

449. Otero K, Shinohara M, Zhao H, et al. TREM2 and β-Catenin Regulate Bone Homeostasis by Controlling the Rate of Osteoclastogenesis. *J Immunol*. 2012;188(6):2612-2621. doi:10.4049/JIMMUNOL.1102836

450. Cella M, Buonsanti C, Strader C, Kondo T, Salmaggi A, Colonna M. Impaired Differentiation of Osteoclasts in TREM-2–deficient Individuals. *J Exp Med*. 2003;198(4):645. doi:10.1084/JEM.20022220

451. Zou W, Reeve JL, Liu Y, Teitelbaum SL, Ross FP. DAP12 Couples c-Fms Activation to the Osteoclast Cytoskeleton by Recruitment of Syk. *Mol Cell*. 2008;31(3):422-431. doi:10.1016/J.MOLCEL.2008.06.023

452. Otero K, Turnbull IR, Poliani PL, et al. Macrophage colony-stimulating factor induces the proliferation and survival of macrophages via a pathway involving DAP12 and β-catenin. *Nat Immunol 2009 107*. 2009;10(7):734-743. doi:10.1038/ni.1744

453. Hume DA, Caruso M, Ferrari-Cestari M, Summers KM, Pridans C, Irvine KM. Phenotypic impacts of CSF1R deficiencies in humans and model organisms. *J Leukoc Biol*. 2020;107(2):205-219. doi:10.1002/JLB.MR0519-143R

454. Satoh JI, Kino Y, Yanaizu M, Saito Y. Alzheimer's disease pathology in Nasu-Hakola disease brains. *Intractable Rare Dis Res*. 2018;7(1):32-36. doi:10.5582/IRDR.2017.01088

455. Klünemann HH, Ridha BH, Magy L, et al. The genetic causes of basal ganglia calcification, dementia, and bone cysts: DAP12 and TREM2. *Neurology*. 2005;64(9):1502-1507. doi:10.1212/01.WNL.0000160304.00003.CA

456. Turnbull IR, Gilfillan S, Cella M, et al. Cutting Edge: TREM-2 Attenuates Macrophage Activation. *J Immunol*. 2006;177(6):3520-3524. doi:10.4049/JIMMUNOL.177.6.3520

457. Ito H, Hamerman JA. TREM-2, triggering receptor expressed on myeloid cell-2, negatively regulates TLR responses in dendritic cells. *Eur J Immunol*. 2012;42(1):176-185. doi:10.1002/EJI.201141679

458. Hamerman JA, Jarjoura JR, Humphrey MB, Nakamura MC, Seaman WE, Lanier LL. Cutting Edge: Inhibition of TLR and FcR Responses in Macrophages by Triggering Receptor Expressed on Myeloid Cells (TREM)-2 and DAP12. *J Immunol*. 2006;177(4):2051-2055. doi:10.4049/JIMMUNOL.177.4.2051

459. Gao X, Dong Y, Liu Z, Niu B. Silencing of triggering receptor expressed on myeloid cells-2 enhances the inflammatory responses of alveolar macrophages to lipopolysaccharide. *Mol Med Rep*. 2013;7(3):921-926. doi:10.3892/MMR.2013.1268/HTML

460. Thornton P, Sevalle J, Deery MJ, et al. TREM2 shedding by cleavage at the H157-S158 bond is accelerated for the Alzheimer's disease-associated H157Y variant. *EMBO Mol Med*. 2017;9(10):1366-1378. doi:10.15252/EMMM.201707673

461. Schlepckow K, Monroe KM, Kleinberger G, et al. Enhancing protective microglial activities with a dual function TREM2 antibody to the stalk region. *EMBO Mol Med*. 2020;12(4). doi:10.15252/EMMM.201911227

462. Schlepckow K, Kleinberger G, Fukumori A, et al. An Alzheimer-associated TREM2 variant occurs at the ADAM cleavage site and affects shedding and phagocytic function. *EMBO Mol Med*. 2017;9(10):1356-1365. doi:10.15252/EMMM.201707672

463. Feuerbach D, Schindler P, Barske C, et al. ADAM17 is the main sheddase for the generation of human triggering receptor expressed in myeloid cells (hTREM2) ectodomain and cleaves TREM2 after Histidine 157. *Neurosci Lett*. 2017;660:109-114. doi:10.1016/J.NEULET.2017.09.034

464. Savage JC, Jay T, Goduni E, et al. Nuclear Receptors License Phagocytosis by Trem2+ Myeloid Cells in Mouse Models of Alzheimer's Disease. *J Neurosci*. 2015;35(16):6532. doi:10.1523/JNEUROSCI.4586-14.2015

465. Daniel B, Nagy G, Hah N, et al. The active enhancer network operated by liganded RXR supports angiogenic activity in macrophages. *Genes Dev*. 2014;28(14):1562-1577. doi:10.1101/GAD.242685.114

466. Zhao Y, Bhattacharjee S, Jones BM, et al. Regulation of TREM2 expression by an NF-κB-sensitive miRNA-34a. *Neuroreport*. 2013;24(6):318. doi:10.1097/WNR.0B013E32835FB6B0

467. Bhattacharjee S, Zhao Y, Dua P, Rogaev EI, Lukiw WJ. microRNA-34a-Mediated Down-Regulation of the Microglial-Enriched Triggering Receptor and Phagocytosis-Sensor TREM2 in Age-Related Macular Degeneration. *PLoS One*. 2016;11(3):e0150211. doi:10.1371/JOURNAL.PONE.0150211

468. Kleinberger G, Brendel M, Mracsko E, et al. The FTD -like syndrome causing TREM 2 T66M mutation impairs microglia function, brain perfusion, and glucose metabolism . *EMBO J*. 2017;36(13):1837-1853. doi:10.15252/EMBJ.201796516

469. Takahashi K, Rochford CDP, Neumann H. Clearance of apoptotic neurons without inflammation by microglial triggering receptor expressed on myeloid cells-2. 2005;201(4):647-657. doi:10.1084/jem.20041611

470. Takahashi K, Rochford CDP, Neumann H. Clearance of apoptotic neurons without inflammation by microglial triggering receptor expressed on myeloid cells-2. *J Exp Med*. 2005;201(4):647-657. doi:10.1084/JEM.20041611

471. N'Diaye EN, Branda CS, Branda SS, et al. TREM-2 (triggering receptor expressed on myeloid cells 2) is a phagocytic receptor for bacteria. *J Cell Biol*. 2009;184(2):215-223. doi:10.1083/JCB.200808080

472. Nugent AA, Lin K, van Lengerich B, et al. TREM2 Regulates Microglial Cholesterol Metabolism upon Chronic Phagocytic Challenge. *Neuron*. 2020;105(5):837-854.e9. doi:10.1016/J.NEURON.2019.12.007

473. Hutchins PM, Moore EE, Murphy RC. Electrospray MS/MS reveals extensive and nonspecific oxidation of cholesterol esters in human peripheral vascular lesions. *J Lipid Res*. 2011;52(11):2070-2083. doi:10.1194/JLR.M019174

474. Chan RB, Oliveira TG, Cortes EP, et al. Comparative Lipidomic Analysis of Mouse and Human Brain with Alzheimer Disease. *J Biol Chem*. 2012;287(4):2678-2688. doi:10.1074/JBC.M111.274142

475. Wu K, Byers DE, Jin X, et al. TREM-2 promotes macrophage survival and lung disease after respiratory viral infection. *J Exp Med*. 2015;212(5):681-697. doi:10.1084/jem.20141732

476. Otero K, Turnbull IR, Poliani PL, et al. Macrophage colony-stimulating factor induces the proliferation and survival of macrophages via a pathway involving DAP12 and beta-catenin. *Nat Immunol*. 2009;10(7):734-743. doi:10.1038/NI.1744

477. Deczkowska A, Keren-Shaul H, Weiner A, Colonna M, Schwartz M, Amit I. Disease-Associated Microglia: A Universal Immune Sensor of Neurodegeneration. *Cell*. 2018;173(5):1073-1081. doi:10.1016/J.CELL.2018.05.003

478. Deczkowska A, Weiner A, Amit I. The Physiology, Pathology, and Potential Therapeutic Applications of the TREM2 Signaling Pathway. *Cell*. 2020;181(6):1207-1217. doi:10.1016/j.cell.2020.05.003

479. Filipello F, Morini R, Corradini I, et al. The Microglial Innate Immune Receptor TREM2 Is Required for Synapse Elimination and Normal Brain Connectivity. *Immunity*. 2018;48(5):979-991.e8. doi:10.1016/J.IMMUNI.2018.04.016

480. Jay TR, von Saucken VE, Muñoz B, et al. TREM2 is required for microglial instruction of astrocytic synaptic engulfment in neurodevelopment. *Glia*. 2019;67(10):1873-1892. doi:10.1002/GLIA.23664

481. Wang ECE, Dai Z, Ferrante AW, Drake CG, Christiano AM. A Subset of TREM2+ Dermal Macrophages Secretes Oncostatin M to Maintain Hair Follicle Stem Cell Quiescence and Inhibit Hair Growth. *Cell Stem Cell*. 2019;24(4):654-669.e6. doi:10.1016/J.STEM.2019.01.011

482. Sasaki A. Microglia and brain macrophages: An update. *Neuropathology*. 2017;37(5):452-464. doi:10.1111/NEUP.12354

483. Ford JW, McVicar DW. TREM and TREM-like receptors in inflammation and disease. *Curr Opin Immunol*. 2009;21(1):38-46. doi:10.1016/J.COI.2009.01.009

484. Ulrich JD, Ulland TK, Colonna M, Holtzman DM. Elucidating the Role of TREM2 in

Alzheimer's Disease. *Neuron*. 2017;94(2):237-248. doi:10.1016/J.NEURON.2017.02.042

485. Zhong L, Wang Z, Wang D, et al. Amyloid-beta modulates microglial responses by binding to the triggering receptor expressed on myeloid cells 2 (TREM2). *Mol Neurodegener*. 2018;13(1). doi:10.1186/S13024-018-0247-7

486. Zhang X, Wang W, Li P, Wang X, Ni K. High TREM2 expression correlates with poor prognosis in gastric cancer. *Hum Pathol*. 2018;72:91-99. doi:10.1016/J.HUMPATH.2017.10.026

487. Zhou Y, Song WM, Andhey PS, et al. Human and mouse single-nucleus transcriptomics reveal TREM2-dependent and TREM2-independent cellular responses in Alzheimer's disease. *Nat Med 2020 261*. 2020;26(1):131-142. doi:10.1038/s41591-019-0695-9

488. Grubman A, Choo XY, Chew G, et al. Mouse and human microglial phenotypes in Alzheimer's disease are controlled by amyloid plaque phagocytosis through Hif1α. *bioRxiv*. Published online May 17, 2019:639054. doi:10.1101/639054

489. Alsema AM, Jiang Q, Kracht L, et al. Profiling Microglia From Alzheimer's Disease Donors and Non-demented Elderly in Acute Human Postmortem Cortical Tissue. *Front Mol Neurosci*. 2020;13. doi:10.3389/FNMOL.2020.00134/FULL

490. Thrupp N, Sala Frigerio C, Wolfs L, et al. Single-Nucleus RNA-Seq Is Not Suitable for Detection of Microglial Activation Genes in Humans. *Cell Rep*. 2020;32(13). doi:10.1016/J.CELREP.2020.108189

491. Bakken TE, Hodge RD, Miller JA, et al. Single-nucleus and single-cell transcriptomes compared in matched cortical cell types. *PLoS One*. 2018;13(12):e0209648. doi:10.1371/JOURNAL.PONE.0209648

492. Krasemann S, Madore C, Cialic R, et al. The TREM2-APOE Pathway Drives the Transcriptional Phenotype of Dysfunctional Microglia in Neurodegenerative Diseases. *Immunity*. 2017;47(3):566-581.e9. doi:10.1016/J.IMMUNI.2017.08.008

493. Perugorria MJ, Esparza-Baquer A, Oakley F, et al. Non-parenchymal TREM-2

protects the liver from immune-mediated hepatocellular damage. *Gut*. 2019;68(3):533-546. doi:10.1136/GUTJNL-2017-314107

494. Ramachandran P, Dobie R, Wilson-Kanamori JR, et al. Resolving the fibrotic niche of human liver cirrhosis at single-cell level. *Nat 2019 5757783*. 2019;575(7783):512-518. doi:10.1038/s41586-019-1631-3

495. Coelho I, Duarte N, Barros A, Macedo MP, Penha-Gonçalves C. Trem-2 Promotes Emergence of Restorative Macrophages and Endothelial Cells During Recovery From Hepatic Tissue Damage. *Front Immunol*. 2021;11. doi:10.3389/FIMMU.2020.616044

496. Yao Y, Li H, Chen J, et al. TREM-2 serves as a negative immune regulator through Syk pathway in an IL-10 dependent manner in lung cancer. *Oncotarget*. 2016;7(20):29620-29634. doi:10.18632/ONCOTARGET.8813

497. Lavin Y, Kobayashi S, Leader A, et al. Innate Immune Landscape in Early Lung Adenocarcinoma by Paired Single-Cell Analyses. *Cell*. 2017;169(4):750-765.e17. doi:10.1016/J.CELL.2017.04.014

498. Wu R, Li X, Xu P, et al. TREM2 protects against cerebral ischemia/reperfusion injury. *Mol Brain*. 2017;10(1). doi:10.1186/S13041-017-0296-9

499. Jin SC, Benitez BA, Karch CM, et al. Coding variants in TREM2 increase risk for Alzheimer's disease. *Hum Mol Genet*. 2014;23(21):5838-5846. doi:10.1093/HMG/DDU277

500. Thornton P, Sevalle J, Deery MJ, et al. TREM2 shedding by cleavage at the H157-S158 bond is accelerated for the Alzheimer's disease-associated H157Y variant. *EMBO Mol Med*. 2017;9(10):1366-1378. doi:10.15252/EMMM.201707673

501. Schlepckow K, Kleinberger G, Fukumori A, et al. An Alzheimer-associated TREM2 variant occurs at the ADAM cleavage site and affects shedding and phagocytic function. *EMBO Mol Med*. 2017;9(10):1356-1365. doi:10.15252/EMMM.201707672

502. Woollacott IOC, Nicholas JM, Heslegrave A, et al. Cerebrospinal fluid soluble

TREM2 levels in frontotemporal dementia differ by genetic and pathological subgroup. *Alzheimers Res Ther*. 2018;10(1). doi:10.1186/S13195-018-0405-8

503. Weber GE, Koenig KA, Khrestian M, et al. An Altered Relationship between Soluble TREM2 and Inflammatory Markers in Young Adults with Down Syndrome: A Preliminary Report. *J Immunol*. 2020;204(5):1111-1118. doi:10.4049/JIMMUNOL.1901166/-/DCSUPPLEMENTAL

504. Suárez-Calvet M, Morenas-Rodríguez E, Kleinberger G, et al. Early increase of CSF sTREM2 in Alzheimer's disease is associated with tau related-neurodegeneration but not with amyloid-β pathology. *Mol Neurodegener*. 2019;14(1):1-14. doi:10.1186/S13024-018-0301-5/FIGURES/4

505. Suárez-Calvet M, Kleinberger G, Caballero MÁA, et al. sTREM2 cerebrospinal fluid levels are a potential biomarker for microglia activity in early-stage Alzheimer's disease and associate with neuronal injury markers. *EMBO Mol Med*. 2016;8(5):466-476. doi:10.15252/EMMM.201506123

506. Suárez-Calvet M, Caballero MÁA, Kleinberger G, et al. Early changes in CSF sTREM2 in dominantly inherited Alzheimer's disease occur after amyloid deposition and neuronal injury. *Sci Transl Med*. 2016;8(369). doi:10.1126/SCITRANSLMED.AAG1767

507. Piccio L, Deming Y, Del-Águila JL, et al. Cerebrospinal fluid soluble TREM2 is higher in Alzheimer disease and associated with mutation status. *Acta Neuropathol*. 2016;131(6):925-933. doi:10.1007/S00401-016-1533-5/TABLES/2

508. Piccio L, Buonsanti C, Cella M, et al. Identification of soluble TREM-2 in the cerebrospinal fluid and its association with multiple sclerosis and CNS inflammation. *Brain*. 2008;131(11):3081-3091. doi:10.1093/BRAIN/AWN217

509. Heslegrave A, Heywood W, Paterson R, et al. Increased cerebrospinal fluid soluble TREM2 concentration in Alzheimer's disease. *Mol Neurodegener*. 2016;11(1):1-7. doi:10.1186/S13024-016-0071-X/TABLES/1

510. Falcon C, Monté-Rubio GC, Grau-Rivera O, et al. CSF glial biomarkers YKL40

and sTREM2 are associated with longitudinal volume and diffusivity changes in cognitively unimpaired individuals. *NeuroImage Clin*. 2019;23:101801. doi:10.1016/J.NICL.2019.101801

511. Deczkowska A, Weiner A, Amit I. The Physiology, Pathology, and Potential Therapeutic Applications of the TREM2 Signaling Pathway. *Cell*. 2020;181(6):1207-1217. doi:10.1016/J.CELL.2020.05.003

512. Rauchmann BS, Schneider-Axmann T, Alexopoulos P, Perneczky R. CSF soluble TREM2 as a measure of immune response along the Alzheimer's disease continuum. *Neurobiol Aging*. 2019;74:182-190. doi:10.1016/J.NEUROBIOLAGING.2018.10.022

513. Liu D, Cao B, Zhao Y, et al. Soluble TREM2 changes during the clinical course of Alzheimer's disease: A meta-analysis. *Neurosci Lett*. 2018;686:10-16. doi:10.1016/J.NEULET.2018.08.038

514. Wu K, Byers DE, Jin X, et al. TREM-2 promotes macrophage survival and lung disease after respiratory viral infection. *J Exp Med*. 2015;212(5):681-697. doi:10.1084/JEM.20141732

515. Zhong L, Chen XF, Wang T, et al. Soluble TREM2 induces inflammatory responses and enhances microglial survival. *J Exp Med*. 2017;214(3):597-607. doi:10.1084/JEM.20160844

516. Zhong L, Xu Y, Zhuo R, et al. Soluble TREM2 ameliorates pathological phenotypes by modulating microglial functions in an Alzheimer's disease model. *Nat Commun 2019 101*. 2019;10(1):1-16. doi:10.1038/s41467-019-09118-9

517. Turnbull IR, Gilfillan S, Cella M, et al. Cutting edge: TREM-2 attenuates macrophage activation. *J Immunol*. 2006;177(6):3520-3524. doi:10.4049/JIMMUNOL.177.6.3520

518. Bosch-Queralt M, Cantuti-Castelvetri L, Damkou A, et al. Diet-dependent regulation of TGFβ impairs reparative innate immune responses after demyelination. *Nat Metab 2021 32*. 2021;3(2):211-227. doi:10.1038/s42255-021-

00341-7

519. Berner DK, Wessolowski L, Armbrust F, et al. Meprin β cleaves TREM2 and controls its phagocytic activity on macrophages. *FASEB J*. 2020;34(5):6675-6687. doi:10.1096/FJ.201902183R

520. Stuart T, Butler A, Hoffman P, et al. Comprehensive Integration of Single-Cell Data. *Cell*. 2019;177(7):1888-1902.e21. doi:10.1016/J.CELL.2019.05.031

521. Trapnell C, Cacchiarelli D, Grimsby J, et al. The dynamics and regulators of cell fate decisions are revealed by pseudotemporal ordering of single cells. *Nat Biotechnol 2014 324*. 2014;32(4):381-386. doi:10.1038/nbt.2859

522. Ericson JA, Duffau P, Yasuda K, et al. Gene Expression during the Generation and Activation of Mouse Neutrophils: Implication of Novel Functional and Regulatory Pathways. *PLoS One*. 2014;9(10):e108553. doi:10.1371/JOURNAL.PONE.0108553

523. Wu K, Byers DE, Jin X, et al. TREM-2 promotes macrophage survival and lung disease after respiratory viral infection. *J Exp Med*. 2015;212(5):681-697. doi:10.1084/JEM.20141732

524. Pfirschke C, Engblom C, Gungabeesoon J, et al. Tumor-Promoting Ly-6G + SiglecF high Cells Are Mature and Long-Lived Neutrophils. *Cell Rep*. 2020;32(12). doi:10.1016/J.CELREP.2020.108164

525. Ryu S, Shin JW, Kwon S, et al. Siglec-F-expressing neutrophils are essential for creating a profibrotic microenvironment in renal fibrosis. *J Clin Invest*. 2022;132(12). doi:10.1172/JCI156876

526. Ogawa K, Asano K, Yotsumoto S, et al. Frontline Science: Conversion of neutrophils into atypical Ly6G + SiglecF + immune cells with neurosupportive potential in olfactory neuroepithelium. *J Leukoc Biol*. 2021;109(3):481-496. doi:10.1002/JLB.1HI0620-190RR

527. Shin JW, Kim J, Ham S, et al. A unique population of neutrophils generated by air pollutant-induced lung damage exacerbates airway inflammation. *J Allergy Clin*

Immunol. 2022;149(4):1253-1269.e8. doi:10.1016/J.JACI.2021.09.031

528. Calcagno DM, Ng RP, Toomu A, et al. The myeloid type I interferon response to myocardial infarction begins in bone marrow and is regulated by Nrf2-activated macrophages. *Sci Immunol*. 2020;5(51). doi:10.1126/SCIIMMUNOL.AAZ1974

529. Kiwamoto T, Katoh T, Evans CM, et al. Endogenous airway mucins carry glycans that bind Siglec-F and induce eosinophil apoptosis. *J Allergy Clin Immunol*. 2015;135(5):1329-1340.e9. doi:10.1016/J.JACI.2014.10.027

530. Mao H, Kano G, Hudson SA, et al. Mechanisms of Siglec-F-induced eosinophil apoptosis: a role for caspases but not for SHP-1, Src kinases, NADPH oxidase or reactive oxygen. *PLoS One*. 2013;8(6). doi:10.1371/JOURNAL.PONE.0068143

531. Calcagno DM, Zhang C, Toomu A, et al. SiglecF(HI) Marks Late-Stage Neutrophils of the Infarcted Heart: A Single-Cell Transcriptomic Analysis of Neutrophil Diversification. *J Am Heart Assoc*. 2021;10(4):1-39. doi:10.1161/JAHA.120.019019

532. Woodfin A, Beyrau M, Voisin MB, et al. ICAM-1-expressing neutrophils exhibit enhanced effector functions in murine models of endotoxemia. *Blood*. 2016;127(7):898-907. doi:10.1182/BLOOD-2015-08-664995

533. O'Sullivan JA, Carroll DJ, Bochner BS. Glycobiology of eosinophilic inflammation: Contributions of siglecs, glycans, and other glycan-binding proteins. *Front Med*. 2017;4(AUG):116. doi:10.3389/FMED.2017.00116/XML/NLM

534. Boivin G, Faget J, Ancey PB, et al. Durable and controlled depletion of neutrophils in mice. *Nat Commun 2020 111*. 2020;11(1):1-9. doi:10.1038/s41467-020-16596-9

535. Hasenberg A, Hasenberg M, Männ L, et al. Catchup: a mouse model for imaging-based tracking and modulation of neutrophil granulocytes. *Nat Methods 2015 125*. 2015;12(5):445-452. doi:10.1038/nmeth.3322

536. Vafadarnejad E, Rizzo G, Krampert L, et al. Dynamics of Cardiac Neutrophil Diversity in Murine Myocardial Infarction. *Circ Res*. Published online August 19,

2020. doi:10.1161/circresaha.120.317200

537. Zilionis R, Engblom C, Pfirschke C, et al. Single-Cell Transcriptomics of Human and Mouse Lung Cancers Reveals Conserved Myeloid Populations across Individuals and Species. *Immunity*. 2019;50(5):1317-1334.e10. doi:10.1016/J.IMMUNI.2019.03.009

538. Kuppe C, Ramirez Flores RO, Li Z, et al. Spatial multi-omic map of human myocardial infarction. *Nat 2022 6087924*. 2022;608(7924):766-777. doi:10.1038/s41586-022-05060-x

539. Pinto AR, Paolicelli R, Salimova E, et al. An Abundant Tissue Macrophage Population in the Adult Murine Heart with a Distinct Alternatively-Activated Macrophage Profile. *PLoS One*. 2012;7(5):e36814. doi:10.1371/JOURNAL.PONE.0036814

540. Weinberger T, Räuber S, Schneider V, et al. Differential MHC-II expression and phagocytic functions of embryo-derived cardiac macrophages in the course of myocardial infarction in mice. *Eur J Immunol*. 2021;51(1):250-252. doi:10.1002/EJI.202048560

541. Nahrendorf M, Swirski FK, Aikawa E, et al. The healing myocardium sequentially mobilizes two monocyte subsets with divergent and complementary functions. *J Exp Med*. 2007;204(12):3037-3047. doi:10.1084/JEM.20070885

542. Hilgendorf I, Gerhardt LMS, Tan TC, et al. Ly-6Chigh monocytes depend on Nr4a1 to balance both inflammatory and reparative phases in the infarcted myocardium. *Circ Res*. 2014;114(10):1611-1622. doi:10.1161/CIRCRESAHA.114.303204

543. Zernecke A, Erhard F, Weinberger T, et al. Integrated scRNA-seq analysis identifies conserved transcriptomic features of mononuclear phagocytes in mouse and human atherosclerosis. *bioRxiv*. Published online December 10, 2020:2020.12.09.417535. doi:10.1101/2020.12.09.417535

544. Remmerie A, Martens L, Thoné T, et al. Osteopontin Expression Identifies a

Subset of Recruited Macrophages Distinct from Kupffer Cells in the Fatty Liver. *Immunity*. 2020;53(3):641-657.e14. doi:10.1016/J.IMMUNI.2020.08.004

545. Daemen S, Gainullina A, Kalugotla G, et al. Dynamic Shifts in the Composition of Resident and Recruited Macrophages Influence Tissue Remodeling in NASH. *Cell Rep*. 2021;34(2). doi:10.1016/J.CELREP.2020.108626

546. Guilliams M, Bonnardel J, Haest B, et al. Spatial proteogenomics reveals distinct and evolutionarily conserved hepatic macrophage niches. *Cell*. 2022;185(2):379-396.e38. doi:10.1016/J.CELL.2021.12.018

547. Shuey MM, Xiang RR, Elizabeth Moss M, et al. Systems Approach to Integrating Preclinical Apolipoprotein E-Knockout Investigations Reveals Novel Etiologic Pathways and Master Atherosclerosis Network in Humans. *Arterioscler Thromb Vasc Biol*. 2022;42(1):35. doi:10.1161/ATVBAHA.121.317071

548. Cremer S, Schloss MJ, Vinegoni C, et al. Diminished Reactive Hematopoiesis and Cardiac Inflammation in a Mouse Model of Recurrent Myocardial Infarction. *J Am Coll Cardiol*. 2020;75(8):901-915. doi:10.1016/J.JACC.2019.12.056

549. Koelwyn GJ, Newman AAC, Afonso MS, et al. Myocardial infarction accelerates breast cancer via innate immune reprogramming. *Nat Med*. 2020;26(9):1452-1458. doi:10.1038/S41591-020-0964-7

550. Ruparelia N, Godec J, Lee R, et al. Acute myocardial infarction activates distinct inflammation and proliferation pathways in circulating monocytes, prior to recruitment, and identified through conserved transcriptional responses in mice and humans. *Eur Heart J*. 2015;36(29):1923-1934. doi:10.1093/EURHEARTJ/EHV195

551. Reichart D, Lindberg EL, Maatz H, et al. Pathogenic variants damage cell composition and single-cell transcription in cardiomyopathies. *Science (80-)*. 2022;377(6606). doi:10.1126/SCIENCE.ABO1984/SUPPL_FILE/SCIENCE.ABO1984_MDAR_REPRODUCIBILITY_CHECKLIST.PDF

552. Lindsey ML, de Castro Brás LE, DeLeon-Pennell KY, et al. Reperfused vs. nonreperfused myocardial infarction: when to use which model. *Am J Physiol Heart Circ Physiol*. 2021;321(1):H208-H213. doi:10.1152/AJPHEART.00234.2021

11 Abbreviation

ACE	Angiotensin-converting enzyme
ACKR2	Atypical chemokine receptor 2
ADAM10/17	A disintegrin and metalloproteinase domain-containing protein 10/17
ADT	Antibody-derived tags
AEA	Autoimmune encephalomyelitis
AKT1	Serine/Threonine protein kinase 1
ALS	Amyotrophic lateral sclerosis
ApoE	Apolipoprotein E
ATP	Adenosine tryphosphate
BCR	B-cell receptor
BHLHE40	basic-helix-loop-helix family member E40
BM	Bone marrow
BMDMs	Bone marrow-derived macrophages
BMPs	Bone morphogenic proteins
C/EBPα	CCAAT-enhancer-binding protein α
CARD	Caspase activation and recruitment domains
CARD	Caspase recruitment domain
CCL	Chemokine C-C motif ligand
CCR2	C-C chemokine receptor type 2
cDCs	Conventional dendritic cells
cGAS	Cyclic GMP-AMP synthase
CITE-seq	Cellular indexing of transcriptomes and epitopes by sequencing
Clec9a	C-type lectin domain family 9 member A
cMoP	Common monocyte precursor
CMPs	Common myeloid progenitors
Col1a1	Collagen type 1 α1

Col3a1	Collagen type 3 α1
Col4a1	Collagen type 4 α1
Col4a3	Collagen type 4 α3
COX-2	Cyclooxygenase-2
cRTMs	Cardiac tissue-resident macrophages
CSA	Cross-sectional area
CSF-1	Colony-stimulating factor 1
CSF-2	Colony-stimulating factor 2
Ctgf	Connective tissue growth factor
CXCR2	C-X-C motif receptor 2
DAMPs	Danger-associated molecular patterns
DAP	D-glutamyl-meso-diaminopimelic acid
DAP10	DNAX activation protein 10
DAP12	DNAX activation protein 12
DCs	Dendritic cells
DHR123	Dihydrorhodamine-123
DNA	Deoxyribonucleic acid
E. coli	Escherichia coli
ECM	Extracellular matrix
EMPs	Erythro-myeloid precursors
ERK	Extracellular signal-regulated kinase
EVs	Extracellular vesicles
F4/80	EGF-like module-containing mucin-like hormone receptor-like 1
FCS	Fetal calf serum
Flt3	Fms-like tyrosine kinase 3
GATA6	GATA-binding protein 6
G-CSF	Granulocyte colony-stimulating factor
GDFs	Growth differentiation factors
GFI1	Zinc finger protein Gfi-1

GM-CSF	Granulocyte-macrophage colony-stimulating factor
GMPs	Granulocyte macrophage progenitors
GPNMB	Transmembrane glycoprotein NMB
Grn	pro-granulin
HF	Heart Failure
HFrEF	Heart failure with reduced ejection fraction
HIF1α	Hypoxia-inducible factor 1-α
HLA-DR	Human leukocyte antigen-DR
HMGB1	High mobility group box-1
HSCs	Hematopoietic stem cells
HTO	Hashtag oligo
ICAM1	Intercellular adhesion molecule 1
IEG	Immediate early genes
IFNICs	Interferon-inducible cells
IFNγ	Interferon-γ
IGF-1	Insulin-growth factor 1
IL	Interleukin
IL1R	IL1 receptor
ILCs	Innate lymphoid cells
IRAKs	IL1 receptor associated kinases
IRF3	Interferon regulatory factor 3
ITAM	Immune receptor tyrosine-based activation motif
KLF2	Krüpper-like factor 2
KO	knock-out
LAD	Left anterior descending
LAMs	Lipid-associated macrophages
LAP	Latency-associated peptide
LCN2	lipocalin-2
LDNs	Low-density neutrophils

LFA-1	Lymphocyte nfunction-associated antigen 1
LPS	Lipopolysaccharide
LRR	Leucine rich repeat
LTBP	latent TGFβ-binding protein
LXR	Liver X receptor
Ly6C	Lymphocyte antigen 6 complex
Ly6G	Lymphocyte antigen 6g
LYVE-1	Lymphatic vessel endothelial hyaluronan receptor 1
MCP-1	Monocyte chemoattractant protein-1
MDP	Monocyte-dendritic cell progenitors
MDPs	monocyte-macrophage/dendritic cell precursors
MerTK	Proto-oncogene tyrosine-protein kinase MER
Mfge8	milk fat globule epidermal growth factor-like factor 8
MFG-E8	milk fat globule-epidermal growth factor 8
MHCI	Major histocompatibility complex class I
MHCII	Major histocompatibility complex class II
MI	Myocardial infarction
MITF	Microphthalmia-associated transcription factor
MMP	Matrix metalloproteinase
MMPs	Multipotent precursors
moDCs	monocyte-derived dendritic cells
MS	Multiple sclerosis
NACHT	Neuronal apoptosis inhibitory protein CIITA HET-E TP1
NADPH	Nicotinamide adenine dinucleotide phosphate
NDNs	normal-density neutrophils
NETs	Neutrophil extracellular traps
NFkB	Nuclear factor kappa-ligh-chain-enhancer of activated B cells
NLRP3	NLR family pyrin domain containing 3
NLRs	Nucleotide-binding oligomerization domain-like receptors

NOD	Nucleotide-binding oligomerization domain-containing protein
NR4A1	Nuclear receptor 4A1
OSM	Oncostatin-M
PAD4	Protein-arginine deiminase type-4
PAMPs	Pathogen-associated molecular patterns
PBS	Phosphate buffered Saline
PC	Principal component
PCA	Principal component analysis
pDCs	Plasmacytoid dendritic cells
PI3K	Phosphatidylinositol 3-kinase
PPARs	Peroxisome proliferator-activated receptors
PPARγ	Peroxisome proliferator-activated receptors γ
PPRs	Patter recognition receptors
PYD	Pyrin domain
RAGE	Receptor for advanced glycation end-products
ROS	Reactive oxygen species
RXR	Retinoid X receptor
RXRG	RXR gamma
S100A8	S100 calcium-binding protein A8
S100A9	S100 calcium-binding protein A9
SatM	Nucleus-containing atypical Ly6C^{lo} monocytes
ScRNA-seq	Single cell RNA sequencing
SHP-1	Src homology region 2 domain-containing phosphatase-1
SiglecF	Sialic acid-binding Ig-like lectin 8
STAT	signal transducer and activator of transcription
STAT6	Signal transducer and activator of transcription 6
sTREM2	Soluble riggering receptor expressed on myeloid cells 2
Syk	Spleen tyrosine kinase
TAMs	Tumor-associated macrophages

TGFβ	Transforming growth factor β
Th	T helper
TIMD4	T-cell immunoglobulin and mucin domain containing 4
TLRs	Toll-like receptors
TNFRs	Tumor necrosis factor receptors
TNFα	Tumor necrosis factor α
TRAF6	Tumor necrosis receptor associated factor 6
Tregs	T regulatory cells
TREM2	Triggering receptor expressed on myeloid cells 2
TRIB1	Tribbles homolog 1
TSP-1	Thrombospondin-1
UBC13	Ubiquitin-conjugating enzyme 13
UEV1A	Ubiquitin-conjugating enzyme E2 variant 1
UMAP	Uniform manifold approximation and projection
VEGF	Vascular endothelial growth factor
VEGFR	Vascular endothelial growth factor receptor
WGA	Wheat germ agglutinin
α-SMA	α-smooth muscle actin

12 Publications

1. **Giuseppe Rizzo**, Julius Gropper, Marie Piollet, Ehsan Vafadarnejad, Anna Rizakou, Sourish Reddy Bandi, Panagiota Arampatzi , Tobias Krammer, Nina DiFabion, Oliver Dietrich, Anahi-Paula Arias-Loza1, Marco Prinz, Matthias Mack, Kai Schlepckow, Christian Haass, Jean-Sébastien Silvestre, Alma Zernecke, Antoine-Emmanuel Saliba, and Clément Cochain; Dynamics of monocyte-derived macrophage diversity in experimental myocardial infarction. *Cardiovascular Research, July 2022*

2. Ehsan Vafadarnejad*, **Giuseppe Rizzo***, Laura Krampert*, Panagiota Arampatzi, Anahi-Paula Arias- Loza, Yara Nazzal, Anna Rizakou, Tim Knochenhauer, Sourish Reddy Bandi, Vallery Audy Nugroho, Dirk Schulz, Melanie Roesch, Paul Alayrac, Jose Vilar, Jean-Sébastien Silvestre, Alma Zernecke, Antoine-Emmanuel Saliba, Clément Cochain; Dynamics of Cardiac Neutrophil Diversity in Murine Myocardial Infarction. *Circulation Research, August 2020.* *equal contribution

3. **Giuseppe Rizzo***, Rosanna Di Maggio*, Anna Benedetti, Jacopo Morroni, Marina Bouche, and Biliana Lozanoska-Ochser; Splenic Ly6C^{hi} monocytes are critical players in dystrophic muscle injury and repair. *The Journal of Clinical Investigation insight, January 2020.* *equal contribution

4. Biliana Lozanoska-Ochser, Anna Benedetti, **Giuseppe Rizzo**, Valeria Marrocco, Rosanna Di Maggio, Piera Fiore, and Marina Bouche; Targeting eartly PKCθ-dependent T cell infiltration of dystrophic muscle reduces disease severity in a mouse model of muscular dystrophy. *The Journal of Pathology, March 2018.*

13 Statement of individual author contribution

Statement of individual author contributions and of legal second publication rights to manuscripts included in the dissertation

Manuscript 1 (Chapter 3; this manuscript was re-wrote it in this thesis for copyright issue): Vafadarnejad E.*, Rizzo G.*, Krampert L.*, Arampatzi P., Arias-Loza A., Nazzal Y., Rizakou A., Knochenhauer T., Bandi S., Nugroho V., Schulz D., Roesch M., Alayrac P., Vilar J., Silvestre J., Zernecke A., Saliba A., Cochain C. Dynamics of Cardiac Neutrophil Diversity in Murine Myocardial Infarction. *Circulation Research* (2020). *equal contribution					
Participated in	**Author Initials,** Responsibility decreasing from left to right				
Study Design Methods Development	C.C.	A.E.S.	E.V., G.R., L.K.		
Data Collection	G.R., L.K., E.V.	R.A., N. Y., S.D., R.M.	B.S., K.T., Al.PA., A.P.		
Data Analysis and Interpretation	C.C., G.R., K.L., E.V.	R.A., N. Y., S.D., R.M.	B.S., K.T., Al.PA., A.P.		
Manuscript Writing	C.C.	A.E.S	E.V., G.R., L.K		
Writing of Introduction	C.C.	A.E.S	E.V., G.R., L.K		
Writing of Materials & Methods	C.C.	A.E.S	E.V., G.R., L.K		
Writing of Discussion	C.C.	A.E.S	E.V., G.R., L.K		
Writing of First Draft	C.C.	A.E.S	E.V., G.R., L.K		

Explanations (if applicable):

Manuscript 2 (Chapter 4): Rizzo G., Gropper J., Piollet M., Vafadarnejad E., Rizakou A., Bandi S, Arampatzi P., Krammer T., DiFabion N., Dietrich O., Arias-Loza A., Prinz M., Mack M., Schlepckow K., Haass C., Silvestre J., Zernecke A., Saliba A., Cochain C. Dynamic of monocyte-derived macrophage diversity in experimental myocardial infarction. *Cardiovascular Research* (2022)

Participated in	**Author Initials,** Responsibility decreasing from left to right				
Study Design Methods Development	C.C.	A.E.S.	G.R.		
Data Collection	G.R., J.G.	M.Pi, E.V., A.R.	S.R.B., P.A., T.K.	N.D., A.P.A.L.,	K.S.
Data Analysis and Interpretation	G.R., J.G., M.Pi, E.V.	A.R., S.R.B., P.A., T.K.	N.D., A.P.A.L., K.S., C.H.	J.S.S., A.Z., A.E.S., C.C.	
Manuscript Writing	C.C	A.E.S	G.R		
Writing of Introduction	C.C	A.E.S	G.R		
Writing of Materials & Methods	C.C	A.E.S	G.R		
Writing of Discussion	C.C	A.E.S	G.R		
Writing of First Draft	C.C	A.E.S	G.R		

Explanations (if applicable):

If applicable, the doctoral researcher confirms that she/he has obtained permission from both the publishers (copyright) and the co-authors for legal second publication.

The doctoral researcher and the primary supervisor confirm the correctness of the above mentioned assessment.

Giuseppe Rizzo Würzburg

Doctoral Researcher's Name Date Place Signature

Clément Cochain 4.11.22 Würzburg

Primary Supervisor's Name Date Place Signature

14 Statement of individual author contribution to figures/tables

Statement of individual author contributions to figures/tables of manuscripts included in the dissertation

Manuscript 1 (Chapter 3; this manuscript was re-wrote it in this thesis for copyright issue): Vafadarnejad E., Rizzo G., Krampert L., Arampatzi P., Arias-Loza A., Nazzal Y., Rizakou A., Knochenhauer T., Bandi S., Nugroho V., Schulz D., Roesch M., Alayrac P., Vilar J., Silvestre J., Zernecke A., Saliba A., Cochain C. Dynamics of Cardiac Neutrophil Diversity in Murine Myocardial Infarction. *Circulation Research* (2020)

Figure	**Author Initials,** Responsibility decreasing from left to right				
10	C.C.	A.E.S.	E.V	G.R.	L.K
11	C.C.	A.E.S.	E.V	G.R.	L.K
12	C.C.	A.E.S.	E.V	G.R.	L.K
13	C.C.	A.E.S.	E.V	G.R.	L.K
14	C.C.	A.E.S.	E.V	G.R.	L.K

Explanations (if applicable):

Manuscript 2 (Chapter 4): Rizzo G., Gropper J., Piollet M., Vafadarnejad E., Rizakou A., Bandi S, Arampatzi P., Krammer T., DiFabion N., Dietrich O., Arias-Loza A., Prinz M., Mack M., Schlepckow K., Haass C., Silvestre J., Zernecke A., Saliba A., Cochain C. Dynamic of monocyte-derived macrophage diversity in experimental myocardial infarction. *Cardiovascular Research* (2022)

Figure	**Author Initials,** Responsibility decreasing from left to right				
1	C.C	A.E.S	G.R.		
2	C.C	A.E.S	G.R.		
3	C.C	A.E.S	G.R.		
4	C.C	A.E.S	G.R.		
5	C.C	A.E.S	G.R.		
6	C.C	A.E.S	G.R.		

Supplementary Figure I	C.C	A.E.S	G.R.		
Supplementary Figure II	C.C	A.E.S	G.R.		
Supplementary Figure III	C.C	A.E.S	G.R.		
Supplementary Figure IV	C.C	A.E.S	G.R.		
Supplementary Figure V	C.C	A.E.S	G.R.		
Supplementary Figure VI	C.C	A.E.S	G.R.		
Supplementary Figure VII	C.C	A.E.S	G.R.		
Supplementary Figure VIII	C.C	A.E.S	G.R.		

Explanations (if applicable):

I also confirm my primary supervisor's acceptance.

Giuseppe Rizzo Würzburg

_____

Doctoral Researcher's Name Date Place Signature

15 Acknowledgment

First of all, I would like to thank my supervisor Dr. Clément Cochain for giving me the opportunity to work in his team. I thank him for his amazing supervision that let me able to learn a lot and professionally grow up. I thank him for always listening to my questions, supporting me, and giving me the freedom to work on anything I wanted. I am also grateful for the chance to continue working in his group as a Post-Doc.

I would like to thank Prof. Dr. Alma Zernecke for the great opportunity to work in her lab and be part of a very stimulating scientific environment, with weekly seminars in which I was able to present and discuss my project, and also getting a lot of feedback.

I would like to thank the other members of the thesis committee, Prof. Dr. Med. Ulrich Hofmann and PD Dr. rer. nat. Heike Hermanns, for the nice discussion during our annual meeting and the support given to me during these years.

I would like to thank Prof. Dr. Georg Gasteiger, who agreed to be the chairperson for my thesis defense.

I would like to thank Dr. rer. nat. Paula Arias-Loza, who invested so much time in performing my echocardiography experiments and for the incredible help that she gave me with the analysis process.

A special thanks go to my colleagues and friends from Clément´s group. In particular Anna, Sourish and Marie. I could not imagine finding better colleagues than them. I thank them for the irreplaceable help that they gave me at work and during the experiments. Thanks for the great time that we have at work and outside, for the laugh, for the joke, and for the hard time that they helped me to overcome. I couldn´t be more grateful finding wonderful people like them, at professional and human level. Another thanks go to Ecem. Although she started quite recently working with us (at least at the time that I wrote this acknowledgment), I am sure that she will fit very well with all of us and I am looking forward to know her better in the future.

A special thank goes to all the people from the institute of Experimental Biomedicine II. I would like to thank Prof. Dr. Elke Butt and her organization´s talent. I would like to thank the Post-Docs, in particular Nuria, Maja and Sandra. I would like to thank all the PhD students (although some of them are already gone), in particular Sarah, Gina, Janine, Annabelle, and Ruggero. Thanks for the great times during the last 4 years and I am looking forward to have other great times with them in the future. I also would like to thank the technicians, in particular Elfi, Petra, Yvonne and Doris. From all the technicians, a special thank goes to Melanie. Thanks for being there during the “unending” terminations that we were making and for the difficult time that we have been through (do you remember the MI training, eh?). Thanks also for the funny times together.

A very special thank goes to Ivana. I could not imagine my PhD time without her around. She is not a normal colleague, she became also one of my greatest friends and I am so happy that I shared this time with her and I am sure that our time will keep going in the future as well, although you are not living in Würzburg anymore. Thanks for sharing my great moments and my bad ones. I will never forget the great time that we had in the office and outside, together with Kristina, Anna and Sourish. Thank you for everything.

A very special thanks go to Kristina. Thanks for all the good times together and for being able to share my gaming passion with another crazy nerd like me.

Special thanks go to Vanessa, Tatiana, Riccardo, Debora and Antonella. Long-time friends and always present in my life. Thanks for all the laugh and beautiful time together.

Special thanks go to my mother and father-in-law, Eleonora and Alfredo. Thanks for welcoming me in your family and being supportive all the time.

I would like to thank my dad, Arianna, Danilo and aunt Elisabetta for their unconditional love and the support during the last years.

Last but not least, I would like to mention and thanks one person very important to me, Ludovica. We started as Master´s students, then we started to hang out together and discussed our Master´s thesis together. We decided to move abroad, at the beginning in different cities and then in the same one. When I started my PhD, we were boyfriend and girlfriend. Now, we are husband and wife. Thanks for your support during my good and bad times, to pick me up when I reached the bottom and to cheer for me every time. I don´t know how my life will be without you. You made me grow up, you made me stand up and fight for my rights. Just, thanks for choosing me and choosing me every day.

16 Affidavit/Eidessatattliche Erklärung

Affidavit

I hereby confirm that my thesis entitled "Determinants of macrophage and neutrophil heterogeneity in cardiac repair after myocardial infarction" is the result of my own work. I did not receive any help or support from commercial consultants. All sources and / or materials applied are listed and specified in the thesis.

Furthermore, I confirm that this thesis has not yet been submitted as part of another examination process neither in identical nor in similar form.

Würzburg

Place, Date Signature

Eidesstattliche Erklärung

Hiermit erkläre ich an Eides statt, die Dissertation "Determinante der Makrophagen- und Neutrophilien-Heterogenität bei der Herzreparatur nach Myokardinfarkt" eigenständig, d.h. insbesondere selbständig und ohne Hilfe eines kommerziellen Promotionsberaters, angefertigt und keine anderen als die von mir angegebenen Quellen und Hilfsmittel verwendet zu haben.

Ich erkläre außerdem, dass die Dissertation weder in gleicher noch in ähnlicher Form bereits in einem anderen Prüfungsverfahren vorgelegen hat.

Würzburg

Ort, Datum Unterschrift